Cardiff University
School of Medicine
Systems Immunity Research Institute

Prifysgol Caerdydd
Yr Ysgol Meddygaeth
Sefydliad Ymchwil Systemau Imiwnedd

GENOME EDITING APPROACHES FOR DEVELOPMENT OF PAN-POPULATION IMMUNOTHERAPIES

MATEUSZ LEGUT

A thesis submitted to Cardiff University
in candidature for the degree of
Doctor of Philosophy

September 2017

DECLARATION

This work has not been submitted in substance for any other degree or award at this or any other university or place of learning, nor is being submitted concurrently in candidature for any degree or other award.

Signed …… (candidate) Date ……

STATEMENT 1

This thesis is being submitted in partial fulfillment of the requirements for the degree of PhD.

Signed …… (candidate) Date ……

STATEMENT 2

This thesis is the result of my own independent work/investigation, except where otherwise stated, and the thesis has not been edited by a third party beyond what is permitted by Cardiff University's Policy on the Use of Third Party Editors by Research Degree Students. Other sources are acknowledged by explicit references. The views expressed are my own.

Signed …… (candidate) Date ……

STATEMENT 3

I hereby give consent for my thesis, if accepted, to be available online in the University's Open Access repository and for inter-library loan, and for the title and summary to be made available to outside organisations.

Signed …….. (candidate) Date ……

STATEMENT 4: PREVIOUSLY APPROVED BAR ON ACCESS

I hereby give consent for my thesis, if accepted, to be available online in the University's Open Access repository and for inter-library loans **after expiry of a bar on access previously approved by the Academic Standards & Quality Committee.**

Signed …… (candidate) Date ……

ACKNOWLEDGEMENTS

The research described in this Thesis would not have been possible without the contribution of my supervisory team, my colleagues, and my collaborators – both inside and outside Cardiff University.

First of all, I would like to thank my supervisor **Andrew Sewell** for enabling me to undertake this exciting project, as well as for his continuous support and providing me with numerous opportunities to develop as a researcher. Thank you for always finding time to address my questions, and for providing me with feedback even in extremely short time frames. A very special thanks to my mentor **Garry Dolton** for training and fostering my independence as a researcher while providing me with support whenever I needed it. I would also like to thank my second supervisor **John Chester** for his feedback and assistance at the beginning of my PhD.

I would like to acknowledge all the help I received from my colleagues **Meriem Attaf** and **Cristina Rius** – for providing advice on T-cell receptor sequencing and running my samples on MiSeq; **Garry Dolton**, **Cristina Rius** and **Sophie Wheeler** – for their assistance in cell culture; **Michael Crowther** and **Sophie Wheeler** – for working together on whole genome CRISPR approaches; **Catherine Naseriyan** (CBS, Cardiff University) - for cell sorting; and **Barbara Szomolay** – for help with analysing NGS data. I would also like to acknowledge my collaborators from within and outside of Cardiff University, in particular: **Oliver Ottmann**, **Afsar Mian**, **Alan Parker** and **Matthias Eberl** (Cardiff University), as well as **Marco Donia**, **Per thor Straten** and **Inge Marie Svane** (CCIT, Copenhagen) – for providing me with invaluable patient samples; **Sam Menzies** and **Paul Lehner** (University of Cambridge), as well as **Colin Farrell** and **John Phillips** (University of Utah, UT) – for providing me with whole genome CRISPR/Cas9 libraries, and their assistance with HiSeq sequencing. Last but not least, I would like to thank **Neville Sanjana** (New York University, NY) – for interesting discussions and his help with grant applications.

All my colleagues from the **T-cell Modulation Group** have greatly contributed to my overall experience in Cardiff, both in professional and private life. In particular I would like to thank members of the **2F01 office**, **Cristina Rius** and **Sophie Wheeler** - for coffee breaks, conversations about everything, and spending time together outside of work.

Finally, I would like to acknowledge **Cancer Research UK** for funding my PhD. Special thanks to **Phillip Taylor**, **Gareth Jones** and **Ann Ager** for taking time to provide feedback on my annual progress reports; and to **Julie Déchanet-Merville**, **Bernhard Moser** and **Alan Parker** for kindly agreeing to be on my viva examination panel.

SUMMARY

Background - T-cell based immunotherapy is the greatest recent breakthrough in cancer treatment, and can induce complete lasting remission. T-cells are capable of responding to a vast diversity of antigens via their hypervariable T-cell receptor (TCR). However, current immunotherapies rely on αβ T-cells which are restricted to person-specific Human Leukocyte Antigen (HLA) molecules presenting peptides from cancer-specific antigens. Thus, a given αβ TCR therapy is applicable only to a minority of patients. In contrast, γδ T-cells, and some αβ T-cells, recognise diverse cancer types regardless of the HLA type. The aims of my thesis were to investigate the potential of using non-HLA restricted T-cells and their receptors for cancer immunotherapy, and to develop tools to facilitate the study of non-HLA restricted T-cells for cancer treatment.

Results – Initially, I developed a CRISPR/Cas9 method for generation of superior TCR transduced cells, in terms of their anticancer reactivity and antigen sensitivity, in comparison to TCR transduced cells generated by current clinical methodologies. Using this TCR replacement method I demonstrated that the anticancer reactivity of broadly cancer-reactive γδ T-cells derived from a variety of clinically relevant sources is dependent on their TCRs. I also used CRISPR/Cas9 genome editing to generate a panel of cancer cell lines deficient in known ligands of non-HLA restricted T-cells that can be used for initial dissection of their anticancer reactivity. Using this approach, I demonstrated that one of non-HLA restricted T-cell clones I procured recognised targets via CD1a. Finally, I developed a whole genome CRISPR/Cas9 pipeline for discovery of ligands and pathways essential for cancer cell recognition by non-HLA restricted T-cells.

Conclusions – My research demonstrated that TCRs from broadly cancer-reactive T-cells can be used to re-direct primary T-cells to many cancer types regardless of their HLA type, paving the way for pan-population immunotherapy. The discovery of non-HLA ligands for broadly cancer-reactive T-cells can be achieved using whole genome and targeted CRISPR/Cas9 gene editing technology.

Work incorporated in this Thesis:

Legut M, Cole DK & Sewell AK. The promise of γδ T cells and the γδ T cell receptor for cancer immunotherapy. *Cell. Mol. Immunol*. (2015).

Attaf M, **Legut M**, Cole DK & Sewell AK. The T cell antigen receptor: The Swiss Army knife of the immune system. *Clin. Exp. Immunol*. (2015). (article featured on the journal cover)

Legut M, Dolton G, Mian A, Ottmann O, Sewell AK. CRISPR-mediated TCR replacement generates superior anticancer transgenic T-cells*. Blood*, re-submitted after revision (2017).

Other papers published during my PhD:

Legut M, Lipka D, Filipczak N, Piwoni A, Kozubek A, Gubernator J. Anacardic acid enhances the anticancer activity of liposomal mitoxantrone towards melanoma cell lines - in vitro studies. *Int. J. Nanomedicine* **9**, 653–668 (2014).

Uusi-Kerttula H, **Legut M**, Davies J, Jones R, Hudson E, Hanna L, Stanton RJ, Chester JD, Parker AL. Incorporation of Peptides Targeting EGFR and FGFR1 into the Adenoviral Fiber Knob Domain and Their Evaluation as Targeted Cancer Therapies. *Hum. Gene Ther*. **26**, 320–329 (2015).

Donia M, Westerlin Kjeldsen J, Andersen R, Wulff Westergaard MC, Bianchi V, **Legut M**, Attaf M, Dolton G, Lyngaa R, Hadrup SR, Sewell AK, Svane IM. PD-1+ polyfunctional T cells dominate the periphery after tumor-infiltrating lymphocyte therapy for cancer. *Clin. Cancer Res*. (2017).

Maciocia PM, Wawrzyniecka PA, Philip B, Ricciardelli R, Akarca AU, Onuoha S, **Legut M**, Cole DK, Sewell AK, Gritti G, Somja J, Piris MA, Peggs KS, Linch DC, Marafioti T, Pule MA.Targeting T-cell receptor β-constant for immunotherapy of T-cell malignancies. *Nature Medicine*, accepted for publication (August 2017).

Presentations of the results described in this Thesis:

British Society for Gene and Cell Therapy Conference, poster presentation (London 2014)

Cardiff University Division of Infection and Immunity Annual Meeting, poster presentation (Cardiff 2016)

7th International Gamma Delta T-cell Conference, oral presentation (London 2016)

British Society for Immunology Congress, oral presentation (Liverpool 2016)

Autolus Ltd meeting, invited speaker (London 2017)

British Society for Gene and Cell Therapy Conference, oral presentation (Cardiff 2017)

CRISPR gene editing workshop, invited speaker (Cardiff 2017)

ABBREVIATIONS

ACT – adoptive cell transfer
ADCC – antibody dependent cellular cytotoxicity
AIRE – autoimmune regulator
ALL – acute lymphoblastic leukaemia
AML – acute myeloid leukaemia
aPC – allophycocyanin
APC – antigen presenting cell
ApE – a plasmid editor
BC – breast cancer
BCR – B-cell receptor
bp – base pair
BrHPP – bromohydrin pyrophosphate
BTN – butyrophilin
C – constant
CAR – chimeric antigen receptor
CCL – chemokine (C-C motif) ligand
CCR – chemokine (C-C motif) receptor
CD – cluster of differentiation
cDNA – complementary DNA
CDR – complementarity-determining region
CML – chronic myelogenous leukaemia
CMV – cytomegalovirus
CR – complete response
CRISPR – clustered regularly interspaced short palindromic repeats
crRNA – complementary RNA
CTLA – cytotoxic T-lymphocyte associated protein
CXCL – chemokine (C-X-C motif) ligand
CXCR – chemokine (C-X-C motif) receptor
D – diversity
DC – dendritic cell
DMSO – dimethylsulfoxide
DN – double negative
DNA – deoxyribonucleic acid
dNTP – deoxynucleotide
DSB – double strand break
DTT – dithiotreitol
E:T – effector to target
EBV – Epstein-Barr virus
EDTA – ethylenediaminetetraacetic acid
EF – elongation factor
ELISA – enzyme-linked immunosorbent assay
ELIspot – enzyme-linked immunospot
EPCR – endothelial protein C receptor
FACS – fluorescence activated cell sorting
FcRn – neonatal Fc receptor
FITC – fluorescein isothiocyanate
FMO – fluorescence minus one
FPPS – farnesyl pyrophosphate synthase
FSC – forward scatter
GalCer – galactosylceramide
GeCKO – genome-wide CRISPR knock-out

GMP – good manufacturing practice
gRNA – guide RNA
HDR – homology-directed repair
HeBS – HEPES buffered saline
HEPES - 4-(2-hydroxyethyl)-1-piperazineethanesulfonic acid
HFE – human haemochromatosis protein
HLA – human leukocyte antigen
HMBPP - (*E*)-4-Hydroxy-3-methyl-but-2-enyl pyrophosphate
HPLC – high-performance liquid chromatography
HR – homologous recombination
ICS – intracellular cytokine staining
IFN – interferon
IFNAR – interferon α receptor
IL – interleukin
IPP – isopentenyl pyrophosphate
J – joining
JAK – Janus kinase
KO – knock-out
LB – lysogeny broth
LCL – lymphoblastoid cell line
MACS – magnetic activated cell sorting
MFI – median fluorescence intensity
MHC – major histocompatibility complex
MIC – MHC I chain-related polypeptide
MIP – macrophage inflammatory protein
MM – malignant melanoma
MOI – multiplicity of infection
MR1 – MHC-I related 1
MSH – MutS homologue
N – non-template
NBP – aminobisphosphonate
ND – not determined
NE – non evaluable
NGS – next generation sequencing
NHEJ – non-homologous end joining
NK – natural killer
NKG2D – natural killer group 2 member D
ns – not significant
nt – nucleotide
NTC – no template control
OC – ovarian cancer
ORF – open reading frame
P – palindromic
P – progressive disease
PAg – phosphoantigen
PAM – protospacer adjacent motif
PBS – phosphate buffered saline
PCR – polymerase chain reaction
PD – programmed death
PDB – Protein DataBase
PE – phycoerythrin
PHA – phytohaemagglutinin
PIP – prolactin-induced protein
PKI – protein kinase inhibitor

PMA – phorbol myristate acetate
PR – partial response
RACE - rapid amplification of cDNA ends
RBC – red blood cell
RCC – renal cell carcinoma
REP – rapid expansion protocol
RFX – regulatory factor X
RFXANK – RFX associated ankyrin containing protein
RFXAP – RFX associated protein
RNA – ribonucleic acid
SEM – standard error of the mean
SMARTer - switching mechanism at 5’ end of RNA transcript
SPICE – simplified presentation of incredibly complex evaluations
SSC – side scatter
TALEN – transcription activator-like effector nuclease
TAPI – TNFα processing inhibitor
TCR – T-cell receptor
TE – tris-EDTA
TIL – tumour-infiltrating lymphocytes
TNF – tumour necrosis factor
TNFRSF – TNFα receptor superfamily
tracRNA – trans-activating RNA
TRAIL – TNF-related apoptosis inducing ligand
ULBP – UL16 binding protein
V – variable
ZAG – zinc-alpha-2-glycoprotein
ZFN – zinc finger nuclease
β2m – beta-2-microglobulin

TABLE OF CONTENTS

LIST OF FIGURES

LIST OF TABLES

1. Introduction

1.1 The T-cell antigen receptor: a Swiss Army knife of the immune system

The immune surveillance performed by both the innate and the adaptive immune cells is essential for host protection against exogenous (i.e. infections) and endogenous threats (i.e. malignantly transformed cells). The adaptive arm of immunity consists of three components, namely: B cells, and T cells expressing αβ or γδ chains of their defining T-cell receptor (TCR). Such tripartite organisation has been maintained throughout the entirety of jawed vertebrate evolution; and three lineages of adaptive immune cells can be found even in jawless vertebrates[1]. In human, αβ T-cells are the most abundant T-cell subset in the periphery while γδ T-cells constitute 1-10% of all circulating T-cells; however, this ratio can significantly change during infections[2], and is much skewed towards γδ T-cells in tissues that represent the main portals for pathogen entry - such as mucosa and epidermis[3]. This tissue localisation can have important implications for immunosurveillance, with γδ T-cells forming the first line of host defence.

1.1.1 Generation of diversity – V(D)J recombination at *tr* loci

The T-cell antigen receptors are generated early in T-cell ontogeny by somatic gene rearrangement at *tra*, *trb*, *trg* and *trd* loci. As illustrated in **Figure 1.1**, the process involves recombination between one variable (V) segment and one junctional (J) segment that are then juxtaposed by splicing with the respective constant (C) segment (*tra* and *trg* loci). In case of *trb* and *trd* loci, the first recombination event occurs between one of two (*trb*) or up to three (*trd*) diversity (D) segments and a J segment, which is then followed by V to DJ recombination. An additional level of diversity is generated by deletion of template nucleotides at 3' end of V segment or 5' end of J segment due to imperfect non-homologous end joining, or addition of palindromic (P) or non-templated nucleotides (N)[4,5]. In human, there are 46 functional TCR-α V segments (TRAV), 3 exclusively TCR-δ V segments (TRDV) and 5 V segments that can be used in either TCR-α or –δ; as well as 48 functional TCR-β V segments (TRBV) and 4-6, depending on haplotype, TCR-γ V segments (TRGV)[6].

Importantly, *trd* locus is present within the *tra* locus, and the consequence of such genomic organisation is the possibility of generating hybrid TCRs, i.e. resulting from recombination between a TRDV and a TRAJ segment, which are then spliced with the TRAC segment, and paired with a canonical TCR-β chain. The resulting TCRs, termed δ/αβ TCRs, are expressed by a

significant proportion of peripheral T-cells specific for α-galactosylceramide (αGalCer) presented by CD1d molecule[7]. Other hybrid TCRs, especially resulting from trans-rearrangements between *trg* and *trb*, have been reported; however, their physiological relevance has yet to be demonstrated[8]. Most of the tools used to examine TCRs such as TCR chain-specific antibodies fail to detect hybrid TCRs, and it remains possible that hybrid TCRs constitute a significant minority of the entire TCR repertoire.

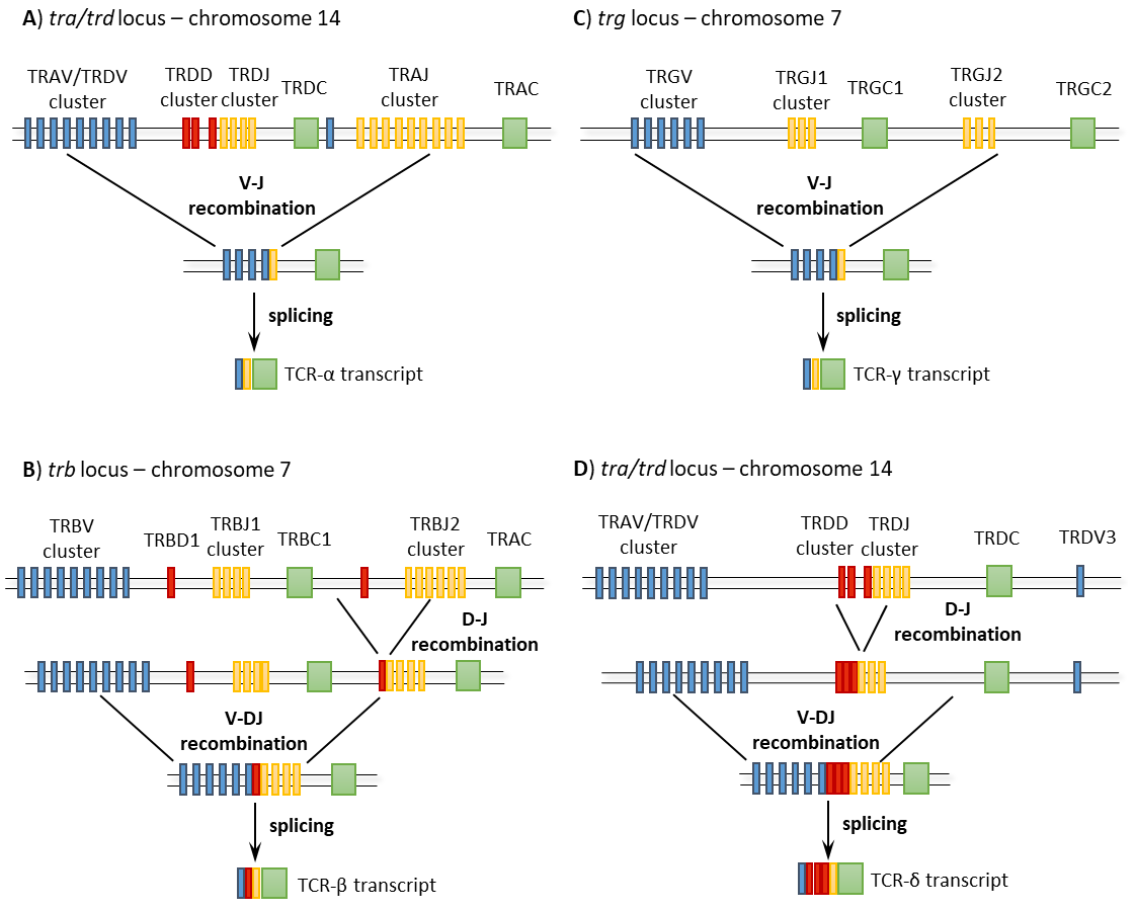

Figure 1.1 Schematic overview of the V(D)J recombination in human *tr* loci. In *tra* and *trg* loci (**A** and **C**, respectively), the recombination occurs between a variable (V) and a joining (J) segment, with non-germine addition/deletion at the V-J junction. The resulting VJ segment is then spliced with the TRAC or one of two TRGC segments, leading to a mature *tra* or *trg* transcript. In *trb* and *trd* loci (**B** and **D**, respectively), the first recombination event occurs between a diversity (D) segment and a J segment (in case of *trd*, multiple D segments may be used). The resulting DJ segment then recombines with a V segment. Non-germline addition/deletion can therefore occur at both recombination junctions (i.e. D/J and V/DJ). Finally, VDJ segment is spliced with one of two TRBC segments or the TRDC segment, leading to a mature *trb* or *trd* transcript. Notably, recombination at *tra* locus leads to the deletion of *trd* segments. Moreover, the chromosomal location of *tra* and *trd* loci, as well as *trb* and *trg*, allows for formation of hybrid TCRs. For the clarity of the figure, only a representation of gene segments was depicted. The organisation of human *tr* loci was adapted from the IMGT database.

The recombination between diverse V segments and diverse J segments, in combination with addition/deletion of random nucleotides at the junctions, can theoretically lead to a vast array of different TCRs (~10^{15} for αβ TCRs and ~10^{18} for γδ TCRs[9]) thus enabling host protection against previously unencountered pathogens. The genetic variability of TCRs is, in effect, translated into highly variegated hairpin loops present at the membrane-distal domain of the receptors (**Figure 1.2**). Every TCR chain possesses three hairpin loops, termed complementarity-determining regions (CDRs); CDR1 and CDR2 are germline-encoded while CDR3 is a result of junctional diversity, and therefore hypervariable. The CDR loops are responsible for the majority, and in most cases entirety, of TCR-ligand contacts[10]. CDR3 length is relatively constricted for TCR-α and TCR-β, in line with the requirement for making a well-defined contact with major histocompatibility complex (MHC) molecules. In contrast, CDR3δ is much longer, on average, than CDR3γ, thus making γδ TCRs more similar to B-cell receptors than αβ TCRs[11]. This observation gave rise to the hypothesis that γδ TCR recognition of ligands resembles that of an antibody; however, the paucity of confirmed γδ TCR ligands seems to contradict this hypothesis.

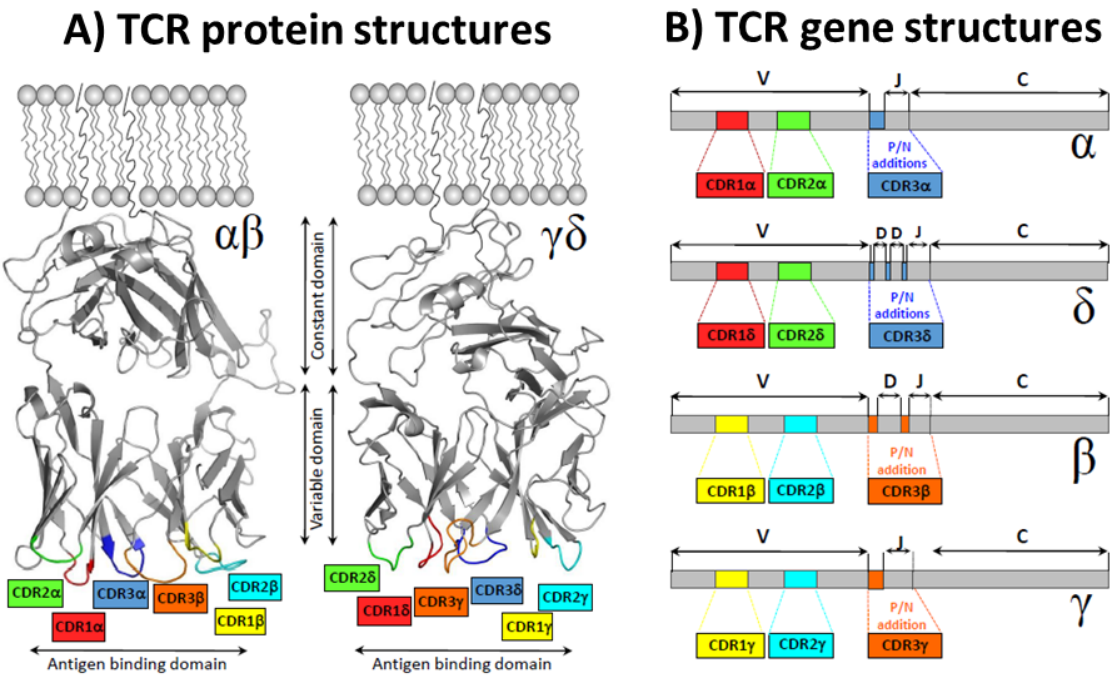

Figure 1.2 The protein and gene structures of αβ and γδ TCRs. The extracellular part of TCR proteins (**A**) is composed of a constant and a variable domain. The variable domain possesses 3 membrane-distal loops, termed complementarity-determining regions (CDR). The CDR loops are colour-coded throughout the Chapter. The correspondence of the protein structure, in particular the CDR loops, to the genetic structure is depicted in **B**. Protein DataBank (PDB) ID: 3HG1 (αβ TCR), 1HXM (γδ TCR). The figure was adapted from Attaf *et al.*, 2015.

1.1.2 Lineage commitment and thymic selection of T-cells

Both αβ and γδ T-cells arise from the same progenitor cells in the thymus which then undergo a differentiation programme that leads to functional and phenotypic divergence down one of these two T-cell lineages. Conventional αβ T-cells are subjected to positive and negative selection in the thymus which results in removal of TCR clonotypes that fail to engage, or engage too strongly, self MHC. Thymic selection therefore narrows down the quasi-random αβ TCR repertoire generated by V(D)J recombination to clonotypes that are potentially capable of recognising foreign peptides in context of self MHC while simultaneously reducing the risk of harmful autoreactivity. Another consequence of thymic selection is the relatively low affinity of αβ TCRs towards epitopes derived from self-proteins (such as tumour-associated antigens), compared to pathogen-derived antigens[12].

Unlike αβ T-cells, the putative mechanism of (thymic) selection of γδ T-cells remains poorly defined. For example, γδ T-cells develop normally in absence of autoimmune regulator (AIRE), a transcriptional regulator crucial for negative selection of αβ T-cells[13]. In contrast, a butyrophilin-like molecule Skint-1 has been shown as indispensable for the development of a subset of murine epidermal γδ T-cells[14]. Skint-1, however, is not a direct ligand of γδ TCRs, and thus its exact role in T-cell selection remains unresolved, especially because it has no human orthologue. Conversely, a pair of other butyrophilin-like molecules, Btnl1 and Btnl6, have recently been identified as drivers of expansion of mouse Vγ7^{+} T-cells in the gut[15]. Importantly, butyrophilin-like molecules BTNL3 and BTNL8 expressed in human gut epithelium drive TCR-dependent proliferation of Vγ4^{+} T-cells, indicating that butyrophilin-like molecules may play a more universal role in selecting for local, tissue specific γδ TCR repertoires.

Furthermore, the commitment of precursor T-cells to either αβ or γδ T-cell lineage has not been fully elucidated yet, as the rearrangement at *trb, trg* and *trd* loci is thought to occur simultaneously. As a result, immature T-cells can express both a γδ and a pre-TCR (TCR-β paired with the invariant Tα) at the same time. The initial experiments demonstrated that a strong signal transmitted *via* a γδ TCR induced precursor commitment to the γδ lineage while the absence thereof – *tra* rearrangement and αβ lineage commitment[16]. Further studies showed that in cells simultaneously expressing a γδ TCR and a pre-TCR, even a weak signal transmitted *via* the former can lead to γδ lineage commitment if accompanied by signals from the latter[17]. This mechanism can therefore be considered a form of positive, ligand-driven selection of functional γδ TCRs in the thymus. Indeed, the concept of positive selection of γδ T-cells is further supported by the observation that the majority of γδ T-cells in the periphery express CD73, a molecule that becomes upregulated in the thymus upon strong γδ TCR signalling, and can thus

be used as the earliest marker of γδ lineage commitment[18]. It should be noted, however, that Sherwood *et al.* challenged the concept of simultaneous rearrangement at *trg* and *trb* loci, demonstrating that in human the vast majority of αβ T-cells possess a rearranged TCR-γ while only a minor fraction of γδ T-cells had a rearranged TCR-β[19].

1.1.3 Conventional and unconventional ligands of T-cell receptors

1.1.3.1 Conventional MHC molecules

By far the best-studied T-cell ligands are peptides (both self and foreign) presented by highly polymorphic MHC molecules, and such ligands have therefore come to represent the convention. The exceedingly high polymorphism of MHC molecules allows presentation of variegated peptides, thus ensuring sufficient host protection against pathogenic challenge at the population level. In human, there are two classes of MHC molecules, namely MHC I [comprising human leukocyte antigen (HLA) –A, -B, and –C], and MHC II (comprising HLA –DR, -DP, and –DQ). The former is structurally composed of a polymorphic α-chain and a non-polymorphic molecule β-2-microglobulin (β2m) while the latter comprises two polymorphic chains α and β (apart from HLA-DR where only the β chain is polymorphic). While the majority of αβ T-cells in the periphery recognise peptide-MHC complexes (recently reviewed by Attaf *et al.*[20]), the evidence of MHC restriction by γδ T-cells remains conspicuously absent. The only well-defined example of a γδ T-cell clone recognising a classical MHC molecule is clone LBK5 specific for mouse MHC-II molecule I-E (Ref.[21]). However, in that case the recognition was specific only for the I-E molecule, irrespective of presented peptides, in contrast with peptide-specific αβ TCR-MHC interactions.

1.1.3.2 Unconventional MHC molecules

Apart from classical MHC-I molecules (termed MHC-Ia), both αβ and γδ TCRs can recognise products of MHC-related genes, termed MHC-Ib, with or without bound antigen (**Table 1.1**). In evolutionary terms, MHC-Ib comprise a highly variegated group of molecules but their diversity, in terms of the number of different alleles present in the population, is much more restricted than that of conventional MHC molecules (reviewed by Rodgers and Cook[22]). Structurally, the majority of MHC-Ib consist of a heavy chain non-covalently linked to β2m, and possess a (putative) antigen-binding groove (**Figure 1.3**). Interestingly, some MHC-Ib molecules, such as CD1d and MR1, can be bound by both αβ and γδ TCRs (Refs. [23–25]; and Jamie Rossjohn, personal communication, London 2016), while the others have so far been shown as ligands for only one or the other TCR heterodimer. Certain MHC-Ib molecules, specifically MHC class I chain-related sequence (MIC) A/B, endothelial protein C receptor (EPCR), CD1, and UL16-binding proteins

(ULBPs), can become upregulated during cellular stress or tumorigenesis. The role of these molecules in activating γδ T-cells will be discussed later (**Section 1.2.2**).

Table 1.1 Human MHC-Ib molecules.

HLA, human leukocyte antigen; MR1, major histocompatibility complex class I related 1; MIC, major histocompatibility complex class I-related chain; ULBPs, UL-16 binding proteins; EPCR, endothelial protein C receptor; HFE, human hemochromatosis protein; FcRn, neonatal Fc receptor; ZAG, zinc alpha2 glycoprotein; PIP, prolactin induced protein; ND, not determined; β2m, beta-2 microglobulin.

*readily dissociates, stable as open conformer; #co-complex structure available.

	Ligand	Associates with β2m?	Binds αβ TCRs?	Binds γδ TCRs?
HLA-E	peptide	Yes	Yes#	ND
HLA-F	ND	Yes*	Yes	ND
HLA-G	peptide	Yes	Yes	ND
MR1	metabolite	Yes	Yes#	ND
MICA/B	-	No	ND	Yes
ULBPs	-	No	ND	Yes
EPCR	lipid, protein C	No	ND	Yes
CD1a	lipid	Yes	Yes#	ND
CD1b	lipid	Yes	Yes	ND
CD1c	lipid	Yes	Yes	Yes
CD1d	lipid	Yes	Yes#	Yes#
HFE	transferrin receptor	Yes	ND	ND
FcRn	albumin, IgG	Yes	ND	ND
ZAG	fatty acids, PIP	No	ND	ND

Of note, the mouse MHC-Ib family member T22 has been confirmed as a γδ TCR ligand on a structural level[26]. T22 shows high structural similarity to MHC-Ia; however, it is incapable of presenting peptides in its antigen-binding groove[27]. The crystal structure of G8 TCR in complex with T22 showed that the relatively long CDR3δ loop fitted into the empty antigen-binding groove on T22 (**Figure 1.4**). The majority of the interaction was mediated *via* the germline-encoded residues within CDR3δ (W…EGYEL motif) while the hypervariable residues only modulated the affinity[28,29]. As a result of this semi-invariant mode of recognition, T22-reactive γδ T-cells constitute a significant proportion of murine γδ T-cells (0.2-2% of splenic γδ T-cells)[30]. However, the exact physiological relevance of T22 recognition remains elusive. Importantly, there is no human orthologue of T22, and the mode of target recognition based exclusively on germline-encoded residues within CDR3 has not been observed in case of human γδ T-cells.

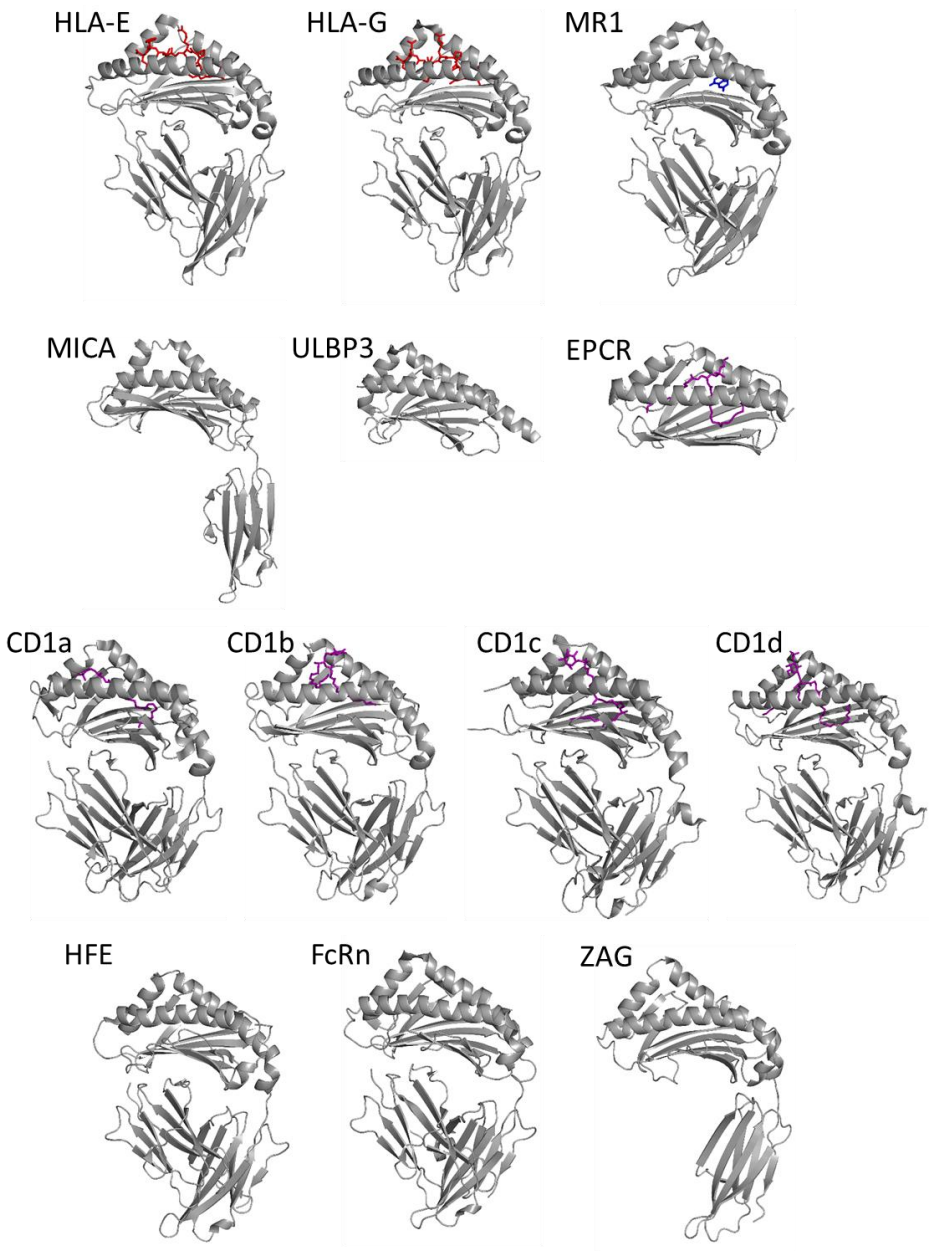

Figure 1.3 The structures of human MHC-Ib molecules. Similar to MHC-Ia, the heavy chain of MHC-Ib molecules is composed of α1 and α2 domains which form the (putative) antigen binding and presentation platform (three α-helices surrounding a β-sheet platform), and α3 domain which is then linked to the plasma membrane. In some cases the heavy chain forms a non-covalent complex with β-2-microglobulin. MHC-Ib can present peptides (depicted in red), metabolites (depicted in blue) and lipids (depicted in purple). For ULBP3 and EPCR, only the platform is shown, due to the availability of structural data. For clarity of the picture, proteinaceous ligands of HFE, FcRn and ZAG were not depicted. HLA, human leukocyte antigen; MR1, major histocompatibility complex class I related 1; MIC, major histocompatibility complex class I-related chain; ULBPs, UL-16 binding proteins; EPCR, endothelial protein C receptor; HFE, human hemochromatosis protein; FcRn, neonatal Fc receptor; ZAG, zinc alpha2 glycoprotein. Protein DataBank (PDB) IDs: HLA-E (3BZE), HLA-G (1YDP), MR1 (5D7I), MICA (1HYR), ULBP3 (1KCG), EPCR (1LQV), CD1a (4X6C), CD1b (1GPZ), CD1c (3OV6), CD1d (4MNG), HFE (1DE4), FcRn (4N0F), ZAG (1ZAG).

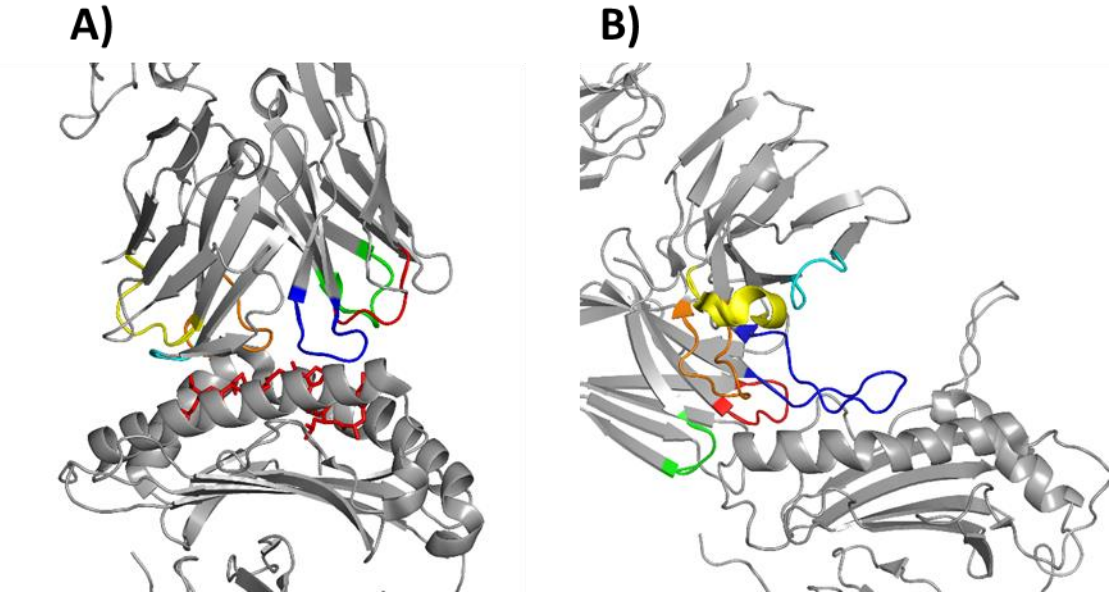

Figure 1.4 Comparison of the docking mode of a conventional αβ TCR onto peptide-MHC I *versus* mouse γδ TCR (G8) onto MHC-Ib molecule T22. αβ TCR docks orthogonally onto the peptide-MHC complex (**A**), with the majority of the TCR-peptide contacts being mediated *via* CDR3α and CDR3β loops (coloured blue and orange, respectively). The peptide presentation platform of the MHC molecule is mostly contacted by CDR1 and CDR2 loops. Conversely, the G8 TCR binds T22 at a more tilted angle (**B**), with CDR3δ loop (blue) filling in the empty groove on T22, and no major binding contributions from the TCR-γ chain. PDB IDs: αβ TCR-pMHC (5EU6), G8-T22 (1YPZ).

1.1.3.3 Non-MHC ligands

While nearly all αβ T-cells, regardless of tissue localisation, are restricted to MHC molecules, be they conventional or non-conventional, a small proportion of αβ TCRs have been shown to bind non-MHC targets, such as self-proteins[31,32,33] or haptens[34]. It should be noted, however, that the αβ TCR-non-MHC interactions have been observed in absence of thymic selection or in pathological settings, and remain mostly anecdotal rather than generic.

Unsurprisingly, γδ T-cells can recognise a variety of non-MHC molecules, including a microbial molecule phycoerythrin[35], haptens[36] and self-proteins [insulin-derived peptides[37], tRNA synthetases[38], MutS homologue 2 (Ref.[39])]. Notably, the majority of peripheral blood T-cells can mount a response to small metabolites from the isoprenoid synthesis pathway (termed phosphoantigens), possibly indirectly - through other proteins, such as butyrophilin 3A1[40,41] and/or F1-ATPase[42]. Since recognition of some of these targets can be a form of γδ T-cell mediated tumour surveillance, the putative mechanisms of recognition will be discussed in later sections.

1.1.4 Diversity of T-cell receptor repertoires

As discussed above, TCR heterodimers are generated in the thymus as a result of V(D)J recombination giving rise to an extremely diverse TCR repertoire. TCR diversity is a prerequisite of an efficient adaptive immune response, and lack thereof invariably leads to higher susceptibility to infections[43]. TCR repertoire diversity, however, is not achieved in a completely stochastic manner but is rather tightly controlled at every stage of T-cell development. For example, the composition of the pre-selection thymic repertoire is strongly dependent on genetic and epigenetic mechanisms, irrespective of the *mhc* haplotype (reviewed elsewhere[44]). Subsequently, thymic selection narrows down the repertoire of αβ TCRs based on the landscape of the presented antigens – which in turn is affected by the polymorphisms in the antigen processing and presentation machinery[45,46]. The resulting repertoire is then shaped in the periphery based on antigen exposure and clonal fitness.

Recent advances in high-throughput sequencing have made it possible to systematically investigate the composition of TCR repertoires in physiological and pathological settings, providing a potent statistical descriptor of T-cell homeostatic maintenance and response to disease. The highest directly measured diversity so far was observed by sampling the entirety of human thymus, showing that the pre-selection diversity of TCR-α exceeded that of TCR-β (up to 100×10^6 unique TCRα sequences and up to 70×10^6 unique TCR-β sequences)[47]. This repertoire, however, was very dynamic due to extensive clonal deletions and generation of different clones at different time points, leading to significant decrease of, in particular, TCR-α diversity in the periphery. As the thymus undergoes involution with age, the diversity of the naïve repertoire is intuitively expected to shrink, thus contributing to reduced immune competence in the elderly. In contrast, a study by Qi *et al.* suggested that even though the naïve TCR repertoire in the elderly undergoes some contraction, it remains nevertheless highly diverse, maintained by homeostatic proliferation[48]. Thus, the reason behind the impaired immune response related to aging lies, as Qi *et al.* proposed, in skewing of the clonal distribution.

The amino acid sequence of the CDR3 loops of TCRs is responsible, in most cases, for the antigen specificity. However, at the present moment it is impossible to predict that specificity based on the primary TCR sequence. That being said, TCR repertoires of T-cell subsets engaging structurally distinct antigens show significant differences. For example, TCR-β sequences from $CD8^+$ (specific for MHC-I) and $CD4^+$ (specific for MHC-II) T-cells showed very little overlap (1% or less), as well as statistically disparate preferences for amino acid composition of CDR3 loops[49]. Furthermore, self-reactive T-cells are characterised by CDR3β loops enriched in hydrophobic

amino acids at positions 6 and 7 (Ref. [50]). TCR repertoire, therefore, can be used as a predictor of susceptibility to autoimmune diseases, even before the onset of clinical presentation (discussed extensively in [51]).

Moreover, T-cell derived lymphoid malignancies result in oligo- or even monoclonal expansions, and therefore lead to TCR repertoire skewing. Deep sequencing of TCR repertoires in cutaneous T-cell lymphoma, for example, demonstrated that patients with TCR repertoires highly dominated by a monoclonal TCR population suffered from more severe clinical manifestation of disease that patients with less clonally focused repertoire[52]. Therefore, estimation of the TCR repertoire can enable improved patient stratification. Finally, numerous studies have addressed the question of the composition of TCR repertoires in cancer patients, in particular comparing the peripheral blood repertoire with the tumour-infiltrating one. A study conducted by my colleagues and myself demonstrated that tumour-reactive clonotypes present in the tumour infiltrating lymphocyte (TIL) products persist in the periphery of complete remission patients for months after adoptive cell transfer, potentially protecting against cancer recurrence[53]. Other groups demonstrated that TCR repertoire signature in the peripheral blood could be a predictor of TCR composition in the tumour, and as such be used to monitor the responsiveness to therapy[54,55]. High throughput sequencing of antigen-specific T-cells can also be a source of therapeutically relevant TCRs, providing an alternative to low-throughput and time consuming clonal derivation and characterisation[56]. Recent advances in single cell sequencing technologies, such as Drop-seq which enables simultaneous recovery of paired TCR sequences, are envisaged to facilitate even further the derivation of TCRs for cancer therapy[57].

While the TCR repertoires of αβ T-cells have been extensively characterised in diverse settings, comprehensive descriptions of γδ TCR repertoires are only starting to emerge. Antibody staining and low-throughput TCR clonotyping showed that the peripheral blood TCR-γ repertoire in human is highly enriched in TRGV9-TRGJP rearrangement, paired with TCR-δ chains expressing TRDV2 segment. This repertoire skewing is believed to be a consequence of a post-natal microbial exposure and (super)antigen-driven expansion of that T-cell subset. However, a study by Vermijlen and colleagues indicated that even the foetal repertoire as early as 23rd week of gestation is dominated by a public, germline-encoded TRGV9-TRGJP sequence (CALWEVQELGKKIKVF)[58]. Since no particular preference for Vγ9Vδ2 TCRs can be observed in human thymocytes[59], dominance of foetal repertoire by an invariant TCR-γ chain could be a result of a positive selection in the foetus in preparation for microbial exposure after birth. Conversely, congenital infection with cytomegalovirus (CMV) induces expansion and differentiation of Vδ1^{+} T-cells, and more importantly, of a public Vγ8Vδ1 TCR (CDR3γ: CATWDTTGWFKIF, CDR3δ: CALGELGDDKLIF)[60]. The T-cell clones bearing the public TCR could

recognise CMV-infected cells in a TCR-dependent manner, thus offering some antiviral protection *in utero*. However, the ligand for that public TCR remains unknown. Another example comes from an acute lymphoblastic leukaemia patient treated with donor lymphocyte infusion where donor-derived Vδ4$^+$ T-cell clones showed persistence and clonal expansion, plausibly in response to recipient's leukemic cells[61]. Finally, of all eight possible TRDV segments, two segments, TRDV1 and TRDV2, substantially dominate the human repertoire, again hinting at a potential for positive selection[62].

Similar to αβ T-cells, the diversity of peripheral γδ TCR repertoire was shown to decrease with age, resulting from a substantial skewing towards oligoclonality[63]. In line with these findings, the absolute number of γδ T-cells as well as the frequency of Vδ2$^+$ cells was found to be decreased in the elderly population when compared to a young cohort[64]. Moreover, cytomegalovirus (CMV) seropositivity leads to inflation of the Vδ1$^+$ compartment in the elderly, similar to αβ T-cells[65]. Finally, Vγ9Vδ2-dominated T-cell repertoire can be *de novo* reconstituted in immunocompromised individuals (e.g. as a result of HIV infection[66]), indicating yet again that extrathymic factors play a major role in generation and maintenance of human γδ T-cell repertoires.

Two recent studies described the composition of human peripheral γδ TCR repertoire in a high throughput manner. Davey *et al.* showed that the Vδ1$^+$ TCR repertoires were highly private, resulting from unlikely recombination events (*i.e.* requiring addition of multiple non-template nucleotides), contrary to more public Vγ9Vδ2 TCR repertoires. Moreover, the initial Vδ1$^+$ TCR repertoire in the neonates was shown to be highly diverse, without any apparent clonal dominance, while in some adults the Vδ1$^+$ TCR repertoire showed indication of clonal expansion, and effector memory phenotype of the expanded clonotypes – in contrast with the naïve phenotype of non-expanded clonotypes[67]. While such clonal expansion and acquisition of a memory phenotype is reminiscent of the antigen-induced adaptive response of αβ T-cells, the putative antigens driving the expansion of selected Vδ1 clonotypes remain opaque. In another study, Ravens *et al.* showed that CMV reactivation in allogeneic haematopoietic stem cell transplant patients induced strong clonal proliferation of several (private) γδ T-cell clonotypes which dominated the *de novo* reconstituted TCR repertoire, thus demonstrating a very textbook example of an antiviral adaptive immune response[68]. Taken together, those two high throughput TCR repertoire studies clearly indicate the adaptive nature of human γδ T-cells, in particular T-cells belonging to the non-Vγ9Vδ2 compartment.

1.2 Recognition of cancer antigens by γδ T-cells and γδ TCRs

As mentioned above, γδ T-cells are an important component of adaptive immune system. γδ T-cells can play both a protective (in case of infectious diseases of viral and bacterial origin), as well as a detrimental role (in case of autoimmune diseases) in vertebrate physiology. Description of all aspects of γδ T-cell biology is however beyond the scope of this Introduction, and has been amply discussed elsewhere[69,70]. Here I will focus on the anticancer role performed by γδ T-cells, especially in human. Indeed, γδ T-cells play a non-redundant function in cancer immunosurveilance within epithelial tissues, as demonstrated in the seminal paper by Hayday and colleagues[71]. The delineations of exact mechanisms of cancer cell recognition by γδ T-cells, in particular on the structural and molecular level of γδ TCR:cognate ligand interactions, have only recently begun to emerge. I will therefore present evidence indicating that γδ T-cells are capable of targeting cancer through a number of different ligands, most of which belong to MHC-Ib family, in particular within a broader cellular stress context (summarised in **Figure 1.5**). Finally, I will discuss the potential methods for re-targeting γδ T-cells to cancers.

1.2.1 Sensing of metabolic intermediates

One of the earliest identified activators of human γδ T-cells were small molecular weight compounds derived from mycobacterial lysates[72]. These mycobacterial lysates retained their ability to stimulate γδ T-cells irrespective of protease treatment while being sensitive to phosphatase treatment, giving the first indications about the non-proteinaceous nature of these antigens – in contrast with their capability of stimulating αβ T-cells. Subsequent studies demonstrated that Vγ9Vδ2 T-cell clones that mediated a response to mycobacterial lysates could also recognise some cancer cell lines, such as the Burkitt's lymphoma line, Daudi, thus indicating that the mechanism of recognition (and the nature of the ligand) was highly similar in both cases[73]. Tanaka *et al.* showed that the naturally occurring compounds responsible for Vγ9Vδ2 T-cell activation were metabolic intermediates of polyisoprenoid synthesis pathways[74]. In case of human cells, the identified compound was isopentenyl pyrophosphate (IPP), a substrate of the mevalonate pathway, while the microbial-derived antigen was (E)-4-hydroxy-3-methyl-but-2-enyl pyrophosphate (HMBPP), an intermediate of the non-mevalonate pathway. Collectively, these compounds are termed "phosphoantigens" (PAgs hereafter).

HMBPP is a non-redundant metabolic substrate for the *Mycobacterium* genus and other pathogenic bacteria[75], as well as malaria-causing protozoans[76]. As it is not produced by a human host, HMBPP can act as a metabolic indicator of infection, and induces a strong response of peripheral Vγ9Vδ2 T-cells. On the contrary, IPP is an intermediate of host's own metabolism.

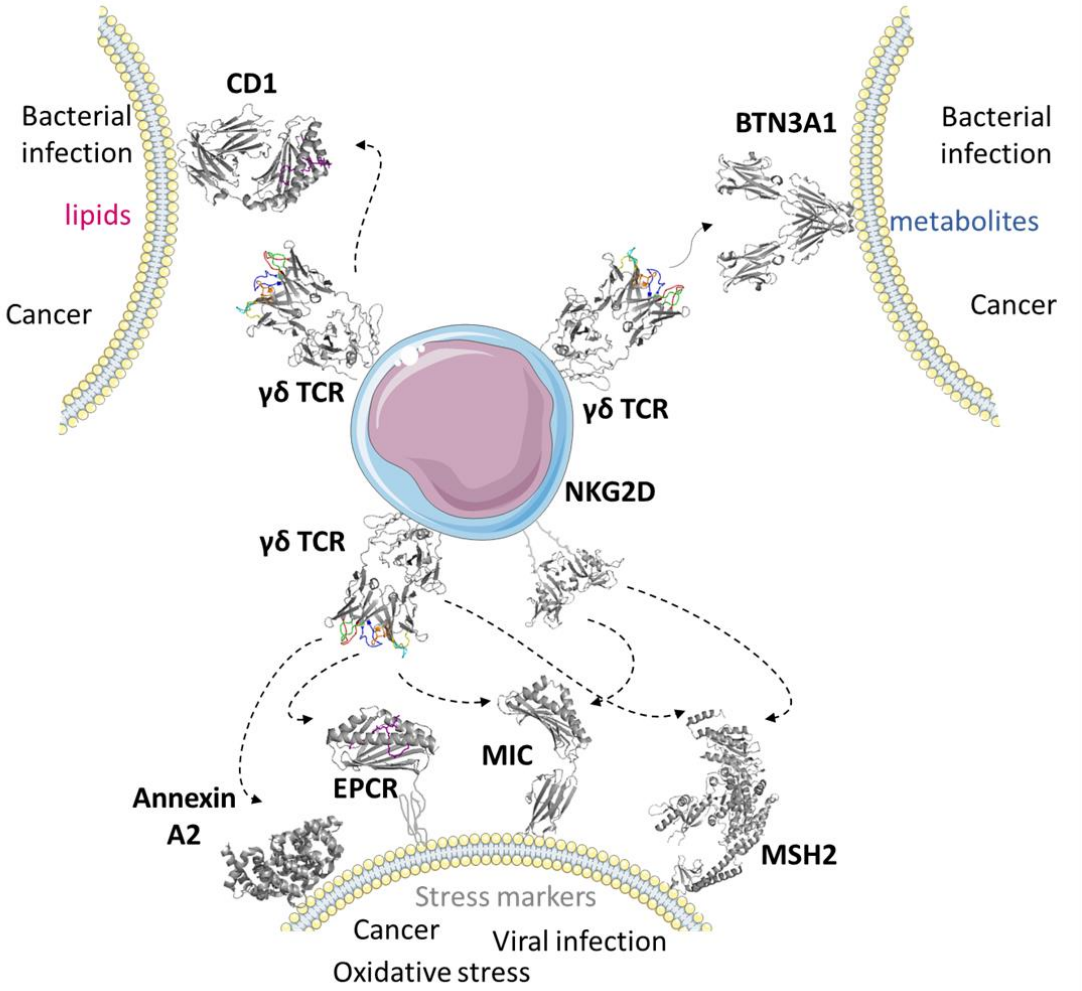

Figure 1.5 Overview of the major ligands of human γδ TCRs, in particular in context of cancer. The ligands of γδ TCRs, confirmed by structural and/or biophysical studies, encompass MHC-Ib molecules such as CD1 (in particular CD1d), EPCR and MICA/B, as well as MHC-like molecule BTN3A1 (putative ligand), and MHC-unrelated MSH2 and annexin A2. CD1 can present diverse lipids to γδ T-cells, including self-derived, bacterial and cancer-specific lipids. In a similar manner, binding of a bacterial (or endogenous) metabolite by BTN3A1 induces a conformational shift of the molecule, and results in TCR signalling (although the exact TCR ligand has yet to be identified). Finally, cellular stress (in particularly caused by viral infection or cancer) leads to upregulation of EPCR, MICA/B, ULBPs (not shown), MSH2 or annexin A2, and thus the cell can be recognised by γδ T-cells. Some of the stress markers (MICA/B, ULBPs, MSH2) are also ligands for another immunoreceptor, NKG2D. Therefore, NKG2D can contribute to TCR-mediated stress sensing by providing a co-stimulatory signal. Detailed description can be found in the main body of the text. EPCR, endothelial protein C receptor; MIC, major histocompatibility complex class I-related chain; BTN3A1, butyrophilin 3A1; MSH2, MutS homologue 2; ULBPs, UL-16 binding proteins; NKG2D, natural-killer group 2, member D. PDB IDs: MICA (1HYR), EPCR (1LQV), CD1d (4MNG), MSH2 (2O8E), γδ TCR (4MNG), NKG2D (1HYR), annexin A2 (2HYW).

However, excessive intracellular accumulation of IPP (and resulting activation of γδ T-cells) can result from dysregulation of the cellular metabolism which often accompanies tumorigenesis[77]. As expected, IPP is a less potent stimulator, by several orders of magnitude, than HMBPP – thus allowing Vγ9Vδ2 T-cells to perform immunosurveillance in cases of significant metabolic dysregulation while preventing harmful autoreactivity due to activation by physiological levels of IPP.

Since IPP is an intermediate of an endogenous metabolic pathway, its levels in the cells can be subject to pharmacological manipulation. For instance, a group of drugs named aminobisphosphonates (NBPs), such as zoledronate, risedronate or pamidronate, inhibit farnesyl diphosphate synthase (FPPS), and therefore lead to T-cell stimulation *via* intracellular IPP accumulation (**Figure 1.6**)[78]. Alkylamines show a similar inhibitory effect on FPPS, although with lower potency than NBPs[79]. Furthermore, phosphoantigens can be chemically modified to increase their potency and/or stability[80,81]. Conversely, it is not surprising that the inhibition of mevalonate pathway upstream of IPP abrogates activation of Vγ9Vδ2 T-cells[82]. Such inhibition can be achieved using statins (*e.g.* mevastatin) which target HMG-CoA reductase. The application of phosphoantigen-modulating compounds for potentiation of cancer immunotherapy will be discussed in later sections.

Despite decades of investigation, only recently has the exact molecular mechanism of phosphoantigen recognition begun unravelling. As the attempts to show a direct, charge-dependent interactions between a TCR and PAgs have failed[83], the existence of a putative cell-surface antigen presenting molecule was proposed. Indeed, my group showed that PAg recognition is dependent on cell-cell contact, and that the presenting cell needs to be of human (rather than rodent) origin[84]. Virtually any nucleated human cells could present PAgs to Vγ9Vδ2 T-cells, indicating the ubiquitous nature of the presenting molecule, and raising questions about how the recognition is regulated.

1.2.1.1 Antigen presenting molecules for phosphoantigens

Scotet *et al.* demonstrated that a Vγ9Vδ2 TCR could bind a mitochondrial protein, F1-ATPase, with μM affinity[42]. F1-ATPase could become ectopically expressed on tumour cells, and subsequently bind its natural ligand apolipoprotein A-I, thus potentiating T-cell activation. Interestingly, the Vγ9Vδ2 TCR tested showed also a μM affinity towards apolipoprotein A-I alone. Further research from the Champagne group indicated that PAg recognition may indeed occur on the cell surface, with IPP binding to F1-ATPase as a nucleotide derivative[85].

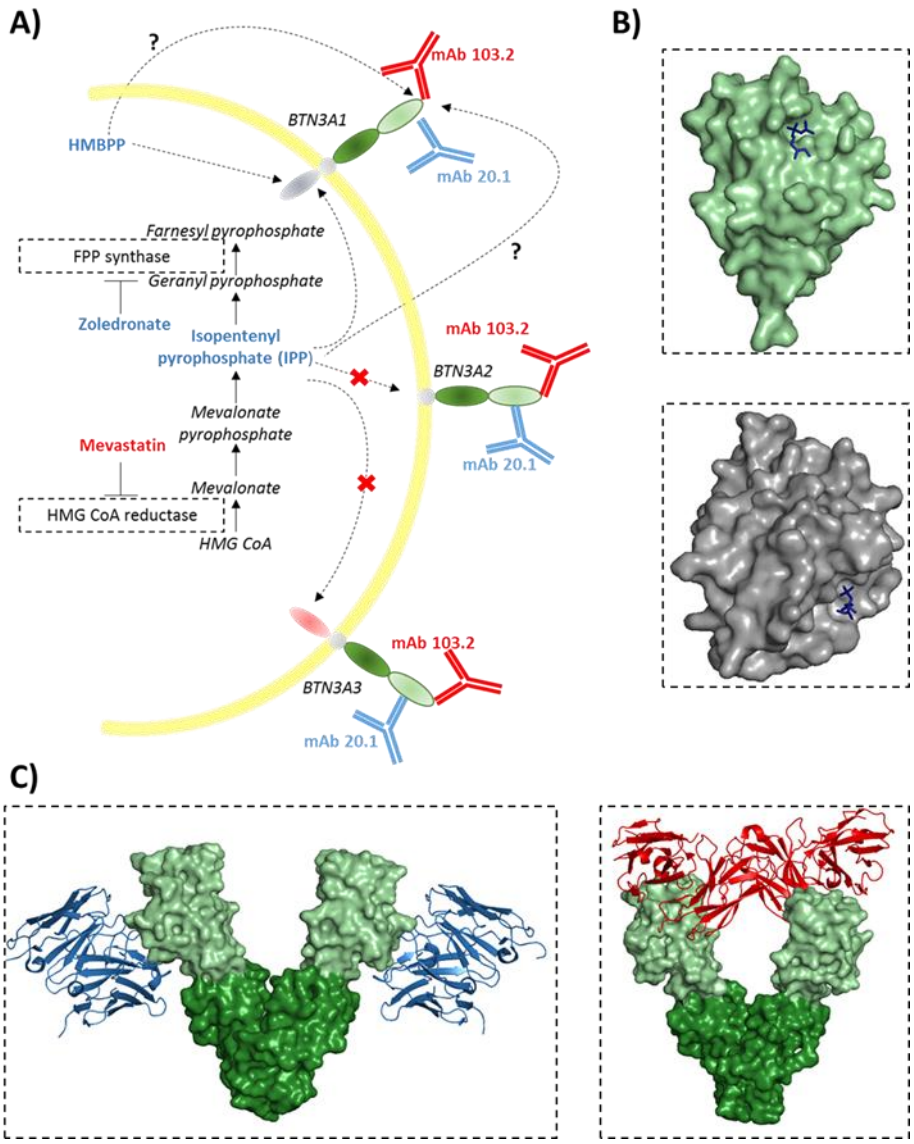

Figure 1.6 Phosphoantigen presentation pathway. (**A**) Schematic representation of the putative phosphoantigen presentation pathways in human cells. Small molecules [zoledronate, (E)-4-hydroxy-3-methyl-but-2-enyl pyrophosphate (HMBPP), isopentenyl pyrophosphate (IPP)] or macromolecules (mAb 20.1) known to stimulate Vγ9Vδ2^{+} T-cells are depicted in blue, while inhibitors of phosphoantigen recognition (mevastatin, mAb 103.2) are shown in red. The mechanism of phosphoantigen transport across plasma membrane remains unresolved. Two putative structures of phosphoantigen binding by butyrophilin(BTN)-3A1 molecule are depicted in **B** (upper – phosphoantigen bound in the extracellular IgV domain of BTN3A1, lower – phosphoantigen bound in the intracellular B30.2 domain). (**C**) mAb 20.1 and mAb 103.2 bind different epitopes on BTN3 (left and right, respectively), thus stabilising an activating or non-activating conformation, respectively. For the clarity of the figure, BTN3 molecules are represented as monomers in (A). Only the BTN3A1 isoform is capable of Vγ9Vδ2^{+} T-cell stimulation in response to phosphoantigen accumulation. Detailed description can be found in the main body of the text. PDB IDs: panel B, upper (4K55), panel B, lower (4N7U), panel C, left (4F9L), panel C, right (4F9P).

However, the vast body of literature supports the concept that another molecule, belonging to butyrophilin family, is crucial for phosphoantigen presentation to human Vγ9Vδ2 T-cells. Butyrophilins are single-pass transmembrane proteins composed of two Ig-like extracellular domains V and C, and in some cases an intracellular B30.2 domain. Butyrophilins are located within the MHC-I locus on human chromosome 6, and belong to B7 superfamily of receptors, many of which play an important role in co-stimulating or co-inhibiting T-cell response[86]. Moreover, members of BTN3 family (BTN3A1, BTN3A2 and BTN3A3, known also as CD277 isoforms) show high sequence similarity to the extracellular domain of Skint-1, the only known molecule required for positive selection of murine γδ T-cells. However, no direct orthologues of BTN3 can be found in rodents, in line with the fact that these animals lack γδ T-cell subsets that mount a response to phosphoantigens. Indeed, genes encoding BTN3, and Vγ9 and Vδ2 TCR domains seem to have co-evolved together, and are present predominantly, although not exclusively, in primates[87].

A study by Vavassori *et al.* elegantly showed, using mouse-human hybrid cell lines bearing different parts of human chromosomes to avoid biased assumptions, that the antigen presenting molecule required for phosphoantigen stimulation of Vγ9Vδ2 T-cells is located on chromosome 6, and then narrowed it down to BTN3A1 isoform[40]. Indeed, the role of BTN3A1 in stimulating T-cells has been confirmed by numerous groups[88,89,90]. For instance, an antibody raised against the extracellular domain of BTN3, termed 20.1, induced a robust Vγ9Vδ2 T-cell response (but no response from other γδ T-cells or αβ T-cells) even without exogenously supplied phosphoantigens, while another α-BTN3 antibody, 103.2, abrogated the T-cell response to phosphoantigens[89]. This phenomenon was addressed by solving crystal structures of BTN3 bound either by 20.1 or 103.2 antibody[91]. BTN3 was shown to exist as a dimer, with two possible conformations – either V-shaped and rising above the cell membrane (Dimer 1) or head-to-tail dimer lying flat on the cell surface (Dimer 2). Indeed, antibody 20.1 bound from the side of BTN3 V domain, enforcing the Dimer 1 conformation and crosslinking the dimers, while antibody 103.2 bound BTN3 from the top (**Figure 1.6**). The physiological existence of these dimers, as well as phosphoantigen-mediated conformational shift into Dimer 1 state has only recently been confirmed[92].

The exact mechanism linking phosphoantigens to T-cell activation *via* BTN3A1 remains controversial[93,94]. De Libero and colleagues proposed that phosphoantigens bind in a shallow pocket within the extracellular domain of BTN3A1 and are thus presented to γδ T-cells in a manner similar to peptide-MHC presentation[40]. In stark contrast, Sandstrom *et al.* showed that phosphoantigens are bound in the intracellular B30.2 domain, and that binding event translates into the extracellular conformational change, and subsequent T-cell stimulation[41]. Indeed, only

the B30.2 domain from BTN3A1 isoform contains a positively charged pocket that can bind a negatively charged pyrophosphate group, and charge-reversal mutations in that pocket abrogate the stimulatory capacity of phosphoantigens. BTN3A2 lacks B30.2 domain while BTN3A3 contains an arginine instead of histidine in the B30.2 binding pocket which prevents phosphoantigen association *via* steric hindrance – thus explaining why only BTN3A1 is capable of activating γδ T-cells. Recent research demonstrated that while the B30.2 domain is capable of binding various small molecules endowed with a negative charge, only phosphoantigens could induce a conformational shift in the B30.2 which then plausibly translated to conformational changes in the whole molecule[95]. Finally, the affinity of HMBPP towards B30.2 exceeds that of IPP by several orders of magnitude, thus explaining the difference in stimulatory potency between the two compounds[41].

Nevertheless, BTN3A1 alone is not sufficient for inducing phosphoantigen-mediated activation of T-cells when rodent cells are used for antigen presentation. A study by Herrmann and colleagues indicated that additional genes located on human chromosome 6 were required for efficient T-cell activation[96]. Whether the products of these genes act as a direct binding partner for Vγ9Vδ2 TCRs, or play a role in phosphoantigen transport and loading, remains unknown despite extensive investigations. Discovery of an actual TCR ligand, especially coupled with a crystal structure of the co-complex, would be of great interest. A co-complex structure between a Vγ9Vδ2 and its cognate ligand could pave way for design of high affinity γδ TCRs which then could serve as a pan-population immunotherapeutic, surpassing high affinity αβ TCRs[97]. While the TCR ligand has yet to be discovered, diverse components of phosphoantigen sensing machinery, such as cytoskeletal adaptor periplakin[98] and small GTPase RhoB[92], have been uncovered. It is therefore not unconceivable that the phosphoantigen presentation pathway could rival that of peptide-MHC in terms of complexity.

Finally, the models of target recognition by Vγ9Vδ2 T-cells (direct binding to F1-ATPase or BTN3A1 in complex with phosphoantigens, or binding to a molecule recruited by a conformational shift of BTN3A1) need not be mutually exclusive but rather dependent on the TCR studied. It is possible that all three putative ligands raise a response from different Vγ9Vδ2 TCR repertoires – a question that could be addressed only recently, thanks to the advances in high throughput sequencing.

1.2.2 Recognition of MHC-Ib molecules

1.2.2.1 CD1 molecules present lipids to γδ T-cells

In human, there are four CD1 family members (CD1a-d) that are capable of presenting lipid antigens to T-cells, in association with β2-microglobulin. CD1 molecules are not ubiquitously expressed but rather restricted to professional antigen-presenting or epithelial cells. The fifth CD1 family member, CD1e, is expressed in the intracellular compartments and plays a role in loading of lipids into other CD1 isoforms but does not present lipids at the cell surface[99]. CD1 family members CD1a-d differ in terms of lipid antigens they can present, the mode of presentation, and the subsets of αβ T-cells they stimulate (recently reviewed by Attaf *et al.*[20]). More importantly, all four surface expressed CD1 family members have been reported to stimulate human tissue-resident γδ T-cells, by presenting either natural or synthetic phospholipids[100].

CD1c can present diverse lipids endowed with a polar headgroup, such as bacterial phosphomycoketides[101], cancer-derived methyl-lysophosphatidic acids[102], as well as undefined self-lipids[103]. Initial research established that CD1c restriction was a common occurrence among tissue-specific γδ T-cells, and occurred even in absence of exogenous (i.e. bacterial or synthetic) lipids[104,105]. Recognition of CD1c was TCR-mediated, and all CD1c-reactive γδ T-cell clones expressed a Vδ1 TCR chain. However, only recently has it become possible to study γδ T-cell response to CD1c in a more systematic manner, by using CD1c tetramers to pull out antigen-specific T-cells from the peripheral blood[106]. As shown before, all CD1c-specific T-cells expressed a Vδ1 TCR chain but differed in Vγ usage. In fact, Vγ segments differentially modulated the affinity towards CD1c loaded with different lipids, showing that in case of some TCRs, TCR-γ contacts must play an important role in ligand discrimination. However, more detailed analysis of the molecular and genetic basis of CD1c recognition awaits resolution of a co-complex crystal structures and high-throughput repertoire studies of antigen-specific populations.

To date, the best studied antigens presented by CD1d are self-derived lipids called sulphatides (sulphated galactosylceramides), and αGalCer. The latter was initially derived from a marine sponge and is used as a model antigen; however, recent research demonstrated that αGalCer can also be a product of mammalian metabolism, and plays a role in regulating the immune response[107]. CD1d is also capable of presenting tumour-restricted lipids[108] and its expression can be a prognostic marker in leukaemia[109], thus highlighting the emerging role of that antigen-presenting molecule as a target for cancer immunotherapy. While CD1d-lipid complexes have been mostly studied in context of recognition by semi-invariant αβ T-cells called invariant

natural killer (iNK) T-cells, recent evidence makes a compelling case for CD1d restriction of a subset of γδ T-cells. Adams and colleagues solved the crystal structure of CD1d-sulphatide bound by a Vγ4Vδ1 TCR[24] while Uldrich *et al.* described the complex between CD1d-αGalCer and a Vγ5Vδ1 TCR[110]. Both structures showed a striking difference in terms of the mode of TCR recognition (**Figure 1.7**). In case of CD1d-sulphatide, the recognition was mediated exclusively *via* the TCR-δ chain – CD1d was contacted mostly by germline-encoded residues from CDR1δ and CDR2δ while sulphatide was bound by the hypervariable CDR3δ loop, in particular by P/N nucleotide-encoded amino acids[24]. Conversely, the interactions between CD1d-αGalCer and Vγ5Vδ1 TCR were mediated by both TCR chains, with TCR-δ contacting CD1d *via* the germline-encoded residues while the lipid cargo was recognised by the hypervariable CDR3γ loop[110]. Indeed, the majority of peripheral blood γδ T-cells that are reactive to CD1d express a Vδ1 TCR, arguing for the germline-encoded recognition of the antigen-presenting molecule[111]. Notably, a structure of a hybrid TCR (δ/αβ) complexed with CD1d-αGalCer has recently been reported[7]. The TCR was composed of the Vδ1 segment that recombined with a Jα segment (a recombination event made possible due to the fact that *trd* locus is present within *tra* locus), followed by splicing with the Cα segment and conventional pairing with a TCR-β chain. As before, the interactions with CD1d were mediated through the germline-encoded Vδ1 residues while the lipid was contacted exclusively by TCR-β. The affinity of this interaction was higher than either Vγ4Vδ1 TCR:CD1d-sulphatide or Vγ5Vδ1 TCR:CD1d-αGalCer, or even type I NK T-cell derived TCR:CD1d-αGalCer[112,113] (**Table 1.2**). Most importantly, such hybrid δ/αβ TCRs are more than just an anecdotal aberration; in fact, they can constitute a major portion of human CD1d-αGalCer reactive T-cells[7].

The two modes of CD1d-lipid recognition by γδ TCRs, albeit different, highlight the importance of the Vδ1 chain in binding the non-polymorphic antigen-presenting molecule (CD1d) while lipids are bound by the non-germline encoded residues. These binding modes allow speculation that γδ TCRs could potentially discriminate between different lipid antigens, and that the mode of target recognition is adaptive, rather than semi-invariant and innate-like.

Table 1.2 Affinity parameters of TCR:CD1d interactions

iNKT, invariant natural killer T-cell; αGalCer, α-galactosylceramide; K_D, dissociation constant.

TCR	Ligand	K_D [μM]	PDB code	Reference
Vγ4 Vδ1	CD1d-sulphatide	5.6	4MNG	Luoma *et al.* , 2013
Vγ5 Vδ1	CD1d-αGalCer	16	4LHU	Uldrich *et al.*, 2013
Vδ1/Cα Vβ2	CD1d-αGalCer	0.066	4WO4	Pellicci *et al.*, 2014
iNKT TCR	CD1d-αGalCer	0.1	2PO6	Cantu *et al.*, 2003; Borg *et al.*, 2007

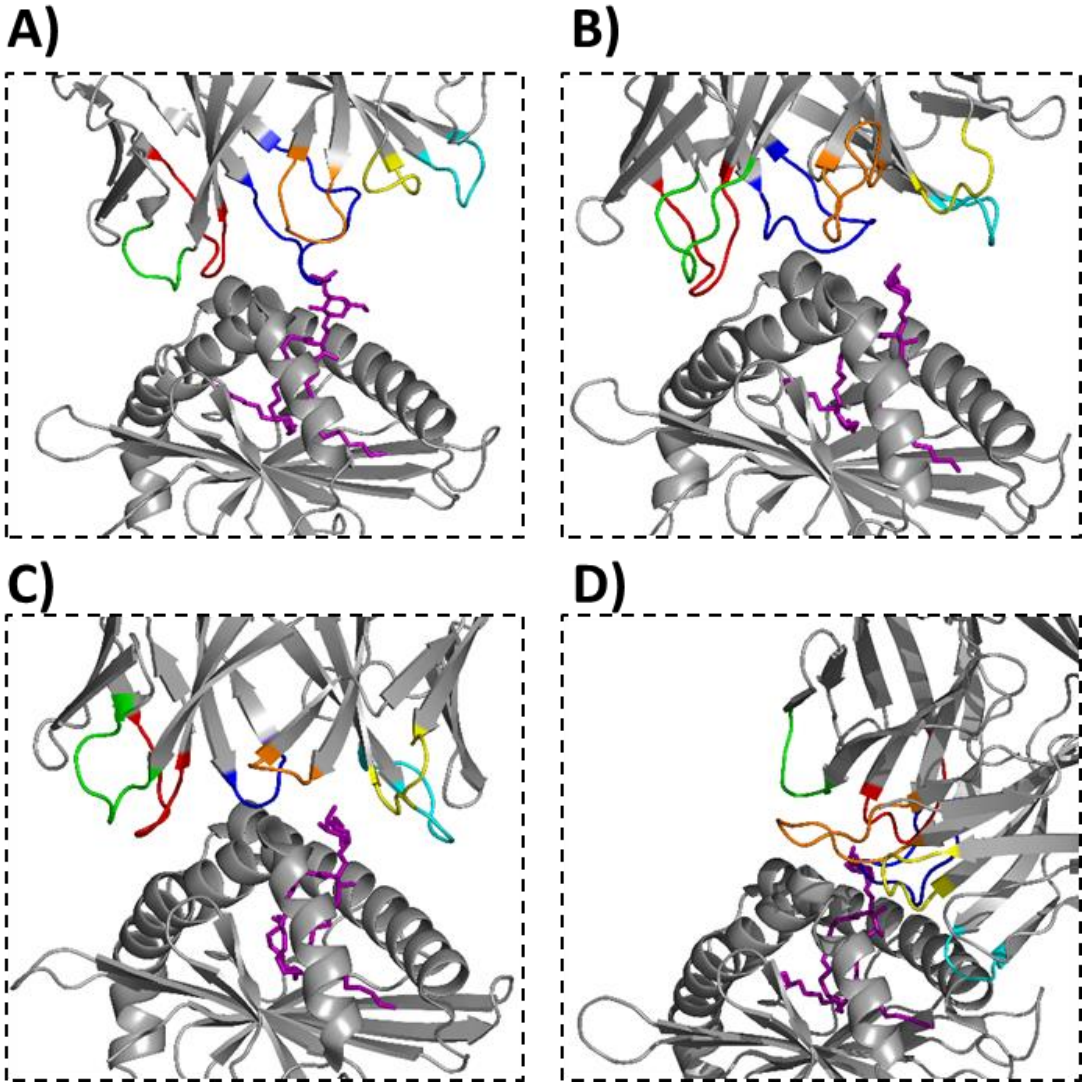

Figure 1.7 Distinct modes of CD1d-lipid complex recognition by TCRs. Recognition of CD1d presenting sulfatide (**A**) or αGalCer (**B**) by γδ TCRs. In brief, the lipid is contacted by hypervariable CDR3 loops while the antigen-presenting molecule in bound by germline-encoded CDR1 and CDR2 (colour-coded). A similar docking mode is observed in case of a hybrid Vδ Jα-Cα TCR (**C**), although the CDR3 loops are much shorter than in case of γδ TCRs. (**D**) Conversely, an invariant natural killer T-cell (iNKT) derived αβ TCR, specific for CD1d-αGalCer, adopts a distinctly different binding mode, contacting CD1d from the side rather than binding in the orthogonal position. Detailed description can be found in the main body of the text. PDB IDs: A (4MNG), B (4LHU), C (4WO4), D (2PO6).

1.2.2.2 EPCR is a shared ligand recognised by tumour- and CMV-specific γδ T-cells

Human CMV is a common pathogen belonging to the *Herpesviridae* family, infecting 50-90% of the population. While asymptomatic in healthy adults, CMV can cause severe morbidity and mortality in immunocompromised individuals and in congenital infections. It has been long known that CMV infection causes expansion of γδ T-cells in the peripheral blood, in particular of the subset that does not express a Vδ2 TCR (termed Vδ2$^-$ T-cells)[114,115]. Such expansion was shown to result in the resolution of the infection[116], as well as in development of a differentiated γδ T-cell subset that could respond to the second CMV challenge in a memory-like manner, again arguing for the adaptive role of γδ T-cells[117]. Furthermore, CMV drives the inflation of highly differentiated Vδ2$^-$ T-cells with age, despite the fact that the overall pool of γδ T-cells is significantly diminished in the elderly[65,118]. One of the notable consequences of maintaining differentiated Vδ2$^-$ T-cells that confer reactivity to CMV is a reduction in susceptibility to cancer. Indeed, Couzi *et al.* showed that kidney transplant patients in whom CMV infection resulted in expansion of γδ T-cells were less likely to develop cancer after transplantation[119]. The reduction of cancer risk conferred by CMV-reactive Vδ2$^-$ T-cells can be explained by the observation that those T-cells could also recognise, and lyse, various epithelial tumours *in vitro*[120] and *in vivo*[121]. Moreover, in patients undergoing allogeneic stem cell transplant, CMV reactivation was associated with reduced risk of leukemic relapse[122]. Again, this phenomenon could be at least partially explained by the fact that CMV reactivation induced selective expansion of γδ T-cells that could directly recognise primary leukemic blasts[123]. Therefore, it has become apparent that CMV infection and malignant transformation could activate an overlapping population of γδ T-cells, possibly though inducing a generic cellular stress signature on target cells. However, to date only one γδ TCR ligand induced both by tumorigenesis and CMV infection has been identified.

Willcox *et al.* demonstrated that endothelial protein C receptor (EPCR) acts as a binding partner for a Vγ4Vδ5 TCR[124]. EPCR shows high sequence and structure similarity to CD1 molecules, and is capable of presenting phospholipids in its antigen-binding groove[125]. Additionally, EPCR expression, or over-expression, has been found to be associated with higher metastatic potential and resistance to apoptosis in different cancer types[126–130], and thus it is not surprising that EPCR is a target for the immune system. In fact, cancer cells can actively shed EPCR, indicating a potential means of immune evasion[131]. The EPCR-reactive Vγ4Vδ5 TCR was isolated from a clone that dominated the peripheral repertoire of a CMV-infected transplant patient (>20% of all peripheral T-cells[132]). The clone could recognise both CMV-infected fibroblasts *in vitro*, as well as a wide panel of cancer cell lines of epithelial origin, in a TCR-dependent manner[120,124]. Generation of blocking antibodies targeting one of the recognised cancer cell lines

led to identification of EPCR as a ligand of the Vγ4Vδ5 TCR, subsequently showing that TCR:EPCR interaction is indispensable for recognition of both CMV-infected and transformed cells. The affinity of the interaction was relatively low ($K_D \approx 90$ μM), and relied on the hypervariable CDR3γ loop. The exact molecular mechanism of the interaction, however, awaits a solution of the co-complex structure. Importantly, EPCR is not a ubiquitous, innate-like target recognised by all CMV and cancer dual-reactive γδ T-cells. In fact, the reactivity of other CMV-reactive clones, even those expressing a Vδ5 TCR, was not abrogated by EPCR blocking antibodies, again arguing for the adaptive nature of γδ T-cell reactivity. Finally, it should be noted that EPCR on its own, even though indispensable for the target recognition, was not sufficient to confer T-cell reactivity to uninfected normal cells (e.g. fibroblasts). Indeed, the reactivity was present only after CMV infection, even though the expression of EPCR remained unchanged by the virus, thus suggesting the productive T-cell activation required an additional co-stimulation, *i.e.* cellular stress context. In accordance with a requirement for an additional costimulatory receptors, transferring of a dual-reactive TCR into T-cell lines conferred reactivity to tumours but not to CMV-infected cells[123,124]. The role of co-stimulatory stress context will be discussed in **Section 1.2.4**.

1.2.2.3 MICA/B are ligands for both TCR and NKG2D

MIC A and B proteins show high structural similarity with MHC-Ia; however, they do not present any antigens in the binding groove, nor do they associate with β2m. MIC proteins have been broadly studied as ligands for an activating NK-type receptor NKG2D[133]. MICA/B exist in the human population in form of over 50 different alleles[134], and the majority of the polymorphisms focus on the membrane distal, α-helical interface where the contact with NKG2D occurs, thus suggesting that the polymorphisms fine tune the binding affinity[135]. A similar interaction is present in rodents, where NKG2D binds an MHC-like family of molecules called RAE-1 (however, RAE-1 homology with MIC is scant)[136]. Other than in NK cells, NKG2D:MIC interaction can deliver a co-stimulatory signal to $CD8^+$ αβ T-cells[137] and γδ T-cells; more importantly, MIC proteins can be a direct ligand for γδ TCRs and act as co-stimulatory molecules at the same time[138]. Indeed, MICA was the first known target expressed by epithelial tumours that were recognised by Vδ1 T-cells[139]. MICA/B appear to be generic markers of cell stress resulting from viral infections[137], oxidative stress[140], DNA damage[141], perturbations in energy metabolism[142], or even chemotherapy[143]. Notably, loss of surface expression of MIC molecules is one of the immune evasion mechanisms employed by tumours[144] or CMV[145].

Even though NKG2D is present in both αβ and γδ T-cells (expressing different Vδ domains), and can play a role in augmenting T-cell activation (discussed in later sections), the direct recognition of MICA/B by γδ TCRs seems to be confined to the Vδ1 subset. Immobilised MICA was found to preferentially expand Vδ1 T-cells[146], and specific binding between MICA and cognate TCRs was confirmed by either staining of MICA/TCR transduced cells with a soluble TCR[147], or multimerised MICA[148], respectively. Despite the availability of crystal structures of MICA[135] and a cognate TCR[138], the crystal structure of a co-complex has yet to be resolved, and thus the molecular mechanism of MICA recognition remains largely a matter of speculation. The kinetic measurements of OTδ1-A5 TCR:MICA interactions indicated that Vδ1 was crucial for binding (with non-germline CDR3δ residues fine tuning the affinity) while the contribution from TCR-γ chain was less important[147]. The affinity of the interaction was relatively high for a self-protein recognition (summarised in **Table 1.3**)[147]. In contrast, Xu *et al.* reported the δ1A/B-3 TCR:MICA binding affinity which was by orders of magnitude weaker than OTδ1-A5 TCR:MICA (**Table 1.3**)[138]. The variability in affinity reported by different studies could reflect differences in the primary TCR and MICA sequences used. Nevertheless, in both cases NKG2D interaction with MICA was stronger than that of a TCR:MICA (**Table 1.3**)[135]. The kinetics of the interactions between MICA and TCR or NKG2D were also found to be strikingly different, with NKG2D binding MICA with fast association and dissociation rates, while TCR binding occurred slower but the resulting complex was less transient than NKG2D:MICA[138]. Taken together with evidence suggesting that TCR and NKG2D bound the same region of MICA in a competitive manner, MICA-mediated recognition of target cells by γδ T-cells was hypothesised to occur in a sequential manner. NKG2D would rapidly scan the cells for the evidence of cellular stress (*i.e.* MIC expression) and, upon encountering it, would give place to a more stable TCR:MICA complex, and the net result would be T-cell activation. Indeed, NKG2D triggering in absence of TCR signalling was insufficient to induce cytotoxicity[149]. The proposed multicomponent mechanism of γδ T-cell activation, a recurrent theme in γδ T-cell recognition of target cells, would therefore prevent robust autoreactivity – especially important since the majority of γδ TCR targets are in essence self-proteins.

Table 1.3 Affinity parameters of TCR/NKG2D:ligand interactions.

NKG2D, natural-killer group 2, member D; MICA, major histocompatibility class I chain-related A; MSH2, MutS homologue 2; K_D, dissociation constant.

receptor	ligand	K_D [μM]	Reference
OTδ1-A5 γδ TCR	MICA*008	2.8	Zhao *et al.*, 2006
δ1A/B−3 γδ TCR	MICA*001	110	Xu *et al.*, 2011
NKG2D	MICA*001	0.3	Li *et al.*, 2001
NKG2D	MSH2	132	Chen *et al.*, 2008

1.2.3 Recognition of ubiquitous stress-associated markers

While the majority of known cancer-associated targets for γδ TCRs belong to MHC-Ib family, the growing body of evidence also suggests that non-MHC molecules that become upregulated or translocated to the cell surface upon cellular stress are also important targets for immunosurveillance. One early example of such cellular stress markers are heat shock proteins, in particular HSP60 and HSP70, which could become overexpressed on cancer cell surface as a result of stress, and subsequently predispose the cells to γδ T-cell mediated lysis[150,151]. Another example of a protein that can become ectopically expressed in certain conditions is human MutS homologue 2 (hMSH2). Under physiological conditions it is restricted to the nucleus, where it constitutes an element of DNA mismatch repair machinery; however, it becomes translocated from the nucleus as a result of cellular stress[152]. hMSH2 has been identified as ligand for γδ T-cells using CDR3δ as a probe, and thus suggesting that the recognition is mediated predominantly *via* TCR-δ (similarly to G8 TCR:T22 interaction)[153]. Ectopic expression of hMSH2 was found on diverse epithelial tumours, as well as on B-cells freshly transformed with EBV, corroborating the role of hMSH2 in cancer surveillance[39]. hMSH2 becomes expressed as a result of oxidative stress and pro-inflammatory cytokines – and both factors are often present in the tumour microenvironment[140]. Interestingly, oxidative stress causes the concomitant expression of MICA/B; moreover, hMSH2 is a ligand for both γδ TCRs and NKG2D (**Table 1.3**), highlighting the similarities between these two indicators of cellular stress. Moreover, UL-16 binding protein 4, expressed by cancer cells and EBV-transformed B-cells, was shown to activate T-cells via both a γδ TCR and NKG2D[154]. Such redundancy in the system, where diverse molecules serve as an indicator of cellular stress and a ligand for distinct immunoreceptors, may counteract immune evasion strategies employed by the tumour.

Finally, a recent study by Marlin *et al.* identified annexin A2 as another ligand of human γδ TCR(s)[155]. Annexin A2 is a phospholipid binding protein normally confined to the cytoplasm but capable of rapid translocation to the extracellular layer of plasma membrane[156]. Annexin A2 expression is upregulated in many cancer cell lines, and can be further enhanced by production of reactive oxygen species[157]. CMV infection was also shown to increase the quantity of annexin A2 on the extracellular layer of plasma membrane[158], indicating that diverse modalities of cellular stress can lead to surface presentation of annexin A2, and subsequent TCR-dependent sensing of cellular stress by γδ T-cell clones. Importantly, annexin A2 induced proliferation of polyclonal T-cell lines derived from healthy donors' peripheral blood, and thus procured annexin A2-reactive γδ T-cell clones expressed diverse Vγ and Vδ TCR segments[155], again arguing for the adaptive rather than innate nature of ligand recognition by γδ T-cells.

1.2.4 Co-stimulatory stress context as a requirement for efficient T-cell activation

The presence of co-receptors has long been established as a requirement for effective engagement of MHC ligands by αβ T-cells. Indeed, co-receptors CD8 and CD4 ensure MHC (class I and class II, respectively) restriction of αβ T-cells from the ontogeny[159]. Furthermore, CD8αβ heterodimer increases the stability of TCR-pMHC-I complex and ensures that CD3ζ becomes fully phosphorylated, thus increasing the sensitivity to the antigen by several orders of magnitude[160–162]. However, the majority of γδ T-cells are CD4/CD8 co-receptor negative, and even in γδ T-cells expressing either (or both) of those co-receptors, the physiological relevance of CD4/CD8 expression remains unclear. It is therefore possible that other molecules act as co-receptors, or provide co-stimulatory signals for γδ TCRs.

In case of EPCR recognition, the putative co-stimulation was provided by adhesion molecules LFA-1 and CD2 binding their ligands CD54 and CD58, respectively, on the target cell[124]. In particular, CD54 became upregulated as a result of CMV infection. However, while EPCR blocking completely abrogated the reactivity, blocking of either LFA-1:CD54 or CD2:CD58 axes merely reduced the activation, indicating that the TCR:ligand contact plays the pre-eminent role in inducing T-cell activation. Furthermore, Kuball and colleagues showed that CD8αα homodimer, preferentially expressed by γδ but not αβ T-cells expanded in CMV infection, is important for target recognition by some, albeit not all, γδ T-cell clones[123]. This differential impact of CD8αα could stem from differences in target specificities or affinities of the cognate TCRs. Notably, CD8αα expression is a feature of epithelium-resident T-cells which constitute the first line antiviral and antibacterial immunity in peripheral tissues[163,164]. CD8αα binds strongly to an MHC-like molecule TL in mice – however, since no human homologue of TL has been identified, the role of CD8αα in T-cell mediated target recognition remains ambiguous[165].

NKG2D, as mentioned before, seems an attractive candidate for a co-stimulatory receptor for γδ T-cells that do not possess a MICA/B-specific TCR. Antibody blocking studies showed that tumour cell recognition by Vγ9Vδ2 T-cells could: 1) predominantly depend on the TCR, 2) depend on both TCR and NKG2D (co-stimulatory scenario), or 3) depend predominantly on NKG2D[166]. The latter scenario raises the possibility of TCR-independent γδ T-cell activation which could have important implications for immunotherapy. In contrast, Yin *et al.* showed that NKG2D engagement alone is not sufficient to trigger cytotoxic activity of γδ T-cells; NKG2D can however synergise with γδ TCR signalling, in a similar manner to signal 1 (TCR) and signal 2 (CD28) in αβ T-cells[149]. Furthermore, NKG2D:MICA axis has been shown to enhance the target recognition of phosphoantigen-specific Vγ9Vδ2 T-cells[167]. The role of NKG2D was, however, more pronounced in absence of any strong TCR stimuli; when the target cells were pulsed with synthetic

phosphoantigens, NKG2D blocking barely affected T-cell activation while TCR blocking fully abrogated the reactivity[168]. Finally, other NK-type receptors such as NKp30 and NKp44 can become expressed on γδ T-cells (in particular on the Vδ1 subset) as a result of *in vitro* expansion conditions[169,170]. Both NK-type receptors were shown to synergise with NKG2D, but not with the cognate TCRs, in inducing cancer cell killing. While their physiological relevance remains to be ascertained, induction of NKp30 and NKp44 on γδ T-cells may prove beneficial in context of cancer immunotherapy.

1.2.5 Targeting γδ T-cells to cancer

γδ are capable of mediating adaptive-like cancer immunosurveillance, as demonstrated by the numerous examples where these lymphocytes recognise cancer cells of diverse origin *via* their cognate TCR (and putative co-stimulatory receptors). However, in some instances cancer cells do not express, or accumulate, the sufficient level of the antigen to induce robust γδ T-cell response. Such immune evasion can be overcome by either pharmacological modulation of tumour metabolism or re-directing T-cells to antigens other than those recognised by the cognate TCRs.

1.2.5.1 Pharmacological modulation of tumour metabolism

The most studied method for increasing tumour recognition by γδ T-cells is induction of intracellular phosphoantigen accumulation by inhibiting FPPS, a key enzyme of mevalonate pathway. This inhibition can be achieved using aminobisphosphonates which are structurally similar to the FPPS substrate, IPP; aminobisphosphonates however competitively bind the ligand-binding pocket of FPPS and induce a conformational change, thus preventing the enzyme from processing IPP[171]. Indeed, aminobisphosphonates have shown promise in preclinical *in vivo* models, delaying the growth of human tumours xenografted in immunodeficient mice, in combination with adoptively transferred Vγ9Vδ2 T-cells[172,173]. A similar approach involves direct activation of γδ T-cells by using synthetic phosphoantigen analogues, such as bromohydrin pyrophosphate (BrHPP/Phosphostim)[80]. Despite the systemic activation and expansion of γδ T-cells induced by BrHPP, no adverse effects were observed in the treated non-human primates[174]. Importantly, BrHPP treatment increased antitumour effect of γδ T-cells *in vivo*, in particular when combined with therapeutic antibodies[175]. However, it should be noted that repeated treatment with either aminobisphosphonates or synthetic phosphoantigens leads to functional exhaustion of Vγ9Vδ2 T-cells[174], as well as activation-induced cell death[176]. Additionally, systematically administered aminobisphosphonates show strong bone-homing properties[177], thus limiting their bioavailability at the tumour site. Moreover, aminobisphosphonates are preferentially taken up by neutrophils, as well as monocytes and macrophages. In the case of

the former, bisphosphonate uptake leads to robust immune suppression of Vγ9Vδ2 T-cells though production of neutrophil-derived hydrogen peroxide and arginase[178]. In the latter case, aminobisphosphonate accumulation causes γδ T-cell induced cytotoxicity towards monocytes and macrophages, as well as a decrease in tumour chemotaxis of γδ T-cells[179,180]. Therefore, a more targeted delivery of aminobisphosphonates to tumour site may prove therapeutically beneficial, by either using liposomal drug delivery systems[181,182], or direct intratumoral injection. The clinical safety and efficacy of Vγ9Vδ2 T-cell activators will be reviewed in the later sections.

Another γδ T-cell ligand that can be pharmacologically modulated using already FDA-approved drugs is MICA/B. MICA/B upregulation, and resulting sensitisation to γδ T-cell mediated cytotoxicity can be achieved by using epigenetic modulators (histone deacetylase inhibitors) such as all-*trans* retinoic acid or valproic acid[183,184]. Notably, the feasibility of increasing MICA/B on cancer cells *in* vivo was shown by intravenous administration of either compound to leukemic patients[185]. Finally, more effective targeting of cancer cells by MICA/B specific γδ T-cells can be achieved by blocking the enzymes responsible for MICA/B shedding[186].

1.2.5.2 Re-directing γδ T-cells to cancer

In absence of known γδ TCR ligands on tumour surface, γδ T-cells can be directed to the tumour by using bi-specific antibodies. Such bi-specific antibodies are engineered to possess a domain that is specific for a tumour surface antigen, and a domain that binds γδ TCR/CD3 complex. As a result, the antibodies cross-link T-cells with target cells, overriding the cognate TCR specificity while ensuring T-cell activation at the same time. While such an approach shows some promise *in vitro*[187] and in *in vivo* mouse models[188], the application of bi-specific antibodies in the clinic may be limited, especially due to poor penetration of solid tumour mass[189]. An interesting alternative to bi-specific antibodies described above is using affinity-enhanced monoclonal TCRs coupled with an anti-CD3 antibody fragment (ImmTAC). ImmTAC reagents allow re-directing a polyclonal population of T-cells to tumours bearing even a very small number of copies of a given peptide-MHC antigen[97]. However, this approach is so far restricted to αβ T-cells, due to the feasibility of engineering high-affinity TCRs and selecting them on structurally well-defined targets. Nevertheless, it is expected that with better understanding of molecular and structural requirements of γδ TCR:ligand interactions, development of γδ ImmTACs will become possible, thus paving way for a HLA-unrestricted, off-the-shelf immunotherapy.

An approach similar to ImmTAC was proposed by Zheng *et al.* by fusing the extracellular domain of a cancer-specific Vγ9Vδ2 TCR with the Fc region of human IgG1 (Ref. [190]). The recombinant protein was shown to bind cancer cells (although the ligand identity has yet to be determined)

and to inhibit cancer growth *in vivo*, through binding to CD16 and inducing antibody-dependent cellular cytotoxicity (ADCC). Indeed, CD16:IgG Fc interaction can stimulate γδ T-cells even in absence of TCR triggering, thus providing another means of target recognition[191]. High CD16 expression can be observed both on Vδ2$^-$ (Ref. [192]) and Vδ2$^+$ (Ref. [191]) cells, presumably as a result of antigenic exposure, and CD16 expression can discriminate between functionally distinct γδ T-cell subsets[193].

Last but not least, γδ T-cells can be re-directed to cancer using genetic engineering (**Figure 1.8**). One option for such redirection is provided by chimeric antigen receptors (CARs). CARs are composed of an extracellular domain targeting the antigen, based on single chain antibody fragments, and an intracellular signalling domain, derived from CD3ζ and co-stimulatory molecules. So far, CAR technology has been mostly applied to αβ T-cells and shown a tremendous potential for treatment of haematological cancers (reviewed by June and colleagues[194]). However, transducing CARs into γδ T-cells may prove beneficial, as these cells exhibit several functional properties that differentiate them from αβ T-cells – *i.e.* direct recognition of ubiquitous tumour antigens, capacity for mounting a rapid response in terms of cytotoxicity and cytokine production, as well as preferential tissue homing[195,196]. Indeed, CD19-specific CAR transduced into a polyclonal γδ T-cell population was capable of inducing the same signalling as the endogenous TCRs, and the transduced γδ T-cells delayed cancer growth in a pre-clinical mouse model[197].

Transduction of well-defined, cancer-specific TCRs can also be used to redirect γδ T-cells. The clinical application of transduced TCRs for cancer therapy, pioneered by Rosenberg and colleagues[198], has shown a great promise for treatment of some cancers, especially melanoma. However, the current clinical protocols involve transducing an αβ TCR into patient's αβ T-cells. As a result, the transduced cells can express two hybrid TCRs, composed of the endogenous and transduced TCR chains. These hybrid receptors can potentially mediate extremely harmful self-reactivity[199,200], and the autoreactivity of transduced TCRs may be difficult to determine in a pre-clinical testing systems[201,202] . However, formation of mixed TCR dimers will not occur if an αβ TCR is transduced into γδ T-cells[203]. The additional advantage of transduced γδ T-cells is the kinetics of the response – αβ TCR-transduced γδ T-cells responded to the cognate peptide antigen markedly faster than αβ T-cells, with similar kinetics of the endogenous γδ TCR-mediated signalling[204]. However, the disadvantage of using γδ T-cells as recipients of αβ TCRs lies in the fact that conventional αβ TCRs require CD8 or CD4 co-receptors for efficient ligand engagement, and γδ T-cells are usually CD4/CD8 co-receptor negative. This problem can be overcome by either co-transduction with the respective co-receptor[205] or using high-affinity TCRs[206]. An

alternative to using HLA-restricted, co-receptor dependent αβ TCRs to induce tumour regression is transducing T-cells with cancer-specific γδ TCRs. This approach, using a Vγ9Vδ2 TCR, has shown some initial promise *in vivo*[207]. Kuball and colleagues showed that transducing different Vγ9Vδ2 TCRs into primary $CD4^+$ cells can be used to select receptors with optimal anticancer receptors (as the exact binding partner for Vγ9Vδ2 TCRs is yet to be identified, the actual affinity maturation of Vγ9Vδ2 TCRs is not feasible)[208]. However, the transduction of an exogenous TCR into primary T-cells usually results in lower antigen sensitivity than would be observed in a T-cell clone bearing the said TCR. This phenomenon is believed to be due to competition for CD3 between endo- and exogenous TCRs[209]. Methodology for improving exogenous TCR expression, and consequently functional avidity, in primary T-cells will be addressed in **Chapter 3.**

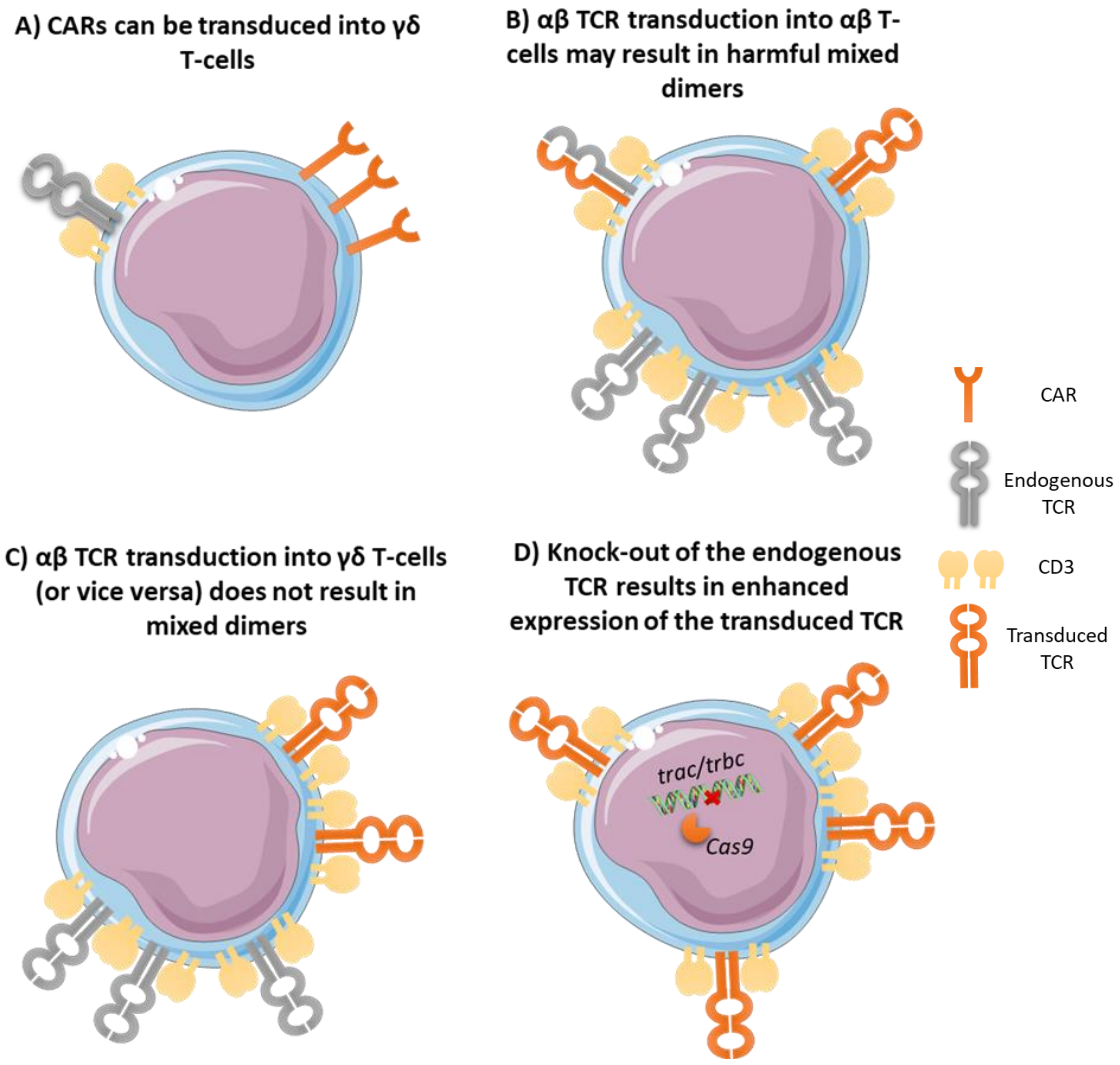

Figure 1.8 Genetic re-targeting of T-cells for immunotherapy. Peripheral T-cells may be engineered to target a chosen (cancer) antigen by transduction with a receptor of known specificity. One of the possibilities is using chimeric antigen receptors (CARs) which are composed of an antibody-derived domain that determines target specificity, and intracellular signalling and co-stimulatory domains (**A**). The other option is using a natural or engineered TCR for transduction. However, the transduction of an αβ TCR into αβ T-cells may give rise to formation of four distinct receptors (**B**), composed of: 1) transduced TCR-α and TCR-β chains; 2) endogenous TCR-α and TCR-β chains; 3) transduced TCR-α and endogenous TCR-β chains (mixed dimer); 4) endogenous TCR-α and transduced TCR-β chains (mixed dimer). Mixed dimers have not undergone the rigours of thymic selection and may have unpredicted (and unpredictable) target specificities which in turn may result in self-recognition and autoimmunity. (**C**) A potential way of avoiding mixed dimers is transduction of an αβ TCR into γδ T-cells (or *vice versa*). However, the co-existence of two distinct TCRs in a single T-cell leads to competition for CD3 and adaptor molecules, and therefore the functional avidity of the transduced TCR may be compromised. TCR competition may be overcome by knocking out the endogenous TCR chains (**D**).

1.3 Cancer immunotherapy – the promise of γδ T-cells?

The role of the immune system in fighting cancer has been investigated for more than half a century[210]. However, only lately has the importance of cancer immunosurveillance become widely acknowledged. In fact, the recent review by Hanahan and Weinberg included immune evasion as an emerging hallmark of cancer cells[211]. The recognition of phenomenon that body's own immune system can mediate reactivity to autologous tumours has led to development of a range of clinical procedures known as cancer immunotherapy, most of which focus on T-cells[212]. Indeed, the potential for inducing complete durable responses, even in patients with multiple metastases that had been refractory to conventional treatment, was acknowledged by the magazine *Science* by naming cancer immunotherapy the Breakthrough of the Year 2013 (Ref. [213]). In this section I will provide a brief overview of T-cell focused immunotherapies, particularly in context of melanoma, and highlight the application of γδ T-cells in the past and potential immunotherapies.

1.3.1 Cancer vaccines

Therapeutic cancer vaccines offer a seemingly simple modality of cancer immunotherapy, as they can be easily manufactured and administered to patients as an off-the-shelf medication. Cancer vaccines are usually composed of short peptides designed for MHC binding or full proteins, with or without adjuvants. The effective cancer vaccine is supposed to target both $CD4^+$ and $CD8^+$ αβ T-cells, and induce a lasting expansion of antigen-specific memory T-cells. However, despite numerous clinical trials, the outcomes after administering cancer vaccines (with the exception of vaccines targeting viral antigens on tumours) have been underwhelming (<7% objective response)[214,215]. One of the reasons for poor clinical efficacy of cancer vaccines is the absence of high-affinity cancer-specific T-cells, which could be robustly primed, in the peripheral repertoire as a result of thymic deletion. Nevertheless, there are on-going attempts to generate optimised peptide antigens through functional (combinatorial peptide libraries[216]) and structural[217–219,] studies, or by leveraging neoantigens from patient's own tumour[220].

Another possible way to break T-cell tolerance to tumour associated self-antigens is using professional antigen-presenting cells (APC) that would process the antigen and present it to T-cells, together with a range of co-stimulatory molecules; thus ensuring a robust response and differentiation of antigen-specific T-cells. The most commonly exploited APCs for cancer immunotherapy are dendritic cells (DCs). However, the generation of sufficient numbers of *ex vivo* differentiated DCs often proves problematic in terms of time and cost effectiveness, as well as may result in sub-optimal DC phenotypes[221].

However, the limitations of DCs for use in cancer vaccines can be overcome by using Vγ9Vδ2 T-cells, which can not only directly recognise and lyse various tumours, but also serve as efficient APCs[222]. Upon *in vitro* activation with phosphoantigens, these cells can cross-present extracellular antigens, thus priming and activating naïve $CD8^+$ αβ T-cells, in a more robust manner than DCs[223]. Further research unravelled that activation of γδ T-cells is not sufficient for them to become APCs – they need to be licenced by interacting with antibodies, for example bound to tumour cells[224]. Another group reported acquisition of APC properties by $V\delta2^+$ T-cells responding to autologous tumour, thus showing that APC licencing can occur in physiological conditions[225]. Apart from their ability to prime αβ T-cells and to induce their antitumour reactivity, γδ APCs inhibited the immunosuppressive functions of regulatory $CD4^+CD25^+$ T-cells. APC properties of Vγ9Vδ2 T-cells have also been identified *ex vivo* in patients infected with *Plasmodium falciparum*[226]. Finally, Khan *et al.* has recently demonstrated the feasibility of generating APCs from peripheral blood $V\delta2^+$ T-cells in cancer patients[227]. These cells could be readily expanded to large numbers, retaining their antigen presenting phenotype, in stark contrast to DCs, thus showing new possibilities for the development of clinically relevant cancer vaccines.

Currently, there are no vaccines *per se* that would target γδ T-cells. However, using phosphoantigens (e.g. BrHPP) or aminobisphosphonates (e.g. zoledronate) can be perceived as analogous to vaccination. Both types of compounds cause expansion, activation and differentiation of peripheral Vγ9Vδ2 T-cells, as discussed above. Indeed, both BrHPP and zoledronate have been used in clinical trials targeting different cancer types, either as a single agent or in combination with other therapeutics. Clinical trials involving γδ T-cells are summarised in **Table 1.4**. Intravenous zoledronate has been shown to be generally well tolerated, and the sporadic acute inflammatory reaction to zoledronate can be reliably predicted by testing the peripheral γδ T-cells *ex vivo* for responsiveness to the drug[228]. Similarly, dose-escalation phase I trial demonstrated that BrHPP together with low dose IL-2 does not cause any grade 4 toxicity, and grade 3 toxicity is observed only sporadically, and at high BrHPP doses[229]. Importantly, BrHPP caused expansion of peripheral γδ T-cells in a dose-dependent manner; the expansion was however decreased with each consecutive administration of the drug, presumably due to T-cell exhaustion and activation-induced cell death. In terms of objective clinical response, zoledronate plus IL-2 was found to be insufficient to generate partial or complete response in renal cell carcinoma[230,231] and malignant melanoma[231], while 2 out of 8 patients with acute myeloid leukaemia achieved partial response[231]. In case of terminal metastatic breast cancer, zoledronate plus IL-2 resulted in 1/10 partial remission and 2/10 stable diseases; the clinical response correlated with the long-lasting maintenance of relatively large

population of Vγ9Vδ2 T-cells in the periphery[232]. A similar result was observed in prostate cancer patients, where treatment with zoledronate and IL-2 induced partial remission in 2/9 cases, which correlated with the sustained presence of an effector γδ T-cell population producing IFN-γ and tumour necrosis factor-related apoptosis inducing ligand (TRAIL)[233]. Conversely, when zoledronate was administered as a single agent, the majority of the patients (8/9) failed to develop a persistent γδ T-cell population in the periphery, and showed no objective response to the treatment. Finally, intravenous zoledronate has been investigated as an adjuvant for conventional chemotherapy for prostate[234], breast[235–238] and lung cancers[239]. Zoledronate was found to yield no improvement over chemotherapy alone in most of the trials, apart from breast cancer where it showed slight improvement for some breast cancer subtypes.

Table 1.4 Clinical trials involving stimulation of patient's γδ T-cells directly *in vivo*.

BrHPP, bromohydrin pyrophosphate; PR, partial remission; SD, stable disease; P, progressive disease; NE, non-evaluable.

Therapeutic agent	Trial stage	Cancer type	Clinical outcome	Reference
zoledronate + IL-2	I	prostate cancer	2 PR, 4 SD, 3 P	Dieli *et al.*, 2007
zoledronate	I	prostate cancer	1 PR, 1 SD, 7 P	Dieli *et al.*, 2007
BrHPP + IL-2	I	various	12 SD, 16 P	Bennouna *et al.*, 2010
zoledronate + IL-2	pilot	renal cell carcinoma	7 SD, 1 P, 4 NE	Lang *et al.*, 2011
zoledronate + IL-2	I/II	melanoma	1 SD, 4 P	Kunzmann *et al.*, 2012
zoledronate + IL-2	I/II	renal cell carcinoma	2 SD, 5 P	Kunzmann *et al.*, 2012
zoledronate + IL-2	I/II	acute myeloid leukaemia	2 PR, 2 SD, 3 P, 1 NE	Kunzmann *et al.*, 2012
zoledronate + IL-2	I	breast cancer	1 PR, 2 SD, 2 P, 5 NE	Meraviglia *et al.*, 2010

1.3.2 Immune checkpoint inhibitors

Immune checkpoint inhibitors are monoclonal antibodies targeting molecules involved in T-cell mediated target recognition and signalling, thus lifting inhibitory signals rather than targeting any particular tumour antigen. So far, antibodies specific for two targets, cytotoxic T-lymphocyte-associated protein (CTLA)-4 and programmed death (PD)-1, have been approved for clinical use in different cancer types[240]. When used alone, anti-CTLA-4 (Ref. [241]) or anti-PD-1 (Ref. [242,243]) antibodies can induce long-lasting objective responses in a fraction of patients (up to 40%

objective response). Moreover, targeting both CTLA-4 and PD-1 simultaneously led to an objective response rate of >50% and reduction of tumour burden by at least 80% (Ref. [244]). It has been demonstrated that the therapeutic success of checkpoint inhibition depends on the initial diversity of peripheral TCR repertoire[245], as well as neoantigenic load of the tumour[246].The majority of checkpoint inhibitor research focuses on αβ T-cells, especially $CD8^+$ subset[56]. However, antigen-specific γδ T-cells can also express PD-1, and PD-1:PD-1 ligand interaction was shown to affect their activation[247]. Therefore, the contribution of γδ T-cells to the clinical outcome of patients treated with checkpoint inhibitors warrants further investigation.

1.3.3 Adoptive cell transfer

Adoptive cell transfer (ACT), pioneered by Rosenberg and colleagues[248], is a highly personalised form of treatment, involving *ex vivo* expansion of patient's own T-cells (up to 10^{11} cells per infusion product), optional genetic engineering or selection for cancer-reactive cells, and re-infusion back into the pre-conditioned patient[249]. Pre-conditioning usually involves non-myeloablative lymphodepleting chemotherapy[250] (fludarabine and cyclophosphamide) and total body irradiation[251]. The purpose of the former is to allow engraftment of adoptively transferred T-cells and to remove potential immunoregulatory cells from tumour microenvironment, while total body irradiation additionally activates the innate immune system *via* translocation of gut microbiota[252]. ACT is currently the most effective treatment for metastatic melanoma, even in cases that had been resistant to checkpoint inhibitor treatments – depending on the regimen, up to 70% patients experienced objective response, and up to 40% underwent complete durable remission ("cure")[251].

1.3.3.1 Procurement of clinical-grade T-cells for adoptive cell transfer

As mentioned before, ACT requires an infusion of high T-cell numbers. These cells need to be derived from the patient, and then expanded in a GMP-compliant system, thus making the therapy time-consuming, technically challenging and expensive. Tumour-infiltrating lymphocytes (TILs) offer an attractive source of T-cells for ACT, especially in melanomas, as they are already enriched in cancer-specific T-cells[251]. The general approach for using TILs in ACT is depicted in **Figure 1.9**. In brief, a tumour explant (1-3 mm^3) is digested to single-cell suspension, and incubated in medium containing IL-2, thus allowing initial expansion of TILs and destruction of the tumour sample [pre-Rapid Expansion Phase (REP)]. Standard TIL expansion protocol requires that TILs are grown as separate cultures from each tumour fragment until reaching >4 $\times 10^7$ cells per culture. Conversely, Young TIL protocol allows combining TILs growing from multiple tumour explants when they collectively reach >5$\times 10^7$ cells. Donia *et al.* showed that T-cells expanded with Young TIL protocol show a less differentiated and thus more functional

phenotype than cells generated with Standard TIL protocol[253]. Additionally, generation of a TIL infusion product with the Young TIL protocol takes on average 3-4 weeks (compared to 5-6 weeks with the Standard TIL protocol) which may be of vital importance when considering a treatment for final stage cancer patients. Standard TIL protocol may also involve testing and selecting TIL subsets with optimal reactivity against the autologous tumour.

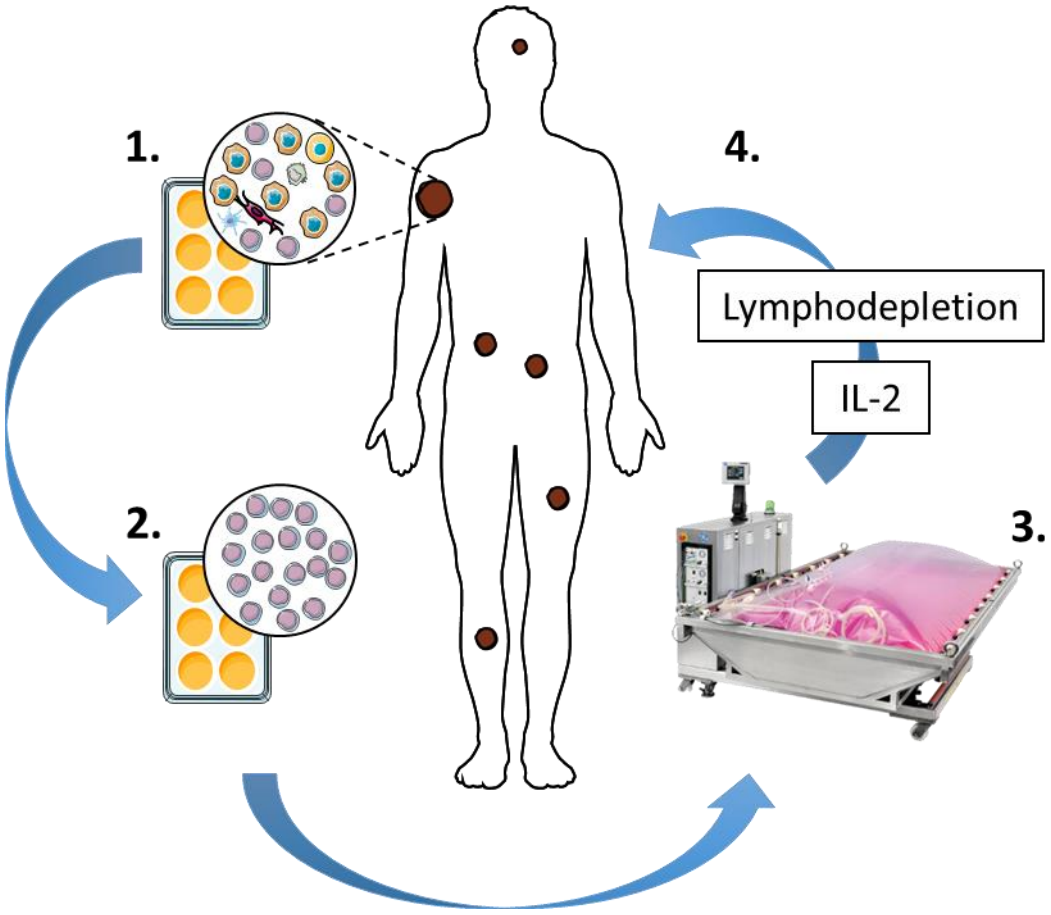

Figure 1.9 Adoptive cell transfer of tumour-infiltrating lymphocytes. In brief, tumour lesion is resected and divided into 1-3 mm^3 fragments (or digested into single cell suspensions), and plated in media containing high dose IL-2 (**1**). The overgrowing tumour-infiltrating lymphocytes (TILs) from the tumour explant (**2**) are then pooled and subjected to Rapid Expansion Protocol (REP), in presence of αCD3 antibody, high dose IL-2 and excess of allogeneic irradiated feeders (an automated, gas-permeable Wave® bioreactor) (**3**). After 14 days of REP, TILs are harvested and can be re-infused into the pre-conditioned patient (after non-myeloablative lymphodepletion with chemotherapeutic agents fludarabine and cyclophosphamide, together with total body irradiation) immediately (**4**), or cryopreserved.

After the pre-REP phase, TILs are rapidly expanded (REP phase) with allogeneic irradiated peripheral blood mononuclear cells (PBMC) and anti-CD3 antibody (OKT3). REP phase may be conducted in a GMP-compliant, closed-system bioreactor (Wave®), thus reducing the workload and facilitating the process[254]. Thus expanded cells are then infused into pre-conditioned patients, together with high[251] or low[255,256] dose of IL-2 – as decreasing the dose of IL-2 reduced the toxic side effects of the treatment while retaining the clinical performance. Importantly, generation of tumour-reactive TIL products for ACT from other cancer types, such as renal cell carcinoma and ovarian cancer, has recently been re-visited, using the methods developed for TIL procurement from melanoma[257]. As reported by Andersen *et al.*, treatment of metastatic melanoma patients with Young TIL infusion product and low dose of IL-2 resulted in objective response rate of over 40% and complete durable remission rate of 20% (Ref. [256]) (ClinicalTrials.gov Identifier: NCT00937625). The dissection of antitumour reactivity of TILs used in the trial NCT00937625 is described in **Chapter 4**.

T-cells from patient's peripheral blood can be used in instances when TILs are not readily available or do not display sufficient antitumour reactivity. Since cancer-specific T-cells are generally rare in the periphery, peripheral T-cell for ACT are usually transduced with a cancer-specific CAR[258] or TCR[198], naturally occurring or engineered for desired affinity[259]. This approach yields a large number of T-cells of known cancer specificity but may result in harmful autoreactivity[201] (as a result of unpredicted TCR cross-reactivity) or facilitate cancer escape[260,261], since normally only one cancer-associated epitope is targeted.

1.3.3.2 γδ T-cells for adoptive cell transfer

It has been observed for over two decades that γδ T-cells can be represented in a relatively high frequency in TILs from different cancer types, in particularly cancers located in the epithelium. This enrichment of γδ T-cells at tumour site should not be surprising, given the tissue localisation and stress surveillance performed by γδ T-cells. The majority of evidence showing tumour infiltration by antitumour γδ T-cells comes from melanomas[262–265], where the infiltrating cells were predominantly $V\delta2^-$, in contrast with the peripheral blood composition. Indeed, Lança *et al.* showed that preferential infiltration of tumours by $V\delta1^+$ but not $V\delta2^+$ T-cells may be mediated *via* CCL2 secretion by tumours and CCR2 expression on $V\delta1^+$ cells[266]. The role of γδ T-cells in other cancer types remains ambiguous; in renal cell carcinoma and gastric cancer, γδ TILs were found to mediate an antitumour activity while in case of breast[267], colorectal[268], pancreatic[269] and hepatocellular[270] cancers the activity of γδ T-cells was found to be impaired or even immunosuppressive.

Since γδ T-cells commonly infiltrate melanoma lesions, they are often present in expanded TIL products for ACT[265]. However, no significant correlation between the percentage of γδ T-cells in TIL products and the clinical outcome (neither was there any correlation between percentages of $CD8^+/CD4^+$ cells or the total number of infused cells, and the clinical outcome)[256]. So far, there has been no clinical trial focusing on TIL-derived γδ T-cells; instead, γδ T-cells used for adoptive cell transfer come from peripheral blood and are enriched in the Vγ9Vδ2 subset (the clinical trials involving ACT of γδ T-cells are summarised in **Table 1.5**). One of the methods for selective expansion of γδ T-cells that has been used in clinical trials involved stimulation with a synthetic phosphoantigen BrHPP (Innacell™ product). In a phase I clinical trial, Bennouna *et al.* showed that the best clinical response to Innacell™ treatment was stabilisation of disease (6/10 patients), despite repeated infusions of the cell product[271]. Similarly, when patients with various solid tumours were treated with autologous expanded Vγ9Vδ2 T-cells, infused together with zoledronate, no objective clinical response was observed[272]. In another study phosphoantigen-expanded T-cells were infused together with IL-2 and zoledronate, resulting in 1/11 of renal cell carcinoma patients achieving complete response[273]. Finally, a small study by Wilhelm *et al.* investigated the possibility of using γδ T-cells from haploidentical donors for ACT, instead of autologous PBMC – since T-cell responses may become dysfunctional in cancer patients[274]. No graft *versus* host disease was observed during treatment, and 3/4 patients demonstrated an initial complete response but relapsed within 8 months after treatment. Therefore, it is apparent that the clinical results of ACT involving γδ T-cells are at best underwhelming, especially when compared with ACT using TILs. One of the potential reasons of failure of γδ T-cell ACT therapies may lie in the fact that the treatment was usually administered without pre-conditioning chemo- and radiotherapy; or in the usage of only Vγ9Vδ2 T-cells, rather than a wider cancer-specific γδ TCR repertoire.

As described above, clinical trials involving γδ T-cells have focused on the Vγ9Vδ2 subset, due to the relative ease and availability of clinical-grade reagents that can be used for their selective expansion. Nevertheless, several groups have developed methods to expand both $V\delta2^+$ and $V\delta2^-$ subsets of human γδ T-cells. For instance, He and colleagues showed that γδ T-cells from TILs or peripheral blood of cancer patients can be efficiently expanded on immobilised anti-γδ TCR antibody without inducing anergy[275,276]. Moreover, Deniger *et al.* engineered a clinical-grade artificial antigen presenting cell line that could be used for an unbiased expansion of γδ T-cells[277]. Indeed, γδ T-cells expanded with that protocol displayed a diverse TCR repertoire and showed superior anticancer activity *in vivo*, compared to only $V\delta2^+$ or only $V\delta1^+$ subsets. Finally, a recent study showed the possibility of clinical-grade expansion of $V\delta1^+$ T-cells without any feeder cells[278]. The cells were expanded only with a tailored combination of antibodies and cytokines,

and showed promising results in preclinical mouse models. It is therefore anticipated that new clinical trials, utilising diverse repertoires of γδ T-cells, will prove more successful than those using phosphoantigen-expanded Vγ9Vδ2 T-cells.

Table 1.5 Clinical trials involving adoptive cell transfer of *ex vivo* expanded γδ T-cells.

BrHPP, bromohydrin pyrophosphate; PAg, phosphoantigen; ZOL, zoledronate; CR, complete response; PR, partial response; SD, stable disease; P, progressive disease; NE, non-evaluable.

[1] autologous, *ex vivo* stimulated PBMC were used as an infusion product, unless stated otherwise.
[2] synthetic phosphoantigen, 2-methyl-3-butenyl-1-pyrophosphate.
[3] PBMC from haploidentical donors were used, following a lymphodepleting regimen.

Therapeutic agent[1]	Trial stage	Cancer type	Clinical outcome	Reference
BrHPP + IL-2	I	renal cell carcinoma	6 SD, 4 P	Bennouna *et al.*, 2008
PAg[2] + ZOL + IL-2	I/II	renal cell carcinoma	1 CR, 5 SD, 5 P	Kobayashi *et al.*, 2011
ZOL	I	various solid tumours	3 SD, 11 P, 1 NE	Nicol *et al.*, 2011
ZOL + other therapies	I	various solid tumours	1 CR, 2 PR	Nicol *et al.*, 2011
[3]ZOL + IL-2	pilot	haematological cancers	3 CR, 1 NE	Wilhelm *et al.*, 2011

Finally, it should be noted that a recent global analysis indicated that of all lymphocyte subsets present within 25 different cancer types (>5,000 individual samples), the strongest positive correlate of a favourable clinical outcome was the presence of γδ T-cells[279]. Other groups have also observed that an elevated frequency of circulating γδ T-cells in cancer patients may be an indicator of a positive outcome and prolonged survival[280–283]. It has therefore become apparent that γδ T-cells play an important role in cancer immunosurveillance, and thus are a valid tool for future cancer immunotherapies.

1.4 Genome engineering for studying the biology of unconventional T-cells

Genome engineering encompasses a broad range of techniques which in essence allow for introducing targeted modifications in the cellular genome, epigenome or transcriptome. Homologous recombination (HR), using exogenously supplied templates flanked with sequences homologous to the target sites, offered the initial potential for generating genetic knock-in or knock-out animal models but its routine application was hampered by extremely low frequency of cells where desired HR occurred[284]. A much more efficient method of genome engineering was discovered in a form of programmable nucleases such as zinc finger nucleases (ZFNs), transcription activator-like effector nucleases (TALENs) and RNA-guided DNA nucleases (e.g. Cas9). ZFNs are composed of Cys2-His2 zinc finger domains which bind to a nucleotide triplet[285] while TALENs are composed of mostly invariant 34-amino acid modules targeting a single nucleotide *via* variable amino acids at positions 12 and 13 (Ref. [286]). The ZF or TALE modules are then combined to target the chosen DNA sequence, and fused with the nuclease domain of FokI, and used as a pair to target both strands of the DNA (**Figure 1.10 A**), and thus induce double strand breaks (DSBs) (**Figure 1.10 B**). The modular assembly of highly repetitive ZF or TALE modules, however, is laborious, requires extensive screening of potential module combinations, and may still show context-dependent specificity[287,288].

Conversely, microbial adaptive immune system CRISPR (clustered regularly interspaced short palindromic repeats), utilising Cas9 DNA endonuclease targeted to the desired DNA sequence with a short RNA RNA sequence *via* Watson-Crick pairing allows for highly efficient, time- and cost-effective disruption of virtually any genomic *loci*[289] (**Figure 1.10 C**). CRISPR/Cas9 system requires also, in addition to Cas9 protein, a short complementary RNA (crRNA) and a *trans*-activating RNA (tracRNA) needed for crRNA processing[290]. Fusing crRNA and tracRNA into one RNA sequence, termed (single) guide RNA (gRNA), was subsequently shown to facilitate Cas9-mediated DNA cleavage[291]. Therefore, Cas9 can be easily directed to the desired genomic *locus via* its cognate gRNA[289,292], and induce DSBs followed either by homology-directed repair (HDR), in presence of a DNA template flanked by sequences homologous to the target, or non-homologous end joining (NHEJ) – an error prone repair mechanism which results in insertion and/or deletion mutations (indels) at the DSB site, and thus a potential frameshift and premature stop codons (**Figure 1.10 B**). The only requirement for a DNA sequence to be targetable with CRISPR/Cas9 system is the presence of a protospacer-adjacent motif (PAM) immediately downstream of the target sequence. For the most commonly used Cas9 orthologue, *Streptococcus pyogenes* Cas9 (*Sp*Cas9), the PAM sequence is 5'-NGG, and thus the

frequency of *Sp*Cas9 targetable sequences in the human genome is 1 in every 8 base pairs (bp)[293]. Importantly from the point of potential off-target effects, 5'-NAG PAM is also an acceptable target for *Sp*Cas9, albeit with reduced cleavage efficiency[293]. While scanning the genome for its targets, Cas9-gRNA complex first binds to the PAM sequences, followed by DNA strand separation and forming a heteroduplex between DNA and gRNA (**Figure 1.10 D**). Following successful binding of the PAM and target sequences, Cas9 changes from target binding to DNA cleavage conformation[294]. Notably, *Sp*Cas9 can tolerate up to 5 mismatches between the gRNA and target DNA sequence[295], and therefore a careful gRNA design is crucial. For limiting the non-specific cleavage, the mismatches between the on-target and potential off-target sequences should be located in the PAM site or the PAM-proximal sequence (8-12 bp upstream of PAM), and preferably clustered either consecutively or within four bp range[293]. Conversely, even a perfect match between the gRNA sequence and the target sequence does not ensure efficient cleavage of the target, as that is dependent on chromatin structure in the target proximity, as well as potential secondary structures formed by the gRNA[296]. While there are numerous gRNA design tools available that score the gRNAs based on predicted off-target reactivity, making predictions about gRNAs with high on-target cleavage efficiencies is more challenging[297,298].

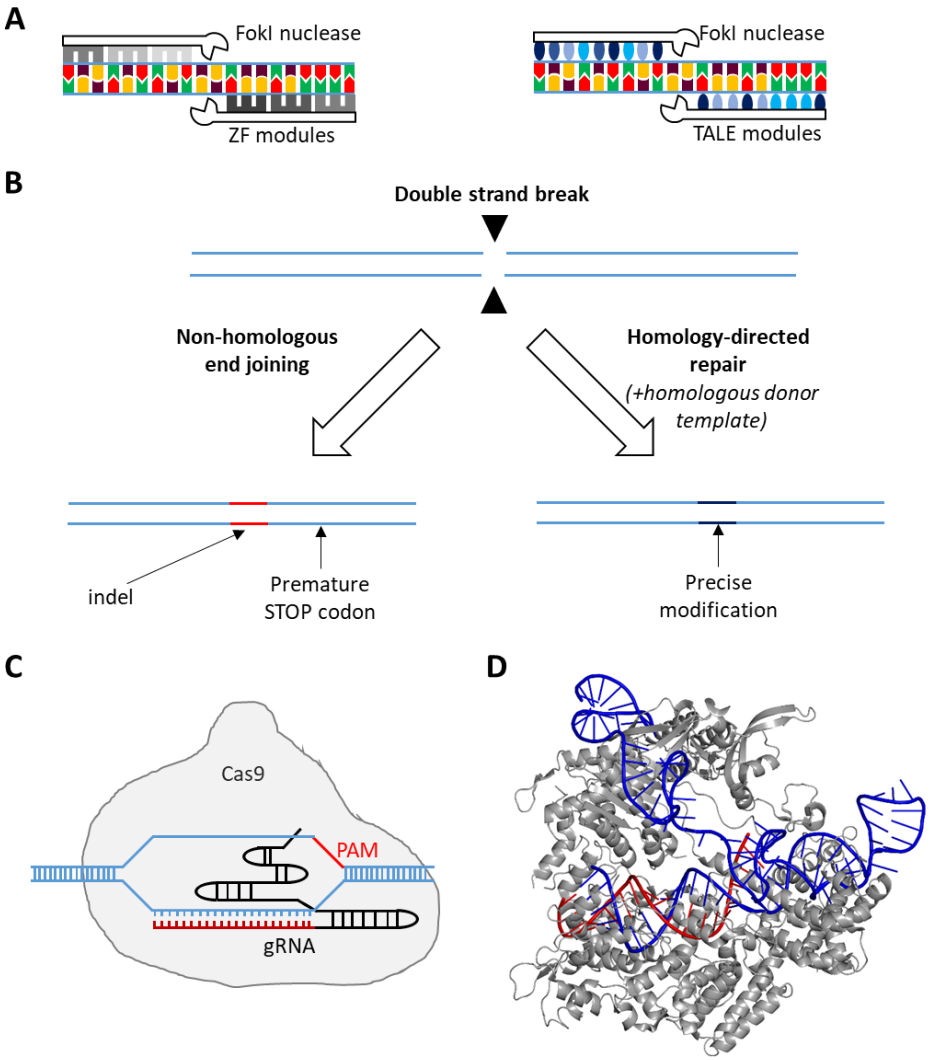

Figure 1.10 Overview of genome engineering tools. (**A**) Genomic *loci* can be targeted *via* an assembly of zinc finger (ZF) modules, each targeting a nucleotide triplet, or an assembly of transcription activator-like effectors (TALE), each targeting a single nucleotide. ZF or TALE modules are then fused with FokI nuclease which induces a double strand break (DSBs) in the target DNA sequences upon dimerisation. (**B**) Double strand breaks are repaired using the endogenous mechanisms, either relying on error-prone non-homologous end joining (NHEJ), or less efficient but highly specific homology-directed repair (HDR) based on the donor DNA template. NHEJ introduces insertion and/or deletion mutations (indels) at the DSB site, thus potentially resulting in a frameshift mutation and premature STOP codons, leading to functional knock-out of the target gene. Conversely, HDR allows for introduction of a specific mutation at the DSB site. (**C**) Cas9 endonuclease is guided to its target sequence by a complex of crRNA and tracRNA which can be fused together into a single molecule called gRNA. A part of gRNA binds to the target DNA sequence through Watson-Crick pairing, and induces endonucleolytic activity of Cas9, thus leading to DSBs at the target sequence. Protospacer-adjacent motif (PAM), absent in the gRNA sequence but present in the target DNA upstream of the sequence bound by gRNA, is required for productive binding of Cas9 to the target DNA. (**D**) Crystal structure of Cas9 protein (in grey) bound to the target DNA sequence (blue). DNA strands are separated by Cas9, allowing for binding of gRNA (red) to its complementary sequence. PDB ID: 4OO8.

The potential applications of CRISPR/Cas9 vastly exceed its the capability for targeting a single *locus*, inducing frameshift mutations *via* NHEJ, or introducing more precise mutations encoded on donor DNA template *via* HDR. Firstly, CRISPR/Cas9 can be easily multiplexed, targeting multiple genomic *loci* at the same time. Initially, Cong *et al.* used an array of gRNAs, separated by direct repeat sequences in a similar manner to the organisation of endogenous CRISPR system in bacteria, to induce DSBs in two genomic *loci* simultaneously[289]. A recent study by Ran *et al.* demonstrated the feasibility of transduction of up to four different gRNAs, each under a different RNA polymerase III, in one vector[299]. Secondly, Cas9 enzyme can be mutated to perform other functions than inducing DSBs at the target site. For instance, mutated Cas9 can induce single strand breaks (so called Cas9 nickase), and therefore reduce off-target reactivity by targeting a single genomic *loci* with a pair of gRNAs[300]. Furthermore, endonuclease activity of Cas9 can be completely abolished, and instead Cas9 can be fused with transcription repressors[301] or factors recruiting transcriptional activators[302], thus resulting in target gene down-regulation or up-regulation, respectively. The potential for gene up-regulation, driven from the endogenous promoter, is of particular interest as it allows to study the gain of function of a given gene in its natural context and at its physiological expression level. Finally, CRISPR/Cas9 system can be used in a library format, combining hundreds of thousands of gRNAs, thus allowing for functional genomic screenings on a whole genome level. Thus generated whole genome CRISPR/Cas9 libraries can be used to interrogate loss[303] or gain of function[302] of every gene in the genome, as well as to discover functional elements located in the non-coding genome[304]. The whole genome CRISPR/Cas9 libraries have so far been used to discover genes essential for cell survival[301,305–307], acquisition of drug resistance by cancer cells[302,303,305,306], resistance to viral infections[308–310], cancer cell metastasis[311], regulation of gene expression[304,306,312,313], and innate immune response to lipopolysaccharide[314].

In this Thesis, CRISPR/Cas9 system was used for generation of gene knock-outs using the NHEJ repair pathway. In particular, in **Chapters 3** and **4** CRISPR/Cas9 was used to improve the sensitivity and anticancer reactivity of broadly-cancer reactive γδ TCRs transduced into primary T-cells while in **Chapter 4** cancer cell lines were engineered *via* CRISPR/Cas9 to be deficient in known and putative ligands of non-HLA restricted T-cells, thus facilitating the dissection of specificities exhibited by unconventional, cancer-reactive T-cells. Finally, **Chapter 5** examines the utility of whole genome CRISPR/Cas9 knock-out libraries for discovery of novel ligands recognised by non-HLA restricted, cancer-reactive T-cells, as well as molecular pathways leading to surface expression of the said ligands.

1.5 Project aims

It is generally acknowledged that γδ T-cells play a vital role in stress/cancer surveillance, predominantly *via* cognate TCR-ligand interactions. However, the exact identity of the cognate ligands, the molecular mechanisms of recognition, as well as breadth of TCR repertoires that respond to the said ligands remain poorly defined. The availability of tools used for studying antigen recognition by γδ T-cells is lagging, compared to the αβ T-cell field. Therefore, my thesis focused on two aspects: first, generating tools for studying antigen recognition by γδ T-cells; and second, applying the generated tools to dissect the antitumour reactivity of γδ T-cells from clinical relevant samples.

- In **Chapter 3** I hypothesised that removal of endogenous αβ TCRs from primary T-cells combined with simultaneous transfer of cancer reactive αβ or γδ TCRs would be feasible and result in generation of functionally superior cancer-specific T-cells.

- In **Chapter 4** I aimed to procure non-HLA restricted, broadly cancer reactive T-cells from a variety of clinical sources. My hypothesis was that TCRs derived from those broadly cancer reactive T-cells could be used for re-direction of healthy peripheral T-cells to a variety of cancers without targeting non-malignant cell lines. I also hypothesised that using CRISPR/Cas9 to knock out single genes encoding (putative) ligands of non-HLA restricted T-cells on tumour cells would facilitate ligand identification of procured clones/TCRs.

- The aim of **Chapter 5** was to investigate the potential of whole genome CRISPR/Cas9 libraries for unbiased identification of surface-expressed ligands (and pathways leading to their expression) on cancer-reactive non-HLA restricted T-cells. I hypothesised that selection of whole genome libraries in a cancer cell line with a cytotoxic T-cell clone would result in specific enrichment of cells transduced with gRNAs targeting the ligands and pathways necessary for productive recognition by T-cell clones tested.

2. Materials and Methods

2.1 Buffers and media for cell culture

Table 2.1 The composition of buffers used throughout the thesis. All buffers were sterile filtered through 0.22 μm filter and stored at 4ºC. All chemicals were purchased from Sigma Aldrich.

Buffer	Composition
Freezing buffer	10% DMSO, 90% foetal bovine serum (FBS)
Red blood cell (RBC) lysis buffer	155 mM NH_4Cl,10 mM $KHCO_3$, 0.1 mM EDTA (pH 7.2-7.4)
MACS buffer	2 mM EDTA, 0.5% bovine serum albumin (BSA) in D-PBS
Fixing buffer	4% paraformaldehyde (PFA) in PBS
FACS buffer	2% FBS in PBS
Tris-EDTA (TE) buffer	10 mM Tris, 1 mM EDTA in ddH_2O (pH=8.0)
Buffered water	2.5 mM HEPES in ddH_2O (pH=7.3)
2xHEPES-buffered saline (HeBS)	0.28 M NaCl, 0.05 M HEPES, 1.5 mM Na_2HPO_4 in ddH_2O (pH=7.0)

Table 2.2 The composition of cell culture media used throughout the thesis. All medium were sterile filtered through 0.22 μm filter, stored at 4ºC and used within 30 days after preparation. All reagents were purchased from Gibco (Paisley, UK), unless specified otherwise.

Medium	Composition
R0	RPMI 1640 supplemented with 100 U/ml penicillin, 2 mM L-glutamine
R5	R0 supplemented with 5% FBS
R10	R0 supplemented with 10% FBS
D10	DMEM supplemented with 10% FBS, 100 U/ml penicillin, 2 mM L-glutamine
D10/F12	DMEM/F12 supplemented with 1 mM sodium pyruvate

T-cell priming medium	R10 supplemented with 10 mM HEPES, 1 mM sodium pyruvate, 1x non-essential amino acids, and 20 IU IL-2 (Proleukin; Prometheus, San Diego, CA)
T-cell expansion medium	T-cell priming medium supplemented with 25 ng/ul IL-15 (PeproTech, Rocky Hill, NJ)
T-cell culture medium	T-cell expansion medium supplemented with 200 IU (final) IL-2
T-cell transduction medium	T-cell culture medium supplemented with 20% (final) FBS
Lysogeny broth (LB)	10 g/l tryptone, 5 g/l yeast extract, 10 g/l NaCl (all from Sigma Aldrich)
LB agar	LB supplemented with 15 g/l bacteriological agar (Sigma)

2.2 Cell culture

2.2.1 Culturing of cell lines

Cell lines were grown at 37^{o}C in humidified atmosphere with 5% CO_2. Unless specified otherwise, the cell lines were procured from ATCC and cultured according to supplier's recommendations. The composition of media used for cell culture is summarised in **Table 2.2** while the cell lines, together with a culture method, are listed in **Table 2.3**. Primary B ALL cells were provided by Oliver Ottmann (Cardiff University) and cultured as described before[315,316]. The cell lines were routinely passaged once they reached 70-80% confluency. In case of suspension cell lines, they were passaged by harvesting, centrifugation, removal of old medium, resuspending in fresh medium, and subsequently seeding an appropriate fraction of cells into a flask with fresh medium. The adherent cell lines were passaged by removal of old medium, washing with Dulbecco's PBS (D-PBS, without Mg^{2+} and Ca^{2+}) followed by non-enzymatic detachment using 2 mM EDTA in D-PBS. The flask was then incubated at 37^{o}C until the cells detached from the surface. The detached cells were then moved to a 50 ml tube, centrifuged at 400 × g for 5 minutes, and the supernatant was aspired. The cell pellet was resuspended in the respective medium and then the cells were seeded into a flask at an appropriate density. If the cells were not confluent enough for passaging, half of the medium was replaced with fresh medium. All the cell lines were routinely tested for Mycoplasma (MycoAlert™ Mycoplasma Detection Kit, Lonza) and found to be negative.

Table 2.3 Cell lines used throughout the thesis. All cell lines were originally obtained from the ATCC and subsequently stored as laboratory stocks. HM, hepatocyte medium; SMCM, smooth muscle cell medium; EpiCM, epithelial cell medium (all from ScienCell).

Cell line	Origin	Culture method, medium
t09, t11, t15, t24, t37, t46 Mel526, Mel624	Malignant melanoma	Adherent, R10
Caki-1	Kidney (carcinoma)	Adherent, D10
HEK 293T	Kidney (embryonic)	Adherent, D10
RCC2, RCC17	Kidney (carcinoma)	Adherent, D10/F12
Colo205, HCT116	Colon (carcinoma)	Adherent, D10
MCF7, MDA-MB231, SKBR3	Breast (adenocarcinoma)	Adherent, R10
Molt3, Jurkat E6.1	T-cell (leukaemia)	Suspension, R10
KBM7, K562	Chronic myelogenous leukaemia (CML)	Suspension, R10
THP-1	Acute monocytic leukaemia	Suspension, R10
T2, C1R	Lymphoblast	Suspension, R10
LCL 146	B lymphoblastoid	Suspension, R10
U266	Multiple myeloma	Suspension, R10
A549	Lung (carcinoma)	Adherent, R10
LnCAP	Prostate (carcinoma)	Adherent, D10
Hela, SIHA, CASKI, MS751	Cervix (carcinoma)	Adherent, D10
TK143, SAOS, U2OS	Bone (osteosarcoma)	Adherent, D10
Hep2	Normal hepatocyte	Adherent, HCM
SM3	Normal smooth muscle	Adherent, SMCM
CIL1	Normal ciliary epithelium	Adherent, EpiCM
MRC5	Normal fibroblast	Adherent, D10

2.2.2 Cell counting

Cells were resuspended at an estimated density of 0.5 to 4 × 10^6 cells/ml. Ten µl of cell suspension was then mixed with 10 µl of 0.4% trypan blue solution (Sigma Aldrich). The resulting mixture was loaded into the haemocytometer, and live cells were counted based on trypan blue exclusion. Cell density (per 1 ml) was then calculated according to the following formula: average cell count from two 16-square grids × 2 (dilution factor) × 10^4.

2.2.3 Cryopreservation and thawing

For cryopreservation, cell pellets were resuspended in the freezing buffer (**Table 2.1**) and then moved to internal thread cryovials (Nunc) as 1 ml aliquots. The cryovials were then cooled down to
-80^{o}C using a controlled-rate freezing device (Mr. Frosty® freezing pot, Nalgene). After five uses, isopropanol in the freezing pot was exchanged for fresh one. After 24 h, cells were moved from -80^{o}C to liquid nitrogen for long term storage. For thawing, cells were removed from liquid nitrogen and thawed in a water bath at 37^{o}C. The thawed cells were diluted 1:10 with warm R10 medium without delay, and centrifuged at 400 × g for 5 minutes. The supernatant was aspired and the cell pellet was resuspended in respective medium, followed by seeding into an appropriate tissue culture flask or plate.

2.2.4 Isolation of peripheral blood mononuclear cells (PBMC)

PBMC were routinely isolated from healthy donors' peripheral blood (either as buffy coats provided by Welsh Blood Service, or obtained through venepuncture from local donors), in accordance with the Human Tissue Act governance and corresponding local ethics. In brief, whole blood was layered on top of Lymphoprep™ in SepMate™ tubes (both from STEMCELL Technologies). The tubes were then centrifuged at 1,200 × g for 10 minutes, and the supernatant containing PBMC was collected. The supernatant was then diluted 1:1 with R0 and centrifuged at 700 × g for additional 10 minutes. Cell pellet was subsequently resuspended in 25 ml of RBC lysis buffer, and the lysis was conducted for 10 minutes in a water bath at 37^{o}C. After lysis, 25 ml of R0 was added to each tube, and the tubes were centrifuged at 300 × g for 6 minutes. RBC lysis was repeated if necessary. The resulting PBMC pellet was resuspended in R10 and cell density was established by counting as described in **Section 2.2.2**. Purified PBMC were either processed immediately or kept at 4^{o}C.

2.2.5 T-cell expansion, cloning and culture

T-cell clones and lines were routinely expanded as described before[317]. In brief, up to 1×10^6 T-cells were placed in a T25 flask in 15 ml T-cell expansion medium together with 1.5×10^7 allogeneic (coming from at least 3 donors, as described in **Section 2.2.4**.) irradiated (3,000 rad) PBMC feeders and 1 µg/ml phytohaemagglutinin (PHA, Fisher Scientific). The flask was placed in a cell culture incubator (37°C, 5% CO_2) at approximately 45° angle to allow better cell-to-cell contact. On day 5 post expansion, half of the medium was replaced with fresh T-cell expansion medium. On day 7, cells were harvested, centrifuged, resuspended in T-cell culture medium, counted and seeded into an appropriate number of wells on a 24 ($3\text{-}4\times 10^6$ T-cells/well) or 48 ($1\text{-}2\times 10^6$ T-cells/well) multiwell plate. T-cells were fed by replacing half of medium three times a week. T-cells were used in functional assays or frozen down during the period of four weeks starting from day 14 post expansion.

T-cell clones were procured by single cell cloning. In brief, T-cells were seeded in 96 U-bottom culture plates in 100 µl T-cell expansion medium (0.5 T-cell/well) with 50,000 allogeneic irradiated feeders and 1 µg/ml PHA. On day 7, wells were topped up with 100 µl T-cell expansion medium. On day 14, wells containing visibly growing T-cell clones were screened in appropriate functional assays. If needed, cloning plates were re-expanded on day 14 by adding 50,000 allogeneic irradiated feeders and 1 µg/ml PHA (final concentration) per well.

2.2.6 T-cell libraries

The methodology for setting up and screening of conventional αβ T-cell libraries has recently been described[216]. In brief, the desired subset of T-cells was purified (as described in **Section 2.3**) and then the T-cells were plated in 96 U-well plates at a density of 200-2,000 T-cells/well, together with DynaBeads® Human T-Activator CD3/CD28 beads[318] (Invitrogen) at 1:3 ratio, in T-cell priming medium. Half of the medium was exchanged three times a week (for T-cell priming medium for the first 7 days, and for T-cell expansion medium onwards; the timing of introducing T-cell expansion medium was adjusted based on T-cell growth). At day 14 after the library setup, representative wells were resuspended and cells were counted (normally 200,000 cells/well). The libraries were then screened by ELISpot for target cell recognition as described in **Section 2.8**.

2.2.7 Magnetic activated cell sorting

2.2.7.1 Isolation based on surface markers

The following T-cell subsets were isolated from freshly prepared or defrosted PBMC: $CD4^+$ cells, $CD8^+$ cells (using CD4 or CD8 MicroBeads, respectively), γδ T-cells and double-negative ($CD4^-$ $CD8^-$) αβ T-cells (using TCR γ/δ+ Isolation Kit or Double-negative T-cell Isolation Kit, respectively; all from Miltenyi Biotec). The magnetic beads based isolation was conducted according to manufacturer's instructions, and the number of cells taken for isolation depended on estimated frequency of the particular subset to be isolated, and on number of cells needed for downstream applications. In brief, the cells were washed with MACS buffer, and then resuspended in 80 µl MACS buffer per 10^7 cells, followed by addition of 20 µl MicroBeads per 10^7 cells. Cells and beads were mixed gently and then incubated for 15 minutes at 4^oC. The cells were then washed with MACS buffer and applied onto a MS or LS column (depending on cell number). MACS buffer was kept on ice at all times, and the centrifugation was conducted at 4^oC, to prevent bead internalisation. Potential cell clumps that would block the column were removed by passing the cell suspension through a 0.22 µm filter. The column was washed three times with MACS buffer, and the enriched cell fraction was then eluted by applying a plunger to the column ($CD4^+$, $CD8^+$ and double negative αβ T-cells), or collected as flowthrough (γδ T-cells).

Magnetic beads were also used to isolate cells (either primary T-cells or cell lines) transduced with a particular gene of interest, co-expressed with a marker gene rat CD2 (positive selection, based on rat CD2 expression) or transduced with CRISPR/Cas9 targeting a particular gene of interest (negative selection, based on the loss of expression of the target gene). In either case, the cells were first stained with a PE-conjugated primary antibody (20 minutes on ice), and then co-incubated with anti-PE MicroBeads (Miltenyi Biotec). Depending on the nature of selection, the fraction of cells bound to the beads, or flowthrough, was collected.

2.2.7.2 TNFα/IFNγ based magnetic pullout

TNFα/IFNγ based magnetic pullout was used to enrich antigen-reactive T-cell lines and procure antigen-reactive T-cell clones, according to manufacturer's instructions (TNFα/IFNγ Secretion Assays, Miltenyi Biotec). One day before the pullout, T-cells were washed extensively with R0 and plated in R5 for resting. The following day T-cells were co-incubated with target cells at 1:1 ratio (typically 50,000 T-cells and 50,000 target cells per well in a 96 U-well plate). After 4h co-incubation, cells were harvested and washed two times with MACS buffer (all centrifugation steps were conducted for 5 minutes at 4^oC, 400 × g). The cells were then re-suspended in MACS buffer and labelled with IFNγ and TNFα Catch Reagents (all reagents from Miltenyi Biotec) for 5

minutes on ice. Catch Reagent binds to a surface marker on all leukocytes and captures IFNγ/TNFα as the cytokines are released from activated T-cells. In our approach we combined the IFNγ and TNFα capture kits to maximise the number of recovered antigen-reactive cells. After labelling with the Catch Reagents, the cells were diluted in warm R5 medium and incubated at 37^{o}C for 45 minutes under slow continuous rotation (cytokine secretion period). The cells were subsequently washed with MACS buffer and incubated with IFNγ/TNFα Detection Antibodies (PE-conjugated) for 10 minutes on ice. After labelling with antibodies, the cells were washed with MACS buffer and incubated with anti-PE MicroBeads for subsequent 15 minutes at 4^{o}C. The bead-labelled cells were subsequently washed with MACS buffer and separated on appropriate columns placed in magnetic field. The cells bound to the column were finally eluted and resuspended in T-cell culture medium. On the following day, the enriched antigen-reactive T-cells were either expanded as a line or cloned (as described in **Section 2.2.5**).

2.3 Lentiviral transductions

2.3.1 Production of lentiviruses

Lentiviruses (2nd or 3rd generation) were produced by co-transfection of packaging, envelope and transfer plasmids into HEK 293T cell line. The 2nd generation transfer plasmid pLentiCRISPR v2 (Ref. [319]) (kindly provided by Dr. Feng Zhang, Addgene plasmid #52961) was co-transfected with packaging plasmid psPAX2 (Addgene plasmid #12260) and envelope plasmid pMD2.G (Addgene plasmid #12259). The 3rd generation transfer plasmid pELNS[320] (kindly provided by Dr. James Riley, University of Pennsylvania, PA) was co-transfected with packaging plasmids pRSV-Rev (Addgene plasmid #12253) and pMDLg/pRRE (Addgene plasmid #12251), and envelope plasmid pMD2.G. The quantities of plasmids used for transfection are listed in **Table 2.4**. The cloning of constructs into transfer plasmids and preparation of transfection-grade plasmids are discussed in **Section 2.11**.

Table 2.4 Plasmids used for production of 2nd and 3rd generation lentiviruses. The quantities of each plasmid (per 1xT175 flask) are given in brackets.

Transfer plasmid	Envelope plasmid	Packaging plasmids
pLentiCRISPR v2 (16 µg)	pMD2.G (8 µg)	psPAX2 (12 µg)
pELNS (15 µg)	pMD2.G (7 µg)	pMDLg/pRRE (18 µg), pRSV-Rev (18 µg)

Plasmids were transfected into HEK 293T cells (60-80% confluent, seeded into T175 flasks at least 24 h before transfection) by calcium phosphate precipitation. In brief, plasmids were

diluted with 1.1 ml of 0.1X TE buffer and 580 µl of buffered water, and then mixed with 188 µl of 2.5 M $CaCl_2$. Finally, 1.9 ml of 2xHeBS was added dropwise to plasmid mixture on a vortex, to ensure formation of a uniform and fine precipitate. The transfection mixture was then incubated at room temperature for 20 minutes to allow precipitate formation, and then was added dropwise to HEK 293T cells. The medium was replaced 16 h post transfection, and lentiviral supernatants were collected 48 h and 72 h post transfection. The supernatants were centrifuged at 400 × g for 5 minutes to remove cell debris, and then filtered through 0.45 µm filters (Millipore). Thus prepared unconcentrated lentiviral supernatants were either stored at 4^{o}C for <7 days, aliquoted and frozen down at -80^{o}C (long term storage), used directly for transduction of cell lines, or concentrated for transduction of primary cells.

Concentration of lentiviral supernatants was achieved by ultracentrifugation at 140,000 × g for 2h at 4^{o}C (Beckman Coulter Optima™ ultracentrifuge using SW28 rotor at 28,000 RPM). The resulting supernatant was removed and lentiviral pellet was resuspended on ice in 100 µl T-cell culture medium. Thus prepared lentiviruses were either stored at -80^{o}C or used immediately to transduce T-cells.

2.3.2 Lentiviral transduction of cell lines

Adherent cell lines were seeded in a 24 multiwell plate a day before transduction, and the cell number was optimised to give 60-80% confluency on the day of transduction. Immediately prior to transduction, all the medium was aspirated and 2 ml of unconcentrated lentiviral supernatant was added, together with 8 µg/ml polybrene (Santa Cruz Biotech).

Suspension cell lines were seeded at the density of 100,000 cells/well in 24 multiwell plate on the day of transduction, in 100 µl medium. Subsequently, 2 ml of unconcentrated lentiviral supernatant was added, together with 8 µg/ml polybrene.

Both adherent and suspension cell lines were then subjected to spinfection (by centrifugation at 500 × g for 2 h). The cells were incubated at 37^{o}C overnight, and the lentivirus-containing medium was replaced with fresh medium the next morning. After 72 h, cells were tested for transgene (or marker gene) expression.

2.3.3 Lentiviral transduction of primary T-cells

Primary T-cells were freshly isolated from PBMC for lentiviral transduction, using $CD4^+$ or $CD8^+$ MicroBeads as described in **Section 2.3.1**. Isolated T-cells were then plated in a 48 multiwell plate (at 0.5 × 10^6 cells/well) in 1 ml T-cell culture medium. T-cells were mixed with CD3/CD28 activation beads at 3 beads to 1 cell ratio, and incubated overnight at 37^{o}C. The next day 900 µl

of medium were aspirated from each well, and concentrated lentiviral particles were added (so that the total volume would not exceed 500 µl), together with 5 µg/ml polybrene (final concentration). On the following day 500 µl of T-cell transduction medium were added to each well. Half of the medium was replaced with fresh T-cell transduction medium three times a week, for the period of 14 days after transduction. During that period T-cells that had taken up lentivirus were selected (the timeline considerations for T-cell transduction are discussed in **Chapter 3**), and, on day 14, expanded with allogeneic feeders and PHA (as described in **Section 2.2.5**).

2.4 Electroporation of Cas9 ribonucleoprotein

When indicated, gene knockouts were achieved through transient delivery of Cas9 protein complexed with *in vitro* transcribed gRNA by electroporation (Neon® Transfection Device, Life Technologies). gRNAs templates were ordered as DNA oligonucleotides and were then used for PCR and *in vitro* transcription according to manufacturer's instructions (GeneArt Precision gRNA Synthesis Kit, Thermo Fisher). Purified gRNA was combined with recombinant Cas9 protein (GeneArt Platinum Cas9 Nuclease) and incubated at room temperature for 10 minutes prior to electroporation into Molt3 cells. Molt3 cells were washed three times with D-PBS and then combined with Cas9-gRNA complex, using 1.5 µg Cas9 protein with 350 ng gRNA for 2×10^5 cells in 10 µl. The following electroporation parameters were used: 1,700 V, 20 ms, 1 pulse. Thus electroporated cells were plated into pre-warmed, antibiotic free medium, and the knockout efficiency was determined after 7 days by flow cytometry.

2.5 Flow cytometry

2.5.1 Surface staining

20,000-50,000 cells were normally stained per tube. Cells were washed two times with PBS to remove the residual proteins from the medium, and then stained for 5 minutes at room temperature in the dark with LIVE/DEAD® Fixable Violet Dead Stain Kit (Thermo Fisher; further referred to as Vivid). Alternatively, LIVE/DEAD® Fixable Aqua Dead Stain Kit was used. After staining with Vivid, primary fluorochrome-conjugated antibodies (for staining of multiple cell surface proteins) or primary unconjugated antibodies (for single staining) were added to the cells, followed by 20 minutes of incubation on ice and in the dark. The cells were then washed twice with PBS (or FACS buffer, if secondary antibodies were used). If needed, secondary antibodies were added and incubated with cells for 20 minutes on ice and in the dark. The cells were subsequently washed twice with PBS and (if needed) fixed in the fixing buffer for 20

minutes on ice, followed by two washes with PBS. The events were then acquired on FACS Canto II (BD Biosciences) and analysed using FlowJo software (Tree Star, Inc.; Ashland, OR). Compensation was performed by single staining of anti-mouse Ig Compensation Particles (BD Biosciences).

The following gating strategy was used. Cells were gated using a typical lymphocyte gate based on forward and side scatters, followed by exclusion of doublets and dead cells. T-cells were then gated based on expression of a surface marker (typically rCD2, CD3, CD8 *etc.*) and analysed further if needed. All gates were set based on appropriate biological and fluorescence minus one controls. The representative gating strategy is shown in **Figure 2.1**. Typically at least 10,000 live events were acquired per sample.

Surface staining-based phenotyping was routinely used to confirm the identity of T-cell clones and lines prior to functional experiments. All the antibodies used are listed in **Table 2.5**.

Table 2.5 The list of antibodies used for flow cytometry staining. All the antibodies were raised in mouse and were reactive against human proteins, unless specified otherwise. [1]used in conjunction with secondary goat anti-mouse Ig, [2]used in conjunction with secondary rabbit-anti goat Ig.

Antibody target	Clone	Fluorochrome(s)	Manufacturer
CD1a	HI149	aPC-Vio770	Miltenyi Biotec
CD1b	SN13	PE-Vio770	Miltenyi Biotec
CD1c	AD5-8E7	FITC	Miltenyi Biotec
CD1d	51.1	APC	Miltenyi Biotec
(rat) CD2	OX-34	FITC, PE	Biolegend
CD3	BW264/56	PerCP, Pacific Blue	Miltenyi Biotec
CD4	M-T466	FITC, PE-Vio770, aPC	Miltenyi Biotec
CD8	BW135/80	PE, aPC, aPC-Vio770	Miltenyi Biotec
CD14	M5E2	Pacific Blue	Biolegend
CD19	HIB19	Pacific Blue, PE	Biolegend
Pan-αβ TCR	BW242/412	FITC, PE	Miltenyi Biotec
Pan-γδ TCR	11F2	FITC, aPC	Miltenyi Biotec
Vδ1 TCR	REA173	FITC	Miltenyi Biotec

Vδ2 TCR	123R3	FITC	Miltenyi Biotec
Vγ9 TCR	REA470	PE	Miltenyi Biotec
iNKT TCR	6B11	aPC	Miltenyi Biotec
HLA-A2	MCA2090F	FITC	Bio-Rad
HLA-ABC	W6/32	aPC	Biolegend
HLA-DR,DP,DQ[1]	Tu39	Unconjugated	Biolegend
CD107a	H4A3	FITC, PE	BD Biosciences
MIP-1β	D21-1351	PE	BD Biosciences
TNFα	cA2	PE-Vio770, PerCP	Miltenyi Biotec
IFNγ	45-15	aPC, PE-Vio770	Miltenyi Biotec
IL-2	MQ1-17H12	aPC	Biolegend
CD69	FN50	FITC	BD Biosciences
CD45RA	T6D11	PE-Vio770	Miltenyi Biotec
CCR7	REA546	PerCP-Vio770	Miltenyi Biotec
CD27	REA499	aPC	Miltenyi Biotec
PD-1	EH12.2H7	PE	Biolegend
NKG2D	1D11	aPC	Biolegend
MICA/B	6D4	PE	Biolegend
BTN3	BT3.1 (20.1)	PE	Biolegend
EPCR[2]	polyclonal	Unconjugated	R&D Systems
PE	PE001	Unconjugated	Biolegend
Mouse Ig	Polyclonal	PE	BD Biosciences
Goat Ig	Polyclonal	FITC	Abcam

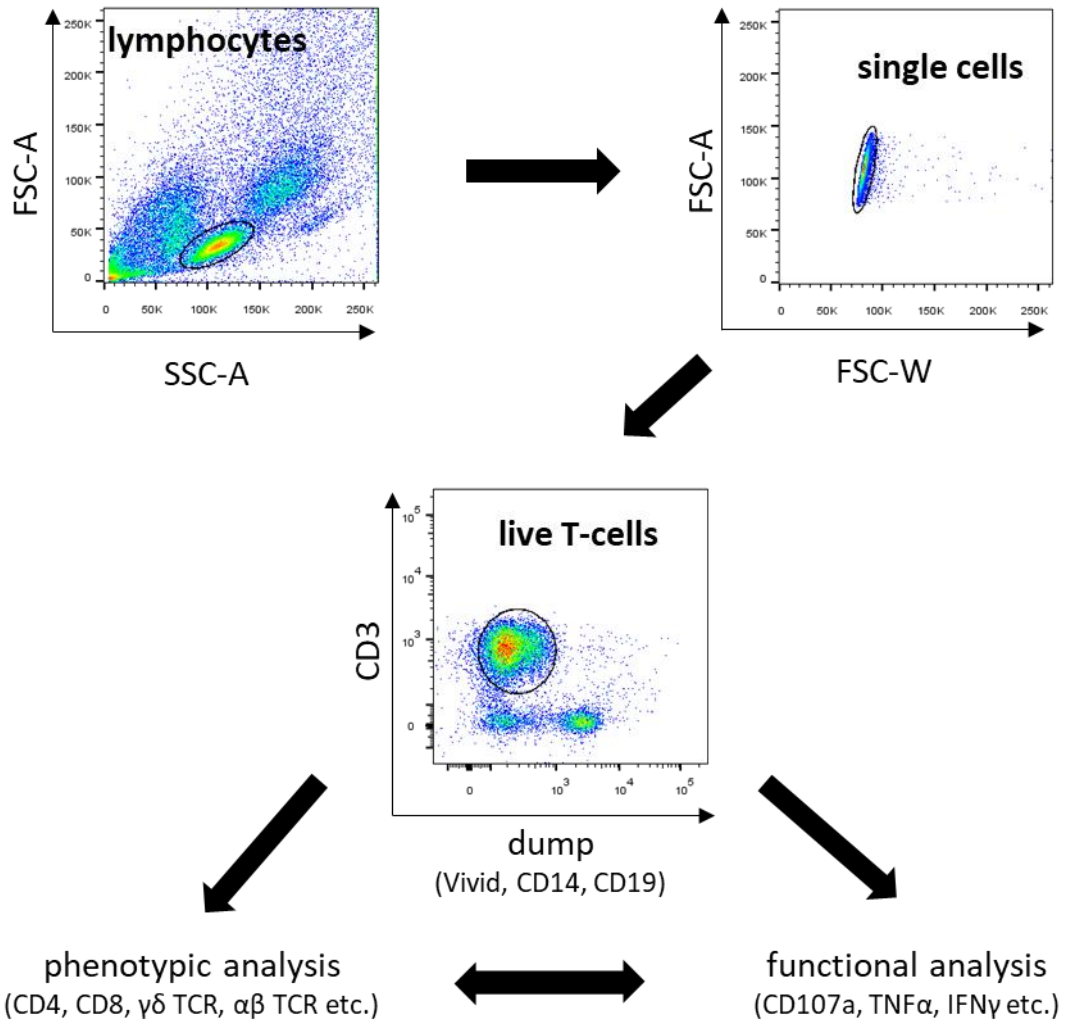

Figure 2.1 Gating strategy for phenotypic and/or functional analysis of T-cells by flow cytometry. The cells were first gated based on characteristic forward and side scatter properties of lymphocytes, followed by exclusion of doublets, and dead and/or $CD3^-$ cells. Thus gated $CD3^+$ cells were then analysed further based on phenotypic and/or functional markers. Representative plots for PBMC co-incubated with autologous tumour are shown. FSC-A – forward scatter-area; FSC-W – forward scatter-width; SSC-A – side scatter-area.

2.5.2 Tetramer staining

The biotinylated peptide-MHC (pMHC) monomers were produced in house as described before[160]. pMHC tetramers were assembled by co-incubation with streptavidin-PE at the molar ratio of 4:1 (pMHC monomer to streptavidin). Streptavidin-PE was added to pMHC monomers in 5 separate steps, each followed by 20 minutes incubation on ice.

For staining, T-cells were transferred to FACS tubes (normally 10^5 cells per stain) and washed with FACS buffer. All the centrifugation steps were conducted at 700 × g for 3 minutes. Cells

were then resuspended in 50 µl of FACS buffer, and 50 ul of 100 nM PKI (Protein Kinase Inhibitor; Dasatinib, Axon Medchen, Reston) solution was added, followed by 30 minutes incubation at 37^{o}C. PKI prevents signal transduction that would result from TCR engagement, and subsequent TCR-pMHC internalisation[321]. After 30 minutes incubation, 0.5 µg tetramer was added to cells (without washing off PKI), and the cells were incubated on ice for another 30 minutes. The cells were then washed twice with PBS and stained with Vivid as described in the **Section 2.5.1**. After staining with Vivid, cells were stained with primary fluorochrome-conjugated antibodies (avoiding PE and PE-based tandem dyes), as well as with primary anti-PE antibody. As demonstrated before by Tungatt *et al.*, addition of anti-fluorochrome antibody improves tetramer staining by stabilising the TCR-tetramer complex on T-cell surface[322,323]. After 20 minutes incubation on ice, the cells were washed twice with PBS and fixed with the fixing buffer prior to acquisition on FACS Canto II.

Apart from the cognate tetramer, the cells were always stained with an irrelevant tetramer, and with only the primary antibody cocktail as controls.

2.5.3 CD69 expression assay

CD69 is a well-validated early marker of activation of T-cells[324]. In our hands, it is also the most sensitive marker of activation of T-cell leukaemia line Jurkat (clone E6.1). In brief, Jurkat cells transduced with TCRs of interest (or untransduced) were incubated for 4 h or 24 h with non-specific stimuli (50 ng/ml PMA, 0.67 µM ionomycin), pan-TCR stimuli (CD3/CD28 activator beads) or cognate antigens of transduced TCRs. The cells were incubated either in R10 or T-cell priming medium. Following stimulation, the cells were washed 1X with PBS, and stained with Vivid and anti-CD69 antibody (clone FN50, BD Biosciences). The events were acquired on FACS Canto II.

2.5.4 Intracellular cytokine staining (ICS)

ICS was used to detect and characterise functional reactivity of T-cell clones and lines against a range of targets. In brief, T-cells were rested in R5 medium for 16-24 h before co-incubation with target cells. On day of the assay, T-cells were combined with target cells at 1:1 ratio (normally 50,000 T-cells per well in a 96 U-well plate), together with protein transport inhibitors brefeldin A and monensin (GolgiPlug™ and GolgiStop™, respectively; BD Biosciences) and anti-CD107a antibody. After 5 h of co-incubation, cells were washed 2X with PBS, and stained with Vivid and surface antibodies as described in **Section 2.5.1**. Following surface staining, cells were fixed and permeabilised using Cytofix/Cytoperm™ reagent (BD Biosciences), according to manufacturer's instructions. After permeabilisation the cells were stained intracellularly with anti-cytokine

antibodies (targeting TNFα, IFNγ, MIP-β and IL-2, or a combination thereof) for 20 minutes on ice. The cells were subsequently washed with PBS and acquired on FACS Canto II. Typically, at least 10,000 live $CD3^+$ events were acquired per sample. The gating strategy was described in **Section 2.5.1**.

2.5.5 Flow cytometry based activation assay

The following assay is a more time-efficient alternative to ICS – however, it can only be used for detection of activation markers CD107a and TNFα. As in case of ICS, T-cells were rested overnight in R5 medium which was followed by co-incubation with target cells at 1:1 ratio. At the start of co-incubation, anti-CD107a and anti-TNFα antibodies were added to the wells, together with 30 µM TNFα processing inhibitor (TAPI)-0 (Sigma Aldrich). TAPI-0 is a selective inhibitor of TNFα converting enzyme, thus inhibiting cleavage of TNFα from the plasma membrane and consequent release into the supernatant[325]. After 5 h of co-incubation, cells were washed 2X with PBS, and stained with Vivid and surface antibodies. After staining, the cells were washed again with PBS and acquired on FACS Canto II. Typically, at least 10,000 live $CD3^+$ events were acquired per sample. The cells prepared thus could also be live sorted on FACS Aria for cell culture or RNA extraction and TCR clonotyping. Contrary to ICS, this assay does not involve fixation and permeabilisation, thus resulting in intact cells.

2.5.6 Long term cytotoxicity assay

Flow cytometry based cytotoxicity assay was used to determine the minimal ratio of T-cells to target cells (effector:target ratio, E:T) that results in complete killing of target cells over a period of 7-21 days. In brief, target cells were plated in duplicate at the density of 50,000 cells/well (suspension cells were plated in 96 U-well plates, adherent cells were plated in 96 flat bottom plates). T-cells were added to target cells at desired E:T ratios (normally between 10:1 and 0.05:1) in a total volume of 200 µl of T-cell priming medium. Target cells were also plated without T-cells, to serve as a 100% survival control. Half of the medium was replaced twice a week. At the chosen time points (normally day 7, day 14 and day 21), the cells were harvested (in case of adherent cells), washed with PBS, and stained with Vivid and anti-CD3 antibody (to exclude T-cells). As an internal control, CountBright™ Absolute Counting Beads (Life Technologies) were added to each well prior to harvesting/washing (approximately 10,000 beads/well). The samples were the acquired on FACS Canto II, and at least 1,000 bead events were acquired per sample. The representative gating strategy is shown in **Figure 2.2**. The survival of target cells was calculated according to the following formula:

$$\%survival = \frac{experimental\ cell\ events/experimental\ bead\ events}{control\ \ cell\ events/control\ \ bead\ events} \times 100\%$$

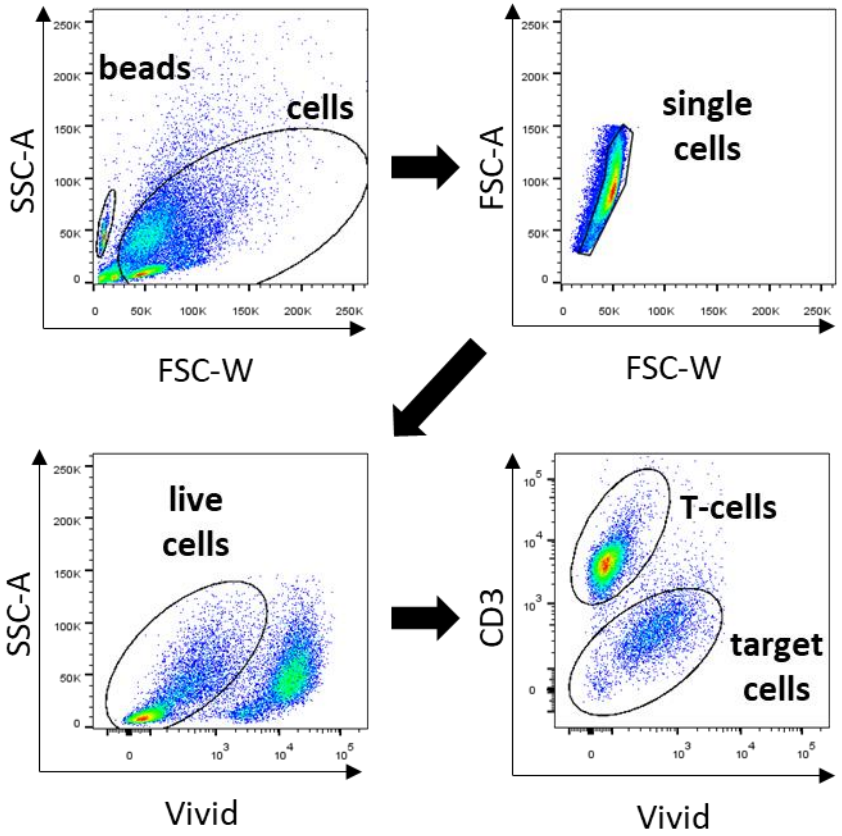

Figure 2.2 Gating strategy for long-term killing assays by flow cytometry. The cells were first gated based on forward and side scatters (with the voltage adjusted so that both T-cells and typically larger target cells could be captured). Counting beads were gated for normalisation and internal control. Doublets were then excluded, and live cells were gated. Thus gated cells were separated by CD3 expression into T-cells and target cells. The survival of target cells was calculated as described in the main body of the text. FSC-A – forward scatter-area; FSC-W – forward scatter-width; SSC-A – side scatter-area.

2.6 Chromium-51 release assay

Chromium-51 release assay was used to measure the short term cytotoxic activity of T-cell clones and lines against a range of target cells. Target cells harvested and washed 2X with D-PBS, and the dry pellets were labelled with ^{51}Cr (sodium chromate, Perkin Elmer) for 1 h at 37^{o}C (30 µCi per 10^6 cells). After labelling, the cells were washed with R0 and resuspended in R10 for leaching of excess ^{51}Cr. The leaching was performed for 1 h at 37^{o}C. Following leaching, the cells were washed with R10 and plated in 96 U-well plates (2,000 cells/well). T-cells were then added to labelled cells at desired E:T ratios, in a total volume of 150 µl R10. Target cells were also incubated with 5% Triton X-100 and medium only, to give total and spontaneous ^{51}Cr release values, respectively. After 4 h or 18 h co-incubation, 15 µl of supernatant was harvested and mixed with 150 µl of Optiphase Supermix Scintillation Cocktail (Perkin Elmer) in polyethylene

terephthalate plates (Perkin Elmer). The quantity of ^{51}Cr in the supernatants was indirectly measured in a 1450-Microbeta™ Counter (Perkin Elmer). The following formula was used to calculate the cytotoxic activity of T-cells:

$$\%lysis = \frac{experimental\ ^{51}Cr\ release - spontaneous\ ^{51}Cr\ release}{total\ ^{51}Cr\ release - spontaneous\ ^{51}Cr\ release} \times 100\%$$

2.7 Enzyme-Linked Immunosorbent Assay (ELISA)

ELISA was performed to detect T-cell activation to a range of stimuli, by measuring the concentration of secreted MIP-1β, TNFα or IFNγ, according to manufacturer's instructions (DuoSet® human ELISA kits, R&D Systems). T-cells were washed in R0 and rested in R5 medium for at least 24 h before co-incubation with stimuli. The co-incubation was conducted in 96 U-well plates for 18 h at 37°C, in 100 µl R5 medium (30,000 T-cells and 60,000 target cells per well). In parallel, a half area flat bottom 96 well plate (assay plate) was coated with 50 µl of mouse anti-human MIP-1β/TNFα/IFNγ capture antibody (1.5 µg/ml in PBS) and incubated overnight at room temperature. Following co-incubation, the plate containing T-cells was centrifuged (400×g, 5 minutes) and 50 µl of the supernatant was harvested (with care as not to harvest any cells) and diluted with 70 µl of R5. The assay plate was washed 3X with 190 µl wash buffer (0.05% Tween-20 in PBS) using an automated plate washer. The assay plate was then blocked with 150 µl of reagent diluent (1% BSA in PBS) for at least 1 h at room temperature. After blocking, the plate was washed and 50 µl of diluted supernatants were added. Recombinant standards for human MIP-1β/TNFα/IFNγ (diluted in reagent diluent for a range of concentrations from 1,000 to 15.6 pg/ml; R&D Systems) were also plated at 50 µl, used to plot a standard curve, and therefore accurately calculate the concentration of MIP-1β/TNFα/IFNγ in experimental samples. The plate with supernatants/standards was incubated at room temperature for 75 minutes and washed. Then, 50 µl of biotinylated anti-MIP-1β/TNFα/IFNγ detection antibody (50 ng/ml in reagent diluent) was added per well and the plate was incubated at room temperature for another 75 minutes. After the incubation, the plate was washed and 50 µl of streptavidin-horseradish peroxidase was added per well. Following 20 minutes of incubation in the dark, the plate was washed and 50 µl of colour reagents A and B (mixed in 1:1 ratio immediately before adding to the plate) was added. After the colours were sufficiently developed, the reaction was stopped by adding 25 µl of 2N sulphuric acid. The OD of each well was measured at 450 nm (with correction at 570 nm) in an iMark microplate reader (Bio-Rad).

2.7.1 Reagents used for treatment of target cells/T-cells

In some instances, target cells were pre-treated with zoledronic acid for 24 h, at 50 μM concentration. IPP (in MeOH) and HMBPP (in DMSO) were purchased from Sigma Aldrich. The target cells were also pre-incubated, when indicated, with the following antibodies: anti-BTN3 (clone 20.1; Biolegend) and anti-HLA ABC (clone W6/32; Biolegend). The pre-incubation was conducted for 30 minutes at 37^{o}C, at 10 μg/ml.

2.8 Enzyme-Linked ImmunoSpot (ELISpot)

IFNγ ELISpot was used to screen T-cell lines (in particular derived from T-cell libraries described in **Section 2.2.6**) for reactivity against target cell lines. T-cells were washed in R0 and rested in R5 medium for 24 h before co-incubation with target cells. MultiScreen™ 96-Well plates (EMD Millipore) were coated with 50 μl of mouse anti-human IFNγ capture antibody (mAb 1-D1K, MabTech; 10 μg/ml) for 18 h at 4^{o}C. The plate was then washed 4X with 200 μl PBS and blocked with 200 μl R10 for 1 h at room temperature. After blocking, T-cells (normally 50,000 per well) and target cells (no more than 30,000 adherent cells and 30,000 suspension cells) were added to the wells and incubated at 37^{o}C for 18 h. The plate was then washed 4X with PBS and incubated with 150 μl of ddH_2O for 10 minutes, followed by one wash with PBS and addition of 50 μl of biotinylated anti-IFNγ antibody (mAb7-B6-1, Mabtech; 1 μg/ml). The plate was incubated for 2 h at room temperature and washed 4X with PBS. Then, 50 μl of streptavidin-alkaline phosphatase was added to each well and incubated for 2 h at room temperature in the dark. Finally, the plate was washed 4X with PBS and incubated with 50 μl of detection reagent (Alkaline Phosphatase Conjugate Substrate Kit, Bio-Rad) per well. After the spots have developed, the reaction was stopped by washing the plate several times with tap water. The plate was then dried overnight and the wells were imaged using the ImmunoSpot® S6 Analyser.

2.9 TCR sequencing

2.9.1 RNA extraction

Total RNA from T-cell clones and lines was extracted using the RNEasy Mini/Micro Plus Kit (Qiagen). Briefly, cell pellet was resuspended in 350 μl of RLT Plus buffer (supplemented with 40 mM DTT) for lysis (alternatively, cells were directly sorted into the RLT Plus buffer). Genomic DNA was then eliminated by passing through gDNA Eliminator spin column, and 70% ethanol was added to the flowthrough at 1:1 ratio. RNA was then bound onto the RNEasy MinElute spin column, washed and finally eluted with 20 μl RNAse-free water. RNA was stored at -80^{o}C or used directly for cDNA synthesis. All the procedures that involved RNA handling were conducted in a

clean, RNAse-free space designated for RNA work, and filtered tips and RNAse-free reagents were used throughout the procedures to ensure no degradation of the sample, and to decrease the chances of contamination.

2.9.2 cDNA synthesis

cDNA synthesis was performed using the SMARTer™ (5' kit (Clontech), according to manufacturer's instructions. In brief, the reaction starts by priming the cDNA synthesis using an oligo (dT) primer which binds to the poly(A) tail of mRNA. The SMARTScribe reverse transcriptase then adds non-template residues to the first strand cDNA as it reaches the end of mRNA transcript. Finally, the SMARTer II Oligonucleotide anneals to the non-template residues on cDNA, and is then used as a template for extension of cDNA (template switching)[326]. Thus generated cDNA molecules contain a universal anchor at the 5' end.

2.9.3 PCR

PCR was designed to capture the whole variable region of the TCR chain (α, β, γ or δ) by using a set of forward primers binding to the universal anchor on every cDNA molecule, and a set of gene specific reverse primers binding to the constant regions of the TCR, thus allowing an unbiased amplification of the TCRs in the sample, regardless of their variable region. All the PCR and sequencing primers are listed in **Appendix Table 8.1.** No template controls (NTC) were set up alongside the samples to test for the presence of contaminations.

The composition of the 1st PCR reaction for TCR cDNA amplification was as follows:

5X Phusion® HF buffer (Thermo Scientific)	10 µl
DMSO	0.5 µl
dNTP (20 mM each)	1 µl
10X Universal primer mix (Clontech)	5 µl
Gene specific primer (10 µM)	1 µl
Phusion® HF DNA polymerase (Thermo Scientific)	0.5 µl
Nuclease-free H_2O	30 µl
cDNA template	2 µl

The composition of the 2st PCR reaction for TCR cDNA amplification was as follows:

5X Phusion® HF buffer (Thermo Scientific)	10 µl
DMSO	0.5 µl
dNTP (20 mM each)	1 µl

10X Short universal primer mix (Clontech)	1 µl
Gene specific primer (10 µM)	1 µl
Phusion® HF DNA polymerase (Thermo Scientific)	0.5 µl
Nuclease-free H_2O	34 µl
Sample after the 1st PCR	2 µl

The following cycling parameters were used for the 1st and 2nd PCR:

Initial denaturation:	94°C, 5 minutes	
Denaturation:	94°C, 30s	
Annealing:	60°C, 30s	30 cycles
Extension:	72°C, 45s	
Final extension:	72°C, 5 minutes	

2.9.4 Agarose gel electrophoresis

1% agarose gel was prepared from agarose powder (Invitrogen) dissolved in TE buffer. Midori Green DNA dye (GeneFlow) was added to the gel before casting. 5X DNA loading buffer (Bioline) was added to the PCR samples from **Section 2.9.3** and thus prepared samples were loaded onto the gel. A DNA ladder (1 kb DNA Ladder, Bioline) was run in parallel. The gels were run for 45 minutes at 80 V and then visualised under a LED illuminator (FastGene) to facilitate cutting out the DNA bands without the risk of UV-induced DNA damage. A representative gel for TCR clonotyping is shown in **Figure 2.3**. DNA was purified from the agarose slices using the NucleoSpin® Gel and PCR Clean-up Kit (Clontech), following manufacturer's instructions.

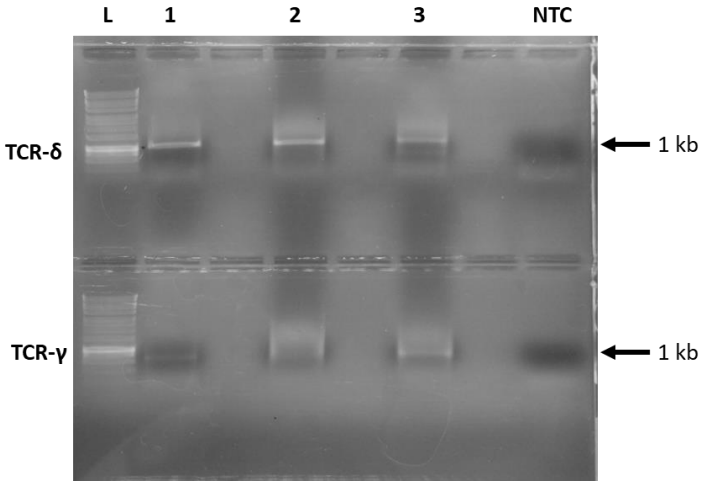

Figure 2.3 Agarose gel electrophoresis of PCR products for γδ TCR clonotyping. SMARTer™ RACE PCR products for TCR-δ and TCR-γ chains were run on 1% agarose gel, visualised and cut out of the gel. No product was observed in the no template control (NTC). L – 1kb DNA ladder; 1, 2 and 3 are representative γδ T-cell clones.

2.9.5 TOPO® cloning

Since the use of Phusion® DNA polymerase leads to blunt-ended PCR products due to polymerase's proofreading capability, the purified PCR products were cloned into the pCR™-Blunt II-TOPO® vector (Invitrogen), according to manufacturer's instructions. In brief, 2 µl of the purified PCR product were combined with 0.5 µl of Salt Solution and 0.5 µl of the vector, followed by 5 minutes of incubation at room temperature to allow the topoisomerase-I mediated ligation to take place. The ligation mixture was then added to OneShot™ TOP10 Chemically Competent *E.coli* (Invitrogen) and incubated on ice for 30 minutes. The cells were then subjected to 30 s heat shock at 42^{o}C followed by additional 2 minutes incubation on ice. Then, pre-warmed Super Optimal Broth (SOC, Clontech) was added, and the cells were moved to the orbital shaker for 1 h (37^{o}C, 220 rpm). Finally, the cells were plated on LB-agar plates containing 50 µg/ml kanamycin and incubated at 37^{o}C overnight.

2.9.6 Colony PCR

Bacterial colonies were screened for the presence of insert by colony PCR. The following MasterMix was prepared:

GreenTaq MasterMix (2X)	12.5 µl
M13 forward primer (10 µM)	1 µl
M13 reverse primer (10 µM)	1 µl
H_2O	10.5 µl
1 bacterial colony on a sterile P10 tip	

The following cycling programme was used:

Initial denaturation:	94^{o}C, 10 minutes	
Denaturation:	94^{o}C, 20s	
Annealing:	57^{o}C, 20s	30 cycles
Extension:	72^{o}C, 45s	
Final extension:	72^{o}C, 5 minutes	

The PCR reactions were run on 1% agarose gel at 80 V for 45 minutes. The colonies that contained an insert were sequenced using the PlateSeq Kit Clone service (Eurofins Genomics). At least 8 colonies were sequenced per TCR chain for TCR clonotyping.

2.9.7 TCR repertoire sequencing and analysis

PCR products amplified from sorted T-cell populations were prepared for next generation sequencing using NEBNext Ultra Library Preparation kit (NEB) to attach Illumina adaptors and sample specific barcodes to the PCR products. Thus prepared libraries were multiplexed and run on Illumina Miseq using MiSeq v2 kit (Illumina), with 2×250 bp paired end reads. Library preparation and MiSeq sequencing were performed in house by Cristina Rius and Meriem Attaf (Cardiff University).

2.10 Molecular cloning

2.10.1 Vector design

Genes to be expressed were cloned into the 3rd generation lentiviral vector pELNS, using XbaI and XhoI restriction sites (**Figure 2.4 A**). The expression of transgenes is driven by the elongation factor (EF)-1α promoter. The pELNS vector contains also the rCD2 marker gene separated from the transgenes of interest by a self-cleaving 2A sequence[327]. The marker gene is flanked by XhoI and SalI restriction sites, thus facilitating its removal if needed. In case of TCRs as transgenes, the individual chains (α and β, or γ and δ) are separated by another 2A sequence containing a unique restriction site for SmaI enzyme, thus ensuring stoichiometric expression of both TCR chains, and allowing for a rapid exchange of individual TCR chains if needed.

Gene to be knocked out were targeted by cloning of an oligonucleotide (serving as a template for gRNA) into the 2nd generation lentiviral vector pLentiCRISPR v2, using an Esp3I restriction site. The gRNA is transcribed from U6 RNA polymerase III promoter while the *Streptococcus pyogenes cas9* gene, linked *via* a 2A sequence with the *pac* marker gene, is transcribed from the short EF promoter (**Figure 2.4 B**). *Pac* gene encodes puromycin N-acetyltransferase which confers resistance to puromycin antibiotic.

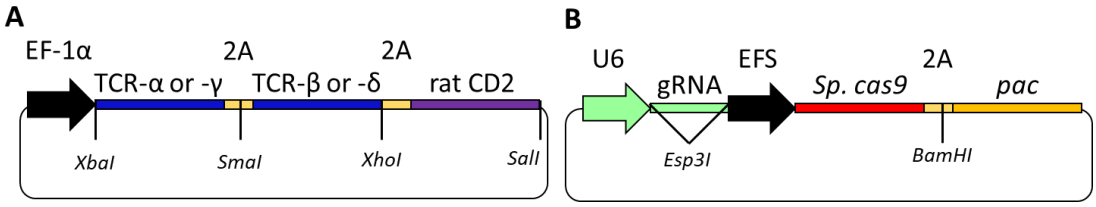

Figure 2.4 Schematic representation of lentiviral transfer plasmids pELNS (A) and pLentiCRISPR v2 (B). The promoters are shown as arrows while the transgenes are shown as bars. Unique restriction sites are marked with the name of restriction enzyme. EF-1α – elongation factor 1α; EFS – short elongation factor; pac – puromycin N-acetyltransferase.

2.10.2 Gene cloning into the pELNS vector

All the constructs to be expressed were codon optimised for *H. sapiens* expression, synthesised and cloned into the pUC57 vector (Genewiz). The protein sequences of all the constructs are listed in **Appendix Tables 8.2 and 8.3**. The vectors were digested for 1-2 h at 37^{o}C, and the composition of the reaction mixture was as follows:

Plasmid DNA	1 µg
10X FastDigest buffer (Thermo Scientific)	2 µl
XbaI (FastDigest, Thermo Scientific)	1 µl
XhoI (FastDigest, Thermo Scientific)	1 µl
Nuclease-free H_2O	to 20 µl

The digested plasmids were loaded directly onto a 1% agarose gel and run at 80 V for 1 h. The appropriate bands (~9 kb for pELNS backbone, ~2 kb for the insert; **Figure 2.5**) were cut from the gel, and DNA was extracted using the Wizard® SV Gel and PCR Cleanup System (Promega), according to manufacturer's instructions. The DNA was eluted in 20 µl nuclease-free water and the concentration of DNA was measured using the NanoDrop™ device (Thermo Scientific). The molar concentration of DNA was calculated according to the following formula:

$$^{ng}/_{\mu l}\ DNA \times \frac{fmol}{660\ fg} \times \frac{10^6 fg}{1\ ng} \times \frac{1}{N} = {}^{fmol}/_{\mu l}\ DNA,$$

where 660 $^{fg}/_{fmol}$ is an average molecular weight of a nucleotide pair, and N is the number of nucleotides.

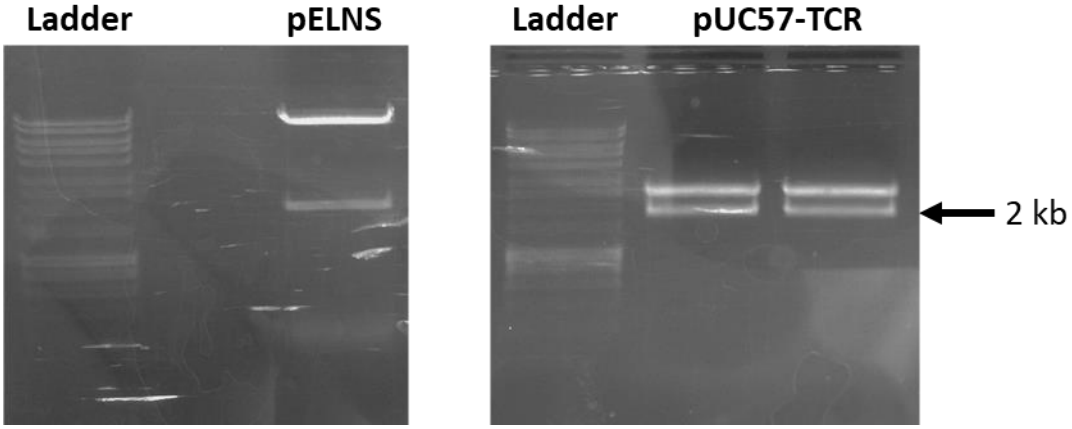

Figure 2.5 Agarose gel electrophoresis after a restriction digest of lentiviral transfer plasmid pELNS and construct plasmid pUC57 carrying a synthesised TCR of interest. Plasmids (1 µg) were digested for 1h with XbaI and XhoI enzymes. 9 kb band from pELNS vector (backbone) and 2 kb band from pUC57-TCR vector (construct) were cut out of the gel, purified and ligated.

The ligation reaction was set up as described below, and conducted for 2 h at room temperature. The combined volumes of insert and vector never exceeded 50% of the total reaction volume. As a control, ligation reaction was set up without an insert.

Vector	30 fmol
Insert	150 fmol
10X T4 DNA Ligase buffer (Thermo Scientific)	2 µl
T4 ligase	1 µl
Nuclease-free H_2O	to 20 µl

The ligation reaction was then used to transform chemically competent XL10-Gold® cells (Agilent Technologies). XL10-Gold® are endonuclease and recombination deficient – since all lentivirus-based vectors contain long terminal repeats, the vectors could recombine, and thus lose the insert, in recombination proficient strains. In brief, 5 µl of the ligation was added to 50 µl of XL10-Gold® cells, followed by incubation on ice for 30 minutes. The cells were subjected to heat shock for 30 s at 42^{o}C, and then were immediately placed on ice for subsequent 2 minutes. Then, 150 µl of pre-warmed SOC medium was added, and the cells were moved to an orbital shaker (37^{o}C, 220 rpm) for 1 h, followed by plating on ampicillin-containing (100 µg/ml) LB agar plates. Inverted plates were incubated overnight at 37^{o}C.

2.10.3 Oligonucleotide cloning into the pLentiCRISPR v2 vector

The gRNA sequences were designed using a free webtool (crispr.mit.edu). The 20 nt gRNA sequences (without PAM) were ordered as a pair of oligonucleotides (Eurofins Genomics) with Esp3I-compatible overhangs as shown below (Ns in Oligo F indicate nucleotides identical to target sequence but without PAM; Ns in Oligo R are complementary to corresponding nucleotides from Oligo F) .

Oligo F	*5'*	-	*CACCGNNNNNNNNNNNNNNNNNN*	-	*3'*
Oligo R	*3'*	-	*CNNNNNNNNNNNNNNNNNNNCAAA*	-	*5'*

All the gRNAs used are listed in **Appendix Table 8.4**. The oligo pair was phosphorylated and annealed as described below:

Forward oligo (100 µM)	1 µl
Reverse oligo (100 µM)	1 µl
10X T4 ligation buffer (NEB)	1 µl
Nuclease-free H_2O	6.5 µl
T4 polynucleotide kinase (NEB)	0.5 µl

The following cycling parameters were used for oligo phosphorylation and annealing:

Phosphorylation:	37°C, 30 minutes
Annealing:	95°C, 5 minutes
	Ramp down to 25°C at 5°C/minute

The transfer vector (lentiCRISPR v2) was digested and dephosphorylated for 1 h at 37°C.

Vector	5 µg
10X FastDigest Buffer (Thermo Scientific)	6 µl
FastDigest Esp3I (Thermo Scientific)	3 µl
FastAP (Thermo Scientific)	3 µl
100 mM DTT (freshly made)	0.6 µl
Nuclease-free H_2O	to 60 µl

The digested plasmid was run on 1% agarose gel, and the appropriate band was extracted as described in **Section 2.10.2.** The ligation was performed for 30 minutes at room temperature by combining the following reagents:

Digested vector	50 ng
Annealed oligo pair (diluted 1:200)	1 µl
2X Quick Ligase Buffer (NEB)	5 µl
Quick Ligase	1 µl
Nuclease-free H_2O	to 10 µl

The ligation was transformed into XL10-Gold® bacteria as described in **Section 2.10.2.**

2.10.4 Validation of the insert sequence

Bacterial colonies transformed with the pELNS vector were screened for the presence of insert by colony PCR. The following MasterMix was prepared:

GreenTaq MasterMix (2X)	12.5 µl
pELNS F1 primer (10 µM)	1 µl
pELNS R2 primer (10 µM)	1 µl
H_2O	10.5 µl
1 bacterial colony on a sterile P10 tip	

The following cycling programme was used:

Initial denaturation:	94^{o}C, 10 minutes	
Denaturation:	94^{o}C, 20s	
Annealing:	60^{o}C, 20s	30 cycles
Extension:	72^{o}C, 2 minutes	
Final extension:	72^{o}C, 5 minutes	

The PCR reactions were run on 1% agarose gel at 80 V for 30 minutes. The colonies that contained an insert were transferred to 5 ml of LB medium supplemented with 100 µg/ml ampicillin and grown overnight at 37^{o}C, 220 rpm. The plasmids were extracted from overnight bacterial cultures using the PureLink® Quick Miniprep Kit (Invitrogen), according to manufacturer's instructions. The purified plasmids were then sequenced using the pELNS F2 and R3 primers (Eurofins Genomics), and the sequencing result was aligned to the reference sequence (ApE, A plasmid Editor, M. Wayne Davis).

Since the size of insert for pLentiCRISPR v2 cloning was small (~20 bp), colony PCR was not performed. Instead, representative colonies were grown overnight in 5 ml LB medium with 100 µg/ml ampicillin, followed by plasmid purification (PureLink® Quick Miniprep Kit) and sequencing using GeCKO F1 primer (Genewiz).

2.10.5 Plasmid maxiprep

The plasmids containing correct inserts were transformed into XL10-Gold® bacteria and inoculated into 250 ml LB medium with 100 µg/ml ampicillin. The bacterial cultures were grown overnight at 37^{o}C, 220 rpm, and centrifuged at 4,000 × g for 10 minutes. The bacterial pellet was then resuspended in R3 buffer containing RNAse A (PureLink® HiPure Plasmid Filter Maxiprep Kit, Invitrogen), lysed using the pre-warmed L7 buffer, neutralised with N4 buffer and applied onto an equilibrated HiPure Filter Column. The column-bound plasmid was then eluted and precipitated using isopropanol (4,000 × g for 1 h at 4^{o}C), followed by washing with 70% ethanol. The purified plasmid pellet was then air-dried, resuspended in TE buffer and stored as aliquots at -20^{o}C. All plasmid maxipreps were tested for presence of correct insert by control restriction digest and Sanger sequencing.

2.11 CRISPR/Cas9 mediated gene knockouts

2.11.1 Genomic DNA extraction

Genomic DNA was extracted from 1-5 $\times$ 10^6 cells (clones and lines transduced with a single gRNA) or 30 $\times$ 10^6 cells (CRISPR/Cas9 libraries), using GenElute™ Mammalian Genomic DNA Miniprep Kit (Sigma Aldrich). The concentration of purified genomic DNA was measured on NanoDrop™ spectrophotometer, and the samples were stored at -20^{o}C.

2.11.2 PCR on genomic DNA

The PCR on genomic DNA was conducted either to amplify the integrated gRNA (for cells transduced with CRISPR/Cas9 libraries, and clones derived from the libraries) or to amplify the gene fragment where CRISPR/Cas9 mediated cleavage was expected to happen. The former PCR was conducted with generic primers binding to regions flanking gRNAs (integrated into the genome) while the latter PCR relied on primer pairs targeting a respective exon. The PCR reaction mixture and cycling parameters for amplifying gRNA are described below (in case of whole genome CRISPR/Cas9 libraries, additional considerations are discussed in **Section 2.12**). No template controls were set up alongside the samples to test for the presence of contaminations.

The following reaction components were used for the 1st PCR:

5X Herculase Reaction Buffer (Agilent)	10 µl
DMSO	1 µl
dNTP (25 mM each)	0.5 µl
GeCKO F1 primer (10 µM)	1 µl
GeCKO R1 primer (10 µM)	1 µl
Herculase II Fusion DNA polymerase (Agilent)	0.5 µl
Nuclease-free H_2O	to 50 µl
DNA template	2.5 µg

The following reaction components were used for the 2st PCR:

5X Herculase Reaction Buffer (Agilent)	10 µl
DMSO	1 µl
dNTP (25 mM each)	0.5 µl
GeCKO F2 primer (10 µM)	1 µl
GeCKO R2 primer (10 µM)	1 µl

Herculase II Fusion DNA polymerase (Agilent)	0.5 µl
Nuclease-free H_2O	to 50 µl
Sample after the 1st PCR	2 µl

The following cycling parameters were used for the 1st and 2nd PCRs:

Initial denaturation:	95°C, 5 minutes	
Denaturation:	95°C, 20 s	
Annealing:	60°C, 20 s	30 cycles
Extension:	72°C, 30 s	
Final extension:	72°C, 5 minutes	

2% agarose gel was prepared from agarose powder (Invitrogen) dissolved in TE buffer. Midori Green DNA dye (GeneFlow) was added to the gel before casting. 5X DNA loading buffer (Bioline) was added to the PCR samples and thus prepared samples were loaded onto the gel. DNA ladder (100 bp DNA Ladder, Bioline) was run in parallel. The gels were run for 45 minutes at 80 V and then visualised under a LED illuminator (FastGene) to facilitate cutting out the DNA bands without the risk of UV-induced DNA damage. A representative gel for gRNA amplification is shown in **Figure 2.6**. DNA was purified from the agarose slices using the QIAEX II Gel Extraction Kit (Qiagen), following manufacturer's instructions.

The extracted DNA was sequenced by Sanger sequencing (Eurofins Genomics) using GeCKO seq primer (in case of clones) or by NGS, as discussed in **Section 2.12.4**.

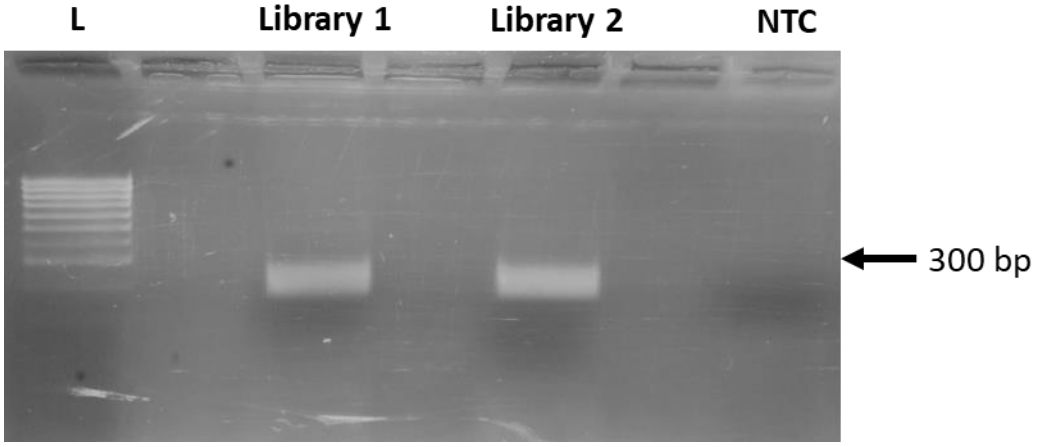

Figure 2.6 Agarose gel electrophoresis of PCR products for GeCKO v2 gRNA sequencing. The genomic DNA used as a template for the PCR was extracted from representative libraries which had undergone selection with T-cell clones/lines of interest. No product was observed in the no template control (NTC). L – 100 bp DNA ladder.

2.12 Whole genome CRISPR/Cas9 libraries

2.12.1 Library description

Human whole genome CRISPR/Cas9 library, termed GeCKO v2 (Genome-scale CRISPR Knock-Out, Addgene plasmid #1000000048, kindly provided by Feng Zhang[319]), was used in this study. The library is divided into two sub-libraries, A and B, which target every coding gene in human genome with 6 independent gRNAs (each binding to first 5' protein-coding exons of a given gene), as well as every miRNA with 4 gRNAs. The library contains also 1,000 gRNAs that do not target any region in human genome, to be used as controls for non-specific target cell survival. Since the pooled library contains >100,000 unique gRNAs, maintenance of the proper representation of gRNA population throughout the library preparation, screening and sequencing is crucial. In some instances, we made use of GeCKO v2 libraries already prepared in a form of target cell (courtesy of Paul Lehner, University of Cambridge, UK) or lentivirus (courtesy of John Phillips, University of Utah, UT). The following methods are based on guidance provided by Feng Zhang and colleagues on www.genome-engineering.org website, or recently published protocols[328].

2.12.2 Library amplification

The sub-libraries were amplified in ElectroCompetent Endura™ cells (Lucigen), by transforming 100 ng library/25 µl cells (5 transformations per sub-library). In brief, bacteria together with plasmid libraries were pulsed at 1,800 V (Bio-Rad MicroPulser™, programme Ec1). Immediately after the pulse, 975 µl of room-temperature Recovery Medium (Lucigen) was added, and the transformed bacteria were moved to a 15 ml tube containing 1 ml of Recovery Medium. The bacteria were then transferred to an orbital shaker (37^{o}C, 250 rpm) for 1 h, followed by plating on LB agar plates containing 100 µg/ml ampicillin. Each sub-library was plated on 20 Petri dishes. In order to calculate transformation efficiency, an aliquot of transformed bacteria was diluted 40,000X and plated on a separate Petri dish. The plates were placed at 32^{o}C for 14 h, and the number of colonies on the dilution plate was counted. The transformation was considered successful if more than 75 colonies were present on each dilution plate (thus giving an average of 3×10^6 colonies per sub-library, and therefore 50X coverage of gRNAs). The transformed bacteria were then harvested from plates and the plasmid DNA was extracted using the PureLink® HiPure Plasmid Filter Maxiprep Kit (Invitrogen), as described in **Section 2.10.5**. No more than 500 mg of bacterial pellet was applied on an individual HiPure Filter column. The starting library aliquots, as well as ready to use lentivirus, were kindly provided by John Phillips (University of Utah, UT).

2.12.3 Library setup and screening

Before transducing the GeCKO v2 library into a new cell line for the first time, the cell line's sensitivity to puromycin was determined. In brief, 1×10^6 cells were plated per well in a 12-well plate. After 24 h, puromycin (Thermo Scientific) was added to the medium at concentrations between 0.1 and 10 μg/ml. The cells were incubated with the antibiotic for 3 days, and then they were detached and re-plated. The cells were detached again 24 h afterwards, and counted by trypan blue exclusion. The lowest concentration of puromycin that resulted in no cell survival was chosen to be used for selection of cells transduced with GeCKO v2 library.

Every stock of GeCKO v2 lentivirus was titrated in target cell lines so that the infection would happen at MOI≈0.4 (thus decreasing the possibility of transducing a single cell with more than one viral particle). In brief, 3×10^6 cells (per well in 6-well plate) were transduced with 0, 25, 50 and 100 μl of lentiviral stock in presence of 8 μg/ml polybrene by spinfection ($500 \times$ g, 2 h). 18 h post infection, the medium was replaced. After 2 days, the cells were split between 2 wells, and puromycin was added to one of the wells. 3 days later, the cells were harvested and re-plated. On the following day, the cells were harvested again and counted. The MOI was calculated according to the formula shown below:

$$MOI = \frac{number\ of\ viable\ cells\ treated\ with\ puromycin}{number\ of\ viable\ cells\ not\ treated\ with\ puromycin}$$

The volume of lentivirus that resulted in MOI between 0.3 and 0.5 was chosen for transduction of the library.

Each GeCKO v2 sub-library was transduced into at least 20×10^6 target cells (thus giving >100X coverage of each sub-library if MOI=0.3-0.5). Thus transduced cells were cultured for 14 days before starting the selection. On day 14, half of the cells from each sub-library were frozen down while the rest was used for screening by co-incubation with T-cell clones and lines. At least 6×10^6 target cells per sub-library were used for screening, to ensure >100X coverage of the library. For screening, 50,000 of target cells were plated in a 96-well plate (flat bottom for adherent cells, U-bottom for suspension cells) in T-cell priming medium, together with T-cells at a defined E:T ratio. In parallel, several wells were set up to contain untransduced target cells to serve as control of the E:T ratio (i.e. to ensure that all the target cells are killed by T-cells at a chosen ratio, thus preventing non-specific survival). After 14 days of co-incubation, surviving target cells were pulled together and re-plated with T-cells at an E:T ratio 2 times higher than the initial one used for screening. After the second round of selection the target cells were cultured to ensure

sufficient cell number for sequencing and functional assays. The practical considerations for GeCKO v2 library screening with cytotoxic T-cells are discussed in more detail in **Chapter 5**.

2.12.4 Library sequencing

The libraries after T-cell selection were initially sequenced as described in **Section 2.11.2**, the rationale being that a successful T-cell selection resulted in survival in only a limited number of cells, and that such representation can be efficiently captured by sequencing only a fraction (5%, normally 2.5 µg) of genomic DNA and sample multiplexing on MiSeq (Illumina). Thus prepared samples were then barcoded and sequenced as described in **Section 2.9.7**.

When indicated, both the control and selected libraries were sequenced exhaustively – i.e. the PCR was performed on the entirety of isolated genomic DNA, using the parameters listed below.

The following reaction components were used for the 1st PCR. A sufficient number of separate reactions was set up to process genomic DNA isolated from at least 20×10^6 cells per sub library. The primer sequences are shown in **Appendix Table 8.5**.

NEBNext High Fidelity PCR Master Mix 2X (NEB)	25 µl
Adaptor F (10 µM)	2.5 µl
Adaptor R (10 µM)	2.5 µl
Genomic DNA	2.5 µg
H_2O	to 50 µl

All the reactions set up from the same genomic DNA sample were then pooled and used as a template for the second PCR. The primers used for the 2nd PCR contain Illumina chip binding adaptors; additionally, Illumina F01-04 primers contain staggers to increase the diversity of the sequenced library while Illumina R primers contain sample specific barcodes. All primers used were purified by HPLC.

NEBNext High Fidelity PCR Master Mix 2X (NEB)	25 µl
Illumina F01-04 (10 µM)	2.5 µl
Illumina R, barcoded (10 µM)	2.5 µl
PCR product	2.5 µl
H_2O	to 50 µl

The following cycling parameters were used for both the 1st and 2nd PCR.

Initial denaturation:	98°C, 30 s
Denaturation:	98°C, 10 s
Annealing:	60°C, 10 s
Extension:	72°C, 15 s
Final extension:	72°C, 2 minutes

The 1st PCR was run for 18 cycles, the 2nd PCR for 24 cycles. The resulting PCR products were then run on 2% agarose gel and extracted as described before. HiSeq sequencing was performed either at University of Cambridge (courtesy of Paul Lehner) or University of Utah (courtesy of John Phillips), with 80 cycles of read 1 and 8 cycles of index 1. Where indicated, the number of reads for each gRNA was normalised using the following formula:

$$normalised\ gRNA\ count = \frac{number\ of\ reads\ per\ given\ gRNA}{number\ of\ reads\ in\ the\ sample} \times 10^6$$

2.13 RNAseq

The transcriptomes of test *vs.* control cells were compared by RNAseq. In brief, total RNA was extracted from 5×10^6 cells using the RNEasy Plus Mini kit (Qiagen), following manufacturer's instructions. The quality and quantity of extracted RNA was determined using 2100 Bioanalyser Instrument (Agilent Technologies). The RNAseq was performed, and data analysed, at the University of Utah (courtesy of John Phillips and Colin Farrell).

2.14 Data analysis

The graphical representations of structural data (deposited at Protein DataBase) were generated using the PyMOL software (The PyMOL Molecular Graphics System, Version 1.8 Schrödinger, LLC.).

The polyfunctionality plots were generated as follows. First, the flow cytometry data were analysed in FlowJo software by sequential gating (to identify T-cells) and Boolean gating (to identify T-cells positive for a given function, or a combination thereof). Thus prepared data were exported to Pestle software and converted to a format recognised by SPICE (Simplified Presentation of Incredibly Complex Evaluations; courtesy of Mario Roederer, NIH) software which was used for the graphical representation of polyfuctionality[329].

The NGS data for TCR repertoire sequencing were analysed in MiXCR software (courtesy of Meriem Attaf and Cristina Rius, Cardiff University). The TCR repertoire data were filtered to remove the reads fulfilling the following quality criteria: low quality of read (lower than Q30), TCRs represented by five reads or less, and TCRs containing CDR3 sequences shorter than 21 nucleotides. The NGS data for GeCKO v2 libraries were analysed in a bespoke web tool (courtesy of Barbara Szomolay, Cardiff University). R software was used for graphical representation of NGS data.

Unless specified otherwise, all other data were analysed in GraphPad Prism software.

3. CRISPR-mediated TCR replacement generates transgenic T-cells with superior anticancer reactivity

3.1 Background

Cancer-specific T-cells exist in virtually every immunocompetent individual, and can be specifically enriched at the tumour site (i.e. tumour infiltrating lymphocytes, discussed in more detail in **Chapter 1**). However, in case of most cancer types, aside from melanoma and few other highly immunogenic cancers, the *in vitro* expansion of sufficiently high numbers of TILs that would confer strong anticancer reactivity has not yet been possible. Furthermore, the tumour microenvironment may be preferentially enriched in regulatory T-cells, the presence of which correlates with poor clinical outcome[330], plausibly due to exerting *in situ* immunosuppression. Regulatory T-cells are therefore undesirable in anticancer TIL infusion products.

Genetic engineering of peripheral T-cells to confer them with anticancer specificity is a clinically relevant alternative to naturally cancer-reactive TILs. Genetic redirecting of peripheral T-cells for clinical application has so far been achieved by transduction of either a CAR or an αβ TCR. While CAR therapy targeting CD19 has shown a particular promise in treating $CD19^+$ blood cancers[331], usage of CAR-modified T-cells for solid tumours has so far led to an underwhelming clinical efficacy, possibly due to issues with tumour homing and persistence of the infusion product[332]. On the other hand, TCR-redirected T-cells have been successfully used for treatment of solid tumours, for example melanoma and synovial cell sarcoma[198,333,334]. It should also be noted, as discussed in **Chapter 1,** that CARs can only target surface-expressed molecules while TCR targets additionally encompass intracellular proteome and metabolome.

Current TCR-based therapies involve transducing an αβ TCR of choice (either natural or affinity-enhanced[259]) into αβ T-cells. The advantages of this approach are twofold – first, αβ T-cells vastly outnumber their γδ counterparts in the periphery, making them easily accessible; and second, αβ T-cells express the necessary co-receptors (either CD8 or CD4) that greatly enhance targeting of cognate antigens (either presented by MHC I or II, respectively) by a given αβ TCR[335]. However, αβ T-cells already express endogenous TCRs. Therefore, transducing an exogenous αβ TCR may result in expression of up to four distinct receptors in a single cell: the transgenic TCR, the endogenous TCR, and mixed dimers formed by mispairing of the endogenous and transgenic receptors. These mixed dimers harbour specificities that are fundamentally unpredictable, and in some cases have been shown to lead to fatal autoreactivity[199,200]. Moreover, every TCR molecule needs to associate with CD3 complex in order to be surface expressed, and

consequently to be functionally reactive. Indeed, the quantity of CD3 has been shown to be the rate limiting factor for TCR surface expression[336]. Consequently, a therapeutically relevant transgenic TCR (be it an αβ or a γδ TCR) needs to successfully compete with endogenous TCRs for CD3 binding and surface expression[209].

Several methodologies have been proposed to overcome, or alleviate, the issue of TCR competition and mispairing in context of αβ TCR transfer. These approaches involve engineering of the variable domains of TCR in order to enhance its affinity for cognate antigens[259], modifications of the constant domain to reduce pairing between the endogenous and transgenic TCRs[337–341], design of single chain TCR constructs[342] or overexpression of CD3 polypeptide chains[336]. Indeed, affinity-enhanced TCRs showed promising clinical efficacy, since even a sub-optimal quantity of TCR molecules on cell surface is sufficient to convey antigen-specific activation due to super-physiological affinity[343]. However, engineered TCRs bypass thymic selection, and therefore may show reactivity to self-antigens that is difficult or impossible to predict. By way of example, the enhanced-affinity TCR targeting a cancer epitope derived from MAGE A3 protein proved to cross-react with a titin-derived epitope expressed solely in adult heart, thus leading to fatal autoreactivity in both patients treated with this TCR[202,344].

3.1.1 Aims

Competition with endogenous TCRs for surface expression and TCR chain mispairing represent substantial potential problems during TCR gene transfer therapy. I aimed to develop a strategy to mitigate these potential problems that could be applied to any TCR. I hypothesised that CRISPR/Cas9 mediated knockout of the endogenous αβ TCR, simultaneous with the transfer of an αβ/γδ TCR of choice, so-called TCR replacement, would result in superior functional activity of thus engineered primary $CD4^+$ and $CD8^+$ T-cells. From our previous experience I knew that some TCRs, in particular γδ TCRs, poorly compete with endogenous αβ TCRs for surface expression. Therefore, developing a system that would improve the expression and functional reactivity of transduced TCRs would be of great interest to researchers, both from the perspective of fundamental research (i.e. new antigen discovery), as well as a pre-clinical proof of concept study. Specifically, my aims were:

- To design new gRNAs targeting *trbc* gene segments that would lead to high knock-out efficiency of endogenous TCRs but would not affect the transduced (codon-optimised) TCR chains;
- To develop a simple transduction system for simultaneous TCR knock-out/knock-in;
- To functionally characterise and compare T-cells transduced with both TCR and CRISPR *versus* TCR only;

- To compare the reactivity of T-cells transduced with only a phosphoantigen-specific γδ TCR *versus* TCR+CRISPR, against a panel of haematological malignancies, as a proof-of-concept for using transduced γδ TCRs in pan-population immunotherapy.

The results from this Chapter formed the basis of a manuscript submitted to ***Blood*** and entitled "**CRISPR-mediated TCR replacement generates superior anticancer transgenic T-cells"** (**Legut** *et al.*, re-submitted after revision, September 2017).

3.2 Results

3.2.1 Design of gRNAs targeting trbc1 and trbc2 gene segments

Human TCR-β locus contains over 40 highly diverse *trbv* gene segments but only two highly homologous *trbc* gene segments. Therefore, targeting the shared sequence between both *trbc* segments with CRISPR/Cas9 system was chosen as a feasible option for disruption of the TCR-β gene, and consequently for abrogation of expression TCR-β protein and αβ TCR heterodimer expression. I designed four distinct guide RNAs that targeted both *trbc1* and *trbc2* gene segments, binding to the 5' end of the first *trbc* exon. Importantly, since I wanted to express not only transgenic γδ TCRs but also αβ TCRs in TCR-β knock-out cells, the gRNAs were designed so that there would be multiple mismatches between the gRNA and codon-optimised TCR-β sequence (while retaining 100% match for both natural *trbc* segments). In particular, mismatches between the gRNA and codon-optimised TCR sequence were desirable at the 3' end, since the CRISPR/Cas9 system may tolerate single/double mismatches at the 5' end but requires perfect match at the 3' end[345]. The alignments of gRNAs with natural and codon optimised *trbc* sequences are shown in **Figure 3.1 A.** The gRNAs, together with *cas9* and puromycin resistance gene, were lentivirally transduced into TCR-proficient Jurkat T-cell leukaemia line for validation of knock-out efficiency. As shown in **Figure 3.1 B**, all four gRNAs resulted in 90-95% knock-out efficiency, in terms of detectable surface expression of αβ TCR-CD3 complex. I chose gRNA 1 to be used for genome editing in primary T-cells, due to high degree of mismatches between the gRNA sequence and codon-optimised TCR-β sequence (5/20 mismatches, including 2 mismatches at the 3' end).

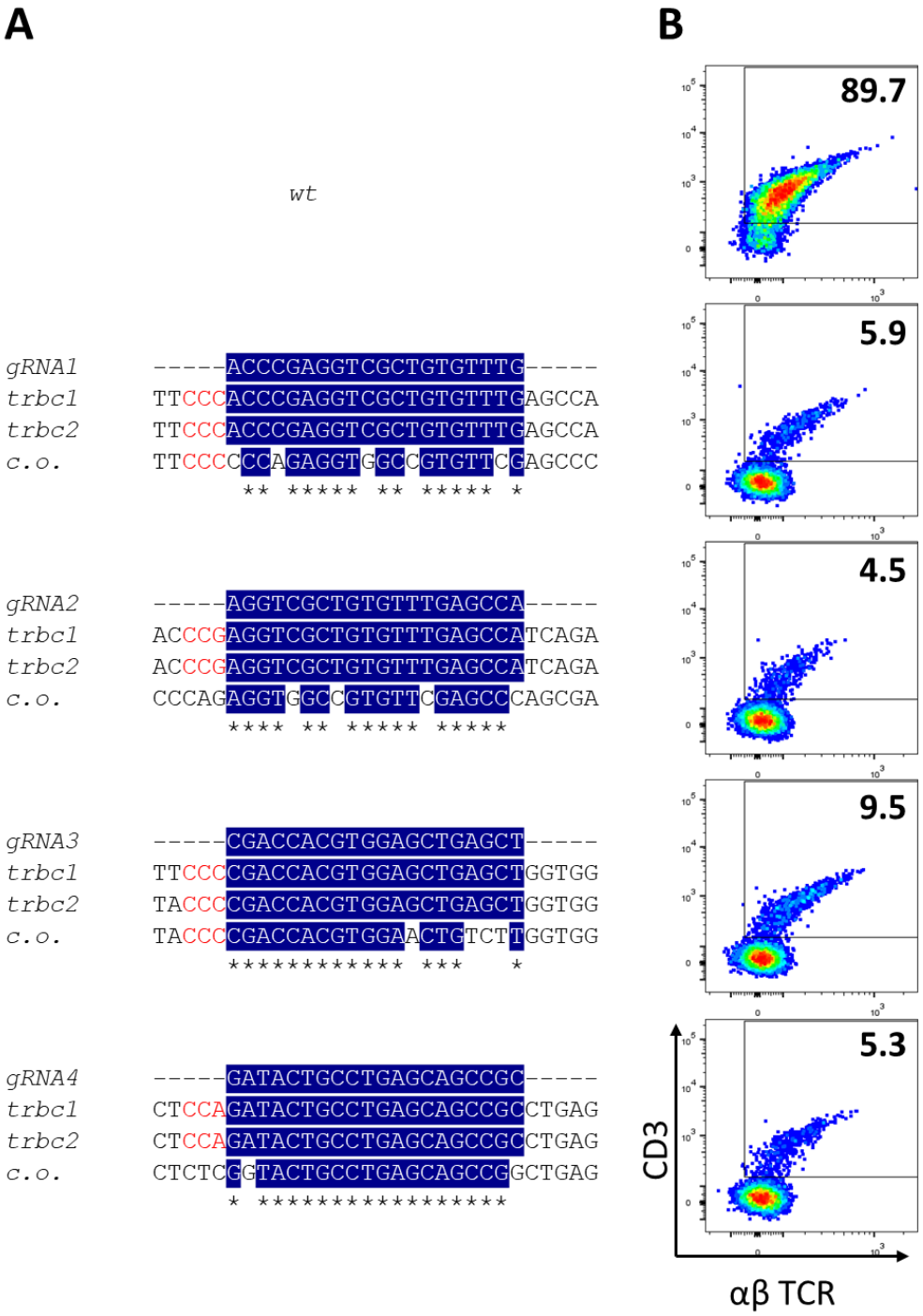

Figure 3.1 Guide RNA design for targeting of *trbc* gene segments. (**A**) gRNAs were designed to perfectly match both *trbc1* and *trbc2* gene segments while avoiding a perfect match with the codon optimised (c.o.) variant of the TCR-β constant domain commonly used in TCR transduction. Nucleotide matches are highlighted in blue and indicated with an asterisk while the protospacer adjacent motif (PAM) is shown in red. The gRNA sequences are shown in reverse. (**B**) Staining of Jurkat cell line for αβ TCR and CD3 complex, either wild type (wt) or transduced with gRNA 1-4, as indicated in panel **A**. Only viable cells were included in the gating. The numbers on dot plots correspond to percentage of αβ TCR-CD3^{+} cells.

3.2.2 TCR-β knock-out in Jurkat improves the magnitude of response to antigen

I first tested the effect of TCR-β knock-out on antigen response of Jurkat cells transduced with a phosphoantigen-specific Vγ9Vδ2 TCR (further referred to as γδ20 TCR). The γδ20 T-cell clone was derived from peripheral blood of a healthy donor based on the response to HMBPP. Jurkat cells are commonly used as a proxy system for studying TCR mediated cell activation, using IL-2 secretion[346] or CD69 upregulation[106,124] as a read-out for activation. Since Jurkat cells produced scant quantities of IL-2 in response to TCR stimuli in our hands (**Appendix Figure 8.1**), I focused on CD69 upregulation as a readout of TCR-specific activation. I compared the activation of Jurkat cells (untransduced, transduced only with γδ20, transduced only with TCR-β CRISPR, or with both TCR and CRISPR) in response to 1 μM HMBPP (cognate antigen of Vγ9Vδ2 TCRs), CD3/CD28 Activator beads (pan-TCR specific stimulus), or PMA/ionomycin (stimulus acting downstream of TCR signalling pathway). The stimulation was conducted for 4 h or 16 h (**Figure 3.2 A,** upper and lower panel, respectively). As expected, all transductant versions of Jurkat responded to non-TCR specific stimulation (PMA/ionomycin), and all TCR-proficient transductants (i.e. apart from Jurkat + CRISPR only) responded to pan-TCR stimulus (CD3/CD28 beads). Only γδ20 TCR-expressing Jurkat responded to HMBPP – and the response of TCR+CRISPR transduced cells was considerably stronger than that of TCR only transduced cells. Despite CD69 being an early marker of activation[324], I detected stronger upregulation of CD69 expression in response to stimuli after 16 h incubation than 4 h incubation. I therefore chose 16 h timepoint for measuring the relative sensitivity of TCR transductants to the cognate antigen HMBPP. As shown in **Figure 3.2 B**, TCR+CRISPR transduced Jurkat exhibited stronger CD69 expression upon antigen stimulation than TCR only transduced Jurkat. The increase in the magnitude of response did not translate though to increased antigen sensitivity as both transductants exhibited similar EC_{50} of HMBPP (in sub-micromolar range). Jurkat cells express only one TCR clonotype and therefore TCR competition may not play an important role in these cells. Therefore, I decided to compare the effect of TCR transduction and TCR replacement in the more sensitive and clinically relevant system of primary T-cells derived from peripheral blood.

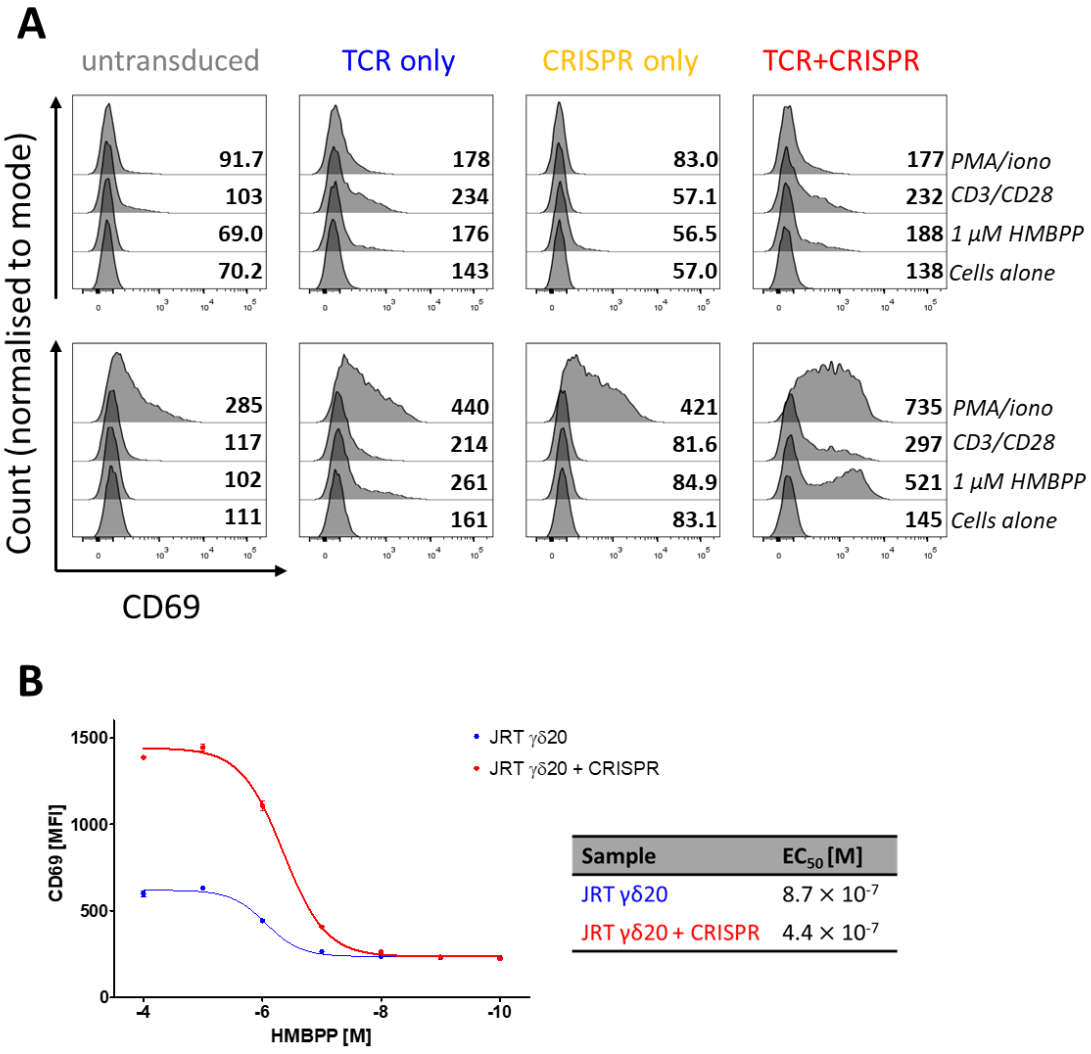

Figure 3.2 Quantification of CD69 expression as a marker of Jurkat activation. (**A**) Jurkat cells, untransduced (grey) or transduced with γδ20 TCR only (blue), TCR-β CRISPR only (orange) or both γδ20 TCR and CRISPR (red), were activated for a period of 4 h (top panel) or 16 h (bottom panel) with 1 µM HMBPP (cognate antigen), pan-TCR activator (CD3/CD28 beads), or a TCR-independent stimulus (PMA+ionomycin). The colour coding is maintained throughout the Chapter. The numbers on histograms correspond to geometric mean fluorescence intensity (MFI) of CD69 staining. Only viable cells were included in the analysis (in case of TCR-transduced Jurkat, additional gating was performed to include only $rCD2^+$ cells). (**B**) Jurkat cells (either transduced with γδ20 TCR alone or in combination with TCR-β CRISPR) were stimulated for 16 h with titrated concentrations of HMBPP, followed by CD69 surface staining. MFI values were fitted with non-linear regression curve to calculate the EC_{50} values. Error bars represent standard error of the mean. The representative data from two independent experiments carried out in duplicate are shown.

3.2.3 Co-delivery of TCR and CRISPR/Cas9 to primary T-cells

Primary T-cells are generally considered to be difficult to transduce by lentivirus – however, the transduction efficiency increases significantly if T-cells are actively dividing (i.e. as a response to TCR and co-stimulatory signalling)[347]. The most common method for inducing T-cell activation (in context of lentiviral transduction) is using CD3/CD28 activator beads (which deliver both TCR and co-stimulatory signal at the same time). However, prolonged culture of T-cells requires supplementation of media with cytokines IL-2 (and optionally IL-15) – and these cytokines lead to loss of CD28 expression on T-cells[348]. The other method for induction of T-cell division is using PHA and allogeneic irradiated feeders (again, to deliver both primary TCR signal, and co-stimulatory signals). The feeder cells can, however, take up lentivirus themselves, thus drastically decreasing the transduction efficiency of T-cells. For the reasons described above I decided to conduct simultaneous transduction of freshly isolated T-cells (pre-activated with CD3/CD28 beads for 24 h) with both TCR and CRISPR/Cas9 encoding lentiviruses. This approach offers the added advantages of simplicity and time-efficiency as only one stimulation and transduction event is required. This methodology is also compatible with any TCR-encoding lentiviral vector and so can be applied in conjunction with existing tools. T-cells engineered by this methodology can also be selected based on marker genes encoded in each lentivirus, producing >95% pure populations that are ready for functional testing as early as 14 or 28 days after the initial transduction (**Figure 3.3 A**). It should be noted that selection of transduced cells based on rat CD2 expression (and puromycin resistance, where applicable) may lead to recovery of less than 10% of starting cell population (**Figure 3.3 B**). Nevertheless, selected transduced cells are capable of expanding equally well as the untransduced cells for at least five consecutive series of T-cell expansions with allogeneic feeders and PHA (**Figure 3.3 C**).

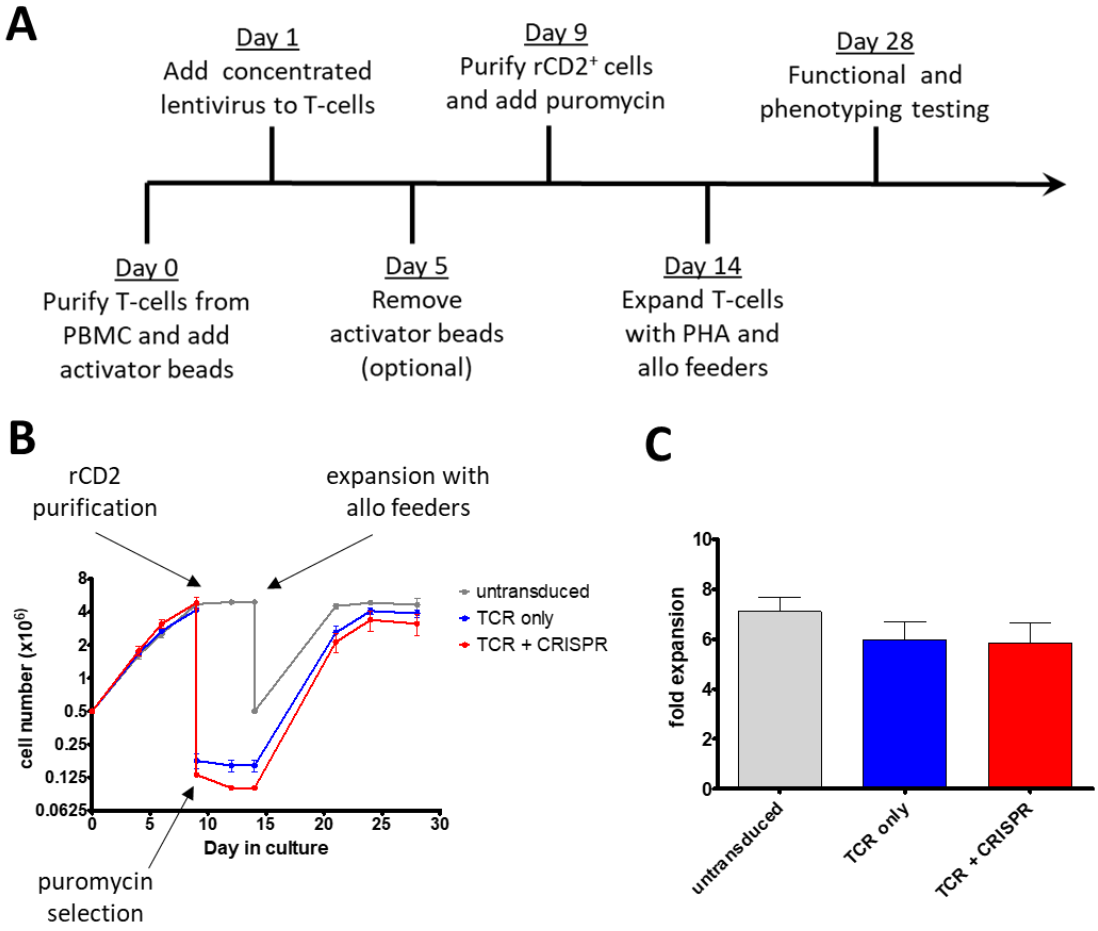

Figure 3.3 Design of a simple system for simultaneous TCR knock-in/knock-out in primary T-cells. (**A**) Timeline for the TCR replacement methodology in primary T-cells. (**B**) Kinetics of T-cell expansion. 5×10^5 T-cells were expanded with CD3/CD28 beads for 14 days. On day 9, TCR-transduced cells were purified based on rCD2 expression and then cultured in presence of 2 μg/ml puromycin (TCR-β CRISPR only). On day 14, all the transduced cells or 5×10^5 untransduced cells were expanded with allogeneic irradiated feeders and PHA. Cells were counted every 2-4 days by trypan blue exclusion. (**C**) Transduced or untransduced T-cells were routinely expanded with allogeneic irradiated feeders and PHA, and the number of viable cells before and after expansion was used to calculate the fold expansion. Standard error of the mean is shown for three donors.

As shown in **Figure 3.4** , the genome editing in T-cells transduced with both TCR and CRISPR/Cas9 lentiviruses followed by selection of cells that had taken up lentiviral cargo is highly efficient. As an example, I used αβ $CD8^+$ T-cells transduced with a γδ TCR. While transduction of these T-cells with the γδ TCR alone resulted only in a minor downregulation of the endogenous αβ TCR, CRISPR/Cas9 co-transduced cells were mostly negative in terms of detectable surface expression of their endogenous αβ TCR. Similar efficiency of TCR knock-out was observed in all the donors tested, thus highlighting the versatility and applicability of the CRISPR/Cas9 mediated TCR replacement.

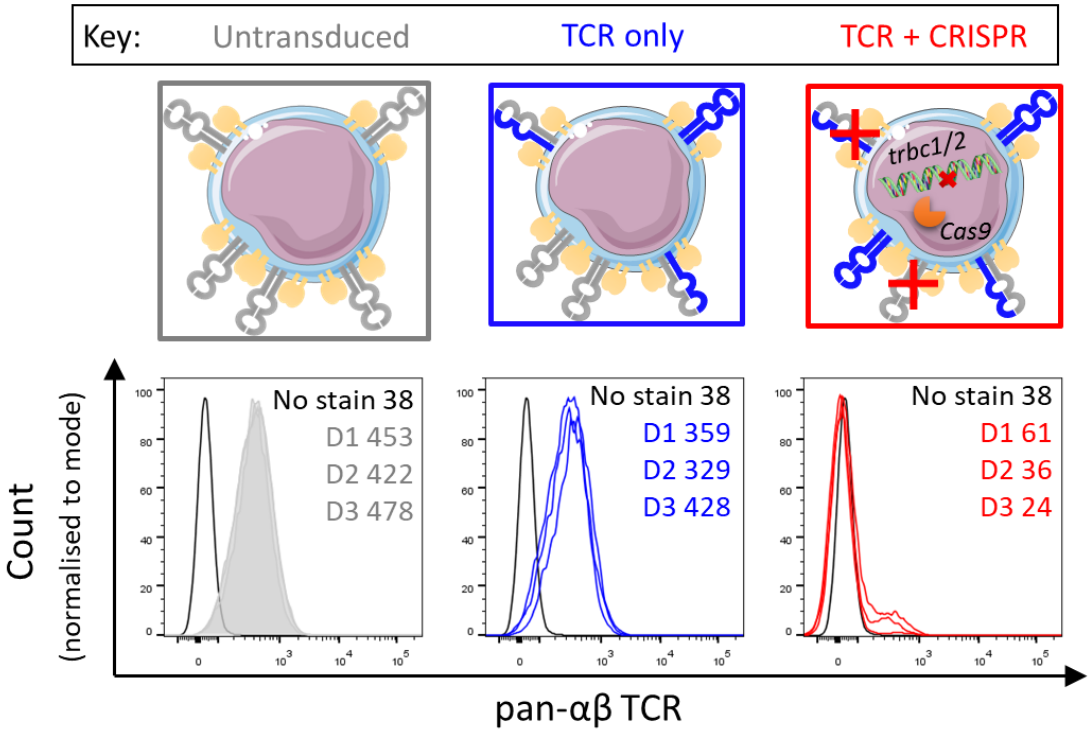

Figure 3.4 Transduction of primary T-cells with TCR-β CRISPR/Cas9 results in highly efficient disruption of the endogenous TCR. Top panel - graphical representation of T-cells: untransduced (expressing only endogenous TCR), transduced only with a TCR (expressing both a transgenic and endogenous TCRs, and up to two potential hybrids), and transduced both with a TCR and TCR-β CRISPR (expressing a transgenic TCR, and potentially a hybrid TCR comprising endogenous TCR-α and transgenic TCR-β). The endogenous TCR chains are shown in grey while the transgenic ones are depicted in blue; CD3 complex is shown in yellow. Bottom panel – corresponding histograms showing the endogenous αβ TCR expression in three donors (D1-D3), as well as a representative unstained control (shown in black). The numbers correspond to MFI values of αβ TCR staining.

3.2.4 Endogenous TCR-β knock-out improves the surface expression of transgenic TCRs

I hypothesised that the removal of the endogenous TCR-β would result in increased expression of transduced γδ and αβ TCRs, by completely abolishing or decreasing the possibility of TCR mispairing and competition, respectively. TCR-β deficient T-cells transduced with a γδ TCR can only express the transgenic TCR since full length TCR-α cannot pair with TCR-γ or TCR-δ on the cell surface. In contrast, TCR-β deficient T-cells transduced with an αβ TCR can potentially express various TCR-α chains paired with the transgenic TCR-β. Therefore, to test the aforementioned hypothesis, I chose a phosphoantigen-specific Vγ9Vδ2 TCR γδ20 I isolated myself from a healthy donor and a melanoma antigen-specific αβ TCR that has been previously described[349] (referred to as Mel13 from hereon and specific for a Melan-A derived epitope EAAGIGILTV, presented by HLA-A2). Removal of endogenous TCR-β resulted in superior expression of both transgenic TCRs in all donors tested, as demonstrated by an up to 10-fold higher mean fluorescence intensity of TCR staining as well as formation of a clearly separated transgenic TCR-positive population of T-cells (**Figure 3.5**). Importantly, this result demonstrated that the wild type TCR-β specific gRNA did not cleave codon-optimised receptors, and that removal of endogenous TCR-β was sufficient to increase the expression of transgenic αβ TCR (despite the presence of endogenous TCR-α).

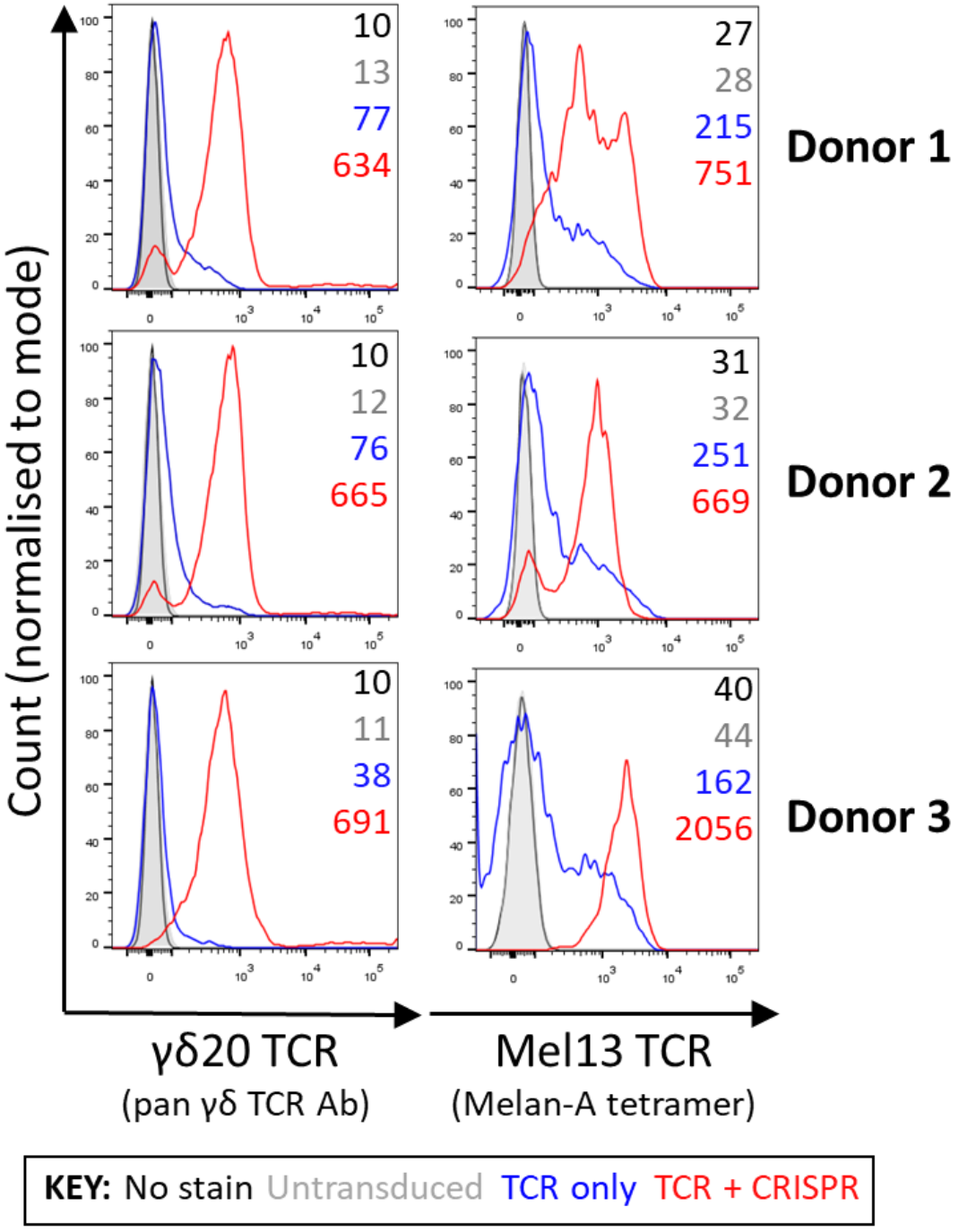

Figure 3.5 TCR-β knock-out increases the surface expression of transgenic TCRs. Primary $CD8^+$ T-cells were transduced either with a γδ20 TCR (detected by staining with a pan-γδ TCR antibody) or a Mel13 αβ TCR (detected by staining with a cognate HLA-A2:EAAGIGILTV tetramer). Unstained controls are shown in black while grey represents untransduced T-cells, blue – transduced only with a TCR, red – transduced with both TCR and CRISPR. The numbers correspond to MFI of staining.

3.2.5 Endogenous TCR-β knock-out improves the functional activity of transgenic TCRs

The quantity of functional TCR molecules on T-cell surface is one of the generally acknowledged factors governing the antigen sensitivity of the cell[350]. I therefore activated the $CD8^+$ T-cells transduced with either γδ20 or Mel13 TCRs (with or without TCR-β CRISPR) with their target cell lines (B-LCL pulsed with zoledronate or a $HLA\text{-}A2^+$ melanoma cell line, respectively). After brief co-incubation, I measured the percentage of T-cells responding to targets by ICS, looking at a marker of cytotoxicity CD107a and two potent antitumour cytokines, TNFα and IFNγ. The majority (up to 90%) of T-cells transduced both with a cancer-specific TCR and TCR-β CRISPR responded to the target cells by expressing at least one of the effector functions measured, in a similar manner to parental T-cell clones (**Figures 3.6 A** and **3.7 A**). Furthermore, TCR+CRISPR transduced cells showed a highly polyfunctional response to their target cancers, with the majority of responding cells expressing simultaneously all three effector functions measured (**Figures 3.6 B** and **3.7 B**). On the other hand, less than 10% of T-cells transduced only with γδ20 TCR, or up to 40% of T-cells transduced only with Mel13 TCR, showed any response to target cells, and the majority of responding cells expressed only one effector function. Overall, the response of TCR+CRISPR transduced cells was significantly stronger, and more polyfunctional, than that of TCR only transduced cells, in all the donors tested (**Figures 3.6 C** and **3.7 C**).

Figure 3.6 TCR-β knock-out augments the strength and polyfunctionality of response to target cells by γδ20 TCR transduced cells. (**A**) Intracellular cytokine staining of primary $CD8^+$ T-cells transduced with γδ20 TCR (with or without TCR-β CRISPR), as well as parental T-cell clone, following 5 h co-incubation with a B LCL line. The B LCL line was derived from the same donor as the parental γδ20 T-cell clone. The LCL line was pre-treated with zoledronate as indicated. The numbers on dot plots refer to percentages of cells positive for a given function. Only viable $CD3^+$ cells were included in the analysis, and the gates were set based on appropriate biological and fluorescence minus one controls. Representative data from three donors are shown.

(Legend continued on the next page)

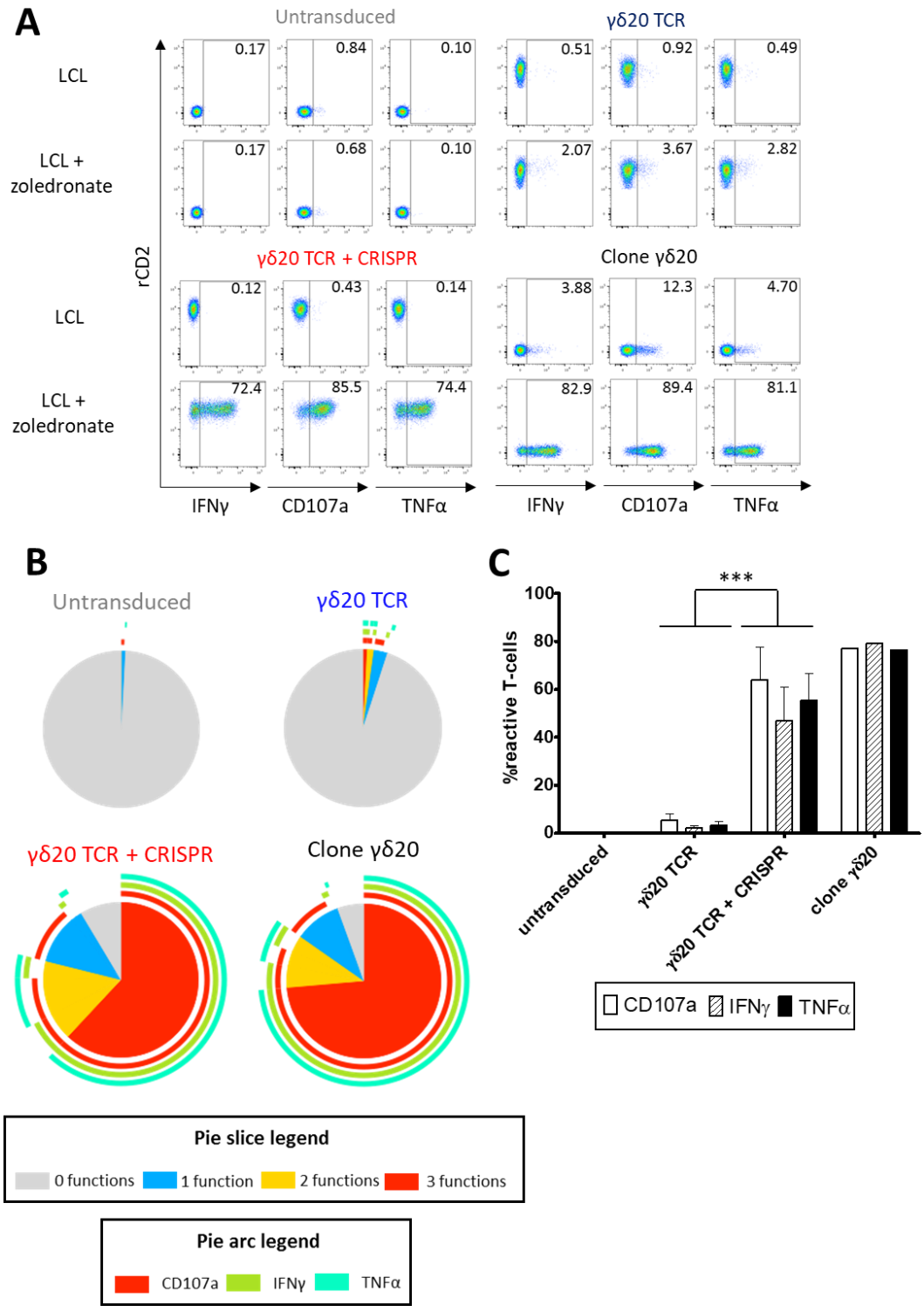

(Legend continued from the previous page) (**B**) The profile of response of transduced T-cells to a B LCL line pre-treated with zoledronate. Pie slices represent fractions of cells positive for a given number of effector functions simultaneously, while arcs specify the effector function. Representative data from three donors are shown. (**C**) The specific response of TCR-transduced T-cells to their target cell lines (calculated by subtracting the percentage of cells positive for a given function after co-incubation with LCL not pre-treated with zoledronate). Standard deviation from the mean of three donors are shown. The statistical significance of difference between responses of T-cells transduced only with γδ20 TCR and γδ20 TCR+CRISPR was calculated using paired t-Student test. ***p=0.0001

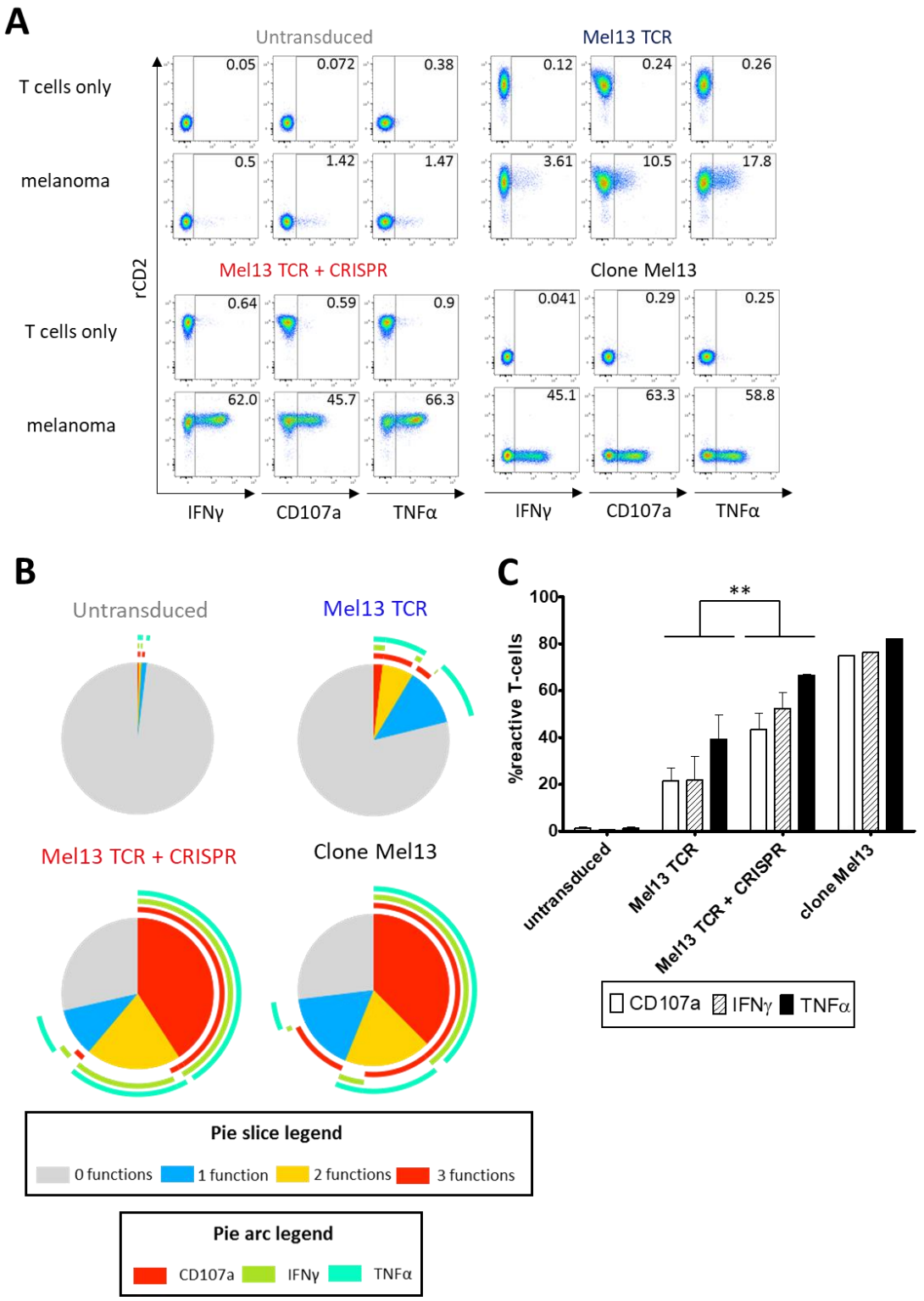

Figure 3.7 TCR-β knock-out augments the strength and polyfunctionality of response to target cells by Mel13 TCR transduced cells. (**A**) Intracellular cytokine staining of primary $CD8^+$ T-cells transduced with Mel13 TCR (with or without TCR-β CRISPR), as well as parental T-cell clone, following 5 h co-incubation with a $HLA\text{-}A2^+$ melanoma line. The numbers on dot plots refer to percentages of cells positive for a given function. Only viable $CD3^+$ cells were included in the analysis, and the gates were set based on appropriate biological and fluorescence minus one controls. Representative data from three donors are shown.

(Legend continued on the next page)

(Legend continued from the previous page) (**B**) The profile of response of transduced T-cells to a HLA-$A2^+$ melanoma line. Pie slices represent fractions of cells positive for a given number of effector functions simultaneously, while arcs specify the effector function. Representative data from three donors are shown. (**C**) The specific response of TCR-transduced T-cells to their target cell lines (calculated by subtracting the percentage of cells positive for a given function incubated alone). Standard deviation from the mean of three donors are shown. The statistical significance of difference between responses of T-cells transduced only with Mel13 TCR and Mel13 TCR+CRISPR was calculated using paired t-Student test. **p=0.002

3.2.6 TCR and CRISPR transduction does not affect the phenotype of the engineered cells

CRISPR mediated TCR replacement resulted in superior activation, in terms of cytotoxicity and cytokine production, of engineered T-cells, compared to standard TCR transfer. The difference between the engineered cells could not, however, be attributed to their differentiation phenotype. The single or double transduced T-cells showed terminally differentiated effector memory phenotype, defined as $CCR7^-CD45RA^+$, with most of the cells being also $CD27^-$ (Ref. [351]). Additionally, the transduced cells gained the expression of an activation marker CD69 (Ref. [352]) but did not express a marker of T-cell exhaustion, PD-1 (Ref. [353]). The exact same phenotype was observed for the matched untransduced control cells, indicating that the phenotypic changes resulted from CD3/CD28 bead expansion and/or subsequent allogeneic feeder and PHA expansion (**Figure 3.8**).

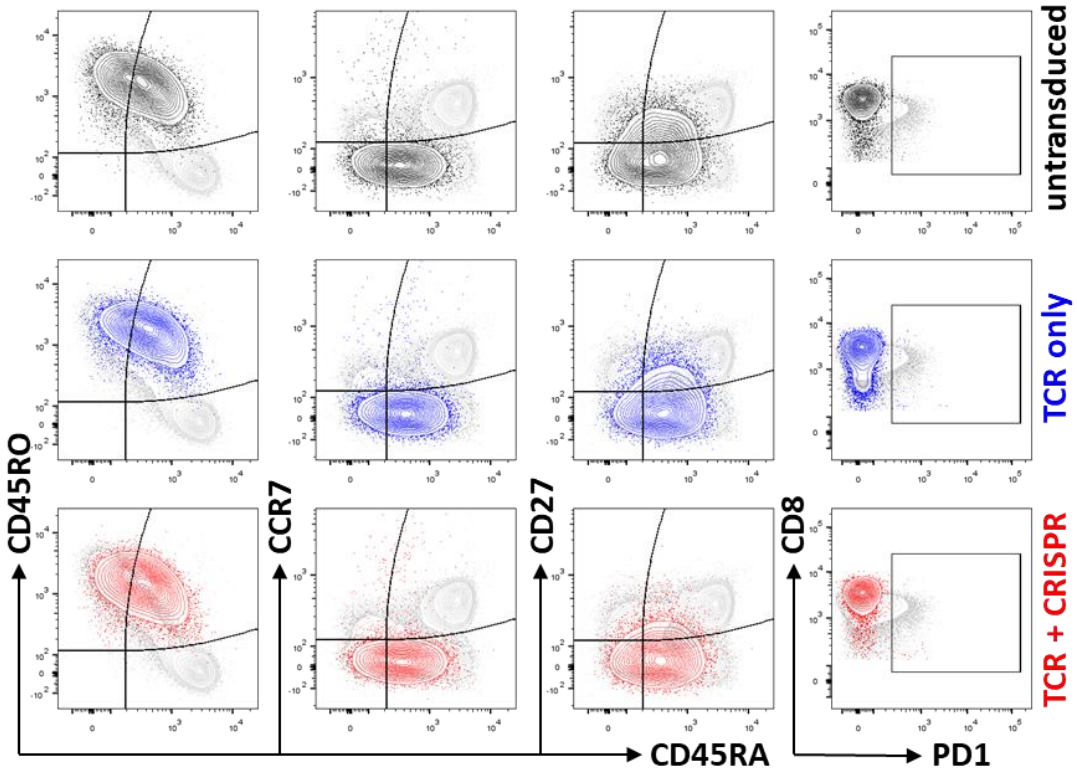

Figure 3.8 Phenotypic profile of single or double transduced T-cells does not differ from the untransduced ones. Donor-matched transduced and untransduced T-cells were stained for phenotypic markers CD45RA, CCR7, CD27, CD69 and PD-1 in parallel with freshly isolated PBMC (shown in grey). Lymphocytes were gated based on size, followed by doublet exclusion. Only live $CD3^{+}CD8^{+}$ cells were taken for analysis. The gates were set based on appropriate fluorescence minus one controls. Representative data from 3 donors are shown.

3.2.7 Endogenous TCR-β knock-out improves the antigen sensitivity of transgenic TCRs

The density of antigen on the surface of target cells is one of the factors determining if a T-cell is going to mount a functional response against the target cell. The most common way of increasing T-cell sensitivity to antigen (thus enabling the T-cell to respond to targets cells where the density of antigen would be suboptimal) is affinity maturation of the TCR[259]. While affinity maturation can be readily applied to HLA-restricted αβ TCRs, owing to the abundance of structural information pertaining to TCR-HLA complexes, no such technology exists for γδ TCRs. Furthermore, affinity matured TCRs have never undergone the rigours of thymic selection, and therefore can harbour unpredicted off-target and on-target off-cancer reactivities[344]. Therefore, I decided to investigate if increasing the number of functional TCR molecules on cell surface via TCR-β knockout would allow the TCR-transgenic T-cell to mount a response to a lower concentration of antigen than TCR-β proficient transgenic T-cells.

$CD8^+$ T-cells, transduced with a γδ20 TCR alone or in combination with TCR-β CRISPR, were incubated with decreasing concentrations of the cognate antigen HMBPP (in presence of T2 cell line, to serve as an antigen presentation platform) for 16 h, followed by quantification of secreted MIP-1β. The parental T-cell clone was tested in parallel. MIP-1β secretion has been shown in our laboratory to be the most sensitive marker of T-cell activation, and thus has become a cornerstone of antigen discovery platform for HLA-restricted T-cells[354–360]. For a side-by-side comparison, I also measured the antigen sensitivity of γδ20 TCR transduced Jurkat cell line. TCR-transgenic Jurkat cell lines have been widely used as a proxy system for studying TCR activation[361], in particular for validation of γδ TCR role in target cell recognition, and discovery of γδ TCR antigens[362,363].

$CD8^+$ T-cells transduced with γδ20 TCR were capable of mounting a response to HMBPP at sub-micromolar concentration. Conversely, T-cells transduced with both TCR and CRISPR still secreted MIP-1β at picomolar concentrations of exogenously supplied HMBPP, closely replicating the sensitivity of the parental T-cell clone (**Figure 3.9 A**), while TCR-transduced Jurkat required micromolar concentrations of HMBPP to become fully activated. In summary, γδ20 TCR+CRISPR transduced T-cells were around 5,000 times more sensitive than γδ20 TCR transduced T-cells, and approximately 50,000 more sensitive than the model proxy system (TCR-transduced Jurkat) (**Figure 3.9 B**). The difference between γδ20 TCR + CRISPR and γδ20 TCR-only transduced cells was even more apparent when IFNγ was used as a marker of activation (**Figure 3.9 C**). TCR-β deficient T-cells replicated the antigen sensitivity of the parental T-cell clone, responding to the antigen even at 0.1 nM concentration while TCR-only transduced cells did not reach the maximal response even at 1 μM concentration of HMBPP.

A

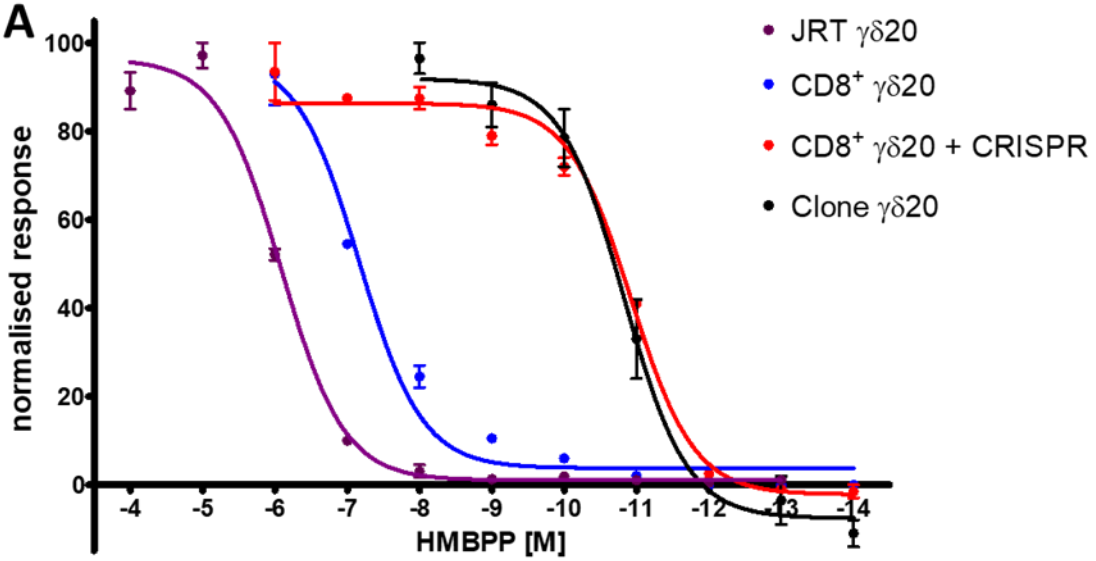

B

Sample	EC_{50} [M]	Fold change of EC_{50}
JRT γδ20	8.1×10^{-7}	0.1
CD8+ γδ20	6.8×10^{-8}	1
CD8+ γδ20 + CRISPR	1.2×10^{-11}	5,000
γδ20 clone	1.5×10^{-11}	5,000

C

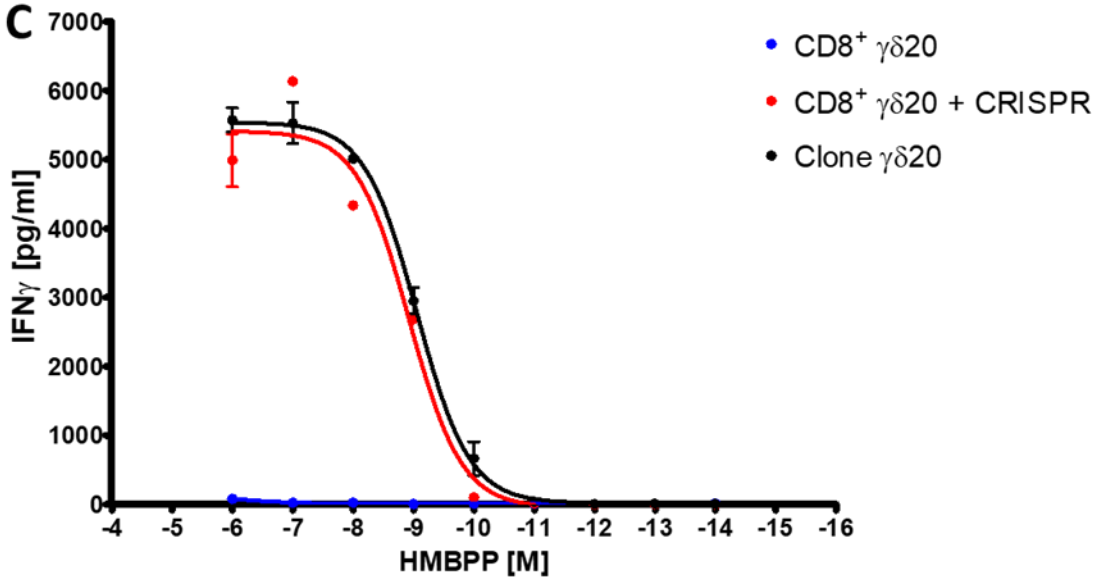

(Legend on the next page)

Figure 3.9 Antigen sensitivity of γδ20 TCR transduced cells. (**A**) $CD8^+$ T-cells transduced with γδ20 TCR with or without TCR-β CRISPR were incubated for 16 h with the indicated concentrations of cognate antigen HMBPP, in presence of T2 cell line, followed by quantification of secreted MIP-1β. The parental T-cell clone was tested in parallel. The activation of Jurkat cells transduced with γδ20 TCR was measured as CD69 upregulation after 16 h stimulation. The response in the absence of HMBPP was normalised to 0 while the maximal response was normalised to 100%, to allow comparison between different conditions. Mean and standard experimental error from duplicate samples is shown, together with fitted nonlinear regression curve. Representative data from two independent experiment are shown. (**B**) EC_{50} values of HMBPP sensitivity as determined by CD69 upregulation (Jurkat) or MIP-1β secretion (T-cells), and then compared to the EC_{50} value of $CD8^+$ T-cells transduced with γδ20 TCR. (**C**) IFNγ secretion by γδ20 TCR transduced $CD8^+$ T-cells and parental clone, after 16 h co-incubation with T2 cell line and varying concentrations of HMBPP.

The increase of sensitivity by Mel13 TCR transduced cells, when combined with TCR-β knockout, was less pronounced that in the case of γδ T-cells (approximately 10-fold increase of sensitivity when MIP-1β or IFNγ secretion were measured; **Figures 3.10 A** and **B**, respectively). Nevertheless, Mel13 TCR + CRISPR transduced cells were capable of exhibiting stronger cytotoxicity against a HLA-$A2^+$ melanoma cell line than Mel13 TCR-only transduced cells, to the same extent at the parental T-cell clone (**Figure 3.10 C**).

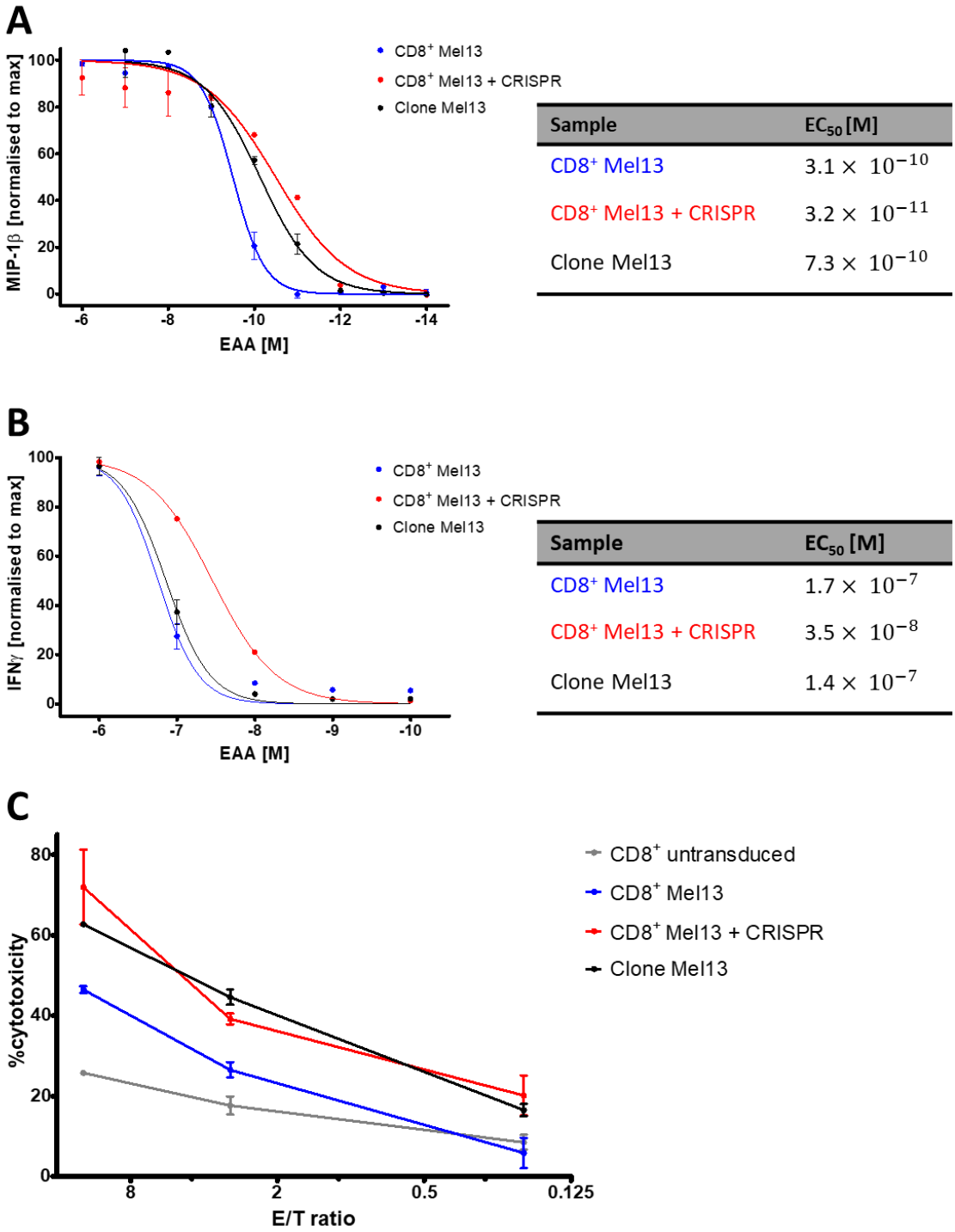

Sample	EC_{50} [M]
$CD8^+$ Mel13	3.1×10^{-10}
$CD8^+$ Mel13 + CRISPR	3.2×10^{-11}
Clone Mel13	7.3×10^{-10}

Sample	EC_{50} [M]
$CD8^+$ Mel13	1.7×10^{-7}
$CD8^+$ Mel13 + CRISPR	3.5×10^{-8}
Clone Mel13	1.4×10^{-7}

Figure 3.10 Antigen sensitivity of Mel13 TCR transduced cells. (**A**) $CD8^+$ T-cells transduced with Mel13 TCR with or without TCR-β CRISPR were incubated for 16 h with the indicated concentrations of cognate peptide EAAGIGILTV, in presence of T2 cell line, followed by quantification of secreted MIP-1β or (**B**) IFNγ. The parental T-cell clone was tested in parallel. The response in absence of peptide was normalised to 0 while the maximal response was normalised to 100%, to allow comparison between different conditions. Mean and standard experimental error from duplicate samples is shown, together with fitted nonlinear regression curve. (**C**) Cytotoxicity of Mel13 transduced $CD8^+$ T-cells and parental clone after 4 h co-incubation with a HLA-$A2^+$ melanoma cell line. Mean and SEM are shown.

3.2.8 TCR replacement enhances targeting of haematological cancers by γδ20 TCR

γδ T-cells expressing Vγ9Vδ2 TCR, recognise phosphorylated metabolites of the isoprenoid pathway, sensed through butyrophilin 3A1 molecule[41]. Metabolic dysregulation, leading to accumulation of these metabolites, is a common feature of many cancers[77], and can be augmented further by clinically approved aminobisphosphonates such as zoledronate[233]. Consequently, Vγ9Vδ2 TCRs offer therapeutic potential for treatment of a wide range of cancers, regardless of patient's HLA type. Haematological cancers are an especially attractive target for Vγ9Vδ2 TCR therapy for a number of reasons[364]. In particular, a successful therapy with Vγ9Vδ2 TCR-engineered T-cells would require simultaneous delivery of both aminobisphosphonate drug and the cellular product. Haematological cancers, being usually disseminated, are easily accessible for systemically delivered therapeutics - in contrast to solid tumours which offer multiple obstacles preventing from efficient infiltration of gene engineered T-cells[365]

Therefore, I compared the cytotoxic activity of standard γδ20 TCR transduced $CD8^+$ T-cells with TCR+CRISPR transduced cells, against a zoledronate-treated B LCL line derived from the same donor as the parental γδ20 T-cell clone (**Figure 3.11**). As expected, based on CD107a expression by transduced T-cells shown in **Figure 3.6**, TCR+CRISPR engineered T-cells exhibited a more potent cytotoxic activity against the B LCL line after 4 h of co-incubation, especially at low effector to target ratios (less than 5% cytotoxicity for γδ20 TCR only transduced cells compared with over 25% cytotoxicity for TCR+CRISPR transduced cells at effector to target ratio below 1:1). Cytotoxicity against the B LCL line untreated with zoledronate was not observed even in case of the parental γδ20 T-cell clone, indicating that the endogenous accumulation of isoprenoid metabolites was not sufficient to induce T-cell activation.

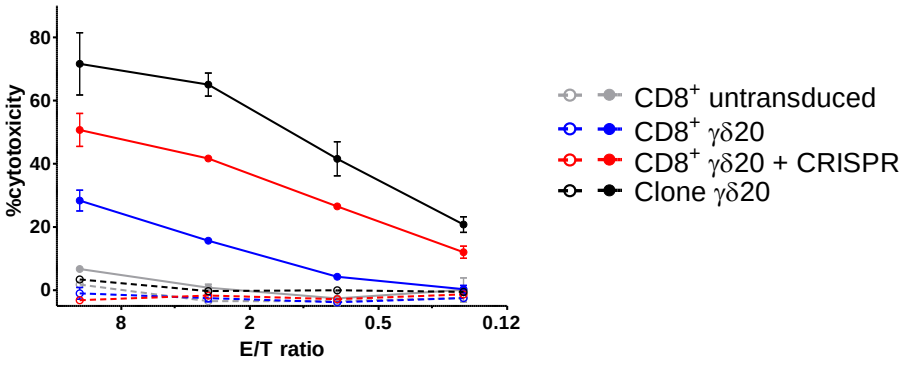

Figure 3.11 TCR-β knock-out enhances cytotoxicity of Vγ9Vδ2 TCR-transduced T-cells. 4 h cytotoxicity of γδ20 TCR transduced $CD8^+$ T-cells and the parental T-cell clone against a γδ20 autologous B LCL. Filled symbols represent B LCL pre-treated with zoledronate while empty symbols indicate no aminobisphosphonate treatment. Standard error of the mean is shown. Representative data from two independent experiments carried out in duplicate, using transduced $CD8^+$ cells from three different donors, are shown.

Since γδ TCRs seem to function independently of classical αβ TCR coreceptors CD4 and CD8, I investigated the potential for re-directing both $CD4^+$ and $CD8^+$ T-cells to haematological malignancies by γδ20 TCR transfer (alone, or in combination with TCR-β CRISPR). I tested a panel of established cancer cell lines encompassing T acute lymphoblastic leukaemia (T-ALL), acute myeloid leukaemia (AML) and multiple myeloma, as well as primary B acute lymphoblastic leukaemia (B-ALL) blasts which closely resemble the phenotypic and genetic features of cancer *in vivo*[315,316]. TCR+CRISPR modified T-cells (both $CD4^+$ and $CD8^+$) were capable of mounting a response (in terms of TNFα and IFNγ secretion) to all the cell lines and primary cells tested (following zoledronate pre-treatment); conversely, single transduced T-cells exhibited a much weaker response, or no response at all (especially towards T-ALL line Molt3 or primary B-ALL blasts; **Figure 3.12**). A similar pattern of response was observed when IFNγ secretion was used as a marker of activation (**Figure 3.13**). There was no specific response to target cells without zoledronate pre-treatment (**Appendix Figure 8.2**), thus indicating that TCR-β knockout did not result in supraphysiological increase of functional avidity.

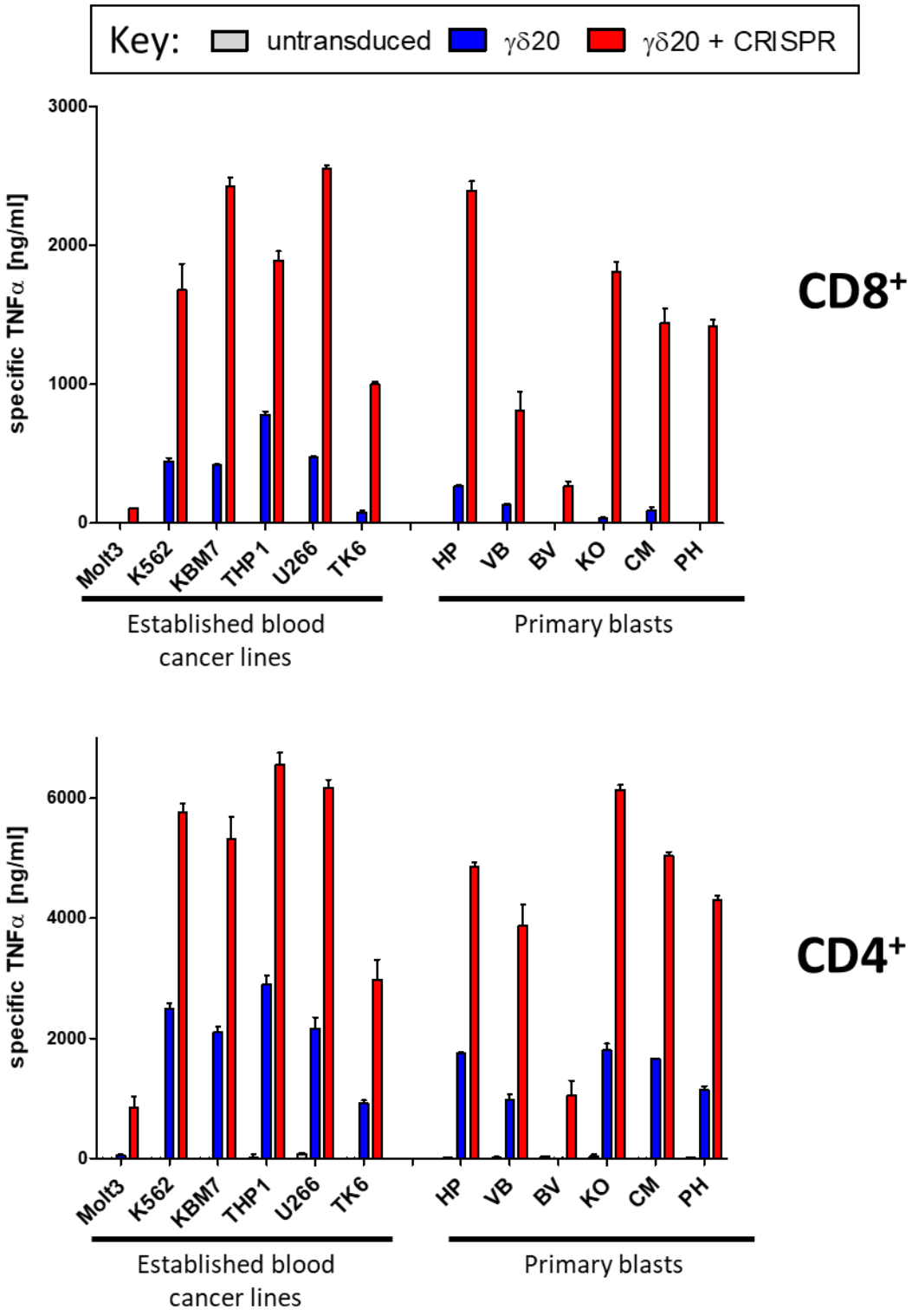

Figure 3.12 TCR-β knock-out enhances TNFα secretion by γδ20 TCR transduced T-cells in response to aminobisphosphonate-treated haematological malignancies. TNFα secretion by γδ20 TCR transduced $CD8^+$ (top) or $CD4^+$ T-cells (bottom) in response to a panel of established blood cancer cell lines of diverse myeloid or lymphoid lineages, as well as primary B lymphoblastic leukaemia blasts. Zoledronate pre-treatment was carried out for 24 h before co-incubation with T-cells. Specific TNFα secretion was calculated by subtracting TNFα secreted from cancer lines alone, and T-cells alone. No specific TNFα release was observed in absence of aminobisphosphonate pre-treatment. Representative data from two experiments carried out in duplicate are shown.

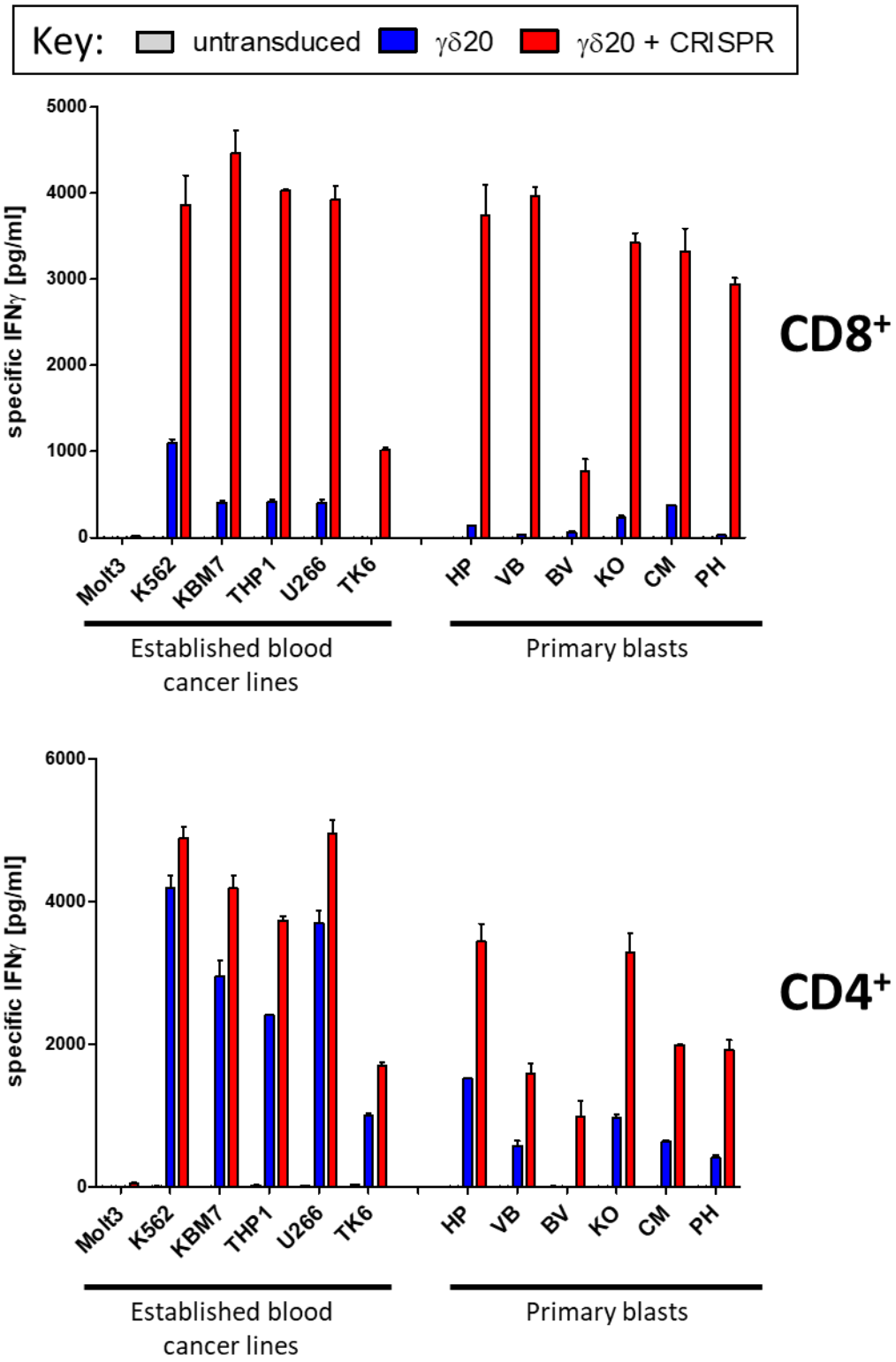

Figure 3.13 TCR-β knock-out enhances IFNγ secretion by γδ20 TCR transduced T-cells in response to aminobisphosphonate-treated haematological malignancies. IFNγ secretion by γδ20 TCR transduced $CD8^+$ (top) or $CD4^+$ T-cells (bottom) in response to a panel of established blood cancer cell lines of diverse myeloid or lymphoid lineages, as well as primary B lymphoblastic leukaemia blasts. Zoledronate pre-treatment was carried out for 24 h before co-incubation with T-cells. Specific IFNγ secretion was calculated by subtracting IFNγ secreted from cancer lines alone, and T-cells alone. No specific IFNγ release was observed in absence of aminobisphosphonate pre-treatment. Representative data from two experiments carried out in duplicate are shown.

3.2.9 Targeting of solid tumours

While systemic administration of aminobisphosphonates may be efficient for sensitising disseminated, easily accessible cancer such as haematological malignancies to Vγ9Vδ2 T-cells, it may be less effective in cases of solid tumours which are not easily penetrable due to their size and limited vascularisation[231]. I therefore compared cytotoxicity of γδ20 TCR transduced $CD8^+$ T-cells (with or without TCR-β CRISPR) against a panel of solid tumours in absence of zoledronate treatment, relying solely on endogenous accumulation of phosphoantigens by the tumours. While some of the tumour lines tested were not recognised at all by γδ20 TCR transduced cells, those that were recognised were lysed more efficiently by γδ20 TCR+CRISPR than γδ20 TCR-only transduced cells, especially all but one melanoma lines, and a prostate cancer line LNCaP (**Figure 3.14**). Therefore, Vγ9Vδ2 TCRs combined with TCR-β knockout may offer a therapeutic benefit in for solid tumours in addition to haematological cancers.

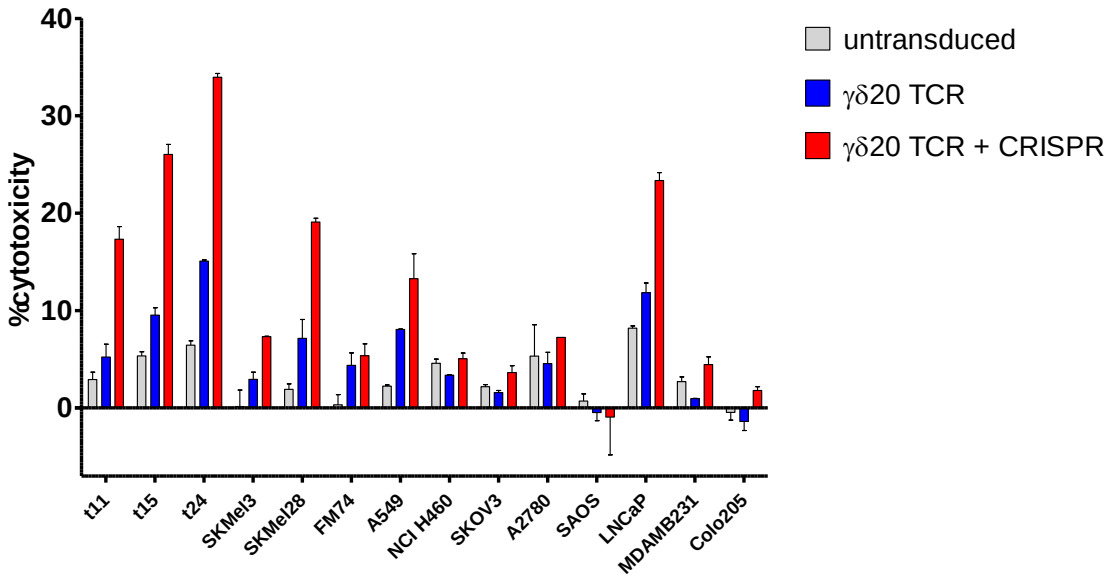

Figure 3.14 TCR-β knock-out increases cytotoxicity of γδ20 TCR transduced T-cells against a panel of solid tumours even in absence of aminobisphosphonate treatment. Cytotoxicity of γδ20 TCR transduced cells was established by 51-Cr release after 6 h of co-incubation with cancer cell lines, at 10:1 effector to target ratio. Mean and SEM are shown. T11, t15, t24, SKMel3, SKMel28 and FM74 are melanoma cell lines; A549 and NCI H460 are lung cancer lines; SKOV3 and A2780 are ovarian cancer lines; SAOS is a bone osteosarcoma line; LNCaP is a prostate cancer line; MDAMB231 is a breast cancer line; and Colo205 is a colorectal cancer line.

3.2.10 On-target off-tumour toxicities

Specific targeting of cancer while limiting the damage to healthy tissue is a prerequisite of every successful cancer therapy. Vγ9Vδ2 T-cell based therapies, in particular concomitant with systemic administration of aminobisphosphonates, have been proven to be generally safe and well tolerated by large cohorts of patients[233,366,228,238], especially when compared with CD19-CAR therapies[367] and affinity-enhanced TCR therapies[344] - both of which have led to severe or fatal toxicities in a fraction of patients. The γδ TCR used here was derived from a T-cell clone present in a healthy individual, without any alterations to the TCR protein sequence. Nevertheless, I decided to investigate if TCR-β knockout which enhanced the targeting of cancers by γδ20 TCR transduced cells also increased the reactivity of the engineered cells against normal, peripheral blood derived cells used directly *ex vivo* (without biases induced by cell culture). Therefore, I isolated B-cells and T-cells from PBMC, based on appropriate surface markers, and pre-treated the cells with zoledronate. 24 h post isolation the cells were co-incubated with engineered T-cells, and secretion of cytokines TNFα and IFNγ (which would indicate productive recognition of target cells) was quantified (**Figure 3.15**). No specific cytokine secretion was observed in response to B-cells, T-cells or whole PBMC by γδ20 TCR-only or TCR+CRISPR transduced cells. By contrast, TCR+CRISPR transduced cells showed much stronger recognition of zoledronate-treated leukaemia (THP1) or myeloma cell lines (U266) that TCR-only transduced cells, in line with the previous results.

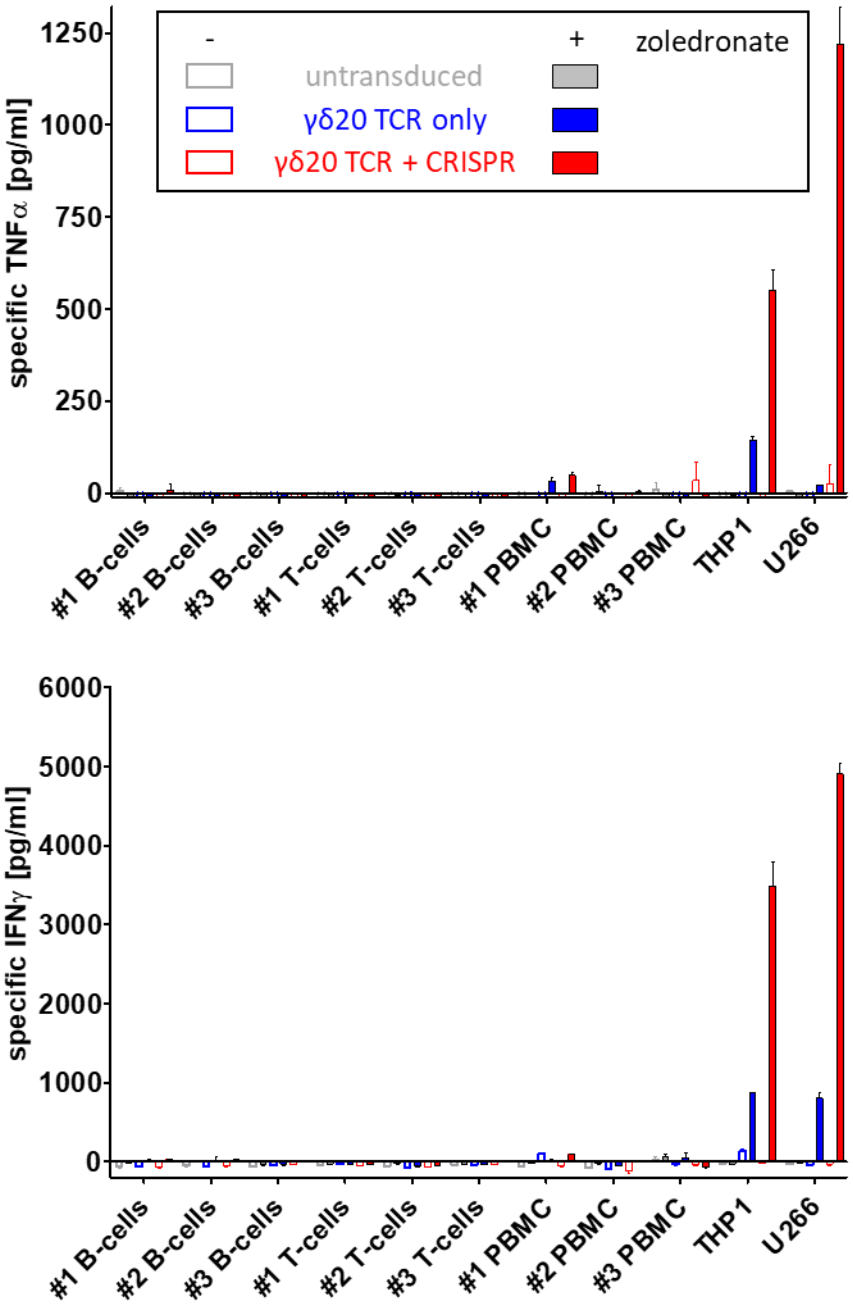

Figure 3.15 TCR-β CRISPR transduced T-cells do not target normal cells derived from peripheral blood. TNFα (top) or IFNγ (bottom) secretion by γδ20 TCR transduced T-cells was determined after 16 h of co-incubation with freshly isolated B-cells ($CD19^+$), T-cells ($CD4^+$) or whole PBMC from three donors. Blood cancer lines THP1 and U266 were included as positive controls. Target cells were pre-incubated with 50 µM zoledronate as indicated in the legend. Specific cytokine concentration was calculated by subtracting the values from T-cells alone and target cells alone. Representative data from TCR transduced cells from two donors are shown.

3.3 Discussion

TCR transfer technology offers an attractive therapeutic potential for generation of a large number of patient-autologous, cancer-specific T-cells. However, due to the presence of endogenous αβ TCR chains in αβ T-cells, therapeutically relevant TCRs have been so far limited to high affinity and/or those known to compete well with endogenous TCRs for cell surface expression. In this Chapter, I have demonstrated the feasibility of redirecting T-cells to cancer by combining poorly competitive γδ or αβ TCRs with CRISPR/Cas9 mediated knockout of the endogenous TCR-β. T-cells engineered using this approach exhibited functional activity and antigen sensitivity closely recapitulating that of parental T-cell clones and vastly outperforming conventional TCR-transduced T-cells. My results suggest that the presence of intact endogenous TCR-α did not have a detrimental effect on functional activity of the transferred melanoma-specific αβ TCR. In fact, when a similar study was conducted, by knocking out endogenous TCRs using zinc finger nuclease technology, in combination with transduction of an αβ TCR, TCR-β deficient cells showed similar performance to TCR-αβ deficient cells[368]. Moreover, since γδ TCR chains cannot form functional hybrids with αβ TCR chains, TCR-β disruption is sufficient for the optimal expression of transgenic γδ TCR.

Endogenous TCR disruption, achieved using a variety of genome editing tools, including zinc finger nucleases[368,369], transcription activator-like effector nucleases[370–372], or CRISPR/Cas9[299,373], has been demonstrated several times before, mostly in context of re-directing T-cells to cancers using CARs. An innovative approach was proposed by Eyquem *et al.*, whereby a CAR was inserted into the endogenous TCR-α locus by leveraging CRISPR/Cas9 homology directed repair, thus achieving simultaneous TCR disruption and physiologically regulated CAR expression driven by TCR promoters[374]. While this method was shown to be highly successful in context of CARs, by preventing premature exhaustion of T-cells, it may be as successful in context of natural cancer-specific TCRs, due to different kinetics and affinity of target binding.

Engineered non-HLA restricted T-cells, such as those redirected by a CAR or unconventional TCR, could potentially be used as an off-the-shelf product since they are deficient in endogenous TCRs and thus likely incapable of causing graft *versus* host disease (GvHD). Such cells could be further modified by gene editing to remove of HLA-I, thus preventing allogeneic rejection by the host. Further modifications might remove checkpoint inhibitors to render the transductants resistant to the immunosuppressive effects of the tumour microenvironmant[373]. Interestingly, off-the-shelf engineered CAR T-cells have been successfully used for treatment of B acute lymphoblastic leukaemia in infants that would not be able to provide an autologous CAR T-cell product[372]. I

therefore believe that the use of genome edited T-cells will become commonplace in clinical setting in the very near future.

Notably, using γδ TCR transgenic T-cells deficient in endogenous TCRs could be a particularly promising avenue for an off-the-shelf cellular therapeutic, due to their potential of targeting diverse cancers without any perceived HLA restriction. As I demonstrated here for the first time, CRISPR/Cas9 mediated removal of the endogenous αβ TCR greatly enhances the surface expression of an otherwise poorly competitive Vγ9Vδ2 TCR with concomitant substantial improvements in the sensitivity of T-cell activation. In particular, TCR+CRISPR engineered cells showed a strikingly more polyfunctional profile of response to target cancer cell lines than standard TCR transduced cells. The majority of TCR+CRISPR engineered cells were capable of simultaneously undergoing cytotoxic degranulation and secreting TNFα and IFNγ cytokines, indicating high level of T-cell activation[355]. Notably, polyfunctional profile of T-cell response has been shown as vital for positive clinical outcome in patients suffering from haematological cancers[375]. Furthermore, this is the first study that compares the antigen sensitivity of T-cell clones and TCR-transduced primary T-cells to TCR transduced Jurkat cell line which is commonly used as a proxy system for studying the role of TCRs, especially non-HLA restricted TCRs, in target cell recognition and antigen discovery. I have further demonstrated that TCR+CRISPR engineered cells closely replicate the antigen sensitivity of the parental T-cell clones, and are orders of magnitude more sensitive to the antigen than the standard model laboratory system, the Jurkat cell line, or clinically applied TCR transduced primary T-cells.

γδ TCRs composed of Vγ9 and Vδ2 chains offer an attractive therapeutic potential, and are likely to be the first γδ TCRs applied clinically[376], due to relatively well understood mechanism of target cell recognition and numerous clinical trials exploiting the Vγ9Vδ2 T-cell subset. Vγ9Vδ2 TCR redirected T-cells could be used in combination with systemic administration of aminobisphosphonates to sensitise cancer cells. Aminobisphosphonate treatment, either relying on *in vivo* expanded Vγ9Vδ2 T-cells, or administered in combination with *ex vivo* expanded T-cells, has been shown to be safe and free from severe adverse effects in spite of ubiquitous expression of mevalonate pathway components and the BTN3A1 molecule[228,231,366,377] . Indeed, aminobisphosphonate administration led to objective clinical response in a small proportion of haematological cancer patients with AML, non-Hodgkin lymphoma or multiple myeloma[231,377]. The overall clinical outcome of aminobisphosphonate/Vγ9Vδ2 T-cell treated cancer patients remains underwhelming, especially when compared with other immunotherapy modalities such as checkpoint inhibitor blockade, and adoptive transfer of TIL or genetically engineered T-cells. The relatively low clinical efficacy of Vγ9Vδ2 T-cell therapies to date may stem from a variety of reasons including use of

a mostly undefined (in terms of clonal composition) and highly variable cellular product, activation-induced death or anergy due to antigen exposure *in vivo* or *ex vivo*, and poor engraftment after adoptive transfer. TCR replacement allows use of a TCR with a desired specificity and sensitivity, thus limiting the variability of the cellular product, transduced into the most clinically desirable subset of autologous (or allogeneic) T-cells[378]. Indeed, as shown in this Chapter, CRISPR mediated TCR replacement resulted in generation of γδ TCR transduced T-cells that could respond, by secretion of TNFα and IFNγ secretion, to all haematological cancer cell lines and primary B ALL blasts in a much stronger manner than cells transduced without CRISPR knockout of endogenous TCR-β chains. Notably, increased TNFα concentration at the tumour site has been shown to be a favourable prognostic marker, and TNFα secretion correlated with anticancer response of cytotoxic T-cells[379]. IFNγ is an important antitumour cytokine, influencing expression of classical and non-classical MHC molecules, as well as other components of antigen processing and presentation[380,381].

In summary, I conclude that the TCR *replacement* system I have developed offers considerable advantages over standard TCR *transfer* technology system for both the potential development of new immunotherapies and for pre-clinical characterisation of relevant TCRs, especially those that show poor competition with endogenous αβ TCR repertoire and/or relatively weak affinity for their respective antigens. While T-cell clones are a gold standard for detailed studies of TCR-mediated antigen recognition, TCR replacement could be used as an alternative when such T-cell clones are unavailable as I have shown that the resultant transductants exhibit a similar level of sensitivity to cognate antigen. TCRs of interest could come from T-cells which grow poorly in culture, for example, in case of T-cell exhaustion resulting from chronic exposure to antigen as in late stage cancer patients[382] , or directly from high throughput paired sequencing of TCR repertoires[57] in antigen reactive populations. Finally, one could envisage that TCR+CRISPR transduced cells, which express only the transgenic TCR and can be generated in practically unlimited numbers, could be used for discovery of new antigens, or new components of known antigen processing machinery, by leveraging whole genome CRISPR/Cas9 knockout libraries[319]. The use of TCR replacement system for selection of potentially pan-cancer specific TCRs is further discussed in **Chapter 4** while antigen discovery using whole genome CRISPR/Cas9 libraries forms the core of **Chapter 5**.

4. Procurement of broadly cancer-reactive, non-HLA restricted T-cell clones and T-cell receptors

4.1 Background

γδ T-cells have been known to play an important role in anticancer immunity for almost three decades[71], and to recognise their targets in a HLA-independent manner[9]. For both reasons, γδ T-cells and their cognate receptors could prove to be an invaluable addition to a new generation cancer immunotherapies[383]. However, the broad application of γδ T-cells in immunotherapy has been hampered by the striking paucity in the understanding of γδ T-cell biology, especially in terms of antigen recognition. The lack of definitive, proven γδ TCR targets has helped fuel an on-going debate whether γδ T-cells fall more into the innate[384] or adaptive[385] immunity category. In fact, even the role of γδ TCRs in target cell recognition has recently been questioned[386].

Antigen recognition by human γδ T-cells in context of cancer has been discussed in **Chapter 1**. Here, I focus on two published γδ TCR ligands, MICA/B[138] and EPCR[362], as well as BTN3A1 – the molecule indispensable for sensing of pyrophosphate metabolites (phosphoantigens) by the main subset of γδ T-cells in peripheral blood that express a Vγ9Vδ2 TCR[89].

MICA/B is an oligomorphic member of the MHC-Ib family, composed of α1 and α2 domains forming a structure reminiscent of MHC-Ia peptide presentation platform and plasma membrane linked α3 domain[138]. MICA/B is not believed to present a specific molecular cargo but is instead a ubiquitous marker of cellular stress that can become ectopically expressed in events of viral infection, cancer or oxidative stress[387]. Together with UL16-binding proteins (ULBP), MICA/B is a target for an activating NK-type receptor NKG2D which can be expressed on T-cells and NK cells. EPCR is also a MHC-Ib molecule expressed on stressed (i.e. virally infected or cancerous) cells[388]. Ample biophysical evidence indicates direct, albeit low affinity interactions between some γδ TCRs and MICA/B[389] or EPCR[362], in a similar affinity range as recognition of self-antigens by αβ TCRs[390]. In contrast, direct binding of Vγ9Vδ2 TCRs to BTN3A1 remains in dispute[40,94]. BTN3A1 is crucial for sensing of intracellular accumulation of pyrophosphate metabolites such as eukaryotic IPP or bacterial HMBPP. While some cancer cells have a naturally elevated level of phosphoantigens due to metabolic dysregulation, further accumulation of phosphoantigens can be induced by use of FDA-approved metabolic inhibitors, aminobisphosphonates[15]. While only one member of BTN3 family, namely BTN3A1, can mediate phosphoantigen recognition, Vγ9Vδ2 T-cell activation can also be induced by using an

"activating" anti-BTN3 antibody which is thought to induce a T-cell stimulating conformation of all three BTN3 isoforms, namely BTN3A1-A3 (Ref.[91]).

As mentioned before, the majority of γδ T-cells in peripheral blood express Vγ9Vδ2 TCRs and are therefore likely to recognise well-described phosphoantigens. Conversely, γδ T-cells present in tissues, in particular epithelial tissues, are mostly Vγ9Vδ2 TCR-negative and may play an important role in cancer immunosurveillance[391]. For instance, our collaborators found elevated frequencies of Vδ1$^+$ T-cells in late-stage melanoma lesions[265]. These tumour-infiltrating Vδ1$^+$ T-cells showed anticancer reactivity *in vitro* but their target specificity has yet to be determined. In this Chapter I performed an initial dissection of anticancer reactivity of tumour-infiltrating γδ T-cells in context of MICA/B, EPCR and BTN3 molecules, on bulk population and single clone levels.

While cancer-reactive γδ T-cells may be enriched at the tumour site, similarly to cancer-reactive αβ T-cells, tumour biopsies usually require invasive methods of acquisition and the sample material they provide may be limited. In contrast, circulating T-cells can be sampled through routine venepuncture but the frequency of cancer-reactive non-Vγ9Vδ2 T-cells in the periphery may be extremely low. The problem of both limited starting material and low frequency of cells of interest can be overcome by using the T-cell library technology, recently developed by my colleagues[216]. In brief, T-cell libraries involve expanding the starting T-cell material in a nearly oligoclonal and TCR-unbiased manner, followed by screening for desired reactivity and enrichment of antigen-reactive cells. So far, the T-cell library method has only been used for procurement of peptide-specific αβ T-cell clones. In this Chapter I applied the T-cell library technology to procure cancer-reactive γδ T-cell clones and TCRs from healthy donors and cancer patients. In parallel, I used the T-cell library technology in attempt to isolate non-HLA restricted cancer-reactive αβ T-cell clones. Since CD4 and CD8 molecules ensure selection of MHC-II and MHC-I restricted αβ T-cells[159], I decided to investigate the potential of CD4CD8-coreceptor deficient (double negative, DN), αβ T-cells as a source of non-HLA restricted, cancer-reactive T-cells alternative to γδ T-cells.

4.1.1 Aims

Broad anticancer reactivity is a well described feature of γδ T-cells (recently reviewed in [20,383]) . However, in order to be of therapeutic application, conferring this broad anticancer reactivity to patient's peripheral T-cells *via* TCR gene transfer seems preferable to isolation and expansion of cancer-reactive γδ T-cells in an autologous setting. Additionally, generation of a cellular platform deficient in known γδ T-cell ligands may help in the prospective selection of γδ TCRs of yet unknown specificities.

Therefore, the specific aims of this Chapter were:

- To investigate γδ T-cells in clinical grade tumour-infiltrating lymphocyte products as a source of broadly cancer-reactive T-cell clones and TCRs;
- To generate a cancer line deficient in γδ TCR ligands MICA/B, EPCR and BTN3 for studying the role of those molecules in cancer cell recognition;
- To determine if TCR transfer of cancer-reactive γδ TCRs into healthy αβ T-cells is sufficient to redirect them to multiple cancer lines;
- To validate the use of T-cell libraries for procurement of cancer-reactive, non-HLA restricted αβ and γδ T-cells;
- To conduct a preliminary dissection of ligand specificity of selected αβ and γδ T-cells.

4.2 Results

4.2.1 Clinical grade TIL products contain cancer-reactive γδ T-cells

Adoptive cell transfer of tumour-infiltrating lymphocytes (TILs) is one of the most successful treatments for metastatic melanoma (MM). Our collaborators at CCIT (Copenhagen, Denmark) have successfully generated therapeutic quantities of TILs from metastatic melanoma, renal cell carcinoma (RCC) and ovarian cancer biopsies, along with matching autologous tumour lines. The recently completed clinical trial using TIL transfer in metastatic melanoma, conducted at the CCIT, resulted in an objective response rate of over 40%, and a complete remission rate of 20% (Ref. [256]). The dissection of anticancer reactivity of TIL products in three complete remission melanoma patients was the focus of another PhD project in our group (V. Bianchi, 2016) while I have had the privileged access to TIL products where the percentage of γδ TCR^+ cells among $CD3^+$ cells exceeded 5%, and where matching autologous tumour was available.

All the tested TIL products showed a response *in vitro* to matching autologous tumours, in terms of CD107a and TNFα expression, and the cancer-reactive population contained γδ TCR^+ cells (between 3% and 90% of all cancer-reactive $CD3^+$ cells; **Figure 4.1**). However, no correlation between *in vitro* reactivity to autologous tumours, or cellular composition in terms of percentages of CD4, CD8 and γδ T-cells, and clinical outcome was found[256]. I have therefore focused on γδ T-cells present in the TIL product of the complete remission patient MM 15, and, albeit to a smaller extent, patient MM 46 who achieved stabilisation of the disease following adoptive transfer of TILs.

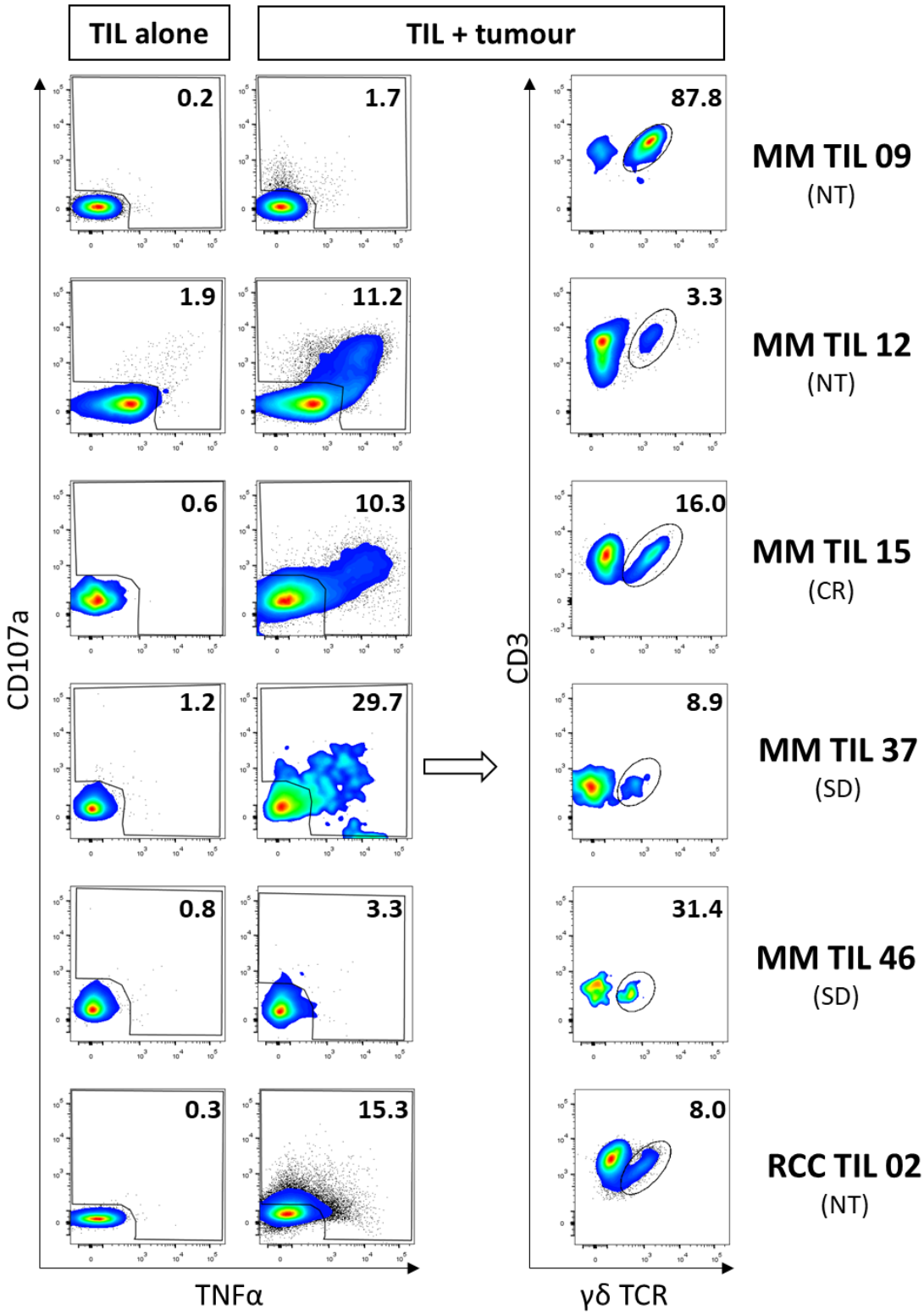

Figure 4.1 Clinical grade tumour-infiltrating lymphocytes contain autologous-tumour reactive γδ T-cells. T-cells were co-incubated with autologous tumour for 5 h, and stained for surface markers CD3, γδ TCR, and activation markers CD107a and TNFα. Only live $CD3^+$ cells were included in the analysis. Cells positive for CD107a and/or TNFα were subsequently gated to calculate the percentage of $γδ\ TCR^+$ cells within the cancer-reactive population. The numbers on dot plots correspond to the percentage of gated population. NT – not treated; CR – complete remission; SD – stable disease.

4.2.2 Autologous tumour-reactive T-cell clonotypes persist in peripheral blood of complete remission patients

Persistence of infused T-cells has been shown as one of the factors correlating positively with tumour regression in melanoma patients[392]. It can also be envisaged that the persistent cancer-reactive T-cell clones following successful TIL therapy are the key players in inducing tumour regression and preventing tumour recurrence, and therefore may be attractive targets for cancer vaccines or source of therapeutically-relevant TCRs. My colleagues and I have therefore combined live sorting of cancer-reactive (CD107a and/or TNFα positive; **Figure 4.2 A**) T-cells with next generation sequencing of TCR repertoires to investigate the breadth of anticancer response, and to discover shared clonotypes between TIL infusion products and peripheral blood 6 months after therapy. We have shown that the TCR-β repertoire of cancer-reactive T-cells becomes broader but also strongly dominated by a single clone in all three complete remission patients tested (Ref. [53] and **Figure 4.2 B**, top panel). My colleagues and I have also determined the HLA restriction and peptide specificity of the cancer-reactive clones that dominated the PBMC repertoire of complete remission patients (unpublished) – discussion of those data, however, exceeds the scope of this thesis.

In parallel with comparing the TCR-β repertoires of complete remission patients, I also looked into the cancer-reactive γδ TCR repertoire of the complete remission patient MM 15. The MM TIL 15 sample contained approximately 10% of γδ TCR^+ cells within the cancer-reactive population (**Figure 4.1**) and showed a striking diversity of clonotypes (over 500 distinct TCR-γ clonotypes and 700 distinct TCR-δ clonotypes), compared to less than 100 tumour-reactive TCR-β clonotypes from the same patient (**Figure 4.2 B**). In contrast, the autologous tumour-reactive T-cells in the peripheral blood after treatment contained less than 3% γδ T-cells (**Figure 4.2 A**), and the TCR repertoire of these tumour-reactive γδ T-cells in PBMC was narrowed down to 10-20 distinct clonotypes, with apparent dominance of 2-3 clonotypes. Similarly to TCR-β repertoires, the dominant cancer-reactive TCR-γ and TCR-δ clonotypes from the peripheral blood could be traced back to the TIL infusion product (**Figure 4.2 B**).

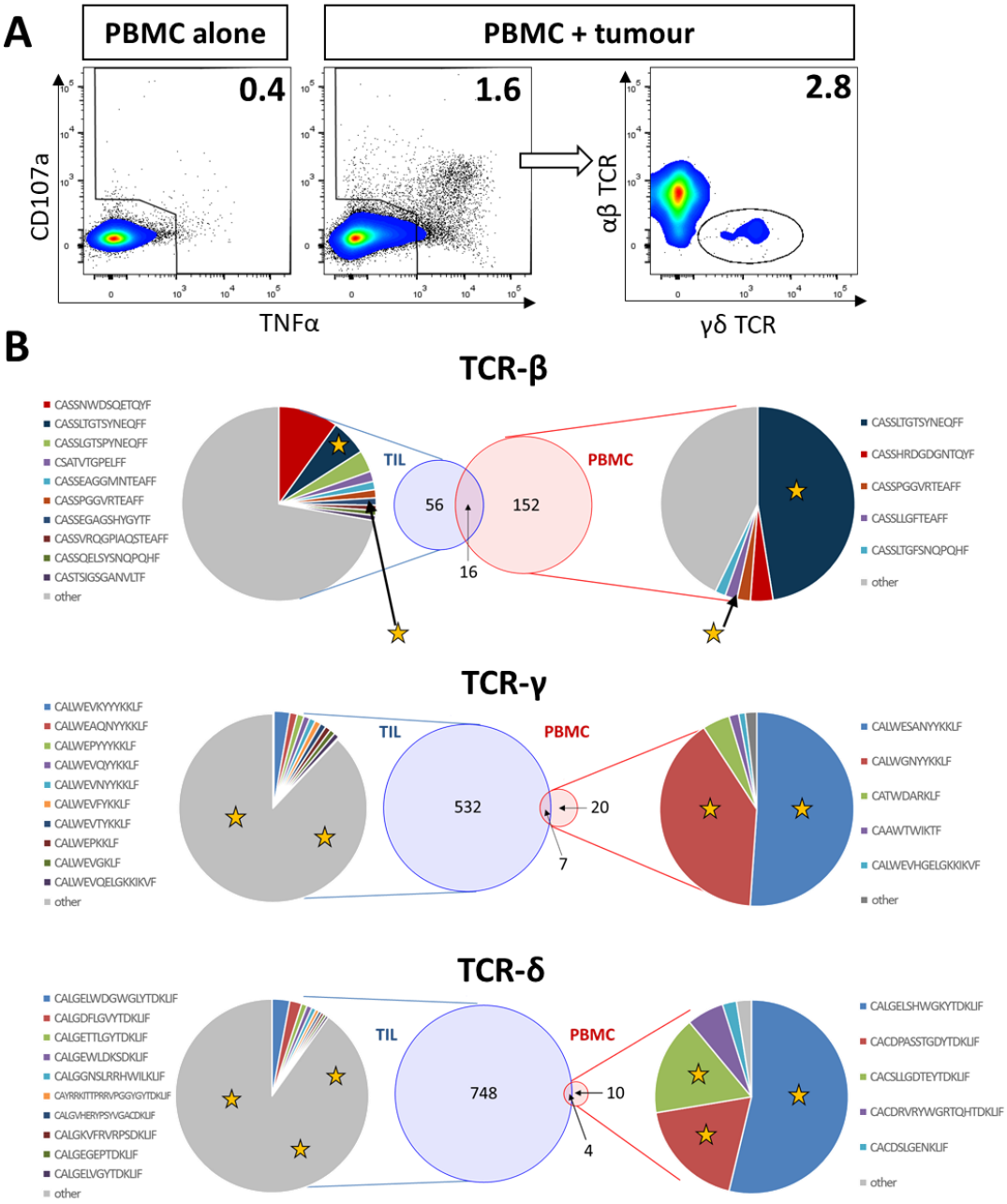

Figure 4.2 Cancer-reactive clonotypes persist in peripheral blood of a complete remission patient MM 15 after adoptive cell transfer. (**A**) PBMC from a complete remission stage IV melanoma patient were collected 6 months after adoptive cell transfer and stored. The PBMC were defrosted one day before co-incubation with autologous tumour. After 5 h of co-incubation, the samples were stained for surface markers CD14, CD19, CD3, αβ TCR and γδ TCR, as well as activation markers CD107a and TNFα. Only live $CD3^{+}$ $CD14^{-}CD19^{-}$ events were included in the analysis. The numbers on dot plots correspond to percentage of gated populations. More than 10,000 reactive (CD107a and/or TNFα positive) T-cells were sorted for TCR repertoire analysis. (**B**) TCR repertoire analysis on cancer-reactive T-cells from TIL and PBMC was performed as described in **Materials and Methods**. Amino acid CDR3 sequences for top 10 (TIL) or top 5 (PBMC) clonotypes are given. The sizes of pie slices correspond to the frequency of a given clonotype in the sample while the sizes of Venn diagrams correspond to the total number of distinct clonotypes (as indicated by numbers on Venn diagrams). Stars indicate clonotypes shared between TIL and PBMC.

4.2.3 Recognition of the autologous tumour by the TIL product from a complete remission patient is independent of known γδ TCR ligands

The use of CRISPR/Cas9 system allows a rapid and efficient generation of cells deficient in a functional product of the target gene, resulting in more robust phenotypes than achievable with siRNA-mediated gene knockdown. I transduced the autologous tumour line from the complete remission patient MM 15 (further referred to as t15) with lentivirus encoding Cas9 and gRNA specific for BTN3, EPCR and MICA/B. The knockout efficiency was up to 95% in cancer cells that had taken up lentivirus (**Figure 4.3 A**), and therefore no single cell cloning was required. Due to heterogeneity within patient-derived melanoma cell lines, single cell cloning could result in selection of cells that were more or less susceptible to T-cell mediated recognition than the parental line, regardless of introduced gene knockout, and thus confound the results (unpublished observations). The t15 line did not express detectable quantities of CD1 molecules (**Appendix Figure 8.3**), and therefore CD1 knockouts of t15 were not generated. Moreover, since the antibodies used for detection of BTN3 and MIC do not discriminate between isoforms, i.e. BTN3 A1-3 and MICA/MICB, I designed guide RNAs that target homologous regions in *btn3a* and *mica/micb* genes (**Figure 4.3 B**). I validated the BTN3 knockout of t15 by testing if this line was recognised by a phosphoantigen-reactive Vγ9Vδ2 T-cell clone. The addition of HMBPP or stimulating anti-BTN3 antibody 20.1 to untransduced tumour resulted in strikingly increased T-cell mediated lysis but had no effect on the lysis of BTN3 knockout tumour (**Figure 4.3 C**). Therefore, I concluded that the generated BTN3 knockout tumour line was deficient in functional BTN3 isoforms as intended.

Apart from being a ligand of some γδ TCRs, MICA/MICB is also a ligand of NK-type receptor NKG2D which is expressed on NK cells, but also γδ T-cells and $CD8^+$ αβ T-cells. I therefore incubated NKG2D positive T-cell clones and lines with MICA/B positive melanoma cell lines, including untransduced t15 and MICA/B knockout line. 5 h co-incubation of target cells with T-cells resulted in NKG2D down-regulation on the T-cells which correlated with the level of MICA/B expression on the cancer cells (**Figure 4.3 D**, left hand side panel). More importantly, no down-regulation of NKG2D expression was observed if T-cells were co-incubated with MICA/B knockout line (**Figure 4.3 D**, right hand side panel). The lack of NKG2D down-regulation indicated the absence of functional MICA/B molecules on the target cell surface and suggested that MICA/B rather than ULBPs were the main target of NKG2D in context of t15 melanoma cell line.

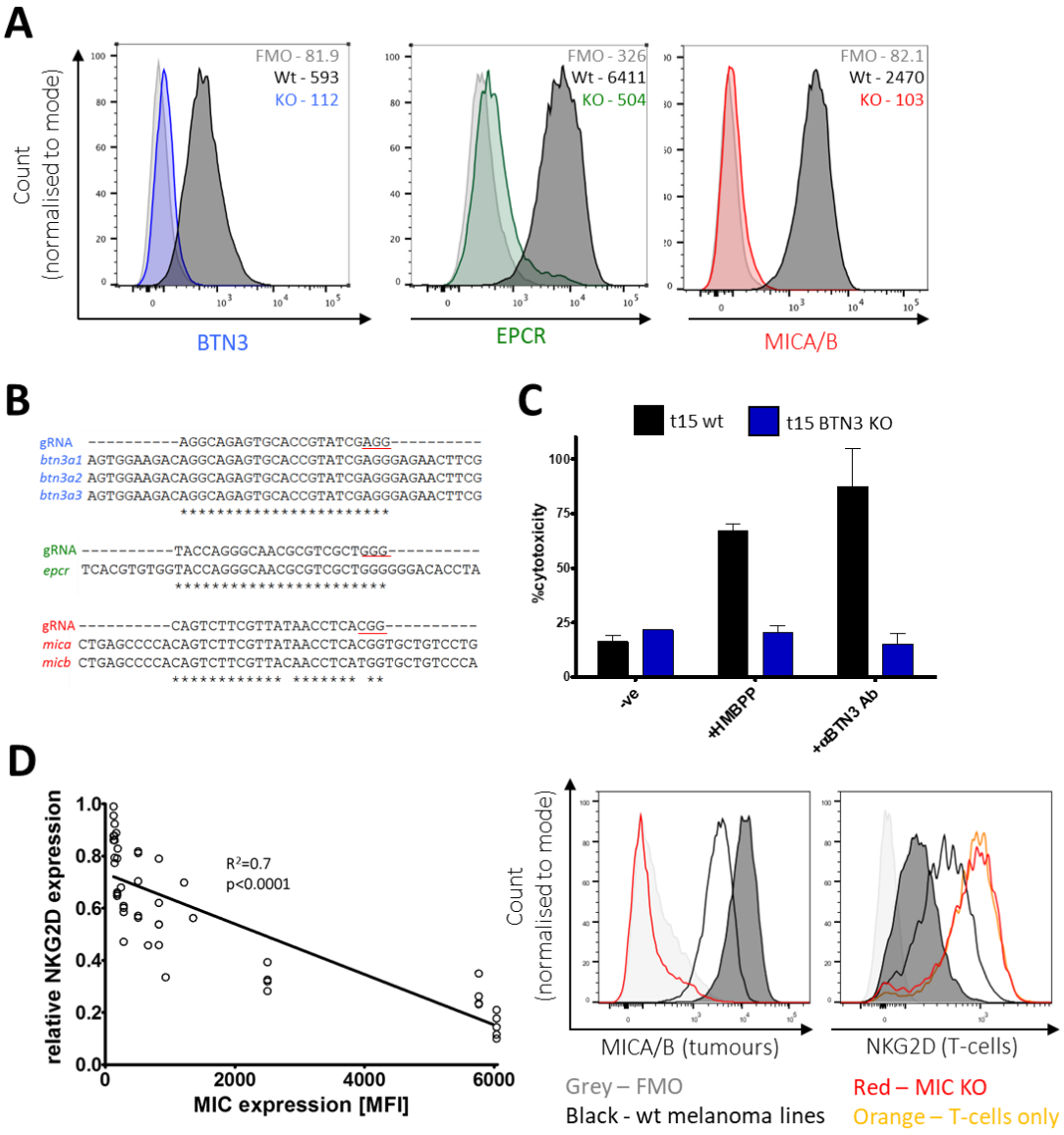

Figure 4.3 Generation of a melanoma cell line deficient in published γδ TCR ligands. (**A**) Melanoma cell line autologous to MM 15 TIL sample (further referred to as t15) was transduced with lentivirus encoding Cas9 and gRNAs specific for BTN3, EPCR and MICA/B. The cells that have taken up lentivirus were stained for surface expression of BTN3, EPCR and MICA/B. The numbers on histograms refer to median fluorescence intensity (MFI) of staining. (**B**) gRNA design for targeting of BTN3 (A1, A2 and A3), EPCR, and MIC A and B. PAM is underlined while stars indicate matching nucleotides between gRNA and target DNA sequences. (**C**) Validation of BTN3 knockout in t15. Untransduced (wt) and BTN3 knockout cells were co-incubated with a conventional Vγ9Vδ2 T-cell clone, in presence of HMBPP or stimulating anti-BTN3 antibody 20.1. Cytotoxicity was determined by ^{51}Cr release after 4 h of co-incubation at effector to target ratio of 5:1. (**D**) NKG2D downregulation on T-cells correlates with the level of MICA/B expression on cancer cells after 5 h co-incubation. NKG2D expression on T-cells was normalised by subtracting the MFI of unstained T-cells (FMO) while the NKG2D expression on T-cells incubated alone was normalised to 1. Left panel - Pearson's correlation between relative NKG2D level and MICA/B expression; right panel - representative histograms of staining of T-cells co-incubated with melanoma lines expressing various levels of MICA/B, or MICA/B knockout.

Finally, I purified γδ T-cells from TIL 15 infusion product and co-incubated the isolated γδ T-cells with wild-type t15 line and BTN3, EPCR or MICA/B knock-outs of this tumour line (**Figure 4.4**). There was no decrease in γδ T-cell reactivity in response to any of these knock-out lines, in terms of either CD107a or TNFα expression, when compared to the reactivity towards the wild-type melanoma line. The slight, albeit insignificant, increase of reactivity towards the knock-out lines could stem from cellular stress as a result of lentiviral infection and integration, and CRISPR/Cas9 mediated DNA damage.

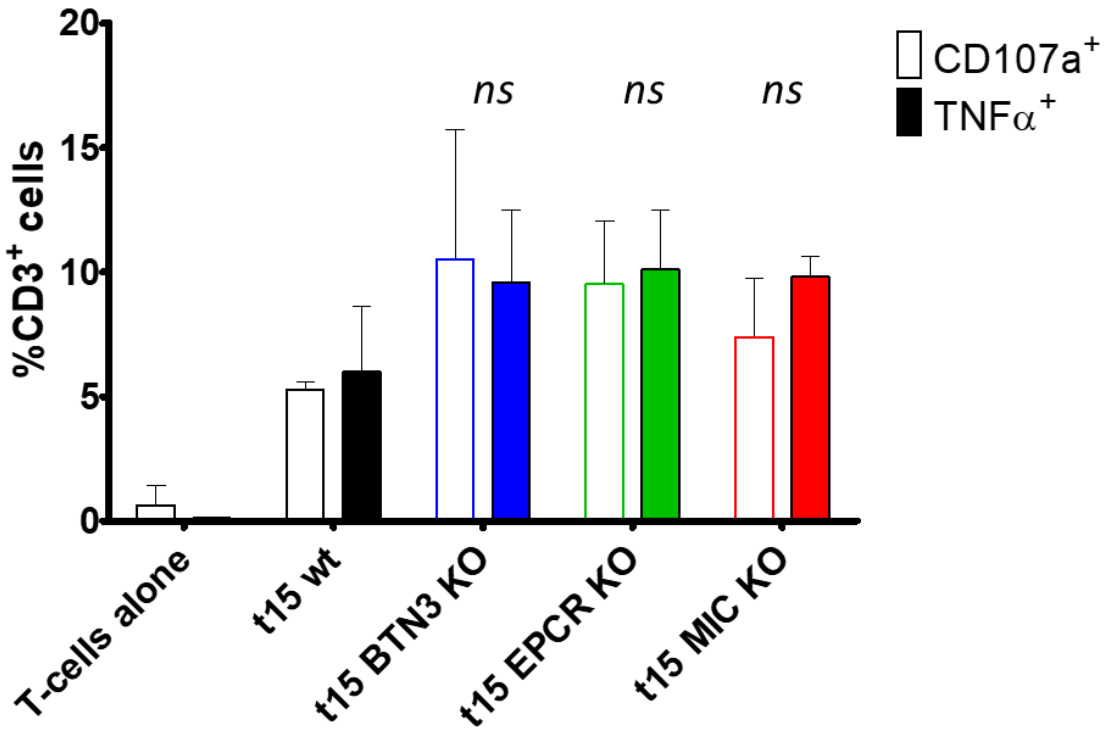

Figure 4.4 BTN3, EPCR and MICA/B are not required for autologous tumour recognition by the majority of γδ T-cells from a clinical grade TIL product. Purified γδ T-cells from MM TIL 15 were co-incubated with the autologous tumour, wild type or deficient in BTN3, EPCR or MICA/B, for 5 h. Mean and standard deviation from three independent experiments are shown. Student's t-test, ns – not significant ($p>0.05$).

4.2.4 Procurement of autologous tumour-reactive γδ T-cell clones from TIL products

T-cell clones are generally considered to be the gold standard for addressing various research questions pertaining to TCR-mediated antigen recognition in a more robust, reliable and reproducible manner than T-cell lines. Furthermore, T-cell clones may be a source of therapeutically relevant, paired TCRs. I therefore undertook single cell cloning of T-cells from TIL 15 and TIL 46 infusion products. The frequency of autologous tumour-reactive γδ T-cells in TIL 15 was relatively high (approximately 1-2%), the cloning was performed directly from the infusion product, without any prior enrichment. Screening of over 700 T-cell clones for

cytotoxicity against the autologous tumours resulted in selection of over different 50 T-cell clones, 14 of which expressed a γδ TCR. The remaining tumour-reactive clones were predominantly $CD8^+$ αβ T-cells, some of which are being used in other studies. In case of TIL 46, procurement of cancer-reactive clones was achieved by co-incubation of TILs with the autologous tumour, followed by live sorting of responding (i.e. TNFα and/or CD107a positive), γδ TCR^+ cells. While this approach resulted in procurement of only 16 clones, 3 out of those 16 clones expressed a γδ TCR, showed robust antitumour activity, and expanded well in culture. The methods for T-cell clone procurement are schematically depicted in **Figure 4.5**.

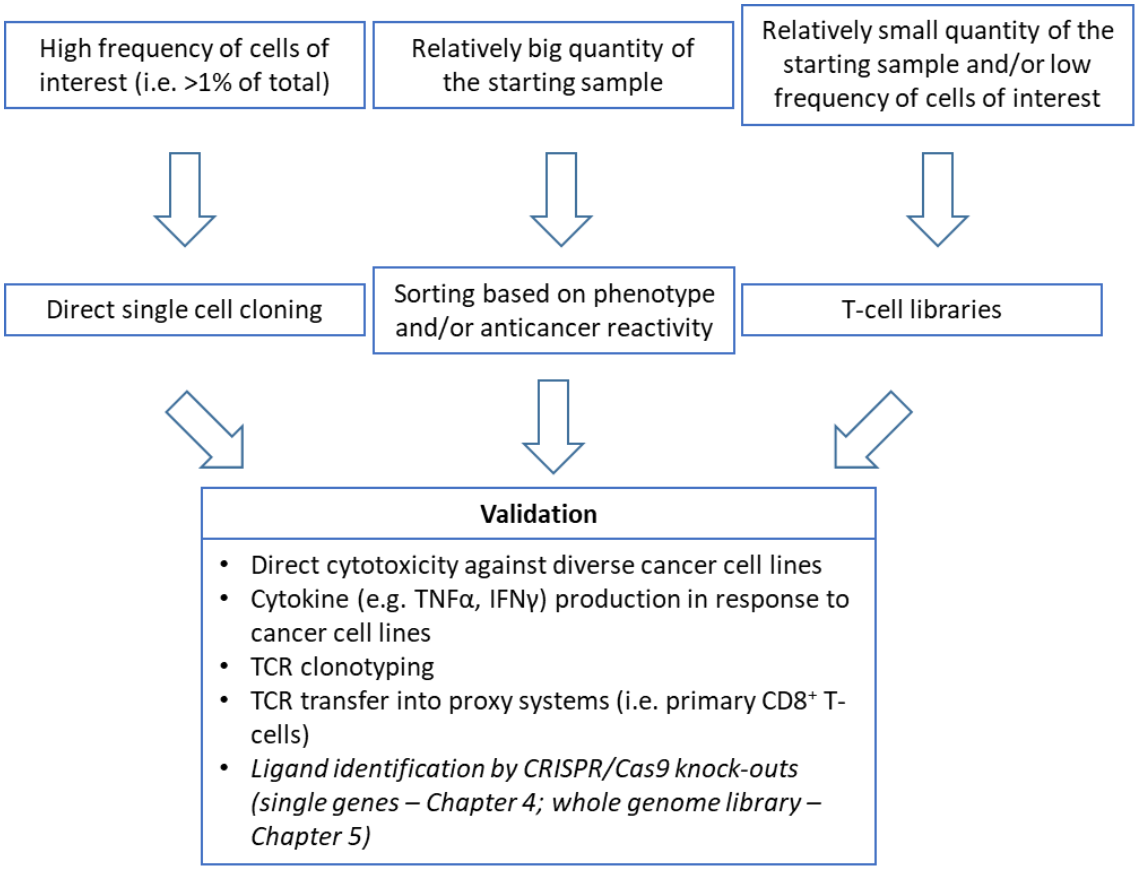

Figure 4.5 Schematic representation of strategies for procurement of broadly cancer-reactive T-cell clones and TCRs used in this Chapter. Depending on number of total cells available, and the estimated frequency of cells of interest, different strategies for enrichment and cloning of T-cells were used, followed by validation against non-HLA matched cancer cell lines of diverse origin.

The selected γδ T-cell clones could efficiently lyse autologous (**Figure 4.6 A**) and allogeneic (**Appendix Figure 8.4**) tumours. In terms of TCR usage, the T-cell clones were predominantly $Vδ1^+$ and $Vγ9^+$, with long and highly diverse CDR3δ sequences (**Figure 4.6 B**). Several clones were then selected for further experiments, based on robust growth parameters and potent anticancer reactivity.

A

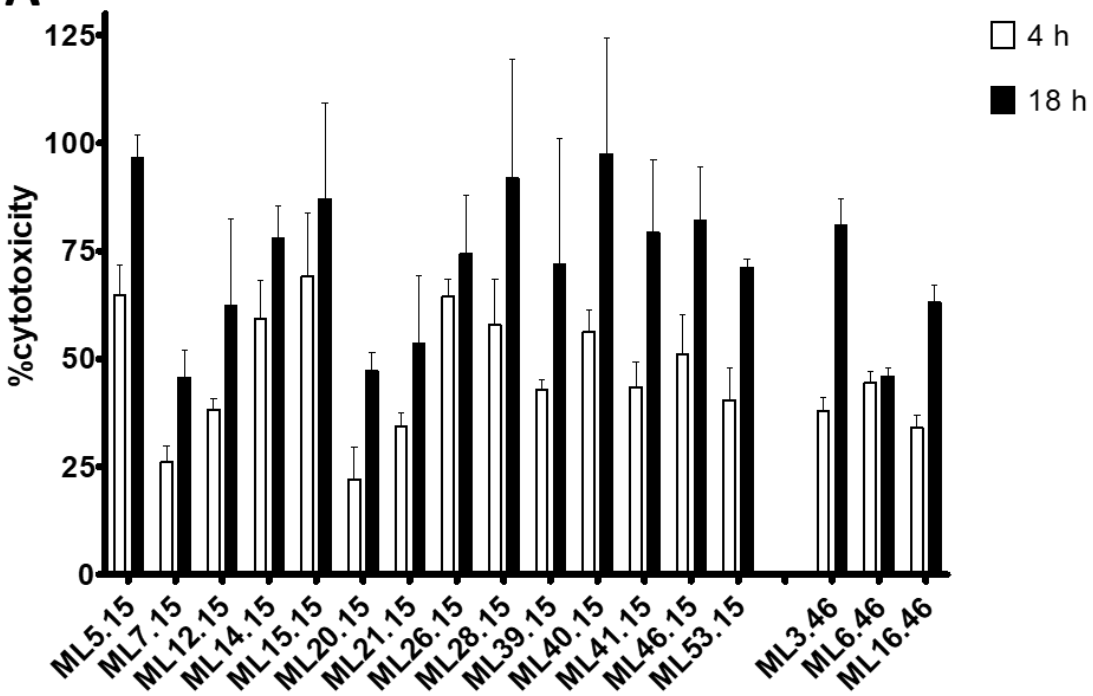

B

Clone	TRDV/TRDJ	TRDD	CDR3δ	TRGV/TRGJ	CDR3γ
ML5.15	TRDV1/TRDJ1	TRDD3	CALGEEWGHTDLGQRFYTDKLIF	TRGV9/TRGJ1	CALW..GSL.YYKKLF
ML7.15	TRDV1/TRDJ1	TRDD2 and TRDD3	CALG.VAAFPITGGL..KLIF	TRGV3/TRGJ1	CATW..EY.YYKKLF
ML12.15	TRDV1/TRDJ1	TRDD3	CALGEPEWGNTDKLIF	TRGV9/TRGJ1	CALWEVHLGD..YKKLF
ML14.15	TRDV1/TRDJ1	TRDD3	CALGELRAPGNRGMGDTDKLIF	TRGV2/TRGJ1	CATWDGPG.YYKKLF
ML15.15	TRDV2/TRDJ1	TRDD3	CACD.LLYWGTPTTDKLIF	TRGV9/TRGJP	CALWEV.QELGKKIKVF
ML20.15	TRDV3/TRDJ1	TRDD2 and TRDD3	CAFRGSKCKGED.DKLIF	TRGV8/TRGJP1	CATWDRP.TGWFKIF
ML21.15	TRDV2/TRDJ1	TRDD3	CACD.PYWGAYTDKLIF	TRGV3/TRGJ1	CATWD.SPSPHPQV.YYKKLF
ML26.15	TRDV2/TRDJ4	TRDD3	CACDTPWGIQGTRPLIF	TRGV9/TRGJ1	CALWEVQEAPNYYKKLF
ML28.15	TRDV3/TRDJ1	TRDD3	CAFDLPASSFLGDTPHTDKLIF	TRGV2/TRGJ1	CATWD.N.YKKLF
ML39.15	TRDV8/TRDJ1	TRDD1 and TRDD3	CAYR.RKITTPRRVPGGYGYTDKLIF	TRGV5/TRGJ2	CATWDRNYYKKLF
ML40.15	TRDV1/TRDJ1	TRDD2 and TRDD3	CALGELQGSYYGRGLLGDGVTDKLIF	TRGV9/TRGJ1	CALWE.GVFRSS.YYKKLF
ML41.15	TRDV1/TRDJ1	TRDD3	CALGEGPRGA.DKLIF	TRGV2/TRGJ2	CATWDGPNYYKKLF
ML46.15	TRDV1/TRDJ1	TRDD2 and TRDD3	CALGEPYVEIP.DKLIF	TRGV9/TRGJP	CALWEVGG...LGKKIKVF
ML53.15	TRDV2/TRDJ1	TRDD3	CACDTGGYMTDKLIF	TRGV2/TRGJP1	CATWD.PHYTTGWFKIF
ML3.46	TRDV1/TRDJ1	TRDD1 and TRDD3	CALGEPPGRKYVLLGDTA.DKLIF	TRGV9/TRGJ1	CALWEVPG.YYKKLF
ML6.46	TRDV1/TRDJ1	TRDD3	CALG.GTGRRGILVRTDKLIF	TRGV9/TRGJ1	CALWEVL.YYKKLF
ML16.46	Vδ2			Vγ9	

Figure 4.6 Autologous tumour-reactive γδ T-cells show limited V segment usage but diverse CDR3 sequences. (**A**) Cytotoxicity of autologous tumour-reactive γδ T-cell clones from MM TIL 15 and MM TIL 46 was determined by ^{51}Cr release after 4 h or 18 h co-incubation with autologous tumours at effector to target ratio of 10:1. (**B**) TCR sequencing was performed as described in Materials and Methods, and the annotation was performed in accordance with the IMGT nomenclature. Non-germline amino acids in CDR3 are shown in red while dots indicate deletions of germline amino acids. The TCR usage of clone ML16.46 was determined only by V segment specific antibody staining.

4.2.5 TIL-derived γδ T-cell clones show robust antitumour response and efficiently lyse diverse cancer lines

I investigated the autologous tumour-directed response of selected γδ T-cell clones in more detail, examining the production of cytokines TNFα, IFNγ and IL-2, the chemokine MIP-1β, in addition to cytotoxicity indicated by expression of a degranulation marker CD107a. TNFα and IFNγ are important drivers of the immune response against solid tumours and haematological cancers[379,380] while IL-2 promotes *in situ* survival, expansion and differentiation of T-cells[393]. Research from our laboratory has shown that MIP-1β secretion is the most sensitive readout of $CD8^+$ and $CD4^+$ αβ T-cell activation[354,356,357]. The T-cell clones ML15.15 and ML6.46 showed a strong and polyfunctional response after co-incubation with the autologous tumour, with the majority of cells expressing multiple functions (**Figure 4.7 A**). The polyfunctional profile of T-cell response has been shown as crucial for cancer eradication[375]. Other clones tested (ML26.15, ML40.15 and ML16.46) displayed a similar profile of polyfunctionality as clones ML15.15 and ML6.46 (**Appendix Figure 8.5**) while clone ML5.15 displayed the weakest reactivity of all the clones tested.

All the γδ T-cell clones tested lysed a diverse panel of cancer cell lines, spanning melanoma, breast cancer, haematological malignancies, cervical cancer and bone osteosarcoma that shared no common HLA (**Figure 4.7 B** and **Appendix Figure 8.6**). The majority of clones tested (ML5.15, ML15.15, ML26.15 and ML16.46) efficiently lysed all but three cancer lines tested, and the unrecognised cell lines were of B-cell origin (T2 cell line, EBV transformed B LCL and Burkitt's lymphoma Daudi). In contrast, clone ML6.46 showed a more pronounced preference for melanoma cell lines, possibly indicating a different antigen specificity than the other clones (**Figure 4.7 B,** bottom panel).

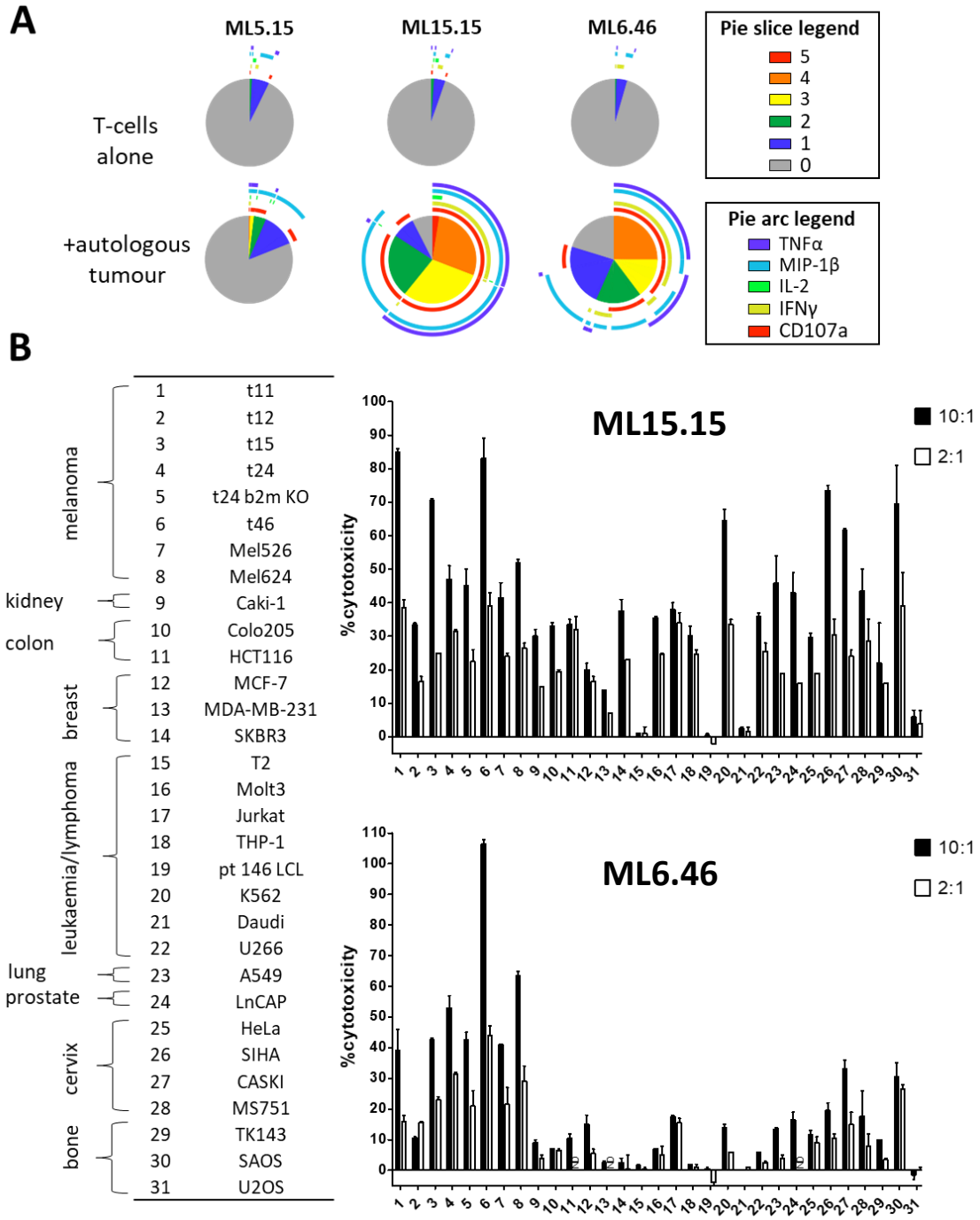

Figure 4.7 TIL-derived γδ T-cell clones show polyfunctional response to the autologous tumour and recognise diverse cancer lines. (**A**) Polyfunctional profile of response of representative γδ T-cell clones to autologous tumours was determined by intracellular cytokine staining after 5 h of co-incubation. Only viable $CD3^+$ cells were included in the analysis, and the gates were set based on appropriate biological and fluorescence minus one controls. Pie slices represent fractions of cells positive for a given number of effector functions simultaneously, while arcs specify the effector function. (**B**) Cytotoxicity against a panel of cancer cell lines (listed on the left hand side) was determined by ^{51}Cr release after 6 h of co-incubation with T-cells at 10:1 and 2:1 effector to target ratio. Representative data from two experiments are shown. ND – not determined.

4.2.6 TIL-derived γδ TCRs are sufficient for re-direction of peripheral αβ T-cells to tumour

As discussed before, the role of γδ TCRs in target recognition remains open to debate. At the same time, using T-cells engineered to express a well-defined γδ TCR seems a more promising and robust immunotherapeutic strategy than generation of patient-autologous γδ T-cell lines of undefined specificity and cellular composition. Therefore, I applied the TCR replacement method described in **Chapter 3** to study the potential of re-directing healthy donor-derived $CD8^+$ αβ T-cells to melanoma line t15. I chose the TCRs from the weakly cancer-reactive clone ML5.15 and strongly cancer-reactive ML15.15 (**Figure 4.8 A** and **B**). When either TCR was transferred into αβ T-cells alone, no specific reactivity to cancer lines was detected. Conversely, when TCR transfer was combined with CRISPR/Cas9 mediated TCR-β knockout, the resulting engineered T-cells showed a striking reactivity against the autologous tumour line t15 or breast cancer line MDA-MB231 (**Figure 4.8 A**). The presence of NKG2D was not sufficient to confer reactivity to cancer lines tested, as both TCR-transduced and untransduced cells expressed this activating NK-type receptor (**Appendix Figure 8.7**).

4.2.7 An unanticipated lack of phosphoantigen self-presentation by a cancer-reactive clone ML15.15

Clone ML15.15 (further referred to as ML15 from hereon) recognises the autologous tumour in a TCR-dependent manner, as well as efficiently lyses numerous cancer cell lines. Moreover, clone ML15 should mount a response to phosphoantigens as it expresses a TCR composed of TRDV2 and TRGV9/TRGJP segments with the germline encoded CDR3γ CALWEVQELGKKIKVF[58]. ML15 TCR also possesses a hydrophobic amino acid, leucine, at position 97 within the CDR3δ, which is thought to predispose Vγ9Vδ2 TCRs towards phosphoantigen reactivity[394]. Despite the primary sequence of the TCR, and capability of mounting a strong functional response as exemplified by recognition of the autologous tumour, clone ML15 failed to secrete MIP-1β or TNFα after stimulation with even micromolar concentrations of HMBPP. Conversely, peripheral blood derived Vγ9Vδ2 T-cell clones tested in parallel were still capable of responding to HMBPP at sub-nanomolar concentrations (**Figure 4.9 A** and **B**). Clone ML15 also failed to respond to IPP concentrations as high as 10 μM (**Appendix Figure 8.8**).

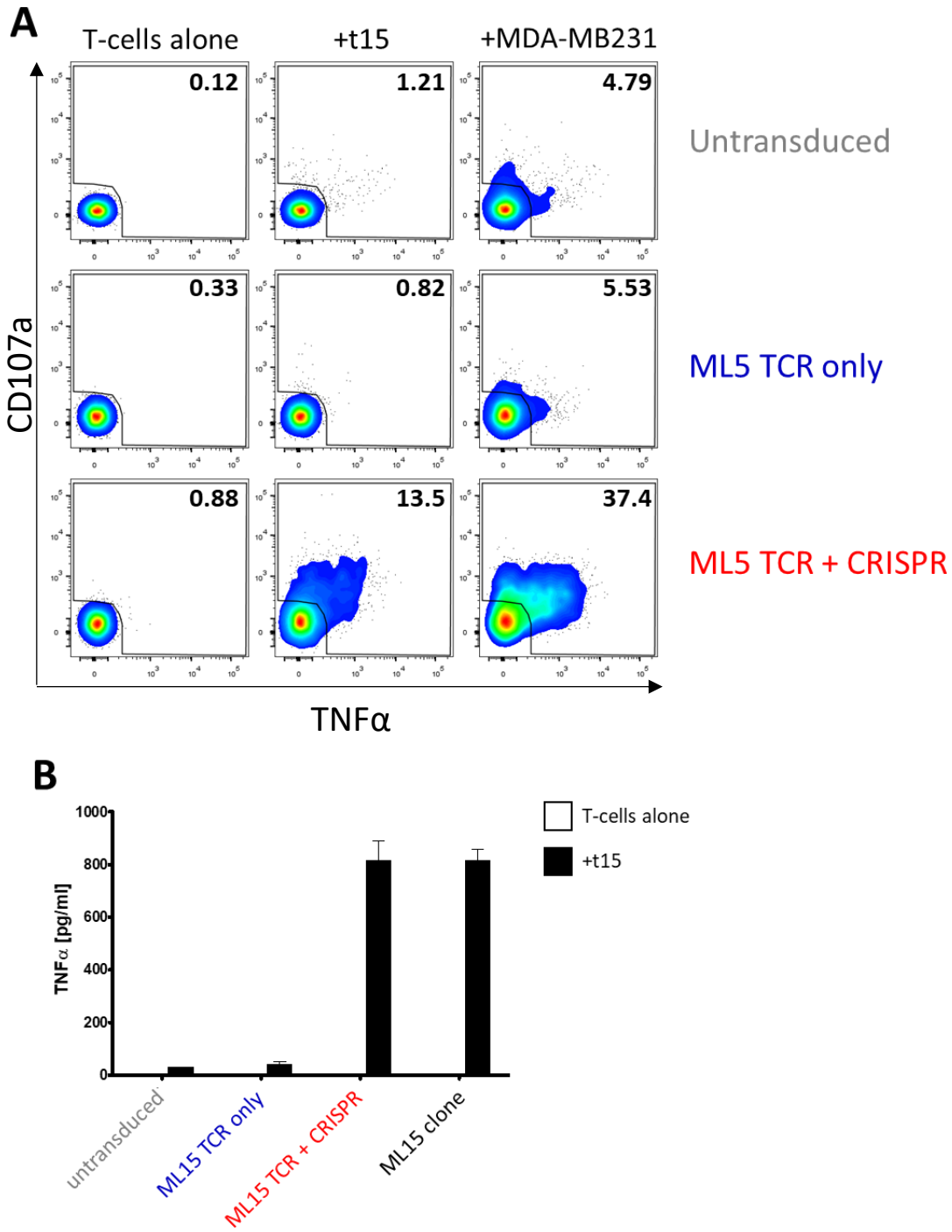

Figure 4.8 TIL-derived γδ TCRs are capable of conferring reactivity to the autologous tumour when transferred to peripheral blood T-cells, together with TCR-β knockout. (**A**) Untransduced, single transduced (ML5 TCR only) or double transduced (ML5 TCR+TCR-β CRISPR) $CD8^+$ αβ T-cells were co-incubated with the autologous tumour t15 or breast cancer line MDA-MB231 for 5 h. Only live $CD3^+$ (and $rCD2^+$, in case of transduced cells) were included in the analysis. (**B**) Untransduced, single transduced (ML15 TCR only) or double transduced (ML15 TCR+TCR-β CRISPR) $CD8^+$ αβ T-cells were co-incubated with the autologous tumour t15 for 16 h, followed by quantification of secreted TNFα by ELISA. Parental clone ML15.15 was tested in parallel.

Clone ML15 expressed a similar level of BTN3 molecules on the cell surface as a phosphoantigen-reactive clone tested in parallel (**Figure 4.9 C**). Despite the abundance of BTN3 on cell surface, clone ML15 failed to respond to the stimulating anti-BTN3 antibody 20.1 or zoledronate in absence of antigen presenting cells (**Figure 4.10**). However, clone ML15 was capable of exhibiting a statistically significant response to the antibody 20.1 or zoledronate when T2 cell line was used for antigen presentation. Neither zoledronate nor 20.1 antibody could increase the response of clone ML15 to the autologous tumour. Finally, TNFα production by ML15 in response to t15 was decreased only by 20-30% in case of BTN3 knock-out while MICA/B and EPCR knock-outs did not affect the T-cell response (**Figure 4.11**). Notably, clone ML15 strongly down-regulated CD3-TCR complex after co-incubation with the autologous tumour, as well as MICA/B and EPCR knock-out tumour line, but only a minor down-regulation of CD3-TCR was observed after co-incubation with the BTN3 knock-out (**Appendix Figure 8.9**).

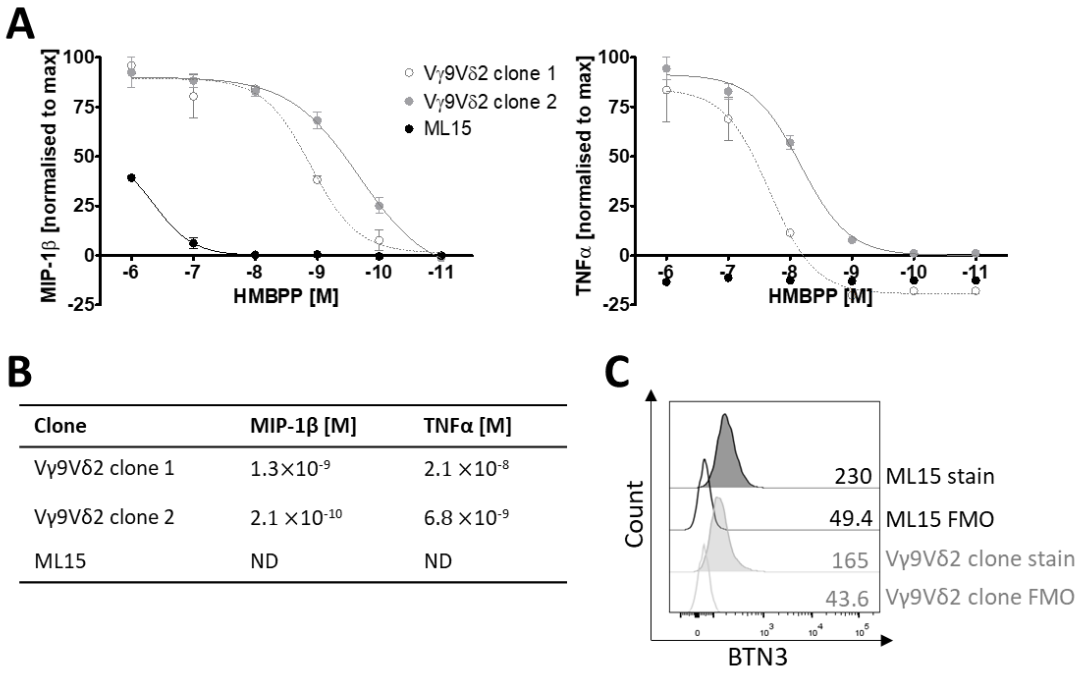

Clone	MIP-1β [M]	TNFα [M]
Vγ9Vδ2 clone 1	1.3×10^{-9}	2.1×10^{-8}
Vγ9Vδ2 clone 2	2.1×10^{-10}	6.8×10^{-9}
ML15	ND	ND

Figure 4.9 TIL-derived Vγ9Vδ2 clone ML15 fails to self-present conventional phosphoantigens. (**A**) Clone ML15 and two peripheral blood derived Vγ9Vδ2 clones, were stimulated with titrated concentrations of HMBPP for 16 h, followed by quantification of secreted MIP-1β or TNFα. The cytokine concentrations were normalised by subtracting the cytokine concentration from unstimulated T-cells, and taking the highest concentration of cytokine as 100%. In case of clone ML15, the highest concentration of cytokine was determined by co-incubation with autologous tumour. (**B**) HMBPP concentrations at which the response of T-cells (in terms of MIP-1β or TNFα) achieved 50% of maximal response (EC_{50}). (**C**) BTN3 staining on surface of clone ML15 or a conventional Vγ9Vδ2 clone. Numbers refer to the MFI of staining.

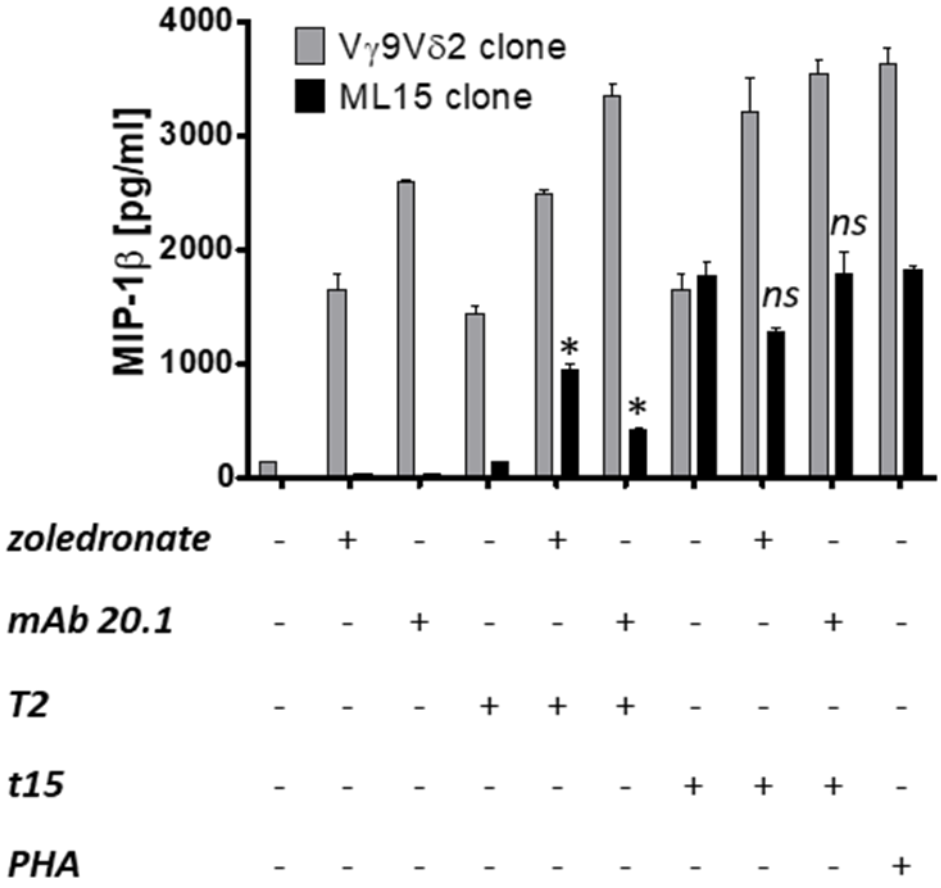

Figure 4.10 TIL-derived Vγ9Vδ2 clone ML15 shows a response to phosphoantigen pathway stimuli in presence of antigen-presenting cells. The response of clone ML15 to zoledronate or stimulating anti-BTN3 antibody 20.1 was tested in presence or absence of antigen presenting cells T2 or t15. A conventional Vγ9Vδ2 clone was tested in parallel. PHA was used as a non-specific T-cell stimulus. The concentration of secreted MIP-1β was quantified after 16 h of co-incubation. Student's t-test *$p<0.05$, ns – not significant.

4.2.8 ML15 TCR transduced cells can respond to phosphoantigens and require BTN3 expression to recognise the autologous tumour

The lack of response to phosphoantigens by clone ML15 could stem from a TCR-intrinsic or TCR-extrinsic reasons, i.e. absence or defects in endogenous phosphoantigen processing and presentation machinery, or in putative co-stimulatory molecules. Therefore, I tested the ML15 TCR transduced $CD8^+$ T-cells for activation after stimulation with HMBPP or autologous tumour (**Figure 4.12 A**). In line with previously shown data, clone ML15 produced TNFα in response to autologous tumour but not HMBPP. Conversely, $CD8^+$ T-cells transduced with a conventional Vγ9Vδ2 TCR responded to HMBPP but not t15. Interestingly, ML15 TCR transduced $CD8^+$ T-cells

mounted a strong response both to HMBPP and t15, thus demonstrating that the TCR expressed by clone ML15 shows an intrinsic phosphoantigen specificity.

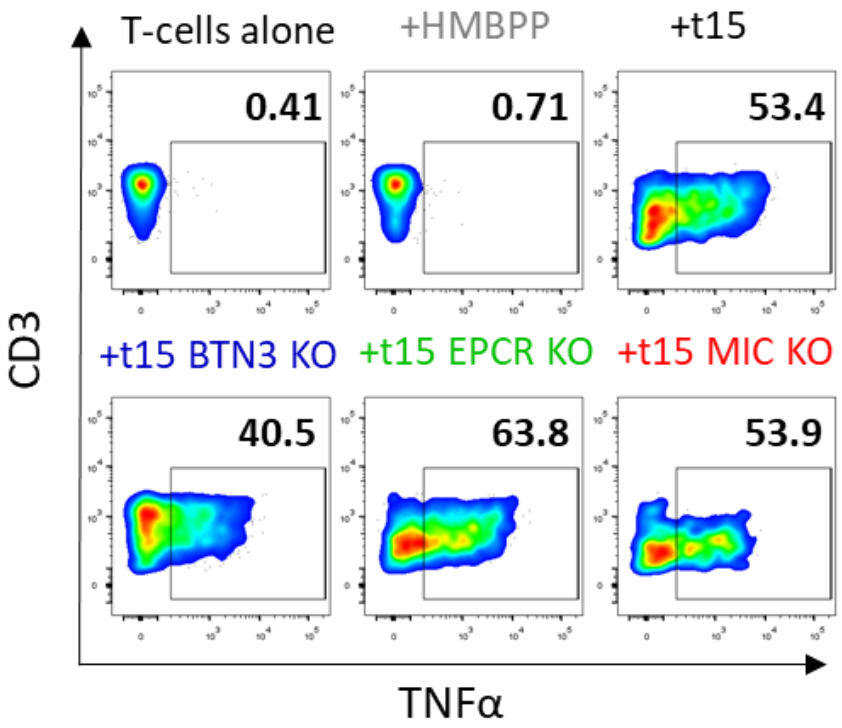

Figure 4.11 BTN3 knock-out does not abrogate the response of clone ML15 to the autologous tumour. Clone ML15 was co-incubated with 1 μM HMBPP, or autologous tumour (wild type or deficient in BTN3, EPCR or MICA/B) for 5 h. Only live $CD3^+$ cells were taken for the analysis. The numbers on dot plots correspond to the percentage of gated populations.

The effect of BTN3 expression on t15 on recognition by the ML15 TCR was subsequently determined. While a conventional Vγ9Vδ2 clone, or $CD8^+$ T-cells transduced with the conventional Vγ9Vδ2 TCR, showed cytotoxicity only towards zoledronate-pretreated, BTN3 expressing t15, ML15 clone and ML15 TCR transduced cells showed strong cytotoxicity against wild type t15 regardless of zoledronate treatment (**Figure 4.12 B**). As shown before, BTN3 knock-out had only a minor effect on t15 recognition by clone ML15. In contrast, BTN3 knock-out resulted in over 95% reduction of cytotoxicity by ML15 TCR transduced cells.

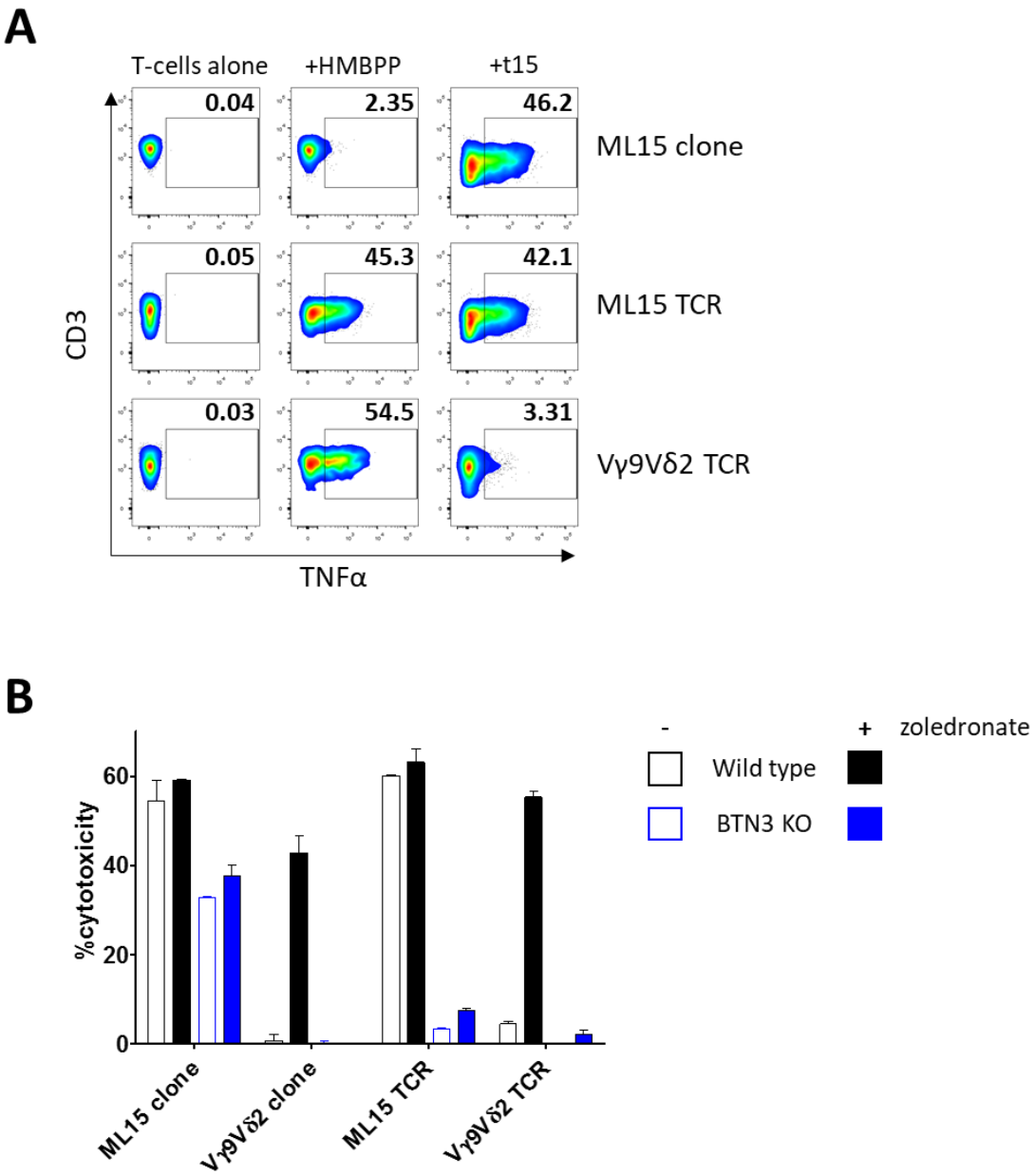

Figure 4.12 ML15 TCR confers the recognition of both autologous tumour and HMBPP to peripheral blood derived CD8$^+$ T-cells. (**A**) CD8$^+$ T-cells transduced with ML15 TCR, or a conventional Vγ9Vδ2 TCR, together with TCR-β CRISPR, were incubated for 5 h with 1 μM HMBPP or autologous tumour t15. The parental clone ML15 was tested in parallel. Only live CD3$^+$ cells were included in the analysis. The numbers on dot plots correspond to percentages of gated populations. (**B**) Cytotoxicity of ML15 or Vγ9Vδ2 clones, as well as CD8$^+$ T-cells transduced with TCR-β CRISPR and ML15 or Vγ9Vδ2 TCRs, was determined by ^{51}Cr release after 4 h co-incubation with target cells (t15, wt or BTN3 knockout) at effector to target ratio of 5:1. The target cells were pre-incubated with 50 μM zoledronate for 24 h before co-incubation with T-cells where indicated.

4.2.9 ML15 TCR efficiently re-directs peripheral T-cells to solid tumours without zoledronate treatment

Given the fact that ML15 TCR transduced cells showed strong cytotoxicity towards autologous tumour without zoledronate pre-treatment, I investigated the capability of ML15 TCR to re-direct peripheral $CD8^+$ T-cells to a panel of cancer cell lines without the need of aminobisphosphonate treatment. As discussed in **Chapter 3**, one of the plausible reasons for low efficacy of Vγ9Vδ2 therapies in solid tumours could be inefficient penetration of the tumour mass by aminobisphosphonates. Therefore, T-cells transduced with a BTN3-specific TCR that efficiently lyse solid tumours in absence of aminobisphosphonate treatment could be of therapeutic interest.

Indeed, ML15 TCR transduced T-cells lysed melanoma cell lines and a representative breast cancer line more efficiently than T-cells transduced with a "conventional" Vγ9Vδ2 TCR (**Figure 4.13 A**). No specific recognition of normal cell lines, including hepatocytes, ciliary epithelial cells or fibroblasts, by ML15 TCR transduced T-cells was observed, further underlining the pre-clinical potential of ML15 TCR (**Figure 4.13 B**). However, only a fraction of cell lines recognised by clone ML15 (**Figure 4.7 B**) were recognised by ML15 TCR-transduced cells, suggesting either TCR-independent manner of recognition of those cell lines, or requirement for specific co-stimulatory receptors that were present on the ML15 T-cell clone but not on ML15 TCR-transduced $CD8^+$ cells.

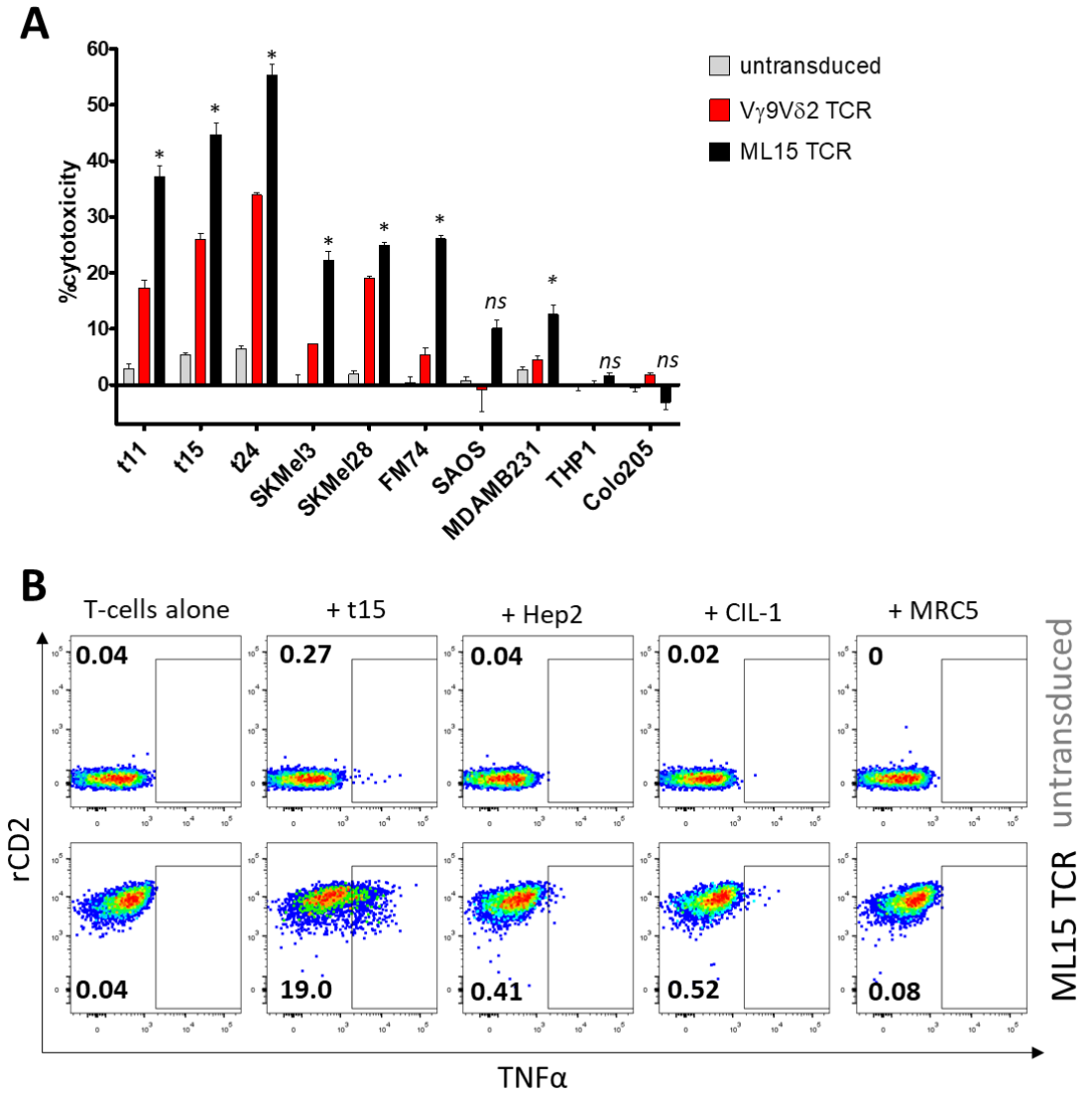

Figure 4.13 ML15 TCR redirects CD8$^+$ T-cells to a range of tumour cell lines without targeting normal cell lines. (**A**) Cytotoxicity of ML15 and Vγ9Vδ2 TCR transduced CD8$^+$ T-cells was determined by ^{51}Cr release after 4 h of co-incubation with tumour cell lines at effector to target ratio of 10:1. CD8$^+$ T-cells were transduced with TCR-β CRISPR together with a γδ TCR. Student's t-test *p<0.05, ns – not significant. (**B**) ML15 transduced T-cells were co-incubated with normal hepatocytes Hep2, ciliary epithelial cells CIL-1 and fibroblasts MRC5 for 5 h. Autologous tumour t15 was used as a positive control. Only live CD3$^+$ cells were taken for analysis. The numbers on dot plots correspond to percentages of gated populations.

4.2.10 T-cell libraries can be used to procure cancer-reactive γδ T-cell clones

While cancer-reactive T-cells are present in the periphery of cancer-free individuals, their frequency is significantly lower than that observed the TIL samples[395]. Therefore, in order to isolate rare cancer-specific γδ T-cell clones from healthy donor PBMC, I modified the T-cell library method developed by my colleagues for isolation of $CD8^+$ T-cells specific for a given peptide-HLA complex[216]. Bulk γδ T-cells were first isolated from healthy donor PBMC by magnetic depletion of other cell types present in the peripheral blood. This approach avoided antibody crosslinking of γδ TCRs leading to cellular activation and potentiallyr activation-induced cell death that might be expected if using positive selection of γδ T-cells using γδ TCR antibody[396]. Selected cells were then physically separated by plating of 2,000 cells per well in 96U wells, and expanded with CD3/CD28 beads to preserve the TCR representation[397]. After 14 days, and approximately 100-fold T-cell expansion, individual wells were assayed for recognition of a small panel of cancer cell lines by IFNγ ELISpot. IFNγ ELISpot is used as a gold standard for detection and quantification of rare antigen specific T-cells[398]. Two out of 96 wells contained T-cells responding to the cancer cell lines (**Figure 4.14**). T-cells from the positive wells were then combined and further enriched by incubation with cancer cell lines and isolation of cytokine-producing cells. Cells isolated in this way were then subjected to single cell cloning in presence of irradiated allogeneic PBMC and PHA, and resulting T-cell clones were screened for recognition of individual cancer cell lines. Two γδ T-cell clones responding to all three cancer cell lines were identified. Both clones, however, expressed Vγ9Vδ2 TCRs and therefore were not pursued any further.

T-cell libraries could also be applied to isolation of cancer-reactive T-cells from ovarian cancer ascites. While ascites is considered an immunosuppressive environment[399], ascites-derived T-cells expanded equally well as T-cells derived from a healthy donor (unpublished observation). The initial isolation of T-cells had to be modified so that positive rather than negative selection of γδ TCR^+ cells was performed, to avoid contaminating the T-cells with cancer cells present in the ascites (**Figure 4.15**). Seven out of 140 wells that were screened contained ovarian cancer reactive T-cells, and following enrichment of cancer-reactive cells from the responding wells one ovarian cancer-reactive Vγ9Vδ2 clone was isolated. In parallel, I isolated five ovarian cancer reactive $CD8^+$ αβ T-cell clones which are being used in another study.

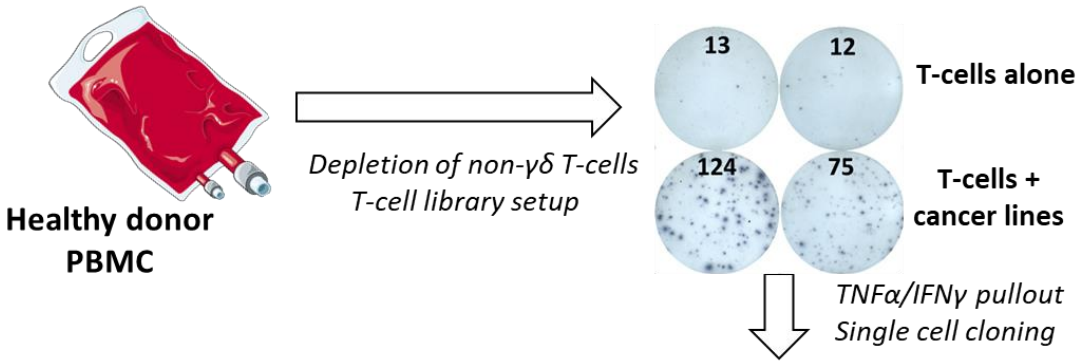

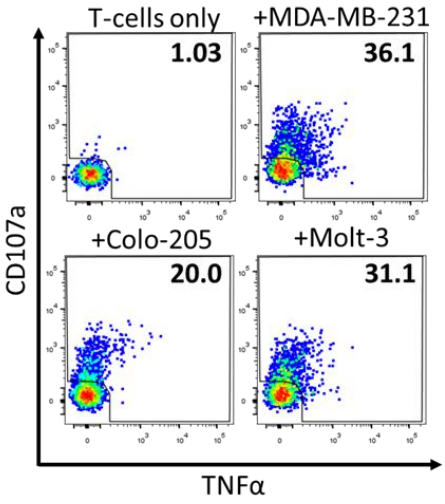

Figure 4.14 T-cell libraries can be used for rapid procurement of cancer-reactive γδ T-cell clones from healthy donors. γδ T-cells were purified by negative selection from fresh healthy donor PBMC and expanded with CD3/CD28 beads as described in **Materials and Methods Section 2.2.6**. 2,000 T-cells were plated per well. After 14 days, each well was tested for response to a small panel of cancer cell lines (MDA-MB-231, Colo-205, Molt-3) by IFNγ ELISpot. The numbers of spots in positive wells are shown. The cancer-reactive wells were then combined and co-incubated with cancer cell lines for 5 h, followed by magnetic purification of TNFα and/or IFNγ secreting T-cells. Cells enriched in this way were single cell cloned tested for recognition of individual cancer cell lines.

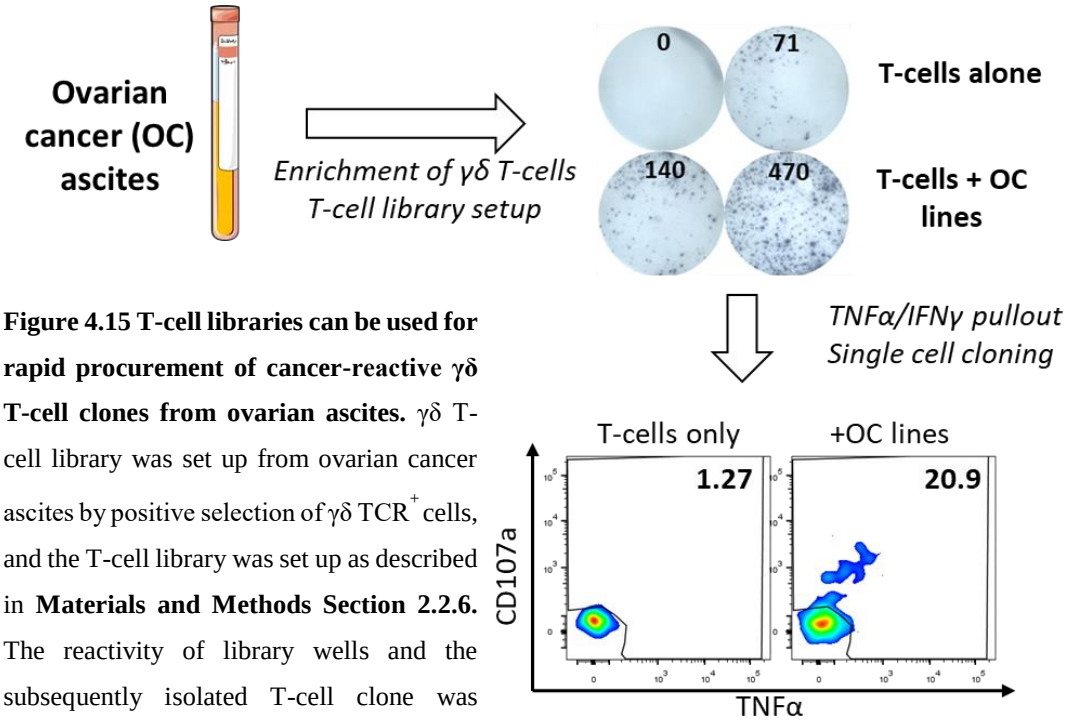

Figure 4.15 T-cell libraries can be used for rapid procurement of cancer-reactive γδ T-cell clones from ovarian ascites. γδ T-cell library was set up from ovarian cancer ascites by positive selection of γδ TCR^+ cells, and the T-cell library was set up as described in **Materials and Methods Section 2.2.6.** The reactivity of library wells and the subsequently isolated T-cell clone was determined against combined ovarian cancer (OC) lines SKOV-3 and A2780.

4.2.11 Procurement of a breast cancer-reactive γδ TCR from breast cancer patient's PBMC

Cancer-specific T-cells are present in the peripheral blood of cancer patients at a generally higher frequency than in healthy individuals, as a result of an ongoing cancer-directed immune response[400]. Therefore, I decided to use T-cell libraries to isolate breast cancer-reactive γδ T-cell clones from the peripheral blood of a breast cancer patient (not treated with any immunotherapeutic modality). One of the advantages of using T-cell libraries is the feasibility of working with relatively limited samples, due to the initial CD3/CD28 bead expansion. For instance, the breast cancer patient's sample discussed here (kindly provided by Matthias Eberl, Cardiff University) consisted of only 1 million viable PBMC upon thawing, which translated to less than 20,000 of purified γδ T-cells. The purified T-cells were plated at 200 cells per 96U well, and expanded approximately 500-fold with CD3/CD28 beads. The library was then screened for reactivity against a small panel of breast cancer lines, and two out of 90 library wells contained breast cancer reactive T-cells (**Figure 4.16 A**). Two γδ T-cell clones were subsequently isolated from the positive library wells. Both γδ T-cell clones showed reactivity towards all three breast cancer lines tested, in particular MDA-MB-231 cell line, (**Figure 4.16 A**) and were found to be sister clones, *i.e.* express the same TCR, further referred to as BC1.18 (**Figure 4.16 B**).

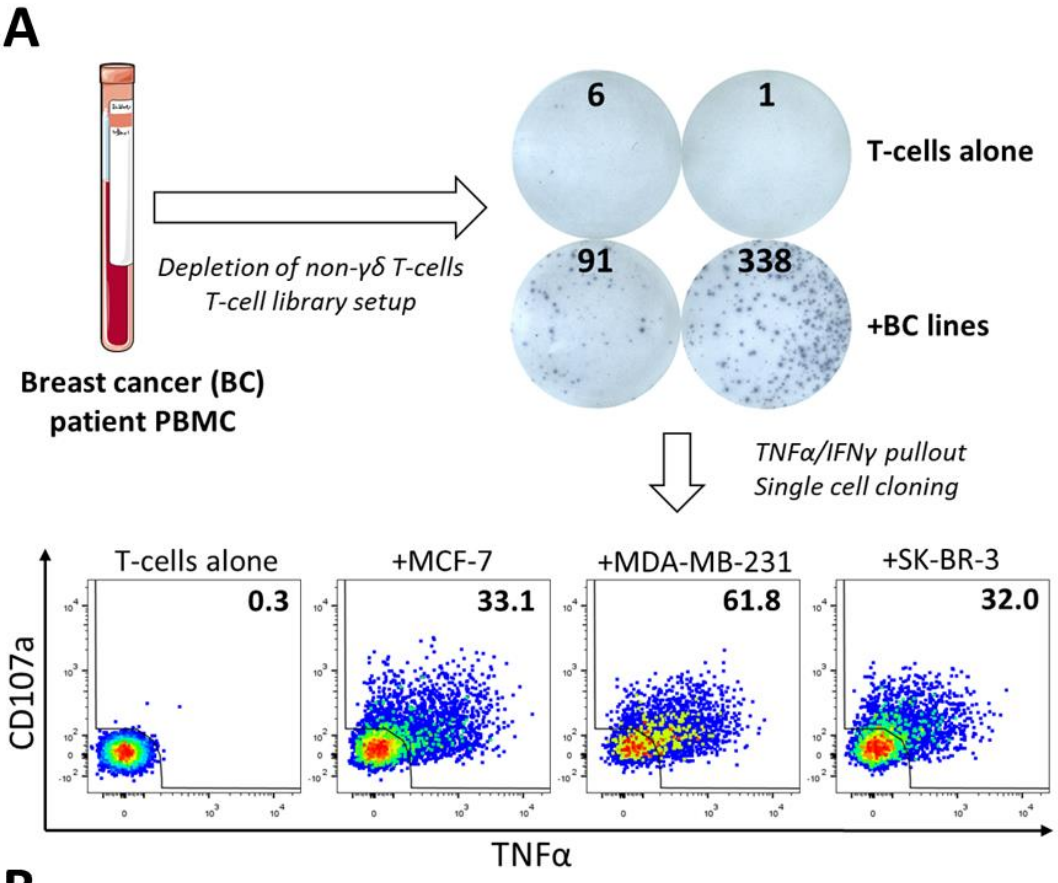

B

TRV	TRD	TRJ	CDR3
TRDV1	TRDD2	TRDJ1	CAL..APRVALVPER..KLIF
TRGV9	-	TRGJ1	CALWE.LLD.YYKKLF

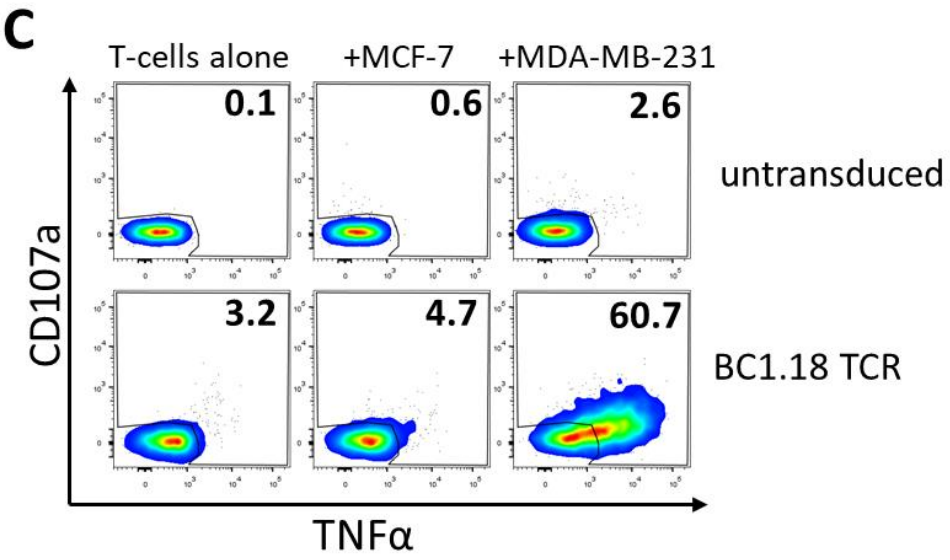

Figure 4.16 Rapid procurement of a cancer-reactive γδ TCR from breast cancer PBMC. *(Legend continued on the next page)*

(Legend continued from the previous page) (**A**) γδ T-cells were purified by negative selection from thawed breast cancer PBMC and expanded with CD3/CD28 beads. 200 cells were initially plated per well. After 14 days, each well was tested for response to a small panel of breast cancer cell lines (MCF-7, MDA-MB-231, SK-BR-3) by IFNγ ELISpot. The numbers of spots in representative wells are shown. The cancer-reactive wells were then combined and co-incubated with cancer cell lines for 5 h, followed by magnetic purification of TNFα and/or IFNγ secreting T-cells. Cells enriched in this way were then single cell cloned tested for recognition of individual cancer cell lines. (**B**) Two cancer-reactive T-cell clones were obtained from the library. Both clones were found to express an identical TCR BC1.18, annotated according to the IMGT nomenclature. Non-germline amino acids in CDR3 are shown in red while dots indicate deletions of germline amino acids. (**C**) $CD8^+$ T-cells, either untransduced or transduced with BC1.18 TCR, were co-incubated with breast cancer cell lines MDA-MB-231 or MCF-7 for 5 h. Only live $CD3^+$ cells were taken for analysis. The numbers on dot plots correspond to percentages of gated populations

When the BC1.18 TCR was transferred into healthy donor $CD8^+$ T-cells, it conferred the cells with specific reactivity towards MDA-MB-231 cell line but not MCF-7 line (**Figure 4.16 C**). The BC1.18 TCR re-directed the healthy CD8+ T-cells not only to the breast cancer line MDA-MB-231 but also to melanoma lines t15 and t24, lung cancer line A549, and ovarian cancer line A2780 (**Figure 4.17**). Importantly, BC1.18 TCR-transduced T-cells did not target the normal fibroblast line MRC5 (**Figure 4.17**). Since BC1.18 TCR-transduced cells recognised melanoma line t15, I was able to determine the role BTN3, EPCR and MICA/B in target cell recognition by BC1.18 TCR, using CRISPR/Cas9 knock-outs generated previously (**Figure 4.3**). However, BC1.18 TCR-transduced T-cells were capable of mounting a strong response to each knock-out, similar to the response against the parental t15 line, therefore indicating that BC1.18 TCR is specific for a novel γδ TCR ligand (**Appendix Figure 8.10**). In summary, T-cell libraries as described here can be used for discovery of broadly cancer-specific γδ TCRs in as little as 10-12 weeks.

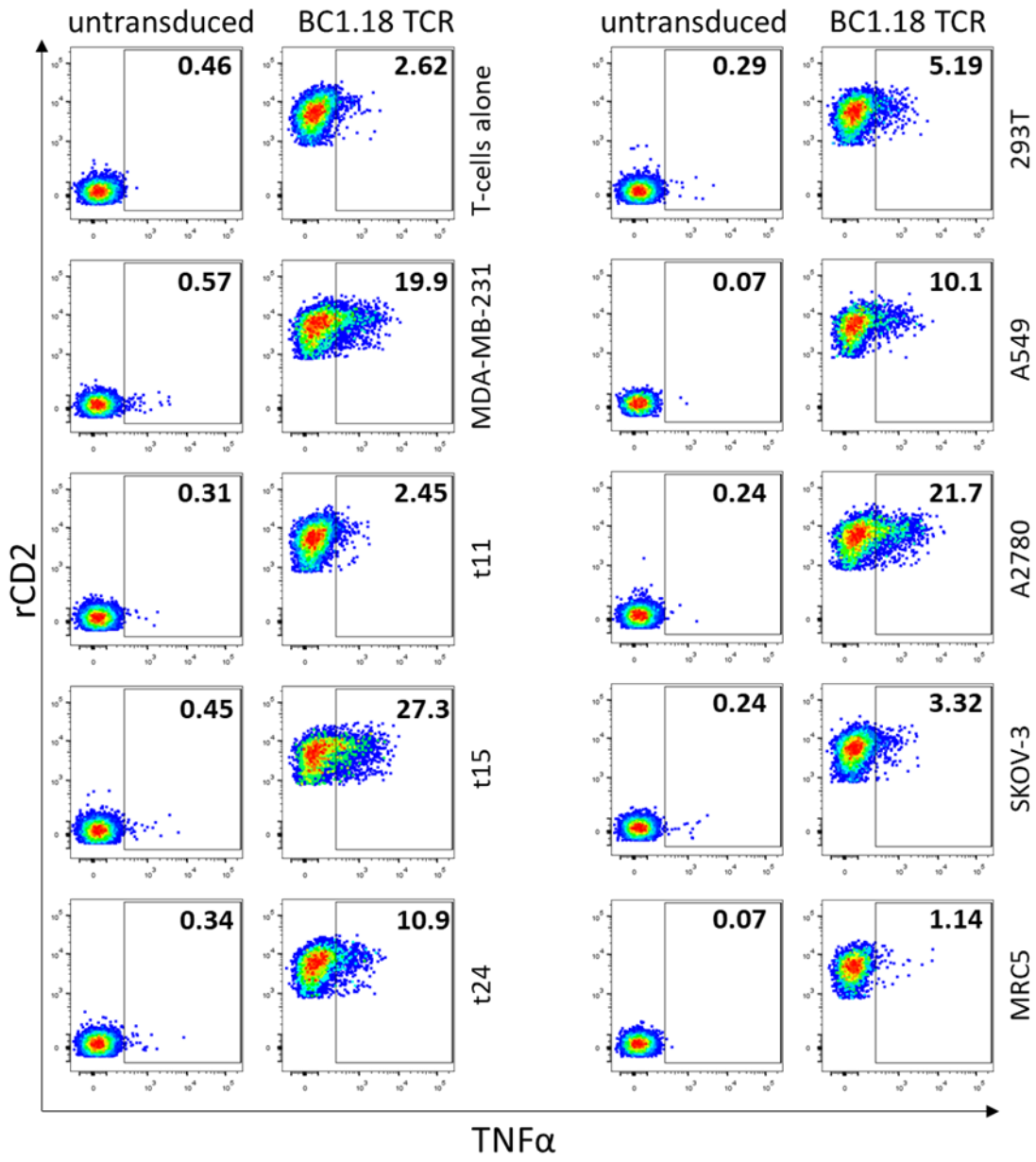

Figure 4.17 BC1.18 γδ TCR successfully re-directs peripheral CD8$^+$ T-cells to a panel of cancer cell lines but not normal fibroblasts. CD8$^+$ T-cells, either untransduced or transduced with BC1.18 TCR, were co-incubated with cancer cell lines as indicated for 5 h. Only live CD3$^+$ (and rCD2$^+$, in case of TCR transduced cells) cells were taken for analysis. The numbers on dot plots correspond to percentages of gated populations. MDA-MB-231 is a breast cancer line; t11, t15 and t24 are melanoma lines; 293T is a kidney cell line; A549 is a lung cancer line; A2780 and SKOV-3 are ovarian cancer lines; while MRC5 is a normal fibroblast line.

4.2.12 Procurement of a cancer-reactive coreceptor double negative αβ T-cell clone

Conventional αβ T-cells are specific for peptide antigens presented by highly polymorphic MHC-Ia and MHC-II molecules, and T-cell restriction is enforced in the thymus by co-receptors CD8 and CD4, respectively[20]. In contrast, less is known about the biology and target recognition of CD4/CD8-coreceptor double negative (DN) αβ T-cells[401]. Importantly, T-cells restricted to monomorphic MHC-Ib molecules such as MR1 or CD1a-CD1d can exhibit CD4/CD8 DN phenotype but the role of MR1 or CD1-restricted T-cells in cancer immunosurveillance remains mostly undefined[402]. Therefore, I decided to apply T-cell libraries to isolate DN T-cell clones with broad anticancer reactivity, without making assumptions regarding their restricting molecule.

Healthy donor PBMC were initially depleted of $CD4^+$, $CD8^+$ and $CD56^+$ cells, followed by positive selection of αβ T-cells, thus removing conventional αβ T-cells, NK cells, iNKT cells, and γδ T-cells. The isolated DN T-cells were plated in 96U wells and expanded with CD3/CD28 beads. Following expansion, the wells were tested for reactivity against a panel of two solid tumour lines (breast cancer MDA-MB-231 and colorectal cancer Colo-205) and one haematological cancer (T-cell leukaemia Molt3). Eighteen out of 96 wells tested contained cancer-reactive cells (**Figure 4.18 A**), and two DN αβ T-cell clones that showed cancer reactivity were subsequently isolated. Interestingly, both clones showed strong response against Molt3 line, in terms of CD107a and TNFα expression, but not against the other two cancer lines tested (**Figure 4.18 A**). Both clones remained phenotypically stable in culture, in terms of CD4 and CD8 expression (**Figure 4.18 B**), and expressed the same TCR, further referred to as 40E.22 (**Figure 4.18 C**). The anticancer reactivity of clone 40E.22 was not confined only to Molt-3 cell line; the clone also produced TNFα (**Figure 4.19 A**) and showed direct cytotoxicity (**Appendix Figure 8.11**) against cancer cell lines of diverse origin, spanning haematological malignancies, as well as bone, lung, breast and ovarian cancer lines - but not melanoma cell lines. No response, in terms of TNFα expression or direct cytotoxicity, was detected when clone 40E.22 DN was incubated with normal cell lines (**Figure 4.19 A** and **Appendix Figure 8.11 A**).

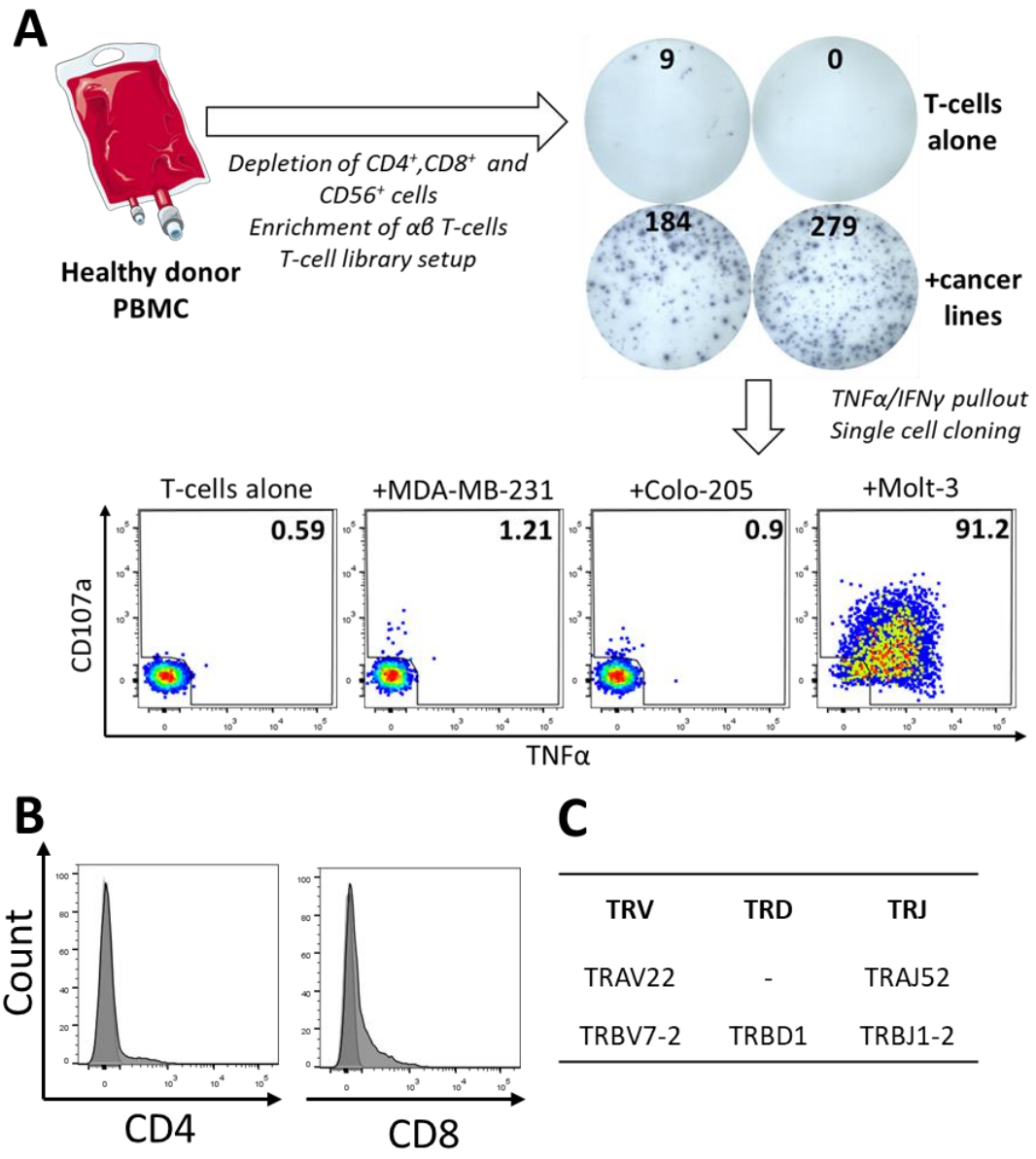

Figure 4.18 T-cell libraries can be used for procurement of cancer-reactive CD4$^-$CD8$^-$ αβ T-cell clones. (**A**) CD4$^-$CD8$^-$ αβ T-cells were purified by depletion of CD4$^+$, CD8$^+$ and CD56$^+$ cells, followed by positive selection of αβ TCR$^+$ cells from fresh healthy donor PBMC, and expanded with CD3/CD28 beads. 2,000 cells were initially plated per well. After 14 days, each well was tested for response to a small panel of breast cancer cell lines (MDA-MB-231, Colo-205, Molt-3) by IFNγ ELISpot. The numbers of spots in representative wells are shown. The cancer-reactive wells were then combined and co-incubated with cancer cell lines for 5 h, followed by magnetic purification of TNFα and/or IFNγ secreting T-cells. Cells enriched in this way were single cell cloned tested for recognition of individual cancer cell lines. (**B**) The cancer-reactive αβ T-cell clones do not express either CD4 or CD8 co-receptor. (**C**) Two cancer-reactive T-cell clones were obtained from the library. Both clones were found to express an identical TCR 40E.22 DN, annotated according to the IMGT nomenclature.

In spite of the absence of strong co-receptor expression, the recognition of peptide-MHC complexes by DN T-cells remains possible, albeit very infrequent[403]. Therefore, the recognition of Molt-3 cell line by clone 40E.22 was tested in presence or absence of HLA-ABC blocking antibody W6/32. Due to lack of readily available, HLA-ABC restricted T-cell clones that recognised wild type Molt-3 cell line to be used as a positive control, the Molt3 cell line was engineered to express HLA-A2 and Melan-A proteins. As expected, HLA-A2 restricted, Melan-A epitope specific T-cell clone Mel13 (described before by my colleagues[321]) showed a specific response to Molt-3 cell line engineered to express both HLA-A2 and Melan-A but not HLA-A2 alone (**Figure 4.19 B**). In the presence of the HLA-ABC blocking antibody, the response of Mel13 clone to Molt-3 cell line decreased by approximately 30%. In contrast, the response of clone 40E.22 DN to engineered Molt-3 cells remained unchanged in presence or absence of the HLA-ABC blocking antibody. Importantly, CRISPR/Cas9 knock-out of β2m, an essential component of the functional MHC-Ia complexes, as well as some MHC-Ib complexes (such as HLA-E, HLA-F, HLA-G, MR1, CD1a-CD1d, HFE and FcRN), in Molt-3 rendered the cell line incapable of triggering any specific response from T-cell clone 40E.22 DN. An initial experiment, using the CRISPR/Cas9 knock-out of MR1 in A549 cell line, generated previously by my colleagues[404], indicated that 40E.22 DN clone recognised its targets independently of MR1 expression (**Appendix Figure 8.12**). Given the fact that Molt3 cell line constitutively expresses high levels of all surface-expressed CD1 isoforms (CD1a-CD1d), I decided to generate Molt-3 lines deficient in each of the CD1 molecules separately.

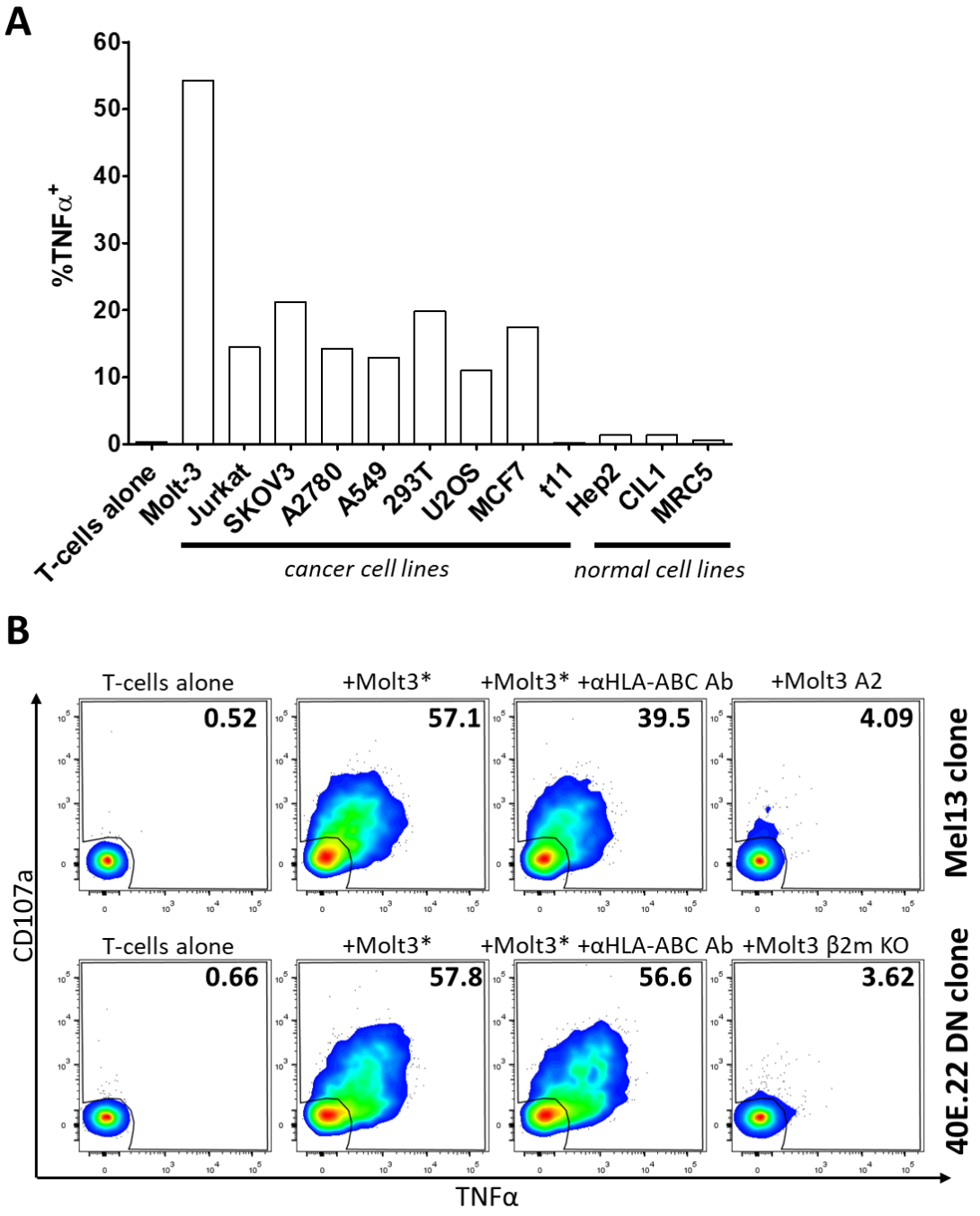

Figure 4.19 Cancer reactive clone 40E.22 DN recognises diverse cancer cell lines, but not normal cells, in a HLA-unrestricted manner. (**A**) TNFα expression of clone 40E.22 DN after 5 h of co-incubation with T-cell leukaemia lines Molt-3 and Jurkat, ovarian cancer lines SKOV3 and A2780, embryonic kidney line 293T, osteosarcoma line U2OS, breast cancer line MCF7, melanoma line t11, or normal cell lines Hep2 (hepatocytes), CIL1 (ciliary epithelium), MRC5 (fibroblasts). (**B**) Clone 40E.22 DN or Melan-A epitope specific, HLA-A2 restricted T-cell clone Mel13, were incubated with Molt3 cell line engineered to express both Melan-A and HLA-A2 (indicated by asterisk *). Where indicated, Molt-3 cell line was pre-incubated with anti-HLA-ABC antibody. Molt-3 cell line was also engineered with CRISPR/Cas9 to be deficient in β-2-microglobulin (β2m), and thus be deficient in conventional or unconventional MHC-I molecules. Representative data from 2 experiments are shown.

4.2.13 Broadly cancer-reactive clone 40E.22 DN requires CD1a for target cell recognition

The CD1 family of molecules possess a high degree of homology at the exonic level. Despite the homology, it is possible to design guide RNAs that target each CD1 family member independently. The design of gRNAs specific for CD1a-CD1d is shown in **Figure 4.20 A**.

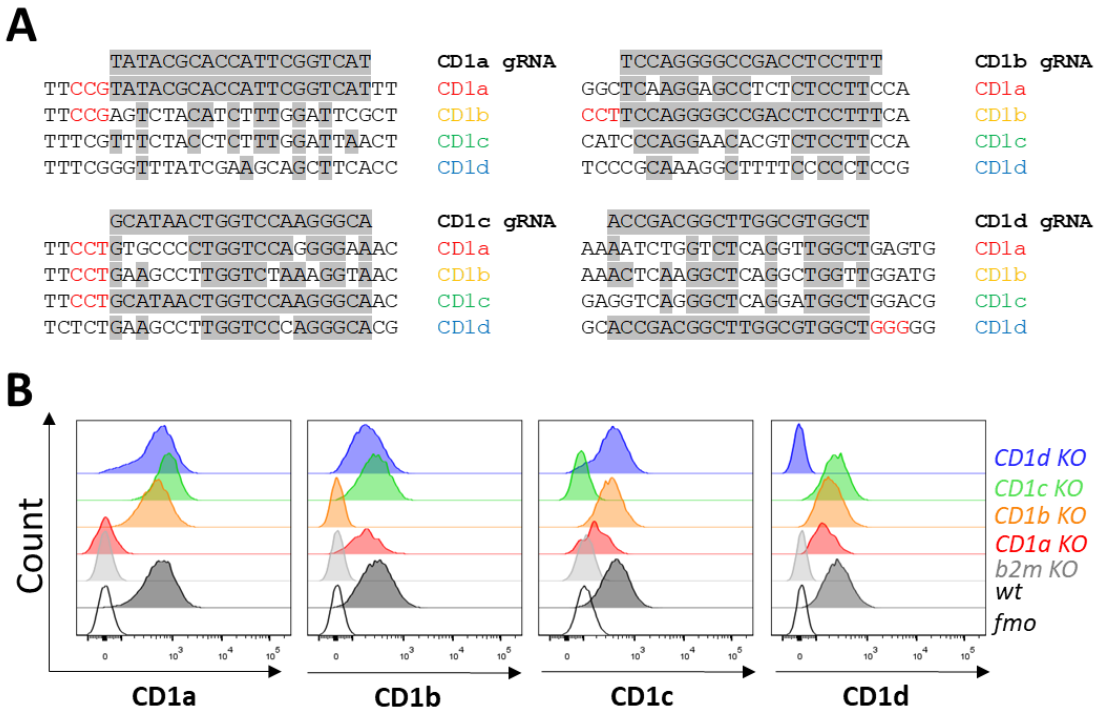

Figure 4.20 Engineering of Molt-3 cell line deficient with each one of CD1 isoforms. (**A**) gRNAs targeting CD1a, CD1b, CD1c and CD1d were designed to target only the chosen CD1 isoform but with multiple mismatches with all the other isoforms. The matching nucleotides are highlighted in grey while PAM is shown in red. (**B**) gRNAs were transduced into Molt3 cell line together with Cas9 protein by electroporation. After 14 days, the cells were subjected to single cell cloning. The clones were then stained for CD1a-d isoforms. Unstained Molt-3 cell line (fmo) and β2m knockout (b2m KO) were used as negative controls while wild type Molt-3 cell line was shown as a positive control.

The designed gRNAs were tested in Molt3 cell line which expresses relatively high levels of CD1a-CD1d molecules (**Figure 4.20 B**). The introduction of CD1-specific CRISPR/Cas9 was performed by electroporation of gRNA complexed with Cas9 protein, to avoid cellular stress associated with lentiviral infection and integration. Engineered cells were single cell cloned to ensure 100% deficiency of a given CD1 molecule. As expected, Molt3 cells deficient in β2m did not stain for any of CD1 molecules on the surface while Molt3 cells transfected with CD1 CRISPRs were deficient for the target CD1 molecule but expressed detectable quantity of other CD1 family members. It should be noted that slight differences in expression level of non-target CD1

molecules between cell clones were observed, probably resulting from variation in the parental cell line, and thus requiring the use of several cell clones in functional assays. Nevertheless, CRISPR/Cas9 knock-out was proven to be specific and restricted only to the target CD1 molecule, as predicted based on sequence alignments. No differences in HLA-ABC expression were observed between CD1 knock-out cells and wild type cells (**Appendix Figure 8.13**).

CD1 knock-out lines of Molt-3 were tested for their ability to activate the clone 40E.22 DN. No major change, in terms of CD107a and TNFα expression, was observed between the response of clone 40E.22 to wild type Molt-3 and CD1b, CD1c or CD1d knock-outs (**Figure 4.21 A** and **B**). Conversely, Molt-3 deficient in CD1a failed to activate the T-cell clone (>95% reduction in CD107a and TNFα expression), to the similar degree as β2m deficient Molt-3. This result suggest that the 40E.22 DN T-cell recognises tumour cells via the MHC-Ib molecule CD1a.

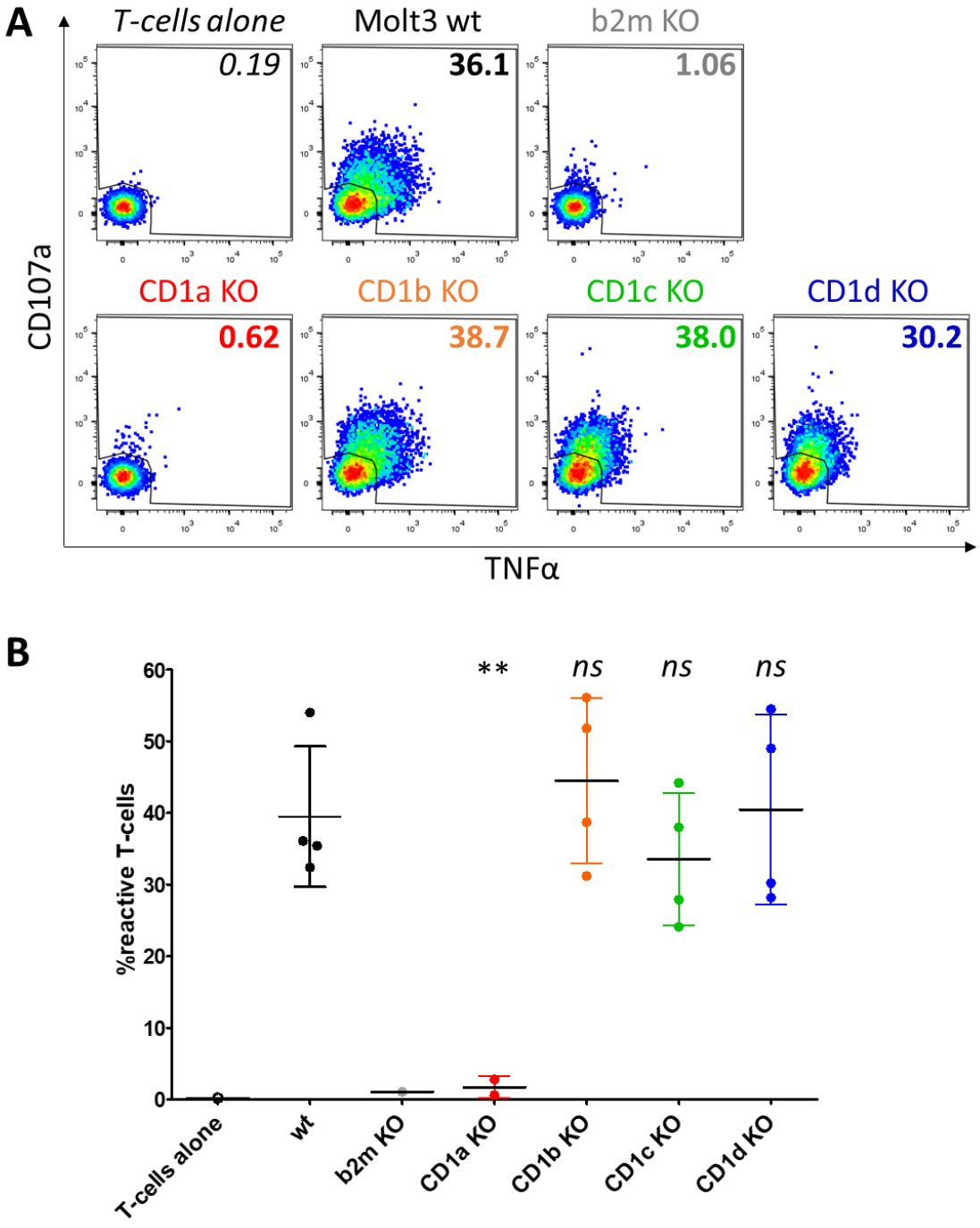

Figure 4.21 The recognition of Molt3 cell line by clone 40E.22 DN requires CD1a expression on cancer cells. (**A**) Clone 40E.22 DN was co-incubated for 5 h with Molt-3 cell line, not transduced (wt) or transduced with β2m, CD1a, CD1b, CD1c or CD1d CRISPR. The reactivity of T-cell clone 40E.22 DN against representative Molt-3 clones is shown. (**B**) Clone 40E.22 DN reactivity (in terms of CD107a and/or TNFα expression) against Molt-3 clones (2-4 per category) is shown after 5 h of co-incubation. Individual data points, corresponding to individual Molt-3 clones, as well as mean and standard deviation are shown. Student's t-test **p<0.01, ns – not significant.

4.3 Discussion

Development of immunotherapies that are safe, curatively efficient and universal, *i.e.* available for cancer patients regardless of their MHC alleles, and spanning multiple cancer types, represents a major challenge in the field. While CARs targeting ubiquitous cancer-associated antigens have been described[405], natural (i.e. non engineered) TCRs may have an advantage over CARs in terms of the safety profile[406], as well as different binding kinetics and affinity parameters[407]. Therefore, in this Chapter I focused on isolation of broadly cancer-reactive, non-HLA restricted T-cells, in particular γδ T-cells. I showed that γδ T-cell clones that exhibit anticancer reactivity can be isolated from a variety of sources, including clinical grade tumour-infiltrating lymphocytes, ovarian cancer ascites, and peripheral blood of cancer patients or healthy donors. Using the TCR transfer system described in **Chapter 3** I demonstrated that TCRs derived from the cancer-reactive γδ T-cells could be used to re-direct primary αβ T-cells to multiple cancer types without targeting normal cells. Moreover, I generated a set of reagents and cell lines for studying the known ligands of γδ TCRs and non-HLA restricted αβ T-cells by leveraging CRISPR/Cas9 mediated genome editing. Finally, using an adapted T-cell library methodology coupled with genome editing I discovered a broadly-cancer reactive αβ T-cell clone that was restricted by CD1a. To author's knowledge, this is the first example of a cancer-reactive, CD1a-restricted αβ T-cell[402].

4.3.1 Procurement of broadly cancer-reactive T-cell clones and T-cell receptors

T-cell clones can be a source of therapeutically valuable, cancer specific TCRs. These TCRs may be used as a soluble therapeutic[97], or used to re-direct T-cells of other specificities to cancer by gene transfer. The low affinitity ligand binding of γδ TCRs reported so far (summarised in [383]) suggest that using these molecules in gene transfer therapies is a more viable solution than as soluble molecules. The identification of promising, broadly cancer reactive γδ TCRs with specificities towards novel ligands is therefore of considerable interest.

Broadly tumoricidal, non-Vγ9Vδ2 T-cell clones have been reported to be sporadically enriched in peripheral blood of some patients, in particular in cases of CMV reactivation[120] or cancer[408]. Epithelial tissues, where γδ T-cells are more abundant than in peripheral blood, are yet another source of cancer reactive T-cells[409]. Additionally, γδ T-cells are capable of undergoing antigen-driven clonal expansions in a similar manner as their αβ counterparts[68]. Therefore, γδ T-cell clones that respond particularly well to cancer may be specifically enriched among the tumour-infiltrating lymphocytes.

The choice of strategy for obtaining cancer-reactive γδ T-cell clones from PBMC, TILs or other tissue materials is dependent on the frequency of these cells within these samples. For instance, cloning of T-cells directly from the starting material is the least biased method that additionally preserves T-cell viability but is only feasible if the frequency of cells of interest is relatively high (>1%) in the starting material. Viable cell sorting based on reactivity towards cancer cells, as determined by markers such as CD107a or TNFα, is another option but the antigen exposure and the process of sorting may have a negative impact on overall viability of T-cells[325,410]. Finally, T-cell libraries as described here are a particularly valuable tool when the number of cells in the starting material is relatively low and/or the frequency of cells with given specificity is expected to be relatively low[216]. T-cell libraries can also be used to select γδ T-cell clones specific for a known ligand, by using a matched cell line proficient and deficient in the given ligand for screening. Notably, γδ TCR-specific antibodies should be avoided, where possible, in purifying cells for T-cell library setup as γδ T-cells have been reported to be susceptible to cell death resulting from TCR-binding antibodies[396,411].

Cancer-reactive γδ T-cell clones may recognise their targets in a TCR-dependent or TCR-independent manner[412]. Furthermore, target recognition can result from additive or synergistic triggering of TCR and co-stimulatory NK type receptors[170,413]. It may also be envisaged that different TCRs require different co-stimulatory receptors, or even co-receptors conceptually similar to CD4 and CD8 co-receptors for αβ T-cells. Therefore, TCR transfer into a sensitive proxy system is crucial for determining if the target cell recognition is mediated by the TCR. As I have shown in this Chapter, when two γδ TCRs were transferred into αβ TCR-proficient T-cells, no cancer-specific reactivity was observed. Such result could lead to a conclusion that given γδ TCRs did not play any role in target cell recognition by parental T-cell clones. However, increasing the sensitivity of the proxy system by TCR-β knockout demonstrated that both γδ TCRs conferred reactivity against the tumour to primary T-cells. Finally, a given γδ T-cell clone can show both TCR-dependent and independent target recognition. Clone ML15 described in this chapter, for instance, was still capable of recognising the autologous tumour line in absence of BTN3 molecules which are necessary for target recognition by ML15 TCR-transduced cells.

Finally, therapeutically relevant TCRs can be derived directly from paired sequencing of TCR repertoires, by single cell PCR or more high throughput technologies such as DropSeq[57]. Such TCRs can only be characterised in proxy systems as the original T-cell clones are not available. A study by Ravens *et al.* showed that CMV reactivation led to clonal expansion of several T-cell clones in haematopoietic stem cell transplant patients[68]. Here, I have transferred one of the dominant TCRs described therein into primary T-cells together with TCR-β knock-out, to test if that TCR emerging with CMV reactivation could also confer reactivity to cancers, which is a

common feature of CMV-reactive γδ T-cells[120]. The TCR-transduced T-cells could mount a specific response to some of the cancer cell lines tested, in particular melanoma and breast cancers (**Appendix Figure 8.14**).

4.3.2 Phosphoantigen sensing by T-cells – an ongoing mystery

While the observation that Vγ9Vδ2 T-cells commonly respond to phosphoantigens was made several decades ago, the main hypothesis as to how this recognition occurs has evolved profoundly, resulting in the phosphoantigen sensing model whereby intracellular binding of phosphoantigens to BTN3A1 molecule induced conformational change of the extracellular BTN3A1 domain, and subsequent activation of T-cells[41]. Numerous molecules have been gradually unveiled as players in phosphoantigen sensing, including cytoskeletal adaptor periplakin and GTP-binding protein RhoB[92,98]. Despite decades of extensive study, several vital questions pertaining to phosphoantigen recognition remain; in particular identity of the actual ligand of Vγ9Vδ2 TCRs. Herrmann and colleagues postulated that additional, yet unidentified genes on located on chromosome 6 other than BTN3A1 are essential for T-cell response to phosphoantigens[96]. Human chromosome 6 contains not only the BTN3 family but also MHC-Ia and MHC-II families, and some members of MHC-Ib family, as well as other genes involved in classical antigen processing and presentation.

The TCR repertoire of phosphoantigen-reactive T-cells is potentially highly diverse[414] – but the functional implications of the said diversity require further investigation. A study by Morita and colleagues indicated that while all CDR loops of γδ TCRs play a role in phosphoantigen recognition, the recognition occurs mostly *via* the germline-encoded residues[394]. On the other hand, Vγ9Vδ2 TCRs which differed only in their CDR3 sequences showed striking differences in response to activating anti-BTN3 antibody[415], thus suggesting that phosphoantigen response may be even more complex than initially expected.

Here I showed that a broadly cancer-reactive Vγ9Vδ2 clone ML15 failed to respond to phosphoantigens in self-presentation experiments, i.e. without any APCs. The clone ML15 expresses a TCR that is capable of conferring recognition of phosphoantigens, as demonstrated by TCR transfer experiments and ML15 clone responses to phosphoantigens in presence of normally not recognised APCs such as T2 cell line. Interestingly, ML15 TCR transduced cells showed a markedly stronger reactivity to a panel of cancer cell lines without bisphosphonate treatment than cells transduced with another, "conventional" Vγ9Vδ2 TCR, possibly indicating that CDR3 loops could influence functional avidity of response to target cells. I concluded that T-cell clone ML15 was deficient in molecule(s) other than BTN3 that are necessary for efficient response to phosphoantigens and stimulating antibody 20.1. This putative deficiency was not a

genetic feature of the patient from whom clone ML15 was isolated as I have successfully procured phosphoantigen-reactive Vγ9Vδ2 T-cell clones from the same patient (**Appendix Figure 8.15**). A comparison of transcriptomes between the donor-matched phosphoantigen-reactive clones and ML15 could possibly unveil new components of phosphoantigen sensing pathway.

4.3.3 Targeting CD1a for cancer therapy

CD1 molecules belong to MHC-Ib family and are located on chromosome 1 in humans. While CD1a-d are expressed on cell surface and present antigens to αβ and γδ T-cells, CD1e is located intracellularly and processes lipid antigens for presentation by, in particular, CD1b[99]. CD1a-CD1d molecules are surface expressed in association with β-2-microglobulin and show structural similarity to HLA-ABC molecules (**Figure 1.3**). While the contributions of CD1b-CD1d restricted T-cells to anticancer immunity, in particular directed against haematological malignancies, have been described before[416–418], no direct role of CD1a restricted T-cells in cancer has been demonstrated yet.

CD1a is expressed almost exclusively on thymocytes and a subset of dendritic cells called Langerhans cells which are resident predominantly in epidermis[419]. Self-reactive CD1a restricted T-cells are very frequent among circulating DN ($CD4^-CD8^-$) and $CD4^+$ T-cells[420], and are capable of skin-specific homing where they produce IL-22 in response to CD1a on Langerhans cells[421]. CD1a presents mostly self-derived lipids, such as sulfatide[422], but was also shown to bind bacterial lipopeptide DDM[423]. A recent study by Birkinshaw *et al.* demonstrated that TCR recognition of CD1a-bound lipids is indirect, i.e. the lipid antigen is buried within the CD1a molecule and thus affects the conformation of the TCR contact area on CD1a surface[424].

The CD1a restricted T-cell clone 40E.22 described in this Chapter was capable of efficient recognition and lysis of several cancer cells without targeting normal cell lines tested. Since the clone was derived from a healthy donor without any apparent autoimmune disorder, it is possible that the clone recognises cancer-derived lipid antigens presented by CD1a which differ from homeostatically presented self-lipids. Whether the recognition is direct, i.e. the TCR forms direct contacts with the putative lipid antigen, or the recognition occurs in indirect manner, similarly to one described by Birkinshaw *et al.*[424], needs to be determined. Nevertheless, cancer-specific T-cells restricted by non-polymorphic CD1 molecules should be investigated in context of pan-population immunotherapies, and the availability of cell lines engineered to be deficient in only one isoform of CD1 at a time should facilitate the said investigations.

In summary, the approaches described in this chapter have enabled me to procure broadly tumoricidal, non-HLA-restricted T-cells that can bear αβ or γδ TCRs. These T-cells may offer exciting opportunities for pan-population, pan-cancer therapies. The initial attempts to dissect the ligand specificity of those broadly cancer-reactive T-cells and TCRs described here focused on CRISPR/Cas9 knock-outs of known ligands, such as BTN3, MICA/B, EPCR or CD1 family molecules. However, it seems likely that the majority of the ligands of non-HLA restricted cells are yet to be discovered, and it is not possible to make assumptions about their identity. Using whole genome CRISPR/Cas9 approaches, described in the following Chapter, offers a potential of unbiased discovery of novel cancer-associated ligands, and pathways necessary for their surface expression.

5. Whole genome CRISPR/Cas9 libraries for identification of genes essential for cancer cell recognition by unconventional T-cells

5.1 Background

Conventional αβ T-cells recognise processed protein antigens in the form of peptide epitopes presented on the cell surface by HLA molecules. The identification of restricting HLA alleles can be routinely achieved by a combination of blocking antibodies, partially HLA-matched cells lines, and validation by knock-in and knock-out of putative HLAs. Subsequently, the presented epitope can be identified by screening the data from combinatorial peptide libraries[356] against bespoke protein databases[425]. This approach, pioneered in my laboratory, is now being routinely used to dissect T-cell cross-reactivity in a variety of disease settings[360]. Discovery of antigens recognised by non-HLA restricted T-cells is less straightforward and to date has required highly sophisticated and time consuming methods. For instance, Vavassori *et al.* identified BTN3A1 gene as required for phosphoantigen presentation by serial generation of mouse-human hybrids carrying whole, or subsequently shorter parts of human chromosomes[40]. An alternative methodology was developed in the Déchanet-Merville's laboratory where mice were immunised with cancer cells recognised by γδ T-cell clones. Antibodies generated by immunised mice were then tested for blocking of the cancer cell recognition by γδ T-cells, and if successful, used for immunoprecipitation of the putative targets. While this approach has been highly successful, leading to identification of two novel γδ TCR ligands, EPCR[362] and annexin A2 (Ref. [155]), it is relatively laborious and allows only for identification of surface-expressed proteins (i.e. *bona fide* TCR ligands).

Forward genetic screens offer an attractive possibility for identifying novel genes essential for recognition of target cells by T-cells, without making any assumptions about the identity, or role, of those putative genes. The principle of forward genetic screens involves generation of a cellular library mutagenised for a single gene per cell, followed by selection of phenotype(s) of interest. The early genetic screens of this type involved libraries of short hairpin RNAs which induced target gene knock-down *via* RNA interference[426]. The RNA interference library screens, however, suffered from off-target effects and incomplete gene knock-downs, thus hampering the interpretation of results[427]. Retroviral gene traps, which inactivate random genes by insertional mutagenesis, were proposed as an alternative to shRNA screens[428]. The gene trap approach was limited only to haploid, or near-haploid, cell lines such as KBM7 leukaemia cell line[429] – since the insertion affected only one allele at the time. Finally, the recent advances of CRISPR/Cas9 technology allow for bi-allelic gene disruptions and could be easily delivered in high

throughput library format, thus making it possible to conduct loss-of-function[319], or gain of function[302], library screens in any cell type. So far, the whole genome CRISPR/Cas9 loss-of-function library screens have been used to discover genes involved in, for instance, conferring drug resistance[303], playing a role in viral entry[308] or contributing to metastasis[311]. The applications of CRISPR/Cas9 screens were reviewed in more detail in **Chapter 1**.

5.1.1 Aims

At the time of conducting experiments for this thesis, no whole genome library screen involving T-cells as the selecting factor had been published. Therefore, my aim was to investigate the potential of using the Genome-scale CRISPR/Cas9 Knock-Out (GeCKO) library to identify new, as well as already published, genes essential for cancer cell recognition by conventional and unconventional T-cells. Specifically, my Aims were to:

- Optimise library screening in terms of effector and target cell numbers, as well as duration of the screen;
- Generate T-cell selected libraries that would be resistant to lysis by the respective T-cell clone;
- Develop a rapid and cost effective method for sequencing of selected libraries;
- Validate selected hit genes from the libraries for their role in activating T-cells.

5.2 Results

5.2.1 Optimisation of T-cell mediated whole genome library screening

The GeCKO v2 library, generated in Zhang laboratory[319] and used throughout this Chapter, is divided into two sub-libraries, A and B, with each containing 3 independent guide RNAs targeting 5' regions in conserved, protein-coding exons of all 19,050 human genes. Each library also contains 1,000 gRNAs designed not to target any human gene as a control in addition to gRNAs targeting miRNAs (4 guides per miRNA, only in sub-library A). The total number of gRNAs, therefore, exceeds 100,000 and thus maintaining the gRNA representation throughout the experiment is an imperative. As a consequence, to ensure sufficient (>300-400X) coverage over the starting library[319], at least 50×10^6 library-transduced cells should be used for each T-cell mediated selection. Due to targeting of all the human genes, the T-cell mediated CRISPR library screening has potential to unveil important genes beyond those that encode for surface expressed TCR ligands. Such genes could be necessary for target expression and could include molecules essential for processing, trafficking, expression (e.g. transcription factors) or other function (e.g. protein folding). The schematic outline of T-cell mediated screening of whole genome libraries is shown in **Figure 5.1**.

The high number of target cells used for screening, exceeding 10^7, requires use of a sufficiently high number of T-cells. Since T-cell clones, in general, can only undergo a finite number of cell expansions before undergoing exhaustion and/or senescence[430], minimisation of T-cell number used for each individual screen is desirable. Additionally, an excess of T-cells could potentially result in off-target or bystander toxicity against target cells that do not express key genes for T-cell recognition. Therefore, I first sought to determine the lowest number of T-cells that would result in complete lysis of target (untransduced) cancer cells. In order to accurately quantify the number of surviving cells, I modified the long term killing assay proposed by Jedema *et al.* to replace CFSE dye with stable GFP expression in target cells[431]. The method also involved using fluorescent beads as an internal control which ensured the acquisition of the same quantity of each sample (**Figure 2.2**). To allow T-cell persistence in the sample for several weeks, culture medium was supplemented with low dose of IL-2 (20 IU/ml). IL-2 supplementation did not affect the growth of cancer cells (**Appendix Figure 8.16**).

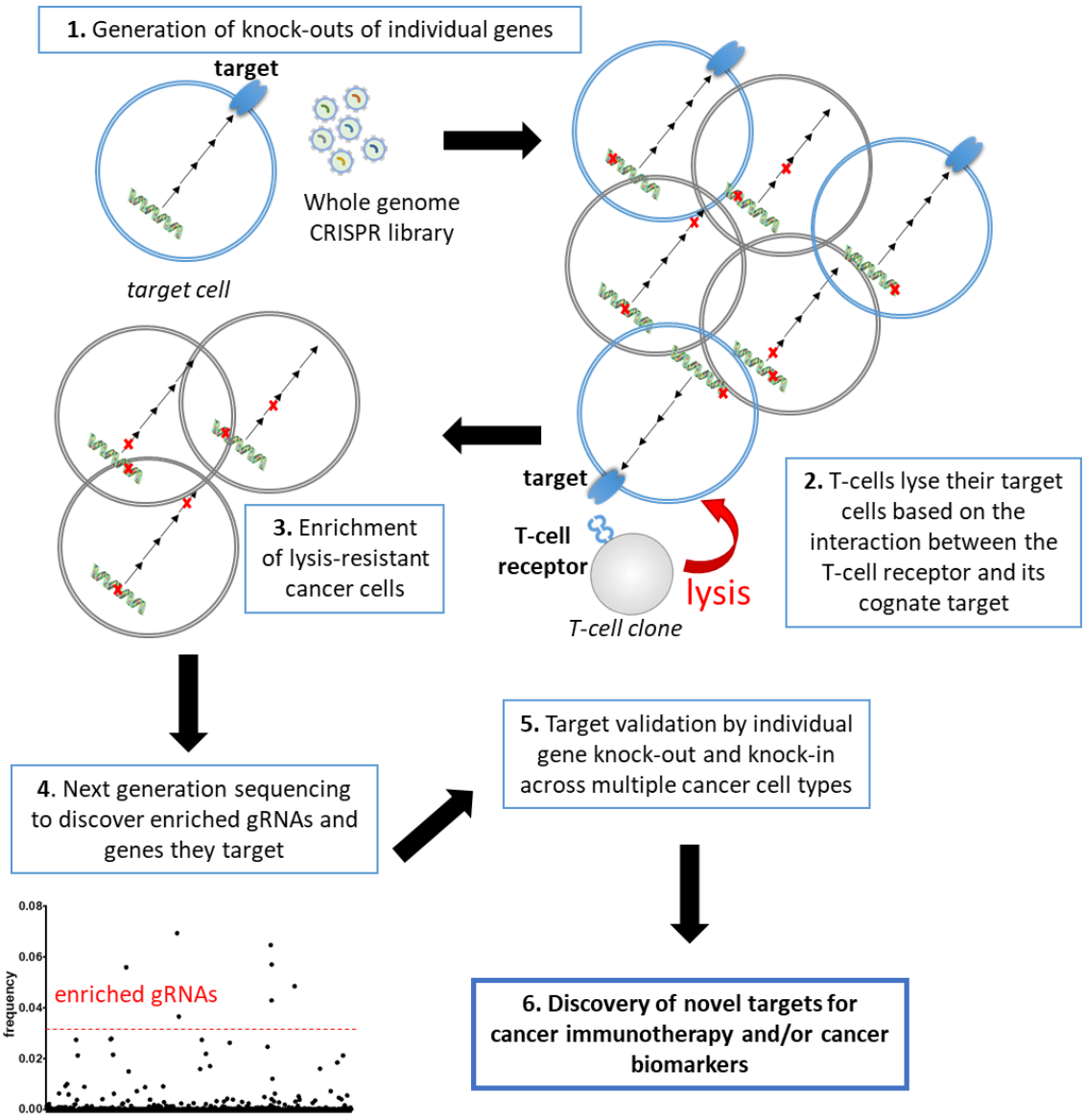

Figure 5.1 Schematic outline of whole genome library screening with cytotoxic T-cells. (**1**) The chosen target cell line is first lentivirally transduced with the whole genome CRISPR/Cas9 library, followed by selection of cells that had taken up lentivirus. Each cell should harbour a CRISPR/Cas9 induced indel in only one gene. (**2**) The library of single gene knock-out targets is then co-incubated with cytotoxic T-cells, resulting in (**3**) enrichment of cells that are more resistant to T-cell mediated lysis. These cells can harbour knock-outs not only in the gene encoding the cognate T-cell target but also in components of the pathway that leads to surface expression of the target. (**4**) The gRNA composition in the enriched library is then sequenced by next generation sequencing; (**5**) the resulting hits are independently validated, potentially leading to discovery of new targets for cancer immunotherapy (**6**).

The optimal E:T ratio was then determined for a Vγ9Vδ1 T-cell clone ML5 and a Vγ9Vδ2 T-cell clone ML15, against the haploid leukaemia line KBM7 (**Figure 5.2 A**). After 7 days of co-incubation, no detectable survival of target cells was seen at E:T as low as 0.2 (for ML5) or 0.1 (ML15). The survival of target cells was monitored for the following 14 days, to ensure that no survival occurred at chosen E:T ratios. Interestingly, a detectable population of surviving KBM7 cells became apparent at day 27 in samples where ML5 clone was present at 0.2 E:T ratio, thus indicating that long-term monitoring of cell survival is essential for choosing the correct E:T ratio (**Figure 5.2 B**). In parallel, autologous tumour t15 was investigated as an alternative to KBM7 cell line – however, the E:T ratios required for complete lysis of t15 were over 10-fold higher than E:T required for complete lysis of KBM7 (**Figure 5.2 C**). Considering that the optimal whole genome library screen would involve the minimum of 50×10^6 transduced cells, and that procurement of more than 50×10^6 of T-cells was not practical or feasible for the majority of T-cell clones investigated, I decided to focus my studies on T-cell clones and cancer cell lines where the optimal E:T ratio was 1:1 or lower.

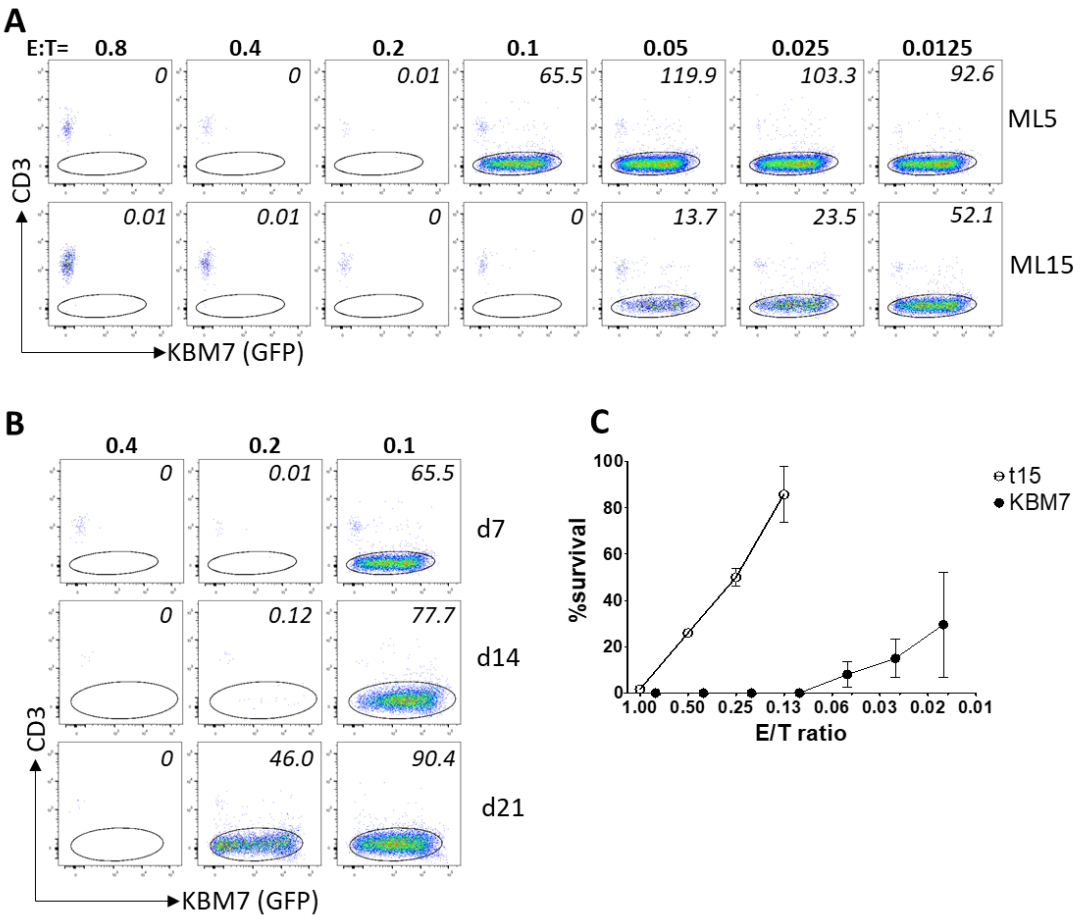

(Legend on the following page)

Figure 5.2 Determining optimal E:T ratios for CRISPR library screening with T-cell clones. (**A**) γδ T-cell clones ML5 and ML15 were co-incubated with KBM7 leukaemia cell line for 7 days at various E:T ratios. KBM7 cell line was engineered to express GFP to facilitate discrimination from T-cells. On day 7 fluorescent beads were added to each well, and T-cells were stained for CD3. 1,000 bead events were acquired per sample, and used to normalise the count of viable KBM7 cells (GFP^+ $CD3^-$). %Survival, shown on dot plots, was calculated by dividing the bead-normalised number of events in experimental wells by number of events in KBM7 only wells. (**B**) The survival of KBM7 cell line co-incubated with clone ML5 was monitored every 7 days as described in **A**. (**C**) Clone ML15 was co-incubated with KBM7 cell line or autologous tumour t15 at specified E:T ratios for 7 days, followed by determination of cancer cell survival. Standard error of the mean is shown.

5.2.2 KBM7 library screening with clone ML15 identifies C1orf74 as a gene essential for target cell recognition

The first whole genome screen was conducted on GeCKO-transduced KBM7 cell line by selection with clone ML15. KBM7 cell line was transduced at MOI<0.4 to prevent multiple gRNAs from being present in a given cell, and then co-incubated with the T-cell clone ML15 at E:T of 0.1 (60×10^6 of KBM7 cells + 6×10^6 of T-cells). The selection was conducted in 96U well plates, to provide optimal contact between T-cells and target cells. A second aliquot of 60×10^6 GeCKO-transduced KBM7 cells were plated without T-cells, to be used as a reference library. In parallel, one 96U well plate was set up with non-transduced KBM7 together with ML15 clone, to ensure that the clone was still capable of lysing all the target cells at the given E:T ratio. The co-incubation was carried out for 14 days, followed by combining all the T-cell selected wells, removal of dead cells and debris, and culturing for 3 days without exogenous IL-2 to remove residual T-cells. The surviving KBM7 cells were then re-plated with a fresh aliquot of T-cells for 14 days, at E:T of 0.2, to remove any residual cells that still expressed T-cell targets. Following this second round of selection and removal of residual T-cells, the ability of selected KBM7 cells to resist T-cell mediated lysis was tested in a ^{51}Cr release assay. These results showed that while the KBM7 cells were only slightly more resistant to lysis than the parental line after one round of selection, the lysis of KBM7 after two rounds of selection was reduced by 70-80% compared to the parental line (**Figure 5.3 A**). The next step involved examining whether any specific gRNAs had been enriched in the T-cell lysis-resistant tumour line.

The gRNA representation in selected libraries was determined by next generation sequencing of respective PCR products, as described in Materials and Methods (**Section 2.12.4**). The minimum of 30×10^6 of cells were used for genomic DNA extraction and subsequent PCR. The distribution

of gRNAs in the reference library plated in parallel with the selected library was highly skewed, and only 30% of all the library gRNAs could be detected, possibly due to proliferation bias (**Appendix Figure 8.17**). Therefore, an aliquot of transduced KBM7 library which was frozen down on the day of library screen setup was used as the reference library. While no obvious enrichment was observed in case of KBM7 cells after the round 1 of selection, the gRNA representation in round 2 was heavily dominated (>97% of reads) by a single guide RNA targeting *c1orf74* gene (**Figure 5.3 B**). The second most frequent hit (approximately 3% of reads) targeted a putative intracellular protein SLFNL1.

In parallel, single cell clones were derived from the KBM7 library after 2 rounds of selection, to validate the sequencing results. All 15 cell clones that were generated contained the *c1orf74*-targeting gRNA, and activated the T-cell clone ML15 to a lesser extent than the parental KBM7 line (**Figure 5.3 C**). I chose clone 2 as a representative clone for further validations as this clone grew particularly well and was subsequently shown to contain a large deletion in the *c1orf74* gene as described below.

The C1orf74 gene (chromosome 1 open reading frame 74) is composed of two exons but only the second exon contains the protein coding region which translates into a 269-amino acid long polypeptide, and does not contain any leader sequences that would target it to plasma membrane or any particular cellular compartment[432]. The PCR performed on C1orf74 exon 2 in wild type KBM7 resulted in an approximately 1 kb product, and the sequence of that product aligned perfectly with the *c1orf74* sequence from the reference genome hg38. In contrast, the C1orf74 amplification in clone 2 resulted in approximately 300 bp product (**Figure 5.3 D**). Sequencing of that PCR product unveiled an over 600 bp deletion, spanning from the sequence targeted by the gRNA towards the 5' end of the exon (**Figure 5.3 E**). Therefore, the gRNA enriched in the selected KBM7 library was functional and caused a surprisingly large deletion in the target region.

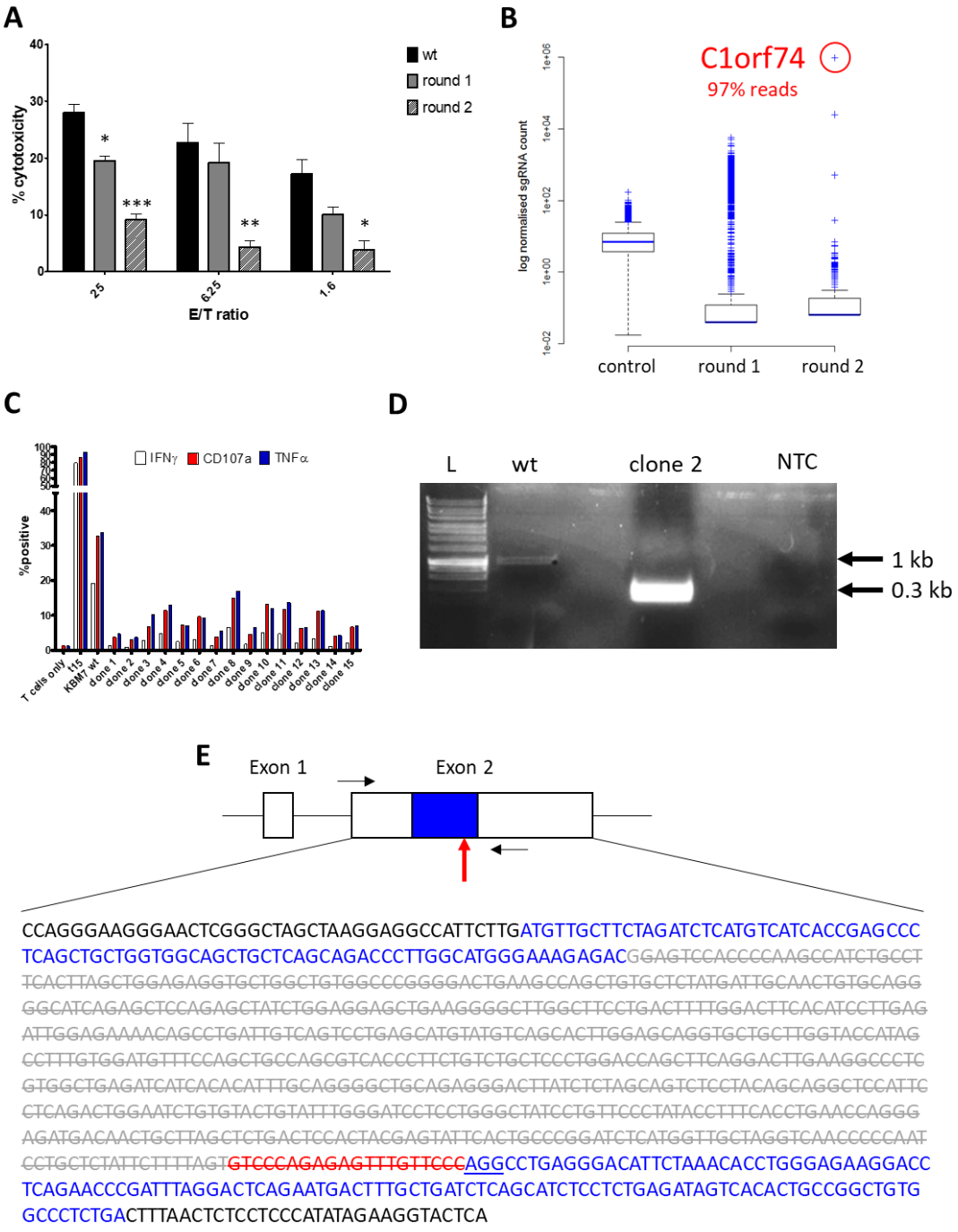

Figure 5.3 C1orf74 is the most enriched gRNA in KBM7 CRISPR library screened with clone ML15. (**A**) KBM7 cell line was transduced with whole genome CRISPR/Cas9 library GeCKO v2 and selected with clone ML15 at E:T=0.1 for 14 days (round 1), followed by re-plating the surviving cells with clone ML15 at E:T=0.2 for 14 days more (round 2). The cytotoxicity of clone ML15 against parental KBM7 line, as well as selected libraries, was determined by ^{51}Cr release after 4 h of co-incubation. Standard error of the mean is shown. Student's t-test *p<0.05, **p<0.01, ***p<0.0001. (**B**) gRNA representation in selected and unselected whole genome GeCKO libraries was determined and normalised as described in **Materials and Methods Section 2.12.4**. The gRNA representation was visualised using the R software. Red circle indicated a gRNA specific for *c1orf74* gene, which was identified in over 97% reads in the sample. The whole genome library was provided and sequenced courtesy of Paul Lehner, Cambridge University.

(Legend continued on the following page)

(Legend continued from the previous page) (**C**) Single cell clones (1-15) were generated from KBM7 library after two rounds of selection. The KBM7 clones, as well as the parental, unselected line, were co-incubated with T-cell clone ML15 for 5 h, followed by enumeration of responding T-cells (in terms of IFNγ, TNFα and CD107a) by ICS. Autologous tumour t15 was included as a positive control. (**D**) Genomic DNA extracted from clone 2 (derived from the selected KBM7 library) and from untransduced KBM7 line was used as a template for PCR directed at the protein-coding exon of *c1orf74*. The PCR products were run on 1% agarose gel. (**E**) The schematic representation of *c1orf74* gene (top panel), as well as sequencing results of the PCR product from clone 2 (bottom panel). Exons are shown as boxes while the protein-coding part of exon 2 is shown in blue. Black arrows indicate binding sites for primers used for PCR while the red arrow indicates the site targeted by the gRNA. gRNA sequence is shown in red, and PAM is underlined. The nucleotide sequence shown in grey and crossed out was absent in the PCR product from clone 2. L – 1 kb DNA ladder; NTC – no template control.

5.2.3 Vγ9Vδ2 T-cell clones recognise target cells regardless of C1orf74 expression

In order to confirm the role of C1orf74 in mediating T-cell recognition of KBM7 line, I designed six guide RNAs targeting the protein coding region of *c1orf74* gene, and transduced them into the parental KBM7 cell line. The sequences of gRNAs are shown in **Appendix Table 8.4**. Guide RNA 5 is identical with the gRNA that dominated the KBM7 library after two rounds of selection. Only three guide RNAs (3, 5 and 6) reduced the response of clone ML15 to KBM7 by at least 20% (**Figure 5.4 A**). Since the activation of clone ML15 could be induced by KBM7 cells in which no disruption of *c1orf74* gene occurred, despite having taken up the lentivirus, single cell clones were procured from each KBM7 line transduced with different gRNAs. When each individual KBM7 clone was tested for activation of T-cell clone ML15, a significant reduction of activation was only observed in case of KBM7 clones transduced with gRNA 5 (**Figure 5.4 B**). Amplification of the *c1orf74* exon 2 was then carried out from genomic DNA extracted from representative cell clones transduced with different gRNAs. Despite the fact that some of the KBM7 clones tested were capable of activating T-cell clone ML15 to the same extent as the parental KBM7 line, all the clones tested showed large deletions in the *c1orf74* locus (**Figure 5.4 C**). The deletions occurred within the protein coding region of *c1orf74* gene, as demonstrated by PCR and Sanger sequencing (**Appendix Figure 8.18**), indicating the lack of functional C1orf74 protein. Furthermore, knocking out *c1orf74* in autologous tumour t15 with two independent gRNAs (3 and 5) failed to abrogate or decrease the cytotoxicity of T-cell clone ML15, or other Vγ9Vδ2 T-cell clones, towards t15 (**Figure 5.4 D**).

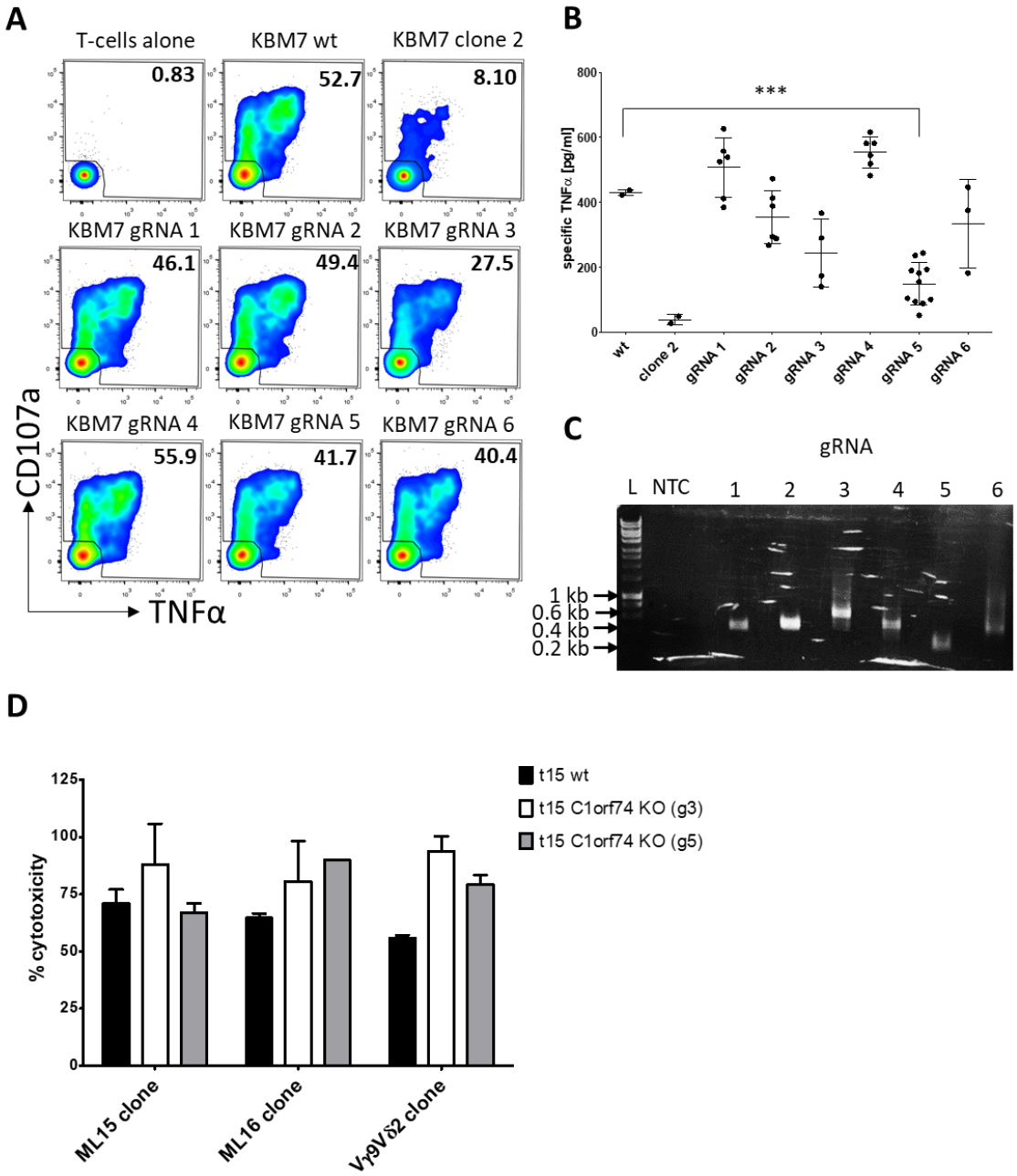

Figure 5.4 Targeting of C1orf74 with different gRNAs does not replicate the phenotype of selected whole genome library in KBM7 cell line. (**A**) Six different gRNAs targeting the protein-coding region in exon 2 of *c1orf74* were designed and lentivirally transduced into KBM7, followed by selection of cells that had taken up lentivirus. The resultant cell lines were co-incubated with clone ML15 for 5 h, and their ability to stimulate the T-cell clone was determined by enumeration of CD107a and/or TNFα-expressing T-cells. (**B**) Single cell clones were generated from KBM7 cell line transduced with six gRNAs targeting *c1orf74*. The KBM7 clones were co-incubated with T-cell clone ML15 for 16 h, followed by quantification of secreted TNFα (normalised by subtracting TNFα secreted by T-cells alone). Each data point represents an individual KBM7 clone derived from respective gRNA-transduced lines. gRNA 5 is identical with the gRNA identified by whole genome library screening. (**C**) PCR was performed on genomic DNA from representative clones from each gRNA-transduced KBM7 line to amplify the protein-coding region of *c1orf74*. The PCR products were run on 1% agarose gel. L – 1kb DNA ladder; NTC – no template control.

(Legend continued on the following page)

(Legend continued from the previous page) (**D**) Autologous (for clone ML15) tumour t15 was lentivirally transduced with *c1orf74*-targeting gRNAs 3 and 5, followed by selection of cells that had taken up lentivirus. The transduced cells, as well as untransduced controls, were co-incubated with T-cell clones at 10:1 E:T ratio for 4 h, and the cytotoxicity was determined by ^{51}Cr release. Standard error of the mean is shown.

I also expressed the protein-coding region of *c1orf74* in T2 cell line which was identified as one of the few cell lines that were not lysed by clone ML15 (**Figure 4.7 B**). C1orf74 was expressed together with marker gene rCD2, separated by a self-cleaving 2A sequence, to allow for selection of cells that had taken up lentivirus. As expected, no increase of T-cell activation was observed when T-cell clone ML15, or other Vγ9Vδ2 T-cell clones, were incubated with T2 cell line over-expressing C1orf74 (**Figure 5.5 A**). Additionally, over-expression of C1orf74 in KBM7 slightly decreased rather than increased susceptibility of the cancer cells to lysis, when incubated with ML15 or other Vγ9Vδ2 T-cell clones (**Figure 5.5 B**).

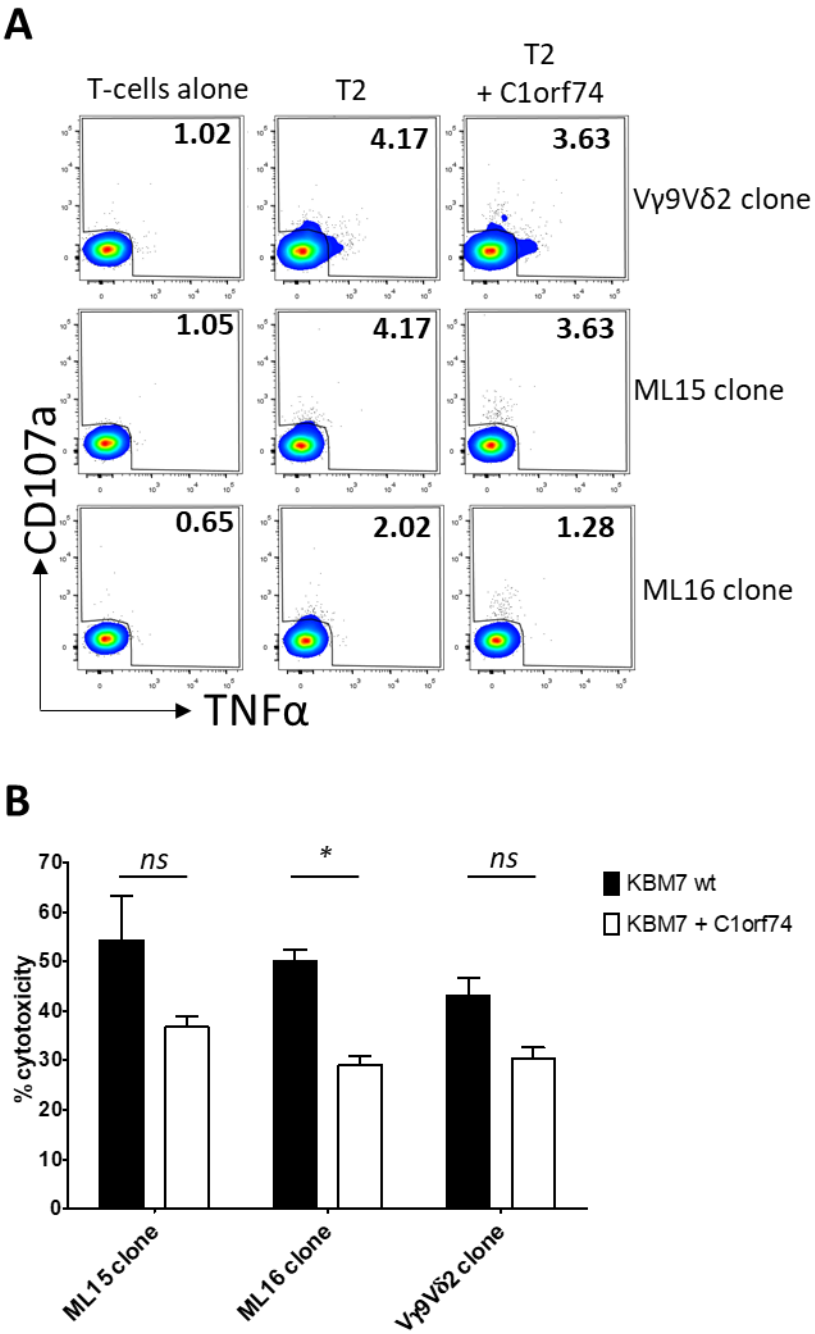

Figure 5.5 The expression of C1orf74 does not influence recognition of cell lines by Vγ9Vδ2 T-cell clones. (**A**) T2 cell line was lentivirally transduced with codon-optimised C1orf74-rCD2 construct, followed by selection of $rCD2^+$ cells. The transduced cells, as well as the untransduced control, were incubated with TIL-derived clones ML15 and ML16, as well as the conventional Vγ9Vδ2 clone. The responding T-cells were enumerating based on CD107a and/or TNFα expression among live $CD3^+$ cells. (**B**) KBM7 cell line was lentivirally transduced with codon-optimised C1orf74-rCD2 construct, followed by selection of $rCD2^+$ cells. The transduced cells, as well as the untransduced control, were co-incubated with T-cell clones at 10:1 E:T ratio for 4 h, and the cytotoxicity was determined by ^{51}Cr release. Standard error of the mean is shown. Student's t-test, *$p<0.05$, ns – not significant.

I therefore concluded that C1orf74 did not play any apparent role in recognition of KBM7 line by clone ML15, and the observed decrease of T-cell activation in case of the CRISPR library or individually transduced gRNAs could stem from other factors. One of the factors could be a deficiency in the phosphoantigen sensing pathway, resulting either from an off-target effect of gRNAs, or heterogeneity of the starting KBM7 population. Aminobisphosphonate treatment showed that the C1orf74-deficient KBM7 library-derived clone 2 was still capable of stimulating ML15 and other Vγ9Vδ2 T-cell clones, in a phosphoantigen specific manner, although to a lesser extent than the parental KBM7 line (**Figure 5.6 A**). Furthermore, pulsing with the activating anti-BTN3 antibody 20.1 sensitised the KBM7 clone 2 to Vγ9Vδ2 T-cell clones, albeit to a lesser extent than with wild type KBM7 (**Figure 5.6 B**). Importantly, no difference in T-cell activation was observed when a Vδ1Vγ9 clone ML3 was incubated with KBM7 clone 2 or untransduced KBM7 parental line, indicating that the mechanism of resistance observed for KBM7 clone 2 affects only the recognition by Vγ9Vδ2 T-cell clones. In order to dissect this mechanism of resistance further, I compared the transcriptomes of KBM7 clone 2 and the parental KBM7 line by RNAseq. The RNAseq analysis revealed that the KBM7 clone 2 differed from the parental line in terms of expression of nearly 5,000 genes (**Appendix Figure 8.19**). Such a vast difference in transcriptomes precluded from any more precise dissections of the resistance mechanism employed by KBM7 clone 2, and my supervisory team advised me not to pursue studies of C1orf74 further.

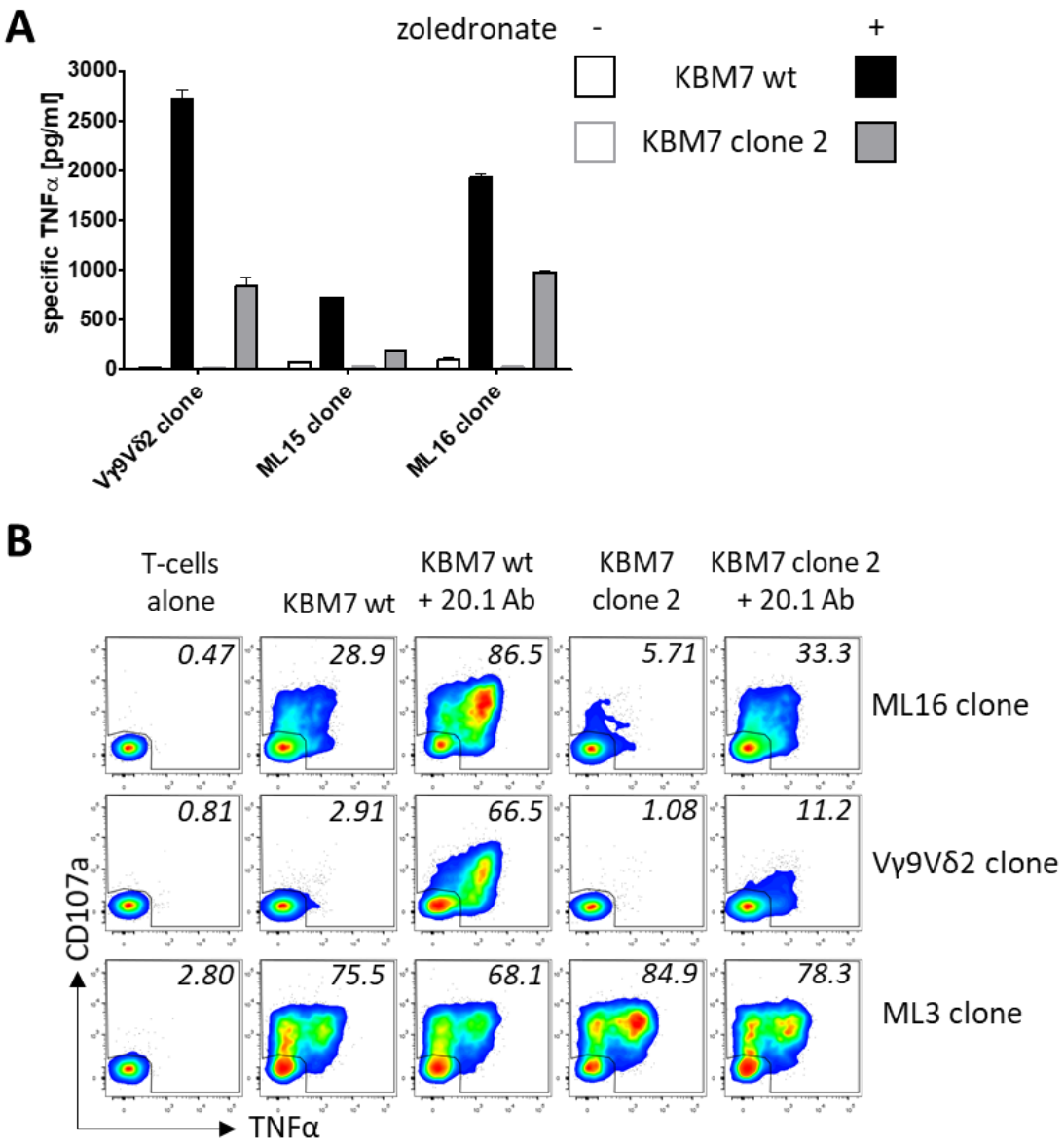

Figure 5.6 C1orf74-deficient KBM7 clone 2 is still capable of stimulating T-cells *via* the phosphoantigen pathway. (**A**) T-cell clones were co-incubated with parental or clone 2 KBM7 cells ± 50 μM zoledronate. TNFα concentration in the supernatants was determined after 16 h of co-incubation. TNFα concentrations were normalised by subtracting the values from T-cells incubated alone. Standard error of the mean is shown. ML15 and ML16 are broadly cancer-reactive Vγ9Vδ2 T-cell clones derived from TILs while the Vγ9Vδ2 clone is a conventional phosphoantigen-reactive T-cell clone derived from peripheral blood. (**B**) T-cell clones were co-incubated with parental or clone 2 KBM7 cells for 5 h after 30 min pre-incubation with the stimulating anti-BTN3 antibody 20.1. ML3 is a broadly cancer-reactive TIL-derived T-cell clone which expresses a Vγ9Vδ1 TCR.

5.2.4 The validation of the whole genome CRISPR library methodology by using a conventional αβ T-cell clone

Despite the use of high cell numbers, ensuring over >400X coverage over the GeCKO library, multiple rounds of selection and exhaustive sequencing of selected and unselected libraries, the screening of KBM7 library with a γδ clone ML15 resulted in false positive hits. Therefore, I decided to validate the screening methodology by transducing GeCKO library into a HLA-A2^{+} melanoma cell line t24, followed by selection with KT B17 – a conventional αβ T-cell clone specific for a Melan-A derived epitope presented by HLA-A2. Each sub-library was transduced into 15×10^{6} cells at MOI=0.4, ensuring >100X coverage over the library. Each sub-library was then subjected to T-cell mediated selection for 14 days, and the surviving cells were re-selected to decrease chances of non-specific survival. Indeed, after two rounds of selection the t24 melanoma lines transduced with sub-libraries A and B were significantly more resistant to lysis by the αβ T-cell clone KT B17 than the unselected t24 line (**Figure 5.7 A**).

The representation of gRNAs in the selected libraries was then determined by "mid-throughput" sequencing on an Illumina MiSeq instrument. The rationale for this approach was that based on the number of cells surviving the selection, the gRNA representation therein was vastly reduced and therefore could be sampled sufficiently by sequencing only a fraction of genomic DNA, and multiplexing the samples by MiSeq (thus resulting in 10^{4}-10^{5} reads per sample, in contrast with 10^{8} reads in HiSeq). The development of this approach was motivated by the need for rapid cost-effective verification that library selection had been successful and allowed the GeCKO gRNAs to be sequenced in the same MiSeq runs as those my laboratory routinely uses for TCR sequencing. The limited sampling accurately represented the diversity observed in all the samples tested, especially for the most frequent gRNAs, as demonstrated by high correlation values between two independent biological replicates coming from the same selected library, and sequenced in the "mid-throughput" manner (**Appendix Figure 8.20**).

The "mid-throughput" sequencing of selected t24 libraries showed that the second round of enrichment resulted in an increased frequency of gRNA targeting HLA-A2, from less than 10% to nearly 30% of the reads in sub-library A (**Figure 5.7 B**), as well as decreased frequency of (plausibly) non-specific gRNAs for miRNA 5659 and C6orf106 (from 40 and 30% of reads, respectively, to 2% or less). HLA-A2 is the antigen presentation platform for KT B17, and therefore it is of no surprise that the knock-out of this gene made the cells resistant to lysis. Another important hit, present in both sub-libraries A and B, albeit at low frequency, was β-2-microglobulin – an essential component of surface-expressed HLA class I. This screen also detected TNFRSF21 (TNF receptor superfamily member 21; a TNFα induced death receptor[433])

in sub-library A. Therefore, the absence of TNFRSF21 on t24 cells could potentially protect them from apoptosis after contact with T-cell derived TNFα. The results from sub-library B were heavily dominated by two gRNAs, specific for C10orf62 and Janus kinase (JAK) 1, and their relative frequency was not substantially enriched by the second round of selection (**Figure 5.7 B**). In order to validate the role of the enriched gRNAs from sub-library B, I transduced them into the parental line t24. No resistance to lysis was observed in case of C10orf62 gRNA-transduced t24 (**Appendix Figure 8.21**), again indicating that the survival of cells bearing this gRNA was likely to be non-specific.

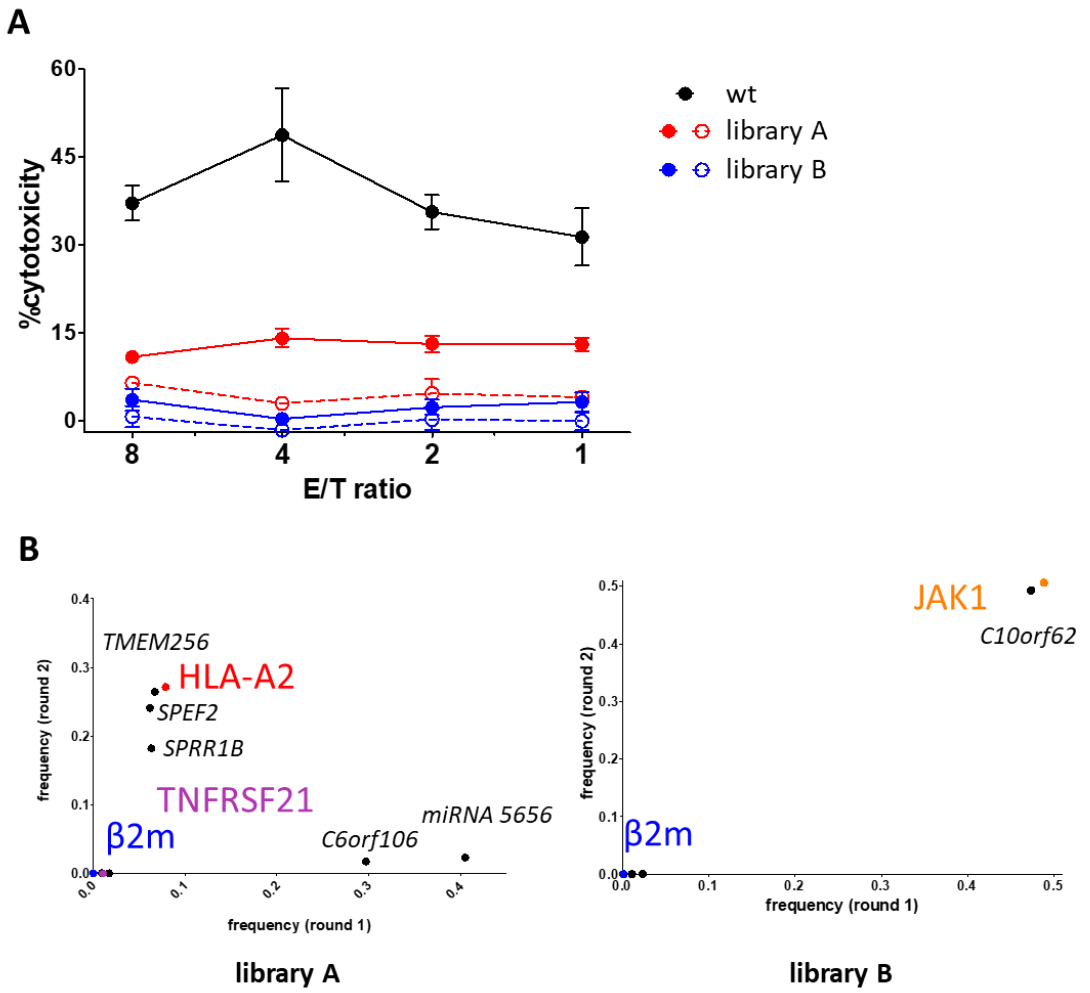

Figure 5.7 Proof-of-concept selection of whole genome libraries in a melanoma cell line with a conventional HLA-A2 restricted αβ T-cell clone. (**A**) Whole genome library GeCKO v2 (sub-libraries A and B) was transduced into a HLA-A2^{+} melanoma cell line t24. The transduced cells were co-incubated with an αβ T-cell clone KT B17 specific for a Melan-A epitope presented by HLA-A2 at E:T of 1:1 for 14 days. The surviving cells after the first round of selection (round 1, filled circles) were incubated with KT B17 clone at E:T of 2:1 for 14 days, and the surviving cells were combined (round 2, empty circles). The cytotoxicity of clone KT B17 against the selected libraries, as well as the parental melanoma line (wt) was determined by ^{51}Cr release after 4 h of co-incubation. The lentivirally packaged whole genome libraries were provided by John Phillips, University of Utah. (**B**) Genomic DNA from sub-library A and sub-library B after the round 1 and round 2 of selection was extracted and sequenced as described in Materials and Methods. The frequencies of gRNAs in round 1 and round 2 of selection are shown. gRNAs targeting genes of known function in antigen processing and presentation are shown in colour. JAK1, Janus kinase 1; TNFRSF21, TNFα receptor superfamily member 21.

Janus kinases are involved in the IFNγ signalling pathway, and loss of function of JAKs through somatic mutations has been shown as a means of acquiring resistance to checkpoint inhibitor blockade in human melanomas[434]. IFNγ, acting *via* Janus kinases, upregulates the expression of MHC molecules and β-2-microglobulin, as well as components of antigen processing pathway[435]. Indeed, low dose IFNγ treatment upregulated conventional HLA class I (A, B and C), as well as HLA-A2 expression on the melanoma cell line t24 (**Figure 5.8 A**). Conversely, no effect of IFNγ on t24 transduced with JAK1 gRNA was observed, thus validating the efficiency of the knock-out. Consequently, JAK1 gRNA-transduced t24 was less susceptible to lysis by Melan-A specific T-cell clones or Melan-A specific TCR-transduced cells (**Figure 5.8 B**). While JAK1 knock-out made the cancer cells more resistant to T-cell mediated lysis, the reduction was not as great as observed in case of the selected sub-library B (**Figure 5.7 A**), indicating the possibility of co-selection of spontaneous mutations in t24 in addition to gRNA-specific phenotypes.

Guide RNAs targeting HLA-A2, β-2-microglobulin and JAK1 have also been found in a replicate GeCKO library, selected independently with KT B17 clone, showing the reproducibility of T-cell screening of whole genome libraries in cancer cells (**Appendix Figure 8.22**). In addition to HLA-A2, β2m and JAK1 gRNAs, the second library also contained gRNAs specific for CD58 and IFN-α/β receptor 2 (IFNAR2). CD58 is a ligand of CD2, expressed on lymphocytes, and acts as an adhesion molecule, potentiating T-cell and NK cell response. Loss of function of CD58 is a common evasion mechanism of different cancer types[436,437]. IFNAR2, conversely, acts upstream of the JAK/STAT pathway and promotes apoptosis of cancer cells[438,439].

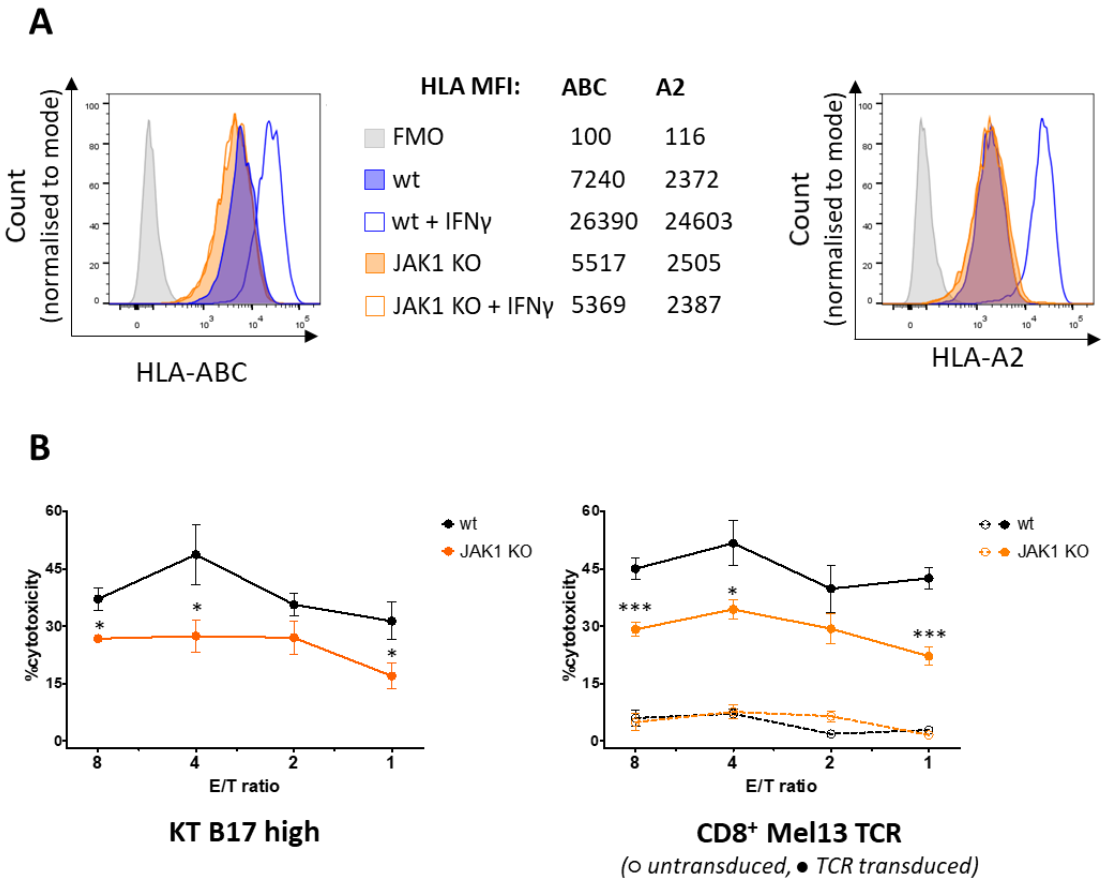

Figure 5.8 Knock-out of JAK1 from a melanoma cell line reduces the susceptibility to lysis by Melan-A specific T-cell clones and TCRs. (**A**) gRNA specific from JAK1, enriched in the selected sub-library B, was independently transduced into the melanoma cell line t24. JAK1 gRNA transduced t24, as well as untransduced parental line (wt, wild type) were cultured for 72 h with or without 200 IU/ml IFNγ, followed by staining for surface expression of conventional HLA class I (A, B and C) or HLA-A2. Mean fluorescence intensities are shown. FMO, fluorescence minus one control. (**B**) The parental t24 line (wt, wild type) and transduced cells (JAK1 KO) were co-incubated for 4 h with either T-cell clone KT B17 high (left panel), or $CD8^+$ T-cells transduced with Mel13 TCR and TCR-β CRISPR and corresponding untransduced $CD8^+$ T-cells (right panel). Cytotoxicity was determined by ^{51}Cr release assay. Standard error of the mean is shown. Student's t-test *$p<0.05$, ***$p<0.005$.

5.2.5 Identification of MR1 as the restricting element of a cancer-reactive αβ T-cell clone

Given the encouraging proof-of-concept demonstrated from screening a conventional T-cell clone shown above, my colleagues and I decided to use this technology to gain insight into the mode of cancer cell recognition by a non-HLA restricted αβ T-cell clone MC.7G5. MC.7G5 recognises diverse cancer lines, but not normal cells, and the recognition is not hampered by anti-MHC I or anti-MHC II blocking antibodies (**Appendix Figure 8.23**). My colleagues and I have therefore transduced the GeCKO library into one of the cell lines lysed by MC.7G5, namely HEK 293T, transducing 40×10^6 cells at MOI=0.4, thus ensuring >100X coverage over the starting library. The transduced cells were then selected with the T-cell clone in two successive rounds of selection, as described above. I have then sequenced gRNA representation in the library after selection, identifying over 300 individual gRNAs. The results were then narrowed down by inclusion of gRNAs only if more than one gRNA was detected for the given gene (**Figure 5.9 A**). The presence of multiple gRNAs targeting a single gene decreases the chances of the gene being a false positive hit[303]. Only five genes remained after filtering the sequencing results based on the presence of multiple gRNA targeting a single gene, namely β2m (five gRNAs), MR1 (two gRNAs), regulatory factor X (RFX, five gRNAs), RFX associated ankyrin containing protein (RFXANK, five gRNAs), and RFX associated protein (RFXAP, three gRNAs). As mentioned before, β2m is an essential component of conventional MHC-Ia protein complexes (HLA-A, B, C) but also some MHC-Ib family members, including CD1 and MR1. RFX, RFXANK and RFXAP are essential components of a protein complex driving the transactivation of β2m and MHC-I promoters[440]. These results clearly pointed out at MR1 as being essential for target cell recognition by MC.7G5. To validate this result, MR1 was knocked out of a melanoma cell line MM909.24, as described before[404], as well as was lentivirally over-expressed in the parental melanoma cell line. The knock-out of MR1 in MM909.24 completely abrogated the recognition of the cell line by MC.7G5 while MR1 over-expression increased the T-cell response (**Figure 5.9 B**). The putative model of target cell recognition by clone MC.7G5 is schematically depicted in **Figure 5.9 C**, including all the proteins identified by CRISPR/Cas9 library screen. Further experiments conducted by my colleague Michael Crowther confirm that the MC.7G5 T-cell clone recognises cancer through a non-MAIT ligand presented in the MR1 binding groove. Indeed, addition of known MAIT ligands to $MR1^+$ cancer cells reduced recognition by MC.7G5 while making the cells targets for MAIT clones in parallel assays. These results suggest that MR1 may present novel, undiscovered ligands on the surface of cancer cells. This project was assigned to my colleague and will therefore not be further discussed in the context of my own work. Nevertheless, my work shows valuable proof-of-concept that whole genome CRISPR can be very valuable for rapid

identification of ligands recognised by 'orphan', non-HLA restricted T-cell clones with unknown targets.

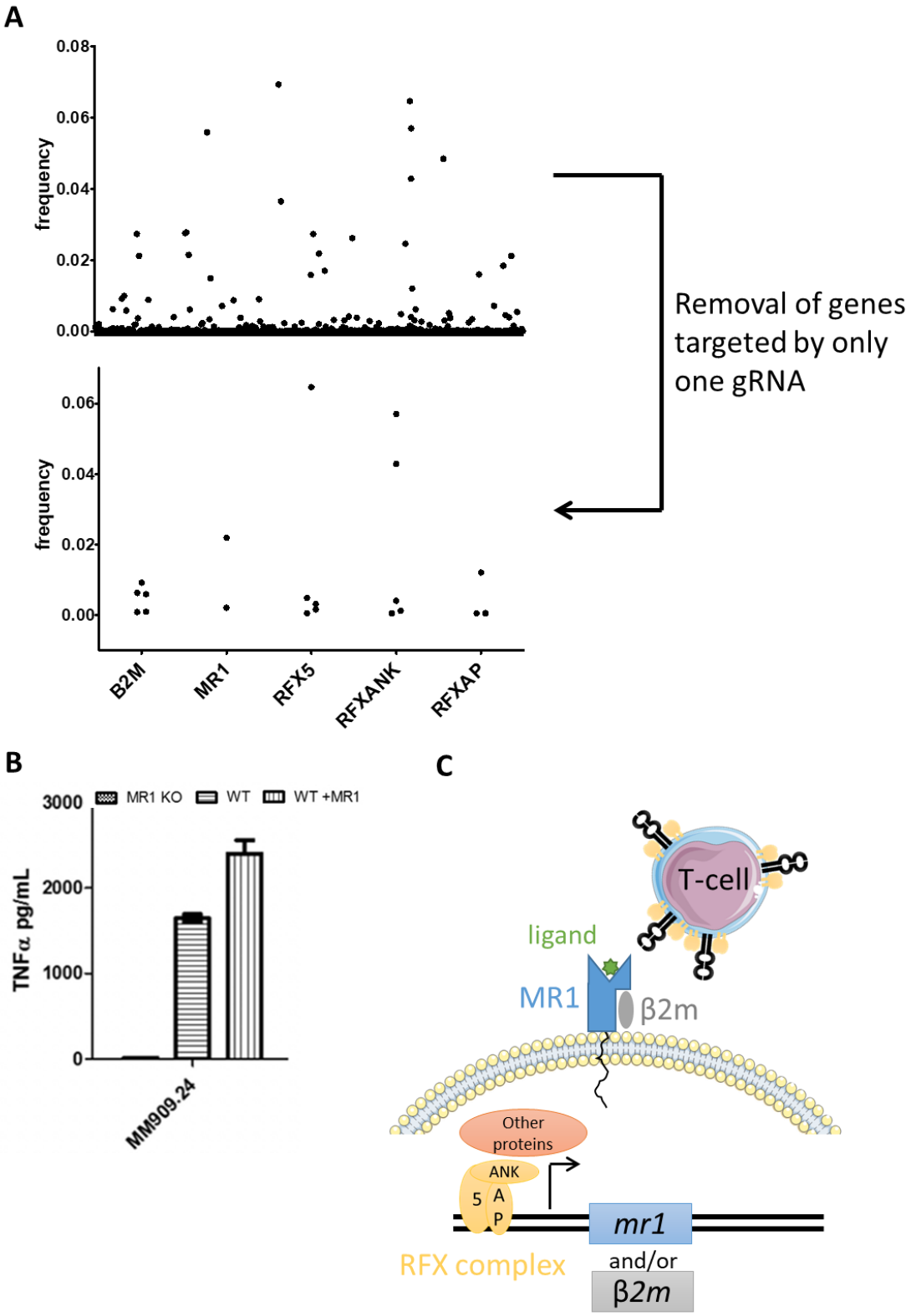

Figure 5.9 Whole genome library screening with a non-HLA restricted αβ T-cell clones identifies MR1 as the restricting molecule. (**A**) HEK 293T cells were transduced with the whole genome library GeCKO v2, and screened with a non-HLA restricted, broadly cancer-reactive αβ T-cell clone MC.7G5

(Legend continued on the following page)

(Legend continued from the previous page) The lentivirally packaged whole genome libraries were provided John Phillips, University of Utah. The transduced cells were subjected to two rounds of screening with T-cells, followed by genomic DNA extraction and sequencing. The frequency of each identified gRNA is shown on the top panel. The gRNAs were then filtered to remove genes targeted by only one gRNA. RFX, regulatory factor X; RFXANK, RFX associated ankyrin containing protein; RFXAP, RFX associated protein. (**B**) Clone MC.7G5 was incubated with a melanoma cell line MM909.24. The cell line was engineered to be deficient in MR1 by CRISPR/Cas9 (MR1 KO) or to overexpress MR1 (WT +MR1). Untransduced cell line was used as a control (WT). The TNFα concentration was measured after 16 h of co-incubation of the T-cell clone MC.7G5 and MM909.24 cell lines. Data provided as a courtesy of Michael Crowther, Cardiff University. (**C**) Schematic representation of cell components essential for target cell recognition by clone MC.7G5. All the components (save the putative MR1 ligand) were identified by whole genome library screening.

5.3 Discussion

Whole genome CRISPR/Cas9 libraries conceptually offer an excellent tool to investigate any selectable biological mechanism of choice, theoretically allowing for a comprehensive identification of every major gene and pathway essential for the given process. When using T-cells as the selecting factor, CRISPR/Cas9 libraries can help identify the actual TCR ligand, co-stimulatory molecules and protein machinery involved in presenting the said ligand on cell surface. In practice, however, T-cell mediated screens of whole genome libraries are challenging due to a variety of factors. First, the screens rely on interactions between two cell types, thus introducing another variability to the experiment. Factors such as the optimal T-cell to library ratio, the duration of co-incubation, and even the type of culture vessel (i.e. ensuring sufficient T-cell to target contact while maintaining optimal cell density) can determine the success or failure of the screen. Second, pre-existing cellular heterogeneity, or that which is unintentionally induced during genome engineering and selection, may ensure the gRNA-independent survival of a given target cell and result in false positive hits. Third, activated T-cells can potentially kill non target cells, i.e. cells that have a productive knock-out that would prevent from them being directly recognised by T-cells, in a bystander manner, either employing Fas-FasL pathway or through cytokine secretion[441].

It may also be envisaged that a given T-cell clone can recognise, and lyse, target cells using more than one mechanism, for instance TCR - ligand and NK receptor – NK ligand, or MHC I – ILT2 (ref. [412]). The TCR itself is capable of recognising diverse targets – which is a well-studied phenomenon, at least in case of αβ TCR cross-reactivity[442]. The actual T-cell target may also be derived from a pathway essential for cell survival – for example, production of IPP in the mevalonate pathway requires HMGR, an essential enzyme in isoprenoid biosynthesis, knock-out of which is lethal for the cell[443,444]. Therefore, it may be that in case of some T-cell clones a knock-out of any single gene is insufficient to protect the target cell from lysis. As demonstrated in this Chapter, selection of KBM7 cell line with ML15 T-cell clone did not result in discovery of a meaningful CRISPR-guided knockout despite apparent gRNA enrichment and resistance to lysis exhibited by the selected library. Indeed, I showed in **Chapter 4** that clone ML15 was still capable of killing the cancer cell line lacking BTN3 molecules, possibly in a TCR-independent manner. Therefore, it may be desirable to use TCR-transduced cytotoxic T-cells instead of γδ T-cell clones, to limit the recognition mechanism to TCR–ligand interactions. Using TCR-transduced cells, which do not express any endogenous TCR through TCR-β knock-out, as described in **Chapter 3**, additionally allows an access to potentially unlimited number of specific T-cells, by repeated transductions into freshly isolated cells, in contrast with T-cell clones which have a limited capacity for continual growth.

After I performed my studies and during the writing of this thesis, two papers addressing the issue of T-cell mediated selection of CRISPR/Cas9 libraries were published in *Nature*. Manguso *et al.* used a bespoke CRISPR/Cas9 library (under 10,000 gRNAs) targeting over 2,000 genes functionally expressed by a mouse melanoma cell line[445]. The CRISPR/Cas9 library was then transplanted into immunocompetent mice treated with a tumour cell vaccine, with or without checkpoint inhibitor therapy directed at PD-1, thus allowing the library to undergo selection under the pressure of adaptive immune system. A reference library was generated by transplanting the engineered melanoma cell line into αβ TCR deficient mice. This innovative approach, involving *in vivo* selection of knock-out library by the endogenous immune system, highlighted the importance of the IFNγ pathway in cancer sensitivity to immunotherapy. In line with the results showed in this Chapter, Manguso *et al.* demonstrated that loss of JAK1, as well as other components of JAK/STAT pathway, increased the resistance of cancer cells to T-cell mediated lysis, as well as made the cells unresponsive to IFNγ signalling. Finally, PTPN2, a protein tyrosine phosphatase acting downstream of interferon receptors IFNAR and IFNGR, was identified as a potential target for immunotherapy - as loss of PTPN2 enhanced interferon signalling and MHC-I antigen presentation pathway.

Another approach was presented by Sanjana and colleagues[446]. Whole genome human CRISPR/Cas9 library GeCKO was transduced into a melanoma cell line and selected with primary $CD8^+$ T-cells transduced with the clinically tested αβ TCR specific for NY-ESO epitope presented by HLA-A2 (Ref. [333]). This approach is highly reminiscent of the one I attempted in this Chapter, but there are several differences. The most important difference seems to be duration of the T-cell mediated screening, being in this case 12 h at T-cell to cancer ratio that resulted in incomplete (approximately 90%) cell lysis, thus potentially preventing from excessive bystander killing and enrichment in spontaneously mutated cells. Indeed, the whole genome library screen conducted by Sanjana and colleagues resulted in a robust identification of known components of MHC-I antigen presentation (including HLA-A2, β2m and TAP), but also adhesion molecule CD58 and members of JAK/STAT signalling pathway – which were also identified in whole genome screens described in this Chapter.

Whole genome CRISPR/Cas9 libraries are therefore a highly versatile and robust tool for identification of new cancer immunotherapy targets and mechanisms of cancer immunoevasion. I strongly believe that combining the library selection parameters described by Sanjana and colleagues[446] with primary T-cells transduced with unconventional, broadly cancer-reactive TCRs (described in **Chapter 4**) and CRISPR/Cas9 specific for endogenous TCRs (described in **Chapter 3**) will shed light on the fundamental biology of unconventional T-cells and lead to identification of cancer-associated targets suitable for pan-population immunotherapy.

6. General discussion and Conclusions

6.1 Summary of work

The work presented in this Thesis is connected by two major underlying themes, one being the broad anticancer reactivity of non-HLA restricted T-cells, most notably expressing γδ TCRs; the other focused on CRISPR/Cas9 mediated genome engineering in T-cells and cancer cell lines. Collectively, research projects described herein combine two of the recent Breakthroughs of the Year chosen by the magazine *Science*, namely cancer immunotherapy[213] (Breakthrough of the Year 2013) and CRISPR/Cas9 mediated genome editing[447] (Breakthrough of the Year 2015) so my work is highly topical.

In **Chapter 3**, I developed a methodology for generation of TCR-transduced primary T-cells exhibiting superior anticancer reactivity and antigen sensitivity, vastly outperforming transgenic T-cells generated using current, clinically-applied methods. This TCR replacement methodology relies on simultaneous delivery of the transgenic TCR and CRISPR/Cas9 specific for endogenous TCRs. As a proof-of-concept, I used TCR replacement methodology to generate primary T-cells expressing a phosphoantigen-specific TCR which showed superior reactivity, compared to T-cells transduced with the standard method, against primary leukemic blasts - without targeting normal cells.

Chapter 4 focused on the procurement and initial characterisation of non-HLA restricted, broadly cancer-reactive T-cell clones derived from a variety of clinical sources, including tumour-infiltrating lymphocytes from a complete remission melanoma patient, peripheral blood T-cells from a breast cancer patient, and ovarian cancer ascites. The role of the TCR in cancer cell recognition by selected broadly cancer-reactive γδ T-cells was investigated using the TCR replacement system described in **Chapter 3**. Indeed, only the TCR replacement, but not standard TCR transfer methodologies, resulted in re-direction of primary T-cells to cancer with TCRs isolated from the broadly cancer-reactive T-cell clones. In **Chapter 4** I also generated a panel of cancer cell lines deficient in known ligands of γδ TCRs, using the CRISPR/Cas9 system. This panel of single gene knock-outs can be useful for initial determination of the contribution of known γδ T-cell ligands to cancer recognition by γδ T-cell lines and clones. Using the TCR replacement and butyrophilin knock-out in the autologous tumour, I described a Vγ9Vδ2 T-cell clone which failed to self-present phosphoantigens, possibly due to intrinsic deficiencies in yet to be identified components of the phosphoantigen presentation pathway. Comparative transcriptomic analysis of this Vγ9Vδ2 T-cell clone, as well as donor-matched Vγ9Vδ2 T-cell clones capable of phosphoantigen presentation, may unravel new mechanisms involved in phosphoantigen

sensing. Finally, using CRISPR/Cas9 I generated a panel of cancer cell lines deficient in members of CD1 family (CD1a-d), and thus determined that the recognition of multiple cancer cell lines by a CD4/CD8 double negative αβ T-cell clone was dependent on CD1a –indicating for the first time that CD1a may be a valid target for cancer immunotherapy.

Single gene knock-out as described in **Chapter 4** can only be used to confirm or disprove the role of a known molecule in target cell recognition. In **Chapter 5** I extended the use of CRISPR/Cas9 technology by investigating an unbiased, genome-wide method for discovery of new T-cell ligands, as well as molecular pathways involved in processing and presentation of these ligands. I used whole genome CRISPR/Cas9 libraries transduced into cancer cell lines recognised by conventional and unconventional T-cells, showing encouraging proof-of-concept results. This work also highlighted some potential pitfalls of the approach resulting from non-specific cell survival. Finally, by using a whole genome CRISPR/Cas9 library I identified MR1 as a restricting element for a non-HLA restricted cancer-reactive T-cell clone in addition to a family of transcription factors necessary for the expression of MR1.

6.2 Future perspectives for pan-population cancer immunotherapy

6.2.1 Choosing the optimal target and the optimal receptor

Adoptive transfer of genetically modified lymphocytes is re-defining cancer treatment, resulting in an unprecedented complete remission rate. Indeed, in August 2017 the FDA approved the first genetically engineered autologous T-cell product, based on anti-CD19 CAR, for treatment of acute B-cell lymphoblastic leukaemia in children and young adults, based on over >80% complete remission rates achieved in clinical trials[448]. While CARs are highly successful therapeutics which can be applied across the population regardless of the HLA type, so far the clinical success of CARs has been limited to haematological malignancies expressing CD19. During my studies, I was lucky enough to be involved in the development of new antibodies and CARs for the diagnosis and treatment of T-cell malignancies. This approach takes advantage of the fact that the human TCR-β locus is a gene duplication. Consequently, T-cells express either a TRBC1 or a TCBC2 TCR. These two TCR subtypes segregate more or less evenly across all known T-cell subsets. In contrast, T-cell cancers are either TRBC1 or TRBC2, opening up the possibility for targeting the malignancy while keeping T-cell immunity intact. This work was recently accepted for publication in *Nature Medicine*[449]. Clinical trials of the approach are set to take place in 2018. Given the success of CD19 CARs for the treatment of B-cell malignancies, there are high hopes that this approach will provide an effective treatment option for the more aggressive malignancies that originate from T-cells. While there is great promise for CAR-T

treatment of soluble cancers, efficient CAR targeting of solid tumours will require additional developments[450].

In contrast to results of CARs in solid tumour treatment, αβ TCR-transgenic T-cells specific for a tumour-associated antigen derived from NY-ESO-1 and presented by HLA-A2 induced objective response in solid tumour patients (synovial cell carcinoma and melanoma)[333]. While CD19 CARs and NY-ESO-1 specific αβ TCRs represent plausibly the best-in-kind therapeutics in clinic, they are limited only to a subset of the population expressing a given HLA type (NY-ESO-1 TCR) and/or an antigen present only in a limited subsets of cancer (CD19 CAR, NY-ESO-1 specific TCR). Therefore, development of a broadly cancer-specific, pan-population immunotherapeutic agents which do not cause unmanageable severe adverse effects has the potential to revolutionise the field of cancer immunotherapy.

The optimal cancer-associated target for a pan-cancer, pan-population immunotherapy can be chosen *a priori*, based on population-wide gene and protein expression data. Such a target would be expressed on multiple cancer types but not on essential tissue, and should preferably be crucial for cancer cell survival, proliferation and/or metastasis – thus preventing cancer immunoevasion by losing the expression of a targeted antigen. For instance, loss of CD19 expression is a common immunoevasion mechanism developed by haematological malignancies under the selective pressure from CD19 CARs[451], and the Melan A gene has been lost from melanomas that were targeted with Melan A-specific TCRs[452]. After the selection of desirable antigens, the challenge of finding an optimal receptor specific for the said antigen needs to be overcome. In case of HLA-restricted αβ TCRs, finding a receptor for a chosen antigen (if the antigen is sufficiently immunogenic) can be achieved using the wealth of pre-existing methodologies, including humanised mouse models immunised with target antigens, *ex vivo* patient samples, *in vitro* priming systems, or, in the future, structure-based TCR protein engineering (reviewed in [453]). In case of HLA-unrestricted TCRs, be they αβ or γδ TCRs, methodologies for procurement of a TCR with a given specificity are in their infancy. One can envisage immunising TCR-humanised mice[454] with a syngeneic cell line over-expressing the antigen of choice, or using donor-matched antigen knock-in/knock-out cell lines for high-throughput selection of antigen-specific T-cell lines and clones (in a T-cell library format, as described in **Chapter 4**). However, all these methods are laborious, and may not result in procurement of antigen-specific TCRs (for instance, if such a TCR is not present in the starting TCR repertoire).

Conversely, the selection of a cancer-associated target recognised by broadly cancer-reactive TCRs can be achieved retrospectively – i.e. through initial isolation of broadly cancer-reactive T-

cell clones and TCRs, followed by identification of the cognate ligand, and pre-clinical safety validation. There are several advantages of this approach, such as feasibility (if the T-cell clone recognises cancer cells *via* its TCRs, then the antigen(s) recognised by the TCR are immunogenic enough to drive an immune response). In addition, TCRs are isolated from T-cell clones present in human subjects without any obvious autoimmune disorders might be expected to have improved safety profile over engineered TCRs. Following isolation of cancer-reactive non-HLA restricted T-cell clones, the identity of putative ligands can be inferred using genome engineering technologies, in particular whole genome CRISPR/Cas9 libraries. As shown in **Chapters 4** and **5**, CRISPR/Cas9 technology was successfully used to identify CD1a and MR1 as putative cancer-associated ligands of broadly cancer-reactive T-cell clones.

Targeting of alterations in intracellular metabolome of cancer cells represents a particularly attractive use of non-HLA restricted T-cells. First of all, metabolic dysregulation is an essential feature of cancer cells, supporting their unrestricted proliferative capacity and invasiveness[211]. Therefore, targeting metabolic pathways that are specifically up-regulated in cancer cells offers a possibility of discrimination between normal and transformed cells, as well as limits the capacity of cancer immunoevasion. Secondly, molecules involved in presentation and/or sensing of metabolic pathways, such as MR1, CD1a-d or BTN3A1, are highly invariant[22] and thus offer a potential target for cancer immunotherapy across the entire population. These molecules can present cancer-specific ligands, as exemplified by CD1c presenting cancer-specific self-lipids to T-cells[102], or act as sensors of metabolic perturbation, without bona fide ligand presentation to T-cells – as exemplified by conformational changes in BTN3A1 (Ref. [41]) or (putatively) CD1a[424], or surface expression upon ligand binding in case of MR1 (Jamie Rossjohn, personal communication). CD1a is an attractive cancer target as it is not expressed on any organs apart from skin, where it is present on highly specialised antigen-presenting cells[421]. Therefore, CD1a-directed immunotherapy using natural T-cell receptors has high potential to be safe and should not cause fatal on-target toxicities. Thirdly, identification of specific molecular pathways, products of which are recognised by T-cells, can lead to development of small molecule drugs targeting the said pathway and sensitising cancer to T-cells. Indeed, the recognised metabolites, or molecules that mimic their structure could be used as an off-the-shelf prophylactic or therapeutic “vaccine” to prime cancer-specific responses *in vivo*. Use of whole genome loss-of-function and gain-of-function CRISPR/Cas9 library screening, coupled with high throughput metabolomics, will certainly aid the identification of new metabolic targets recognised by broadly cancer-reactive T-cells.

Finally, the antigen-sensitivity of TCR-transgenic T-cells towards target cancers requires careful consideration. For instance, an αβ TCR with a very low affinity for its cognate antigen showed

scant anticancer effect in patients[455], while an affinity-enhanced version of the same TCR induced a stronger anticancer response but at cost of severe toxicities[456]. Experiments from my own laboratory in multiple systems indicate that natural anti-cancer TCRs are suboptimal and that some level of affinity enhancement is required to ensure robust recognition of tumour. The corollary of this affinity enhancement is that it bypasses thymic selection and has potential to elicit dangerous autoimmunity[206,359]. Additionally, enhanced affinity towards the cognate ligand could have detrimental effects on the anticancer reactivity of the cellular product beyond on-target off-tumour and off-target toxicities. A side-by-side comparison of a natural TCR specific for a peptide-HLA complex (low affinity) *versus* a CAR specific for the very same peptide-HLA (high affinity) demonstrated the superior activity and specificity of the former[407]. Indeed, the expertise accumulated in the CAR field indicates that too high avidity towards the cognate ligand results in premature exhaustion of the engineered T-cells[374,457]. One could also envisage that strong on-target affinity, resulting from fast association and slow dissociation rate, of a transgenic receptor would preclude the engineered T-cells from penetrating the tumour mass and rather sequester them to tumour periphery. For all the reasons mentioned above, I believe that natural TCRs specific for a given surface molecule (be it a ubiquitous stress marker or metabolite/lipid presented by an invariant molecule) offer a safer, and potentially more efficacious, alternative to using CARs directed against the same surface molecule. While there are no published technologies to enhance the affinity of non-HLA restricted TCRs, in particular γδ TCRs, TCRs with optimal on-target affinity can be selected from the endogenous TCR repertoire[208,469]. Indeed, T-cells engineered to express Vγ9Vδ2 TCRs selected from the endogenous repertoire for optimal activity, developed by a Dutch biotech company Gadeta, are set to be tested in clinic against haematological malignancies and solid tumours in 2018/2019 (Ref. [376]).

6.2.2 Going beyond the antigen receptor

While selection of an optimal cancer-associated target and a TCR specific for the said target are of paramount importance for development of novel immunotherapies, a therapeutically successful cellular product must also meet other criteria, such as engraftment and persistence *in vivo*, clinically manageable adverse reactions, as well as trafficking to the tumour site and exerting anticancer activity even in an immunosuppressive tumour milieu. Here I will briefly discuss the potential of genetic engineering to generate an optimal cellular product (summarised in **Figure 6.1**).

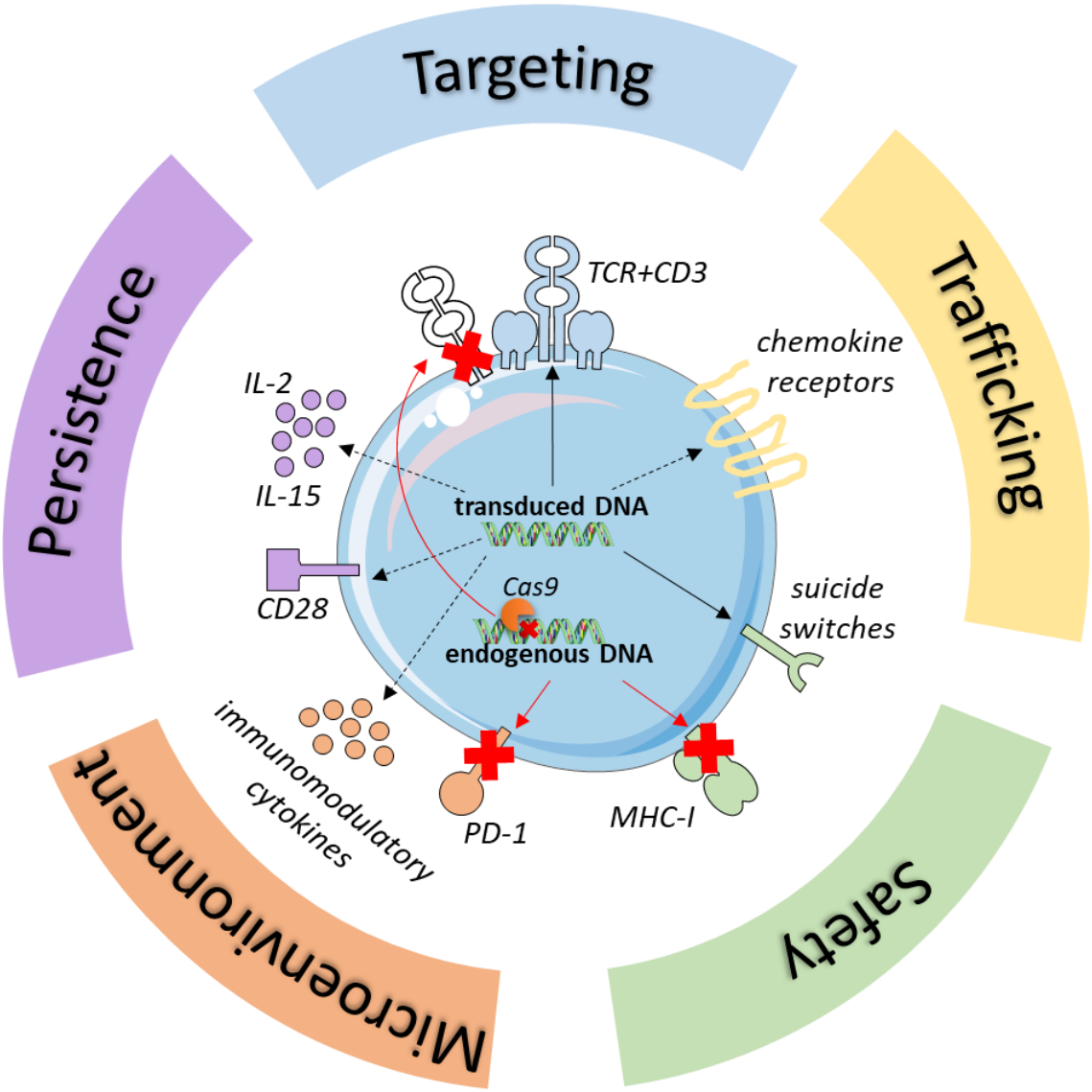

Figure 6.1 Hallmarks of an optimal cellular product for adoptive cell transfer. The optimal T-cell product can be generated by combination of gene knock-ins (delivered in lentiviral vectors) and knock-outs (transiently delivered in a form of Cas9 complexed with gRNAs). While CRISPR/Cas9 can be easily multiplexed to target multiple genes at the same time, the amount of exogenous DNA that can be delivered is limited by the vector packaging limit and cellular fitness considerations. Therefore, using an optimal T-cell subset, exhibiting the desired phenotype, cytokines and chemokine receptors, for starting material may be advantageous. An alternative approach would involve mutant Cas9 which activates gene expression. Finally, a safe off-the-shelf T-cell product should not express endogenous TCRs which can drive GvHD, or endogenous MHC-I molecules which can lead to donor cell rejection. An off-the-shelf T-cell product should target cancer, but not essential tissues, *via* a non-MHC restricted receptor.

Successful engraftment in patients, clonal expansion and persistence of an adoptively transferred T-cell product have been shown as prerequisites of successful CAR[458] or TIL therapy[53,251,253]. While engraftment of adoptively transferred T-cells can be achieved through non-myeloablative lymphodepletion and total body irradiation, together with infusion of exogenous IL-2 (Ref.[249]), efficient T-cell expansion and *in vivo* persistence require that the cellular product does not undergo premature senescence and exhaustion. Senescence and exhaustion can be avoided, or delayed, by modulating the functional avidity of T-cells, as discussed before, but also by selecting the appropriate cell subsets as recipients of TCR gene transfer, and knock-in/knock-out of additional genes. For instance, expression of CD28 and/or IL-15 in T-cells has been shown to prevent senescence by increasing telomerase activity[459,460] and promoting a stem cell memory like phenotype[461]. T-cells exhibiting stem cell memory like and central memory phenotypes have been shown as the most desirable subsets for adoptive transfer, in terms of proliferation and persistence[462,378,463]. Conversely, genetic knock-down or ablation of PD-1 expression on transgenic T-cells prevented the cells from undergoing tumour-induced anergy and exhaustion, as well as promoted their *in situ* anticancer reactivity[464,465].

The main adverse reactions associated with infusion of genetically engineered lymphocytes stem from on-target off-tumour reactivity (a ligand is expressed both on cancer and normal cells), off-target off-tumour reactivity (another ligand is cross-recognised by the receptor, possibly due to an unanticipated structure similarity) and systemic adverse effects, most notably cytokine release syndrome[466]. A plethora of genetic engineering strategies have been designed to control adverse effects of adoptively transferred lymphocytes, including Notch-based ON and OFF switch circuits, druggable suicide switches, and feedback loops that can dampen the T-cell activity at the onset of cytokine release syndrome. The strategies enhancing the safety profile of gene engineered T-cells have recently been reviewed by Lim and June[467].

In order to exert antitumour effects, genetically engineered T-cells must home efficiently to the tumour site, and infiltrate the tumour mass. For instance, chemokines CXCL9 and CXCL10 can drive chemotaxis of T-cells to cancer *via* CXCR3 (Ref. [468]). However, tumour cells often secrete chemokines CCL5, CCL22, and CCL28 which recruit T_{reg} and myeloid-derived suppressor cells which in turn create an immunosuppressive milieu at the tumour site[469–472]. While lymphodepletion and exogenous IL-2 infusion counteract the formation of immunosuppressive milieu[473], additional modifications of infused lymphocytes may promote their tumour homing and resistance to immunosuppression. For instance, engineering T-cells to express CXCR2 enhanced their homing to melanoma *via* CXCL1 and CXCL8 chemokines[474,475] while expression of CCR2 or CCR4 on T-cells re-directed them to mesothelioma[476] or Hodgkin lymphoma[477], respectively. However, it becomes apparent that different cancer types, as well as different

subsets of engineered T-cells, require a different combination of chemokines and chemokine receptors for optimal trafficking, and therefore development of a more general tumour trafficking strategy is needed.

Finally, generation of patient-autologous genetically engineered T-cells is costly, time consuming and requires highly specialised facilities operating under GMP conditions[448]. Moreover, peripheral blood-derived T-cells in cancer patients may be compromised as a result of the on-going disease and previous therapeutic interventions (such as chemotherapy), and thus not proliferate sufficiently to generate therapeutically relevant quantity and/or quality of engineered T-cell product[274]. Additionally, in case of infant cancer patients, it is often impossible to obtain sufficient numbers of donor T-cells for subsequent genetic engineering[372]. Therefore, an off-the-shelf allogeneic T-cell product is highly desirable. Re-targeting of T-cells to cancer *via* non-HLA restricted TCRs offers an alternative to CARs for off-the-shelf allogeneic product as these TCRs should not induce graft versus host disease due to the absence of allogeneic recipient HLA recognition. T-cells engineered to express those non-HLA restricted TCRs should not, however, express any endogenous αβ TCRs that could promote GvHD. Ablation of endogenous αβ TCR expression can be achieved by CRISPR/Cas9 mediated knock-out of the endogenous TCR-β, as demonstrated in **Chapter 3**. Simultaneous with endogenous αβ TCR knock-out, the donor T-cells can be engineered to remove MHC-I, thus removing the potential for allogeneic rejection by the recipient's immune system[372]. Such multiplexed-engineered T-cells could then be expanded, cryopreserved and administered as an off-the-shelf therapeutic to patients most likely to benefit from that kind of therapy.

Notably, a different approach for generation of allogeneic cell products is being commercially pursued by GammaDelta Therapeutics Ltd and Lymphact S.A. whereby a polyclonal population of non-Vδ2 γδ T-cells is derived from tissues or peripheral blood, respectively, and expanded. These cells are then envisaged to be used as an off-the-shelf therapeutic for a variety of malignancies, and the target cancer recognition by such infused T-cells is supposed to occur *via* invariant NK-type receptors[278,391] rather than well-defined TCRs with structurally known ligands. While the infusion of a polyclonal T-cell product reduces the chances of cancer immunoevasion, usage of γδ T-cells in an allogeneic setting has never been extensively tested in patients. MHC-alloreactive γδ T-cells, however, have been identified in mice[21], and therefore it is not inconceivable that MHC-restricted T-cells exist at low frequency within the human γδ T-cell pool. Moreover, infusion of allogeneic NK cells (which are non-MHC restricted) was shown to result in severe GvHD, possibly by augmenting T-cell alloreactivity[478]. I am therefore looking forward to the results of prospective clinical trials using TCR-undefined γδ T-cell populations in an allogeneic settings, as I expect the outcomes may re-define the therapeutic use of γδ T-cells and γδ TCRs.

6.3 Concluding remarks

Cancer immunotherapy has revolutionised current cancer treatments, and its successes are expected to expand to multiple cancer types. In this Thesis, I focused on investigating the immunotherapeutic potential of non-HLA restricted, broadly cancer-specific T-cells and their T-cell receptors, as well as developed genome editing tools for engineering of both T-cells and their target tumours, thus hopefully paving way for discovery of novel therapeutically-relevant receptors and their cognate targets. I believe that the future of cancer immunotherapy lies in allogeneic, off-the-shelf cellular products that can target multiple cancers in an efficacious but safe manner, by leveraging a combination of TCR gene transfer and knock-out of undesirable molecules (e.g. endogenous TCR, HLA, PD-1), *via* CRISPR/Cas9 or alternative systems. The first-in-patient use of genome engineered T-cells[372], as well as a slowly resolving dispute over the CRISPR/Cas9 patents[479], give hope that genome edited T-cell products will soon enter the mainstream clinic, thus allowing us to beat cancer sooner.

7. References

1. Hirano M, Guo P, McCurley N, et al. Evolutionary implications of a third lymphocyte lineage in lampreys. *Nature*. 2013;501(7467):435–438.
2. Hara T, Mizuno Y, Takaki K, et al. Predominant activation and expansion of V gamma 9-bearing gamma delta T cells in vivo as well as in vitro in Salmonella infection. *J. Clin. Invest.* 1992;90(1):204–210.
3. Toulon A, Breton L, Taylor KR, et al. A role for human skin–resident T cells in wound healing. *J. Exp. Med.* 2009;206(4):743–750.
4. Lafaille JJ, DeCloux A, Bonneville M, Takagaki Y, Tonegawa S. Junctional sequences of T cell receptor gamma delta genes: implications for gamma delta T cell lineages and for a novel intermediate of V-(D)-J joining. *Cell*. 1989;59(5):859–870.
5. Desiderio SV, Yancopoulos GD, Paskind M, et al. Insertion of N regions into heavy-chain genes is correlated with expression of terminal deoxytransferase in B cells. *Nature*. 1984;311(5988):752–755.
6. Lefranc M-P. Nomenclature of the Human T Cell Receptor Genes. *Curr. Protoc. Immunol.* 2001;
7. Pellicci DG, Uldrich AP, Le Nours J, et al. The molecular bases of δ/αβ T cell-mediated antigen recognition. *J. Exp. Med.* 2014;211(13):2599–2615.
8. Allam A, Kabelitz D. TCR trans-Rearrangements: Biological Significance in Antigen Recognition vs the Role as Lymphoma Biomarker. *J. Immunol.* 2006;176(10):5707–5712.
9. Chien Y, Meyer C, Bonneville M. γδ T cells: first line of defense and beyond. *Annu. Rev. Immunol.* 2014;32:121–155.
10. Davis MM. The evolutionary and structural “logic” of antigen receptor diversity. *Semin. Immunol.* 2004;16(4):239–243.
11. Rock EP, Sibbald PR, Davis MM, Chien YH. CDR3 length in antigen-specific immune receptors. *J. Exp. Med.* 1994;179(1):323–328.
12. Cole DK, Pumphrey NJ, Boulter JM, et al. Human TCR-binding affinity is governed by MHC class restriction. *J. Immunol. Baltim. Md 1950*. 2007;178(9):5727–5734.
13. Tuovinen H, Pöntynen N, Gylling M, et al. gammadelta T cells develop independently of Aire. *Cell. Immunol.* 2009;257(1–2):5–12.
14. Barbee SD, Woodward MJ, Turchinovich G, et al. Skint-1 is a highly specific, unique selecting component for epidermal T cells. *Proc. Natl. Acad. Sci.* 2011;108(8):3330–3335.
15. Di Marco Barros R, Roberts NA, Dart RJ, et al. Epithelia Use Butyrophilin-like Molecules to Shape Organ-Specific γδ T Cell Compartments. *Cell*. 2016;167(1):203–218.e17.
16. Wilson A, de Villartay JP, MacDonald HR. T cell receptor delta gene rearrangement and T early alpha (TEA) expression in immature alpha beta lineage thymocytes: implications for alpha beta/gamma delta lineage commitment. *Immunity*. 1996;4(1):37–45.
17. Zarin P, Wong GW, Mohtashami M, Wiest DL, Zuniga-Pflucker JC. Enforcement of -lineage commitment by the pre-T-cell receptor in precursors with weak -TCR signals. *Proc. Natl. Acad. Sci.* 2014;111(15):5658–5663.
18. Coffey F, Lee S-Y, Buus TB, et al. The TCR ligand-inducible expression of CD73 marks lineage commitment and a metastable intermediate in effector specification. *J. Exp. Med.* 2014;211(2):329–343.
19. Sherwood AM, Desmarais C, Livingston RJ, et al. Deep Sequencing of the Human TCR and TCR Repertoires Suggests that TCR Rearranges After and T Cell Commitment. *Sci. Transl. Med.* 2011;3(90):90ra61-90ra61.
20. Attaf M, Legut M, Cole DK, Sewell AK. The T cell antigen receptor: The Swiss Army knife of the immune system. *Clin. Exp. Immunol.* 2015;
21. Matis LA, Fry AM, Cron RQ, et al. Structure and specificity of a class II MHC alloreactive gamma delta T cell receptor heterodimer. *Science*. 1989;245(4919):746–749.

22. Rodgers JR, Cook RG. MHC class Ib molecules bridge innate and acquired immunity. *Nat. Rev. Immunol.* 2005;5(6):459–471.
23. Gadola SD, Koch M, Marles-Wright J, et al. Structure and binding kinetics of three different human CD1d–α-galactosylceramide–specific T cell receptors. *J. Exp. Med.* 2006;203(3):699–710.
24. Luoma AM, Castro CD, Mayassi T, et al. Crystal Structure of Vδ1 T Cell Receptor in Complex with CD1d-Sulfatide Shows MHC-like Recognition of a Self-Lipid by Human γδ T Cells. *Immunity*. 2013;39(6):1032–1042.
25. Corbett AJ, Eckle SBG, Birkinshaw RW, et al. T-cell activation by transitory neo-antigens derived from distinct microbial pathways. *Nature*. 2014;509(7500):361–365.
26. Adams EJ, Chien Y-H, Garcia KC. Structure of a gammadelta T cell receptor in complex with the nonclassical MHC T22. *Science*. 2005;308(5719):227–231.
27. Wingren C, Crowley MP, Degano M, Chien Y, Wilson IA. Crystal structure of a gammadelta T cell receptor ligand T22: a truncated MHC-like fold. *Science*. 2000;287(5451):310–314.
28. Adams EJ, Strop P, Shin S, Chien Y-H, Garcia KC. An autonomous CDR3delta is sufficient for recognition of the nonclassical MHC class I molecules T10 and T22 by gammadelta T cells. *Nat. Immunol.* 2008;9(7):777–784.
29. Sandstrom A, Scharf L, McRae G, et al. γδ T cell receptors recognize the non-classical major histocompatibility complex (MHC) molecule T22 via conserved anchor residues in a MHC peptide-like fashion. *J. Biol. Chem.* 2012;287(8):6035–6043.
30. Chien Y, Konigshofer Y. Antigen recognition by γδ T cells. *Immunol. Rev.* 2007;215(1):46–58.
31. Tikhonova AN, Van Laethem F, Hanada K, et al. αβ T cell receptors that do not undergo major histocompatibility complex-specific thymic selection possess antibody-like recognition specificities. *Immunity*. 2012;36(1):79–91.
32. Hanada K -i., Wang QJ, Inozume T, Yang JC. Molecular identification of an MHC-independent ligand recognized by a human / T-cell receptor. *Blood*. 2011;117(18):4816–4825.
33. Barnd DL, Lan MS, Metzgar RS, Finn OJ. Specific, major histocompatibility complex-unrestricted recognition of tumor-associated mucins by human cytotoxic T cells. *Proc. Natl. Acad. Sci. U. S. A.* 1989;86(18):7159–7163.
34. Rao A, Ko WW-P, Faas SJ, Cantor H. Binding of antigen in the absence of histocompatibility proteins by arsonate-reactive T-cell clones. *Cell*. 1984;36(4):879–888.
35. Zeng X, Wei Y-L, Huang J, et al. γδ T Cells Recognize a Microbial Encoded B Cell Antigen to Initiate a Rapid Antigen-Specific Interleukin-17 Response. *Immunity*. 2012;37(3):524–534.
36. Zeng X, Meyer C, Huang J, et al. Gamma delta T cells recognize haptens and mount a hapten-specific response. *eLife*. 2014;3:e03609.
37. Zhang L, Jin N, Nakayama M, et al. Gamma delta T cell receptors confer autonomous responsiveness to the insulin-peptide B:9-23. *J. Autoimmun.* 2010;34(4):478–484.
38. Bruder J, Siewert K, Obermeier B, et al. Target specificity of an autoreactive pathogenic human γδ-T cell receptor in myositis. *J. Biol. Chem.* 2012;287(25):20986–20995.
39. Dai Y, Chen H, Mo C, Cui L, He W. Ectopically Expressed Human Tumor Biomarker MutS Homologue 2 Is a Novel Endogenous Ligand That Is Recognized by Human T Cells to Induce Innate Anti-tumor/Virus Immunity. *J. Biol. Chem.* 2012;287(20):16812–16819.
40. Vavassori S, Kumar A, Wan GS, et al. Butyrophilin 3A1 binds phosphorylated antigens and stimulates human γδ T cells. *Nat. Immunol.* 2013;14(9):908–916.
41. Sandstrom A, Peigné C-M, Léger A, et al. The Intracellular B30.2 Domain of Butyrophilin 3A1 Binds Phosphoantigens to Mediate Activation of Human Vγ9Vδ2 T Cells. *Immunity*. 2014;40(4):490–500.
42. Scotet E, Martinez LO, Grant E, et al. Tumor Recognition following Vγ9Vδ2 T Cell Receptor Interactions with a Surface F1-ATPase-Related Structure and Apolipoprotein A-I. *Immunity*. 2005;22(1):71–80.
43. Nikolich-Žugich J, Slifka MK, Messaoudi I. The many important facets of T-cell repertoire diversity. *Nat. Rev. Immunol.* 2004;4(2):123–132.

44. Ebert A, Medvedovic J, Tagoh H, Schwickert TA, Busslinger M. Control of antigen receptor diversity through spatial regulation of V(D)J recombination. *Cold Spring Harb. Symp. Quant. Biol.* 2013;78:11–21.
45. Messaoudi I, Guevara Patiño JA, Dyall R, LeMaoult J, Nikolich-Zugich J. Direct link between mhc polymorphism, T cell avidity, and diversity in immune defense. *Science*. 2002;298(5599):1797–1800.
46. Reeves E, Edwards CJ, Elliott T, James E. Naturally occurring ERAP1 haplotypes encode functionally distinct alleles with fine substrate specificity. *J. Immunol. Baltim. Md 1950*. 2013;191(1):35–43.
47. Vanhanen R, Heikkilä N, Aggarwal K, et al. T cell receptor diversity in the human thymus. *Mol. Immunol.* 2016;76:116–122.
48. Qi Q, Liu Y, Cheng Y, et al. Diversity and clonal selection in the human T-cell repertoire. *Proc. Natl. Acad. Sci. U. S. A.* 2014;111(36):13139–13144.
49. Li HM, Hiroi T, Zhang Y, et al. TCRβ repertoire of CD4+ and CD8+ T cells is distinct in richness, distribution, and CDR3 amino acid composition. *J. Leukoc. Biol.* 2016;99(3):505–513.
50. Stadinski BD, Shekhar K, Gómez-Touriño I, et al. Hydrophobic CDR3 residues promote the development of self-reactive T cells. *Nat. Immunol.* 2016;17(8):946–955.
51. Attaf M, Huseby E, Sewell AK. αβ T cell receptors as predictors of health and disease. *Cell. Mol. Immunol.* 2015;12(4):391–399.
52. Ruggiero E, Nicolay JP, Fronza R, et al. High-resolution analysis of the human T-cell receptor repertoire. *Nat. Commun.* 2015;6:8081.
53. Donia M, Kjeldsen JW, Andersen R, et al. PD-1 $^{+}$ polyfunctional T cells dominate the periphery after tumor-infiltrating lymphocyte therapy for cancer. *Clin. Cancer Res.* 2017;clincanres.1692.2016.
54. Tamura K, Hazama S, Yamaguchi R, et al. Characterization of the T cell repertoire by deep T cell receptor sequencing in tissues and blood from patients with advanced colorectal cancer. *Oncol. Lett.* 2016;11(6):3643–3649.
55. Sims JS, Grinshpun B, Feng Y, et al. Diversity and divergence of the glioma-infiltrating T-cell receptor repertoire. *Proc. Natl. Acad. Sci. U. S. A.* 2016;113(25):E3529-3537.
56. Gros A, Parkhurst MR, Tran E, et al. Prospective identification of neoantigen-specific lymphocytes in the peripheral blood of melanoma patients. *Nat. Med.* 2016;22(4):433–438.
57. Hanson WM, Chen Z, Jackson LK, et al. Reversible Oligonucleotide Chain Blocking Enables Bead Capture and Amplification of T-Cell Receptor α and β Chain mRNAs. *J. Am. Chem. Soc.* 2016;
58. Dimova T, Brouwer M, Gosselin F, et al. Effector Vγ9Vδ2 T cells dominate the human fetal γδ T-cell repertoire. *Proc. Natl. Acad. Sci.* 2015;112(6):E556–E565.
59. McVay LD, Carding SR, Bottomly K, Hayday AC. Regulated expression and structure of T cell receptor gamma/delta transcripts in human thymic ontogeny. *EMBO J.* 1991;10(1):83–91.
60. Vermijlen D, Brouwer M, Donner C, et al. Human cytomegalovirus elicits fetal γδ T cell responses in utero. *J. Exp. Med.* 2010;207(4):807–821.
61. Xu L, Weng J, Huang X, et al. Persistent donor derived Vδ4 T cell clones may improve survival for recurrent T cell acute lymphoblastic leukemia after HSCT and DLI. *Oncotarget*. 2016;7(28):42943–42952.
62. Takihara Y, Reimann J, Michalopoulos E, et al. Diversity and structure of human T cell receptor delta chain genes in peripheral blood gamma/delta-bearing T lymphocytes. *J. Exp. Med.* 1989;169(2):393–405.
63. Giachino C, Granziero L, Modena V, et al. Clonal expansions of V delta 1+ and V delta 2+ cells increase with age and limit the repertoire of human gamma delta T cells. *Eur. J. Immunol.* 1994;24(8):1914–1918.
64. Tan CTY, Wistuba-Hamprecht K, Xu W, et al. Vδ2+ and α/ß T cells show divergent trajectories during human aging. *Oncotarget*. 2016;

65. Roux A, Mourin G, Larsen M, et al. Differential Impact of Age and Cytomegalovirus Infection on the T Cell Compartment. *J. Immunol.* 2013;191(3):1300–1306.
66. Chaudhry S, Cairo C, Venturi V, Pauza CD. The γδ T-cell receptor repertoire is reconstituted in HIV patients after prolonged antiretroviral therapy. *AIDS Lond. Engl.* 2013;27(10):1557–1562.
67. Davey MS, Willcox CR, Joyce SP, et al. Clonal selection in the human Vδ1 T cell repertoire indicates γδ TCR-dependent adaptive immune surveillance. *Nat. Commun.* 2017;8:14760.
68. Ravens S, Schultze-Florey C, Raha S, et al. Human γδ T cells are quickly reconstituted after stem-cell transplantation and show adaptive clonal expansion in response to viral infection. *Nat. Immunol.* 2017;18(4):393–401.
69. Zheng J, Liu Y, Lau Y-L, Tu W. γδ-T cells: an unpolished sword in human anti-infection immunity. *Cell. Mol. Immunol.* 2013;10(1):50–57.
70. Su D, Shen M, Li X, Sun L. Roles of T Cells in the Pathogenesis of Autoimmune Diseases. *Clin. Dev. Immunol.* 2013;2013:1–6.
71. Girardi M, Oppenheim DE, Steele CR, et al. Regulation of cutaneous malignancy by gammadelta T cells. *Science*. 2001;294(5542):605–609.
72. Pfeffer K, Schoel B, Gulle H, Kaufmann SHE, Wagner H. Primary responses of human T cells to mycobacteria: a frequent set of γ/δ T cells are stimulated by protease-resistant ligands. *Eur. J. Immunol.* 1990;20(5):1175–1179.
73. Davodeau F, Peyrat MA, Hallet MM, et al. Close correlation between Daudi and mycobacterial antigen recognition by human gamma delta T cells and expression of V9JPC1 gamma/V2DJC delta-encoded T cell receptors. *J. Immunol. Baltim. Md 1950*. 1993;151(3):1214–1223.
74. Tanaka Y, Morita CT, Tanaka Y, et al. Natural and synthetic non-peptide antigens recognized by human γδ T cells. *Nature*. 1995;375(6527):155–158.
75. Puan K-J, Jin C, Wang H, et al. Preferential recognition of a microbial metabolite by human V 2V 2 T cells. *Int. Immunol.* 2007;19(5):657–673.
76. Guenot M, Loizon S, Howard J, et al. Phosphoantigen Burst upon Plasmodium falciparum Schizont Rupture Can Distantly Activate Vγ9Vδ2 T Cells. *Infect. Immun.* 2015;83(10):3816–3824.
77. Gober H-J, Kistowska M, Angman L, et al. Human T cell receptor gammadelta cells recognize endogenous mevalonate metabolites in tumor cells. *J. Exp. Med.* 2003;197(2):163–168.
78. Idrees ASM, Sugie T, Inoue C, et al. Comparison of γδ T cell responses and farnesyl diphosphate synthase inhibition in tumor cells pretreated with zoledronic acid. *Cancer Sci.* 2013;104(5):536–542.
79. Thompson K. Alkylamines cause V 9V 2 T-cell activation and proliferation by inhibiting the mevalonate pathway. *Blood*. 2006;107(2):651–654.
80. Espinosa E, Belmant C, Pont F, et al. Chemical synthesis and biological activity of bromohydrin pyrophosphate, a potent stimulator of human gamma delta T cells. *J. Biol. Chem.* 2001;276(21):18337–18344.
81. Belmant C, Espinosa E, Halary F, et al. A chemical basis for selective recognition of nonpeptide antigens by human delta T cells. *FASEB J. Off. Publ. Fed. Am. Soc. Exp. Biol.* 2000;14(12):1669–1670.
82. Thompson K, Rogers MJ. Statins prevent bisphosphonate-induced gamma,delta-T-cell proliferation and activation in vitro. *J. Bone Miner. Res. Off. J. Am. Soc. Bone Miner. Res.* 2004;19(2):278–288.
83. Allison TJ, Winter CC, Fournié JJ, Bonneville M, Garboczi DN. Structure of a human gammadelta T-cell antigen receptor. *Nature*. 2001;411(6839):820–824.
84. Green AE, Lissina A, Hutchinson SL, et al. Recognition of nonpeptide antigens by human V gamma 9V delta 2 T cells requires contact with cells of human origin. *Clin. Exp. Immunol.* 2004;136(3):472–482.

85. Mookerjee-Basu J, Vantourout P, Martinez LO, et al. F1-Adenosine Triphosphatase Displays Properties Characteristic of an Antigen Presentation Molecule for V 9V 2 T Cells. *J. Immunol.* 2010;184(12):6920–6928.
86. Compte E, Pontarotti P, Collette Y, Lopez M, Olive D. Frontline: Characterization of BT3 molecules belonging to the B7 family expressed on immune cells. *Eur. J. Immunol.* 2004;34(8):2089–2099.
87. Karunakaran MM, Göbel TW, Starick L, Walter L, Herrmann T. Vγ9 and Vδ2 T cell antigen receptor genes and butyrophilin 3 (BTN3) emerged with placental mammals and are concomitantly preserved in selected species like alpaca (Vicugna pacos). *Immunogenetics*. 2014;66(4):243–254.
88. Wang H, Henry O, Distefano MD, et al. Butyrophilin 3A1 Plays an Essential Role in Prenyl Pyrophosphate Stimulation of Human V 2V 2 T Cells. *J. Immunol.* 2013;191(3):1029–1042.
89. Harly C, Guillaume Y, Nedellec S, et al. Key implication of CD277/butyrophilin-3 (BTN3A) in cellular stress sensing by a major human T-cell subset. *Blood*. 2012;120(11):2269–2279.
90. Decaup E, Duault C, Bezombes C, et al. Phosphoantigens and butyrophilin 3A1 induce similar intracellular activation signaling in human TCRVγ9+ γδ T lymphocytes. *Immunol. Lett.* 2014;161(1):133–137.
91. Palakodeti A, Sandstrom A, Sundaresan L, et al. The Molecular Basis for Modulation of Human V 9V 2 T Cell Responses by CD277/Butyrophilin-3 (BTN3A)-specific Antibodies. *J. Biol. Chem.* 2012;287(39):32780–32790.
92. Sebestyen Z, Scheper W, Vyborova A, et al. RhoB Mediates Phosphoantigen Recognition by Vγ9Vδ2 T Cell Receptor. *Cell Rep.* 2016;15(9):1973–1985.
93. De Libero G, Lau S-Y, Mori L. Phosphoantigen Presentation to TCR Î³Î´ Cells, a Conundrum Getting Less Gray Zones. *Front. Immunol.* 2015;5:.
94. Gu S, Nawrocka W, Adams EJ. Sensing of Pyrophosphate Metabolites by Vγ9Vδ2 T Cells. *Front. Immunol.* 2014;5:688.
95. Salim M, Knowles TJ, Baker AT, et al. BTN3A1 discriminates γδ T cell phosphoantigens from non-antigenic small molecules via a conformational sensor in its B30.2 domain. *ACS Chem. Biol.* 2017;
96. Riaño F, Karunakaran MM, Starick L, et al. Vγ9Vδ2 TCR-activation by phosphorylated antigens requires butyrophilin 3 A1 (*BTN3A1*) and additional genes on human chromosome 6: Antigen processing. *Eur. J. Immunol.* 2014;44(9):2571–2576.
97. Liddy N, Bossi G, Adams KJ, et al. Monoclonal TCR-redirected tumor cell killing. *Nat. Med.* 2012;18(6):980–987.
98. Rhodes DA, Chen H-C, Price AJ, et al. Activation of Human T Cells by Cytosolic Interactions of BTN3A1 with Soluble Phosphoantigens and the Cytoskeletal Adaptor Periplakin. *J. Immunol.* 2015;194(5):2390–2398.
99. de la Salle H. Assistance of Microbial Glycolipid Antigen Processing by CD1e. *Science*. 2005;310(5752):1321–1324.
100. Russano AM, Bassotti G, Agea E, et al. CD1-restricted recognition of exogenous and self-lipid antigens by duodenal gammadelta+ T lymphocytes. *J. Immunol. Baltim. Md 1950*. 2007;178(6):3620–3626.
101. Roy S, Ly D, Li N-S, et al. Molecular basis of mycobacterial lipid antigen presentation by CD1c and its recognition by T cells. *Proc. Natl. Acad. Sci.* 2014;111(43):E4648–E4657.
102. Lepore M, de Lalla C, Gundimeda SR, et al. A novel self-lipid antigen targets human T cells against CD1c $^{+}$ leukemias. *J. Exp. Med.* 2014;211(7):1363–1377.
103. de Lalla C, Lepore M, Piccolo FM, et al. High-frequency and adaptive-like dynamics of human CD1 self-reactive T cells. *Eur. J. Immunol.* 2011;41(3):602–610.
104. Faure F, Jitsukawa S, Miossec C, Hercend T. CD1c as a target recognition structure for human T lymphocytes: analysis with peripheral blood gamma/delta cells. *Eur. J. Immunol.* 1990;20(3):703–706.
105. Spada FM, Grant EP, Peters PJ, et al. Self-recognition of CD1 by gamma/delta T cells: implications for innate immunity. *J. Exp. Med.* 2000;191(6):937–948.

106. Roy S, Ly D, Castro CD, et al. Molecular Analysis of Lipid-Reactive V 1 T Cells Identified by CD1c Tetramers. *J. Immunol.* 2016;196(4):1933–1942.
107. Kain L, Webb B, Anderson BL, et al. The Identification of the Endogenous Ligands of Natural Killer T Cells Reveals the Presence of Mammalian α-Linked Glycosylceramides. *Immunity*. 2014;41(4):543–554.
108. Gentilini MV, Pérez ME, Fernández PM, Fainboim L, Arana E. The tumor antigen N-glycolyl-GM3 is a human CD1d ligand capable of mediating B cell and natural killer T cell interaction. *Cancer Immunol. Immunother.* 2016;65(5):551–562.
109. Bojarska-Junak A, Hus I, Chocholska S, et al. CD1d expression is higher in chronic lymphocytic leukemia patients with unfavorable prognosis. *Leuk. Res.* 2014;38(4):435–442.
110. Uldrich AP, Le Nours J, Pellicci DG, et al. CD1d-lipid antigen recognition by the γδ TCR. *Nat. Immunol.* 2013;14(11):1137–1145.
111. Bai L, Picard D, Anderson B, et al. The majority of CD1d-sulfatide-specific T cells in human blood use a semiinvariant Vδ1 TCR: Clinical immunology. *Eur. J. Immunol.* 2012;42(9):2505–2510.
112. Cantu C, Benlagha K, Savage PB, Bendelac A, Teyton L. The Paradox of Immune Molecular Recognition of -Galactosylceramide: Low Affinity, Low Specificity for CD1d, High Affinity for TCRs. *J. Immunol.* 2003;170(9):4673–4682.
113. Borg NA, Wun KS, Kjer-Nielsen L, et al. CD1d–lipid-antigen recognition by the semi-invariant NKT T-cell receptor. *Nature*. 2007;448(7149):44–49.
114. Déchanet J, Merville P, Bergé F, et al. Major expansion of gammadelta T lymphocytes following cytomegalovirus infection in kidney allograft recipients. *J. Infect. Dis.* 1999;179(1):1–8.
115. Déchanet J, Merville P, Lim A, et al. Implication of gammadelta T cells in the human immune response to cytomegalovirus. *J. Clin. Invest.* 1999;103(10):1437–1449.
116. Lafarge X, Merville P, Cazin MC, et al. Cytomegalovirus infection in transplant recipients resolves when circulating gammadelta T lymphocytes expand, suggesting a protective antiviral role. *J. Infect. Dis.* 2001;184(5):533–541.
117. Pitard V, Roumanes D, Lafarge X, et al. Long-term expansion of effector/memory Vdelta2-gammadelta T cells is a specific blood signature of CMV infection. *Blood*. 2008;112(4):1317–1324.
118. Alejenef A, Pachnio A, Halawi M, et al. Cytomegalovirus drives Vδ2 ^{neg} γδ T cell inflation in many healthy virus carriers with increasing age: CMV distorts γδ T cells over time. *Clin. Exp. Immunol.* 2014;176(3):418–428.
119. Couzi L, Levaillant Y, Jamai A, et al. Cytomegalovirus-Induced T Cells Associate with Reduced Cancer Risk after Kidney Transplantation. *J. Am. Soc. Nephrol.* 2010;21(1):181–188.
120. Halary F. Shared reactivity of V 2neg T cells against cytomegalovirus-infected cells and tumor intestinal epithelial cells. *J. Exp. Med.* 2005;201(10):1567–1578.
121. Devaud C, Bilhere E, Loizon S, et al. Antitumor activity of gammadelta T cells reactive against cytomegalovirus-infected cells in a mouse xenograft tumor model. *Cancer Res.* 2009;69(9):3971–3978.
122. Elmaagacli AH, Steckel NK, Koldehoff M, et al. Early human cytomegalovirus replication after transplantation is associated with a decreased relapse risk: evidence for a putative virus-versus-leukemia effect in acute myeloid leukemia patients. *Blood*. 2011;118(5):1402–1412.
123. Scheper W, van Dorp S, Kersting S, et al. γδT cells elicited by CMV reactivation after allo-SCT cross-recognize CMV and leukemia. *Leukemia*. 2013;27(6):1328–1338.
124. Willcox CR, Pitard V, Netzer S, et al. Cytomegalovirus and tumor stress surveillance by binding of a human γδ T cell antigen receptor to endothelial protein C receptor. *Nat. Immunol.* 2012;13(9):872–879.
125. Oganesyan V, Oganesyan N, Terzyan S, et al. The crystal structure of the endothelial protein C receptor and a bound phospholipid. *J. Biol. Chem.* 2002;277(28):24851–24854.

126. Antón I, Molina E, Luis-Ravelo D, et al. Receptor of activated protein C promotes metastasis and correlates with clinical outcome in lung adenocarcinoma. *Am. J. Respir. Crit. Care Med.* 2012;186(1):96–105.
127. Schaffner F, Yokota N, Carneiro-Lobo T, et al. Endothelial protein C receptor function in murine and human breast cancer development. *PloS One*. 2013;8(4):e61071.
128. Althawadi H, Alfarsi H, Besbes S, et al. Activated protein C upregulates ovarian cancer cell migration and promotes unclottability of the cancer cell microenvironment. *Oncol. Rep.* 2015;34(2):603–609.
129. Wang Q, Liu Q, Wang T, et al. Endothelial cell protein C receptor promotes MGC803 gastric cancer cells proliferation and migration by activating ERK1/2. *Med. Oncol. Northwood Lond. Engl.* 2015;32(5):162.
130. Lal N, Willcox CR, Beggs A, et al. Endothelial protein C receptor is overexpressed in colorectal cancer as a result of amplification and hypomethylation of chromosome 20q: EPCR overexpression in cancer by amplification and Chr20q hypomethylation. *J. Pathol. Clin. Res.* 2017;3(3):155–170.
131. Ducros E, Mirshahi S, Azzazene D, et al. Endothelial protein C receptor expressed by ovarian cancer cells as a possible biomarker of cancer onset. *Int. J. Oncol.* 2012;41(2):433–440.
132. Lafarge X, Pitard V, Ravet S, et al. Expression of MHC class I receptors confers functional intraclonal heterogeneity to a reactive expansion of γδ T cells. *Eur. J. Immunol.* 2005;35(6):1896–1905.
133. Bauer S, Groh V, Wu J, et al. Activation of NK cells and T cells by NKG2D, a receptor for stress-inducible MICA. *Science*. 1999;285(5428):727–729.
134. Stephens HA. MICA and MICB genes: can the enigma of their polymorphism be resolved? *Trends Immunol.* 2001;22(7):378–385.
135. Li P, Morris DL, Willcox BE, et al. Complex structure of the activating immunoreceptor NKG2D and its MHC class I-like ligand MICA. *Nat. Immunol.* 2001;2(5):443–451.
136. Li P, McDermott G, Strong RK. Crystal Structures of RAE-1β and Its Complex with the Activating Immunoreceptor NKG2D. *Immunity*. 2002;16(1):77–86.
137. Groh V, Rhinehart R, Randolph-Habecker J, et al. Costimulation of CD8alphabeta T cells by NKG2D via engagement by MIC induced on virus-infected cells. *Nat. Immunol.* 2001;2(3):255–260.
138. Xu B, Pizarro JC, Holmes MA, et al. Crystal structure of a T-cell receptor specific for the human MHC class I homolog MICA. *Proc. Natl. Acad. Sci.* 2011;108(6):2414–2419.
139. Groh V, Rhinehart R, Secrist H, et al. Broad tumor-associated expression and recognition by tumor-derived gamma delta T cells of MICA and MICB. *Proc. Natl. Acad. Sci. U. S. A.* 1999;96(12):6879–6884.
140. Mo C, Dai Y, Kang N, Cui L, He W. Ectopic Expression of Human MutS Homologue 2 on Renal Carcinoma Cells Is Induced by Oxidative Stress with Interleukin-18 Promotion via p38 Mitogen-activated Protein Kinase (MAPK) and c-Jun N-terminal Kinase (JNK) Signaling Pathways. *J. Biol. Chem.* 2012;287(23):19242–19254.
141. Lu J, Das M, Kanji S, et al. Induction of ATM/ATR pathway combined with Vγ2Vδ2 T cells enhances cytotoxicity of ovarian cancer cells. *Biochim. Biophys. Acta*. 2014;1842(7):1071–1079.
142. Fu D, Geschwind J-F, Karthikeyan S, et al. Metabolic perturbation sensitizes human breast cancer to NK cell-mediated cytotoxicity by increasing the expression of MHC class I chain-related A/B. *Oncoimmunology*. 2015;4(3):e991228.
143. Lamb LS, Bowersock J, Dasgupta A, et al. Engineered drug resistant γδ T cells kill glioblastoma cell lines during a chemotherapy challenge: a strategy for combining chemo- and immunotherapy. *PloS One*. 2013;8(1):e51805.
144. Groh V, Wu J, Yee C, Spies T. Tumour-derived soluble MIC ligands impair expression of NKG2D and T-cell activation. *Nature*. 2002;419(6908):734–738.

145. Fielding CA, Aicheler R, Stanton RJ, et al. Two Novel Human Cytomegalovirus NK Cell Evasion Functions Target MICA for Lysosomal Degradation. *PLoS Pathog.* 2014;10(5):e1004058.
146. Qi J, Zhang J, Zhang S, Cui L, He W. Immobilized MICA could expand human Vdelta1 gammadelta T cells in vitro that displayed major histocompatibility complex class I chain-related A-dependent cytotoxicity to human epithelial carcinomas. *Scand. J. Immunol.* 2003;58(2):211–220.
147. Zhao J, Huang J, Chen H, Cui L, He W. Vdelta1 T cell receptor binds specifically to MHC I chain related A: molecular and biochemical evidences. *Biochem. Biophys. Res. Commun.* 2006;339(1):232–240.
148. Wu J, Groh V, Spies T. T cell antigen receptor engagement and specificity in the recognition of stress-inducible MHC class I-related chains by human epithelial gamma delta T cells. *J. Immunol. Baltim. Md 1950*. 2002;169(3):1236–1240.
149. Yin S, Zhang J, Mao Y, et al. Vav1-phospholipase C-γ1 (Vav1-PLC-γ1) pathway initiated by T cell antigen receptor (TCRγδ) activation is required to overcome inhibition by ubiquitin ligase Cbl-b during γδT cell cytotoxicity. *J. Biol. Chem.* 2013;288(37):26448–26462.
150. Wei Y, Zhao X, Kariya Y, et al. Induction of autologous tumor killing by heat treatment of fresh human tumor cells: involvement of gamma delta T cells and heat shock protein 70. *Cancer Res.* 1996;56(5):1104–1110.
151. O'Brien RL, Fu YX, Cranfill R, et al. Heat shock protein Hsp60-reactive gamma delta cells: a large, diversified T-lymphocyte subset with highly focused specificity. *Proc. Natl. Acad. Sci. U. S. A.* 1992;89(10):4348–4352.
152. Nadin SB, Cuello-Carrión FD, Sottile ML, Ciocca DR, Vargas-Roig LM. Effects of hyperthermia on Hsp27 (HSPB1), Hsp72 (HSPA1A) and DNA repair proteins hMLH1 and hMSH2 in human colorectal cancer hMLH1-deficient and hMLH1-proficient cell lines. *Int. J. Hyperthermia*. 2012;28(3):191–201.
153. Chen H, He X, Wang Z, et al. Identification of Human T Cell Receptor γδ-recognized Epitopes/Proteins via CDR3δ Peptide-based Immunobiochemical Strategy. *J. Biol. Chem.* 2008;283(18):12528–12537.
154. Kong Y, Cao W, Xi X, et al. The NKG2D ligand ULBP4 binds to TCR 9/ 2 and induces cytotoxicity to tumor cells through both TCR and NKG2D. *Blood*. 2009;114(2):310–317.
155. Marlin R, Pappalardo A, Kaminski H, et al. Sensing of cell stress by human γδ TCR-dependent recognition of annexin A2. *Proc. Natl. Acad. Sci.* 2017;114(12):3163–3168.
156. Deora AB, Kreitzer G, Jacovina AT, Hajjar KA. An Annexin 2 Phosphorylation Switch Mediates p11-dependent Translocation of Annexin 2 to the Cell Surface. *J. Biol. Chem.* 2004;279(42):43411–43418.
157. Huang B, Deora AB, He K-L, et al. Hypoxia-inducible factor-1 drives annexin A2 system-mediated perivascular fibrin clearance in oxygen-induced retinopathy in mice. *Blood*. 2011;118(10):2918–2929.
158. Derry MC, Sutherland MR, Restall CM, Waisman DM, Pryzdial ELG. Annexin 2-mediated enhancement of cytomegalovirus infection opposes inhibition by annexin 1 or annexin 5. *J. Gen. Virol.* 2007;88(1):19–27.
159. Van Laethem F, Tikhonova AN, Singer A. MHC restriction is imposed on a diverse T cell receptor repertoire by CD4 and CD8 co-receptors during thymic selection. *Trends Immunol.* 2012;33(9):437–441.
160. Wooldridge L, van den Berg HA, Glick M, et al. Interaction between the CD8 coreceptor and major histocompatibility complex class I stabilizes T cell receptor-antigen complexes at the cell surface. *J. Biol. Chem.* 2005;280(30):27491–27501.
161. Purbhoo MA, Boulter JM, Price DA, et al. The human CD8 coreceptor effects cytotoxic T cell activation and antigen sensitivity primarily by mediating complete phosphorylation of the T cell receptor zeta chain. *J. Biol. Chem.* 2001;276(35):32786–32792.
162. Holler PD, Kranz DM. Quantitative Analysis of the Contribution of TCR/pepMHC Affinity and CD8 to T Cell Activation. *Immunity*. 2003;18(2):255–264.

163. Zhu J, Peng T, Johnston C, et al. Immune surveillance by CD8αα+ skin-resident T cells in human herpes virus infection. *Nature*. 2013;497(7450):494–497.
164. Van Kaer L, Algood HMS, Singh K, et al. CD8αα$^+$ innate-type lymphocytes in the intestinal epithelium mediate mucosal immunity. *Immunity*. 2014;41(3):451–464.
165. Olivares-Villagómez D, Van Kaer L. TL and CD8αα: Enigmatic partners in mucosal immunity. *Immunol. Lett.* 2010;134(1):1–6.
166. Wrobel P, Shojaei H, Schittek B, et al. Lysis of a Broad Range of Epithelial Tumour Cells by Human ?? T Cells: Involvement of NKG2D ligands and T-cell Receptor- versus NKG2D-dependent Recognition. *Scand. J. Immunol.* 2007;66(2–3):320–328.
167. Das H, Groh V, Kuijl C, et al. MICA engagement by human Vgamma2Vdelta2 T cells enhances their antigen-dependent effector function. *Immunity*. 2001;15(1):83–93.
168. Chitadze G, Lettau M, Luecke S, et al. NKG2D- and T-cell receptor-dependent lysis of malignant glioma cell lines by human γδ T cells: Modulation by temozolomide and A disintegrin and metalloproteases 10 and 17 inhibitors. *Oncoimmunology*. 2016;5(4):e1093276.
169. von Lilienfeld-Toal M, Nattermann J, Feldmann G, et al. Activated gammadelta T cells express the natural cytotoxicity receptor natural killer p 44 and show cytotoxic activity against myeloma cells. *Clin. Exp. Immunol.* 2006;144(3):528–533.
170. Correia DV, Fogli M, Hudspeth K, et al. Differentiation of human peripheral blood V 1+ T cells expressing the natural cytotoxicity receptor NKp30 for recognition of lymphoid leukemia cells. *Blood*. 2011;118(4):992–1001.
171. Kavanagh KL, Guo K, Dunford JE, et al. The molecular mechanism of nitrogen-containing bisphosphonates as antiosteoporosis drugs. *Proc. Natl. Acad. Sci.* 2006;103(20):7829–7834.
172. Di Carlo E, Bocca P, Emionite L, et al. Mechanisms of the antitumor activity of human Vγ9Vδ2 T cells in combination with zoledronic acid in a preclinical model of neuroblastoma. *Mol. Ther. J. Am. Soc. Gene Ther.* 2013;21(5):1034–1043.
173. Santolaria T, Robard M, Léger A, et al. Repeated systemic administrations of both aminobisphosphonates and human Vγ9Vδ2 T cells efficiently control tumor development in vivo. *J. Immunol. Baltim. Md 1950*. 2013;191(4):1993–2000.
174. Sicard H, Ingoure S, Luciani B, et al. In Vivo Immunomanipulation of V 9V 2 T Cells with a Synthetic Phosphoantigen in a Preclinical Nonhuman Primate Model. *J. Immunol.* 2005;175(8):5471–5480.
175. Gertner-Dardenne J, Bonnafous C, Bezombes C, et al. Bromohydrin pyrophosphate enhances antibody-dependent cell-mediated cytotoxicity induced by therapeutic antibodies. *Blood*. 2009;113(20):4875–4884.
176. Michishita Y, Hirokawa M, Guo Y-M, et al. Age-associated alteration of γδ T-cell repertoire and different profiles of activation-induced death of Vδ1 and Vδ2 T cells. *Int. J. Hematol.* 2011;94(3):230–240.
177. Santini D, Galluzzo S, Vincenzi B, et al. New developments of aminobisphosphonates: the double face of Janus. *Ann. Oncol. Off. J. Eur. Soc. Med. Oncol. ESMO*. 2007;18 Suppl 6:vi164-167.
178. Kalyan S, Chandrasekaran V, Quabius ES, Lindhorst TK, Kabelitz D. Neutrophil uptake of nitrogen-bisphosphonates leads to the suppression of human peripheral blood γδ T cells. *Cell. Mol. Life Sci.* 2014;71(12):2335–2346.
179. Fowler DW, Copier J, Dalgleish AG, Bodman-Smith MD. Zoledronic acid causes γδ T cells to target monocytes and down-modulate inflammatory homing. *Immunology*. 2014;143(4):539–549.
180. Fowler DW, Copier J, Dalgleish AG, Bodman-Smith MD. Zoledronic acid renders human M1 and M2 macrophages susceptible to Vδ2+ γδ T cell cytotoxicity in a perforin-dependent manner. *Cancer Immunol. Immunother.* 2017;66(9):1205–1215.
181. Parente-Pereira AC, Shmeeda H, Whilding LM, et al. Adoptive immunotherapy of epithelial ovarian cancer with Vγ9Vδ2 T cells, potentiated by liposomal alendronic acid. *J. Immunol. Baltim. Md 1950*. 2014;193(11):5557–5566.

182. Hodgins NO, Wang JT-W, Al-Jamal KT. Nano-technology based carriers for nitrogen-containing bisphosphonates delivery as sensitisers of γδ T cells for anticancer immunotherapy. *Adv. Drug Deliv. Rev.* 2017;114:143–160.
183. Suzuki T, Terao S, Acharya B, et al. The antitumour effect of {gamma}{delta} T-cells is enhanced by valproic acid-induced up-regulation of NKG2D ligands. *Anticancer Res.* 2010;30(11):4509–4513.
184. Du X, Li Q, Du F, He Z, Wang J. Sodium valproate sensitizes non-small lung cancer A549 cells to γδ T-cell-mediated killing through upregulating the expression of MICA. *J. Biochem. Mol. Toxicol.* 2013;27(11):492–498.
185. Poggi A, Catellani S, Garuti A, et al. Effective in vivo induction of NKG2D ligands in acute myeloid leukaemias by all-trans-retinoic acid or sodium valproate. *Leukemia*. 2009;23(4):641–648.
186. Zocchi MR, Catellani S, Canevali P, et al. High ERp5/ADAM10 expression in lymph node microenvironment and impaired NKG2D ligands recognition in Hodgkin lymphomas. *Blood*. 2012;119(6):1479–1489.
187. Hoh A, Dewerth A, Vogt F, et al. The activity of γδ T cells against paediatric liver tumour cells and spheroids in cell culture. *Liver Int.* 2013;33(1):127–136.
188. Oberg H-H, Peipp M, Kellner C, et al. Novel bispecific antibodies increase γδ T-cell cytotoxicity against pancreatic cancer cells. *Cancer Res.* 2014;74(5):1349–1360.
189. Klinger M, Benjamin J, Kischel R, Stienen S, Zugmaier G. Harnessing T cells to fight cancer with BiTE ® antibody constructs - past developments and future directions. *Immunol. Rev.* 2016;270(1):193–208.
190. Zheng J, Guo Y, Ji X, Cui L, He W. A novel antibody-like TCRγδ-Ig fusion protein exhibits antitumor activity against human ovarian carcinoma. *Cancer Lett.* 2013;341(2):150–158.
191. Couzi L, Pitard V, Sicard X, et al. Antibody-dependent anti-cytomegalovirus activity of human T cells expressing CD16 (Fc RIIIa). *Blood*. 2012;119(6):1418–1427.
192. Fisher JPH, Yan M, Heuijerjans J, et al. Neuroblastoma Killing Properties of V 2 and V 2-Negative T Cells Following Expansion by Artificial Antigen-Presenting Cells. *Clin. Cancer Res.* 2014;20(22):5720–5732.
193. Angelini DF, Borsellino G, Poupot M, et al. FcgammaRIII discriminates between 2 subsets of Vgamma9Vdelta2 effector cells with different responses and activation pathways. *Blood*. 2004;104(6):1801–1807.
194. Maus MV, Grupp SA, Porter DL, June CH. Antibody-modified T cells: CARs take the front seat for hematologic malignancies. *Blood*. 2014;123(17):2625–2635.
195. Vantourout P, Hayday A. Six-of-the-best: unique contributions of γδ T cells to immunology. *Nat. Rev. Immunol.* 2013;13(2):88–100.
196. Mirzaei HR, Mirzaei H, Lee SY, Hadjati J, Till BG. Prospects for chimeric antigen receptor (CAR) γδ T cells: A potential game changer for adoptive T cell cancer immunotherapy. *Cancer Lett.* 2016;380(2):413–423.
197. Deniger DC, Switzer K, Mi T, et al. Bispecific T-cells expressing polyclonal repertoire of endogenous γδ T-cell receptors and introduced CD19-specific chimeric antigen receptor. *Mol. Ther. J. Am. Soc. Gene Ther.* 2013;21(3):638–647.
198. Morgan RA, Dudley ME, Wunderlich JR, et al. Cancer regression in patients after transfer of genetically engineered lymphocytes. *Science*. 2006;314(5796):126–129.
199. Bendle GM, Linnemann C, Hooijkaas AI, et al. Lethal graft-versus-host disease in mouse models of T cell receptor gene therapy. *Nat. Med.* 2010;16(5):565–570.
200. van Loenen MM, de Boer R, Amir AL, et al. Mixed T cell receptor dimers harbor potentially harmful neoreactivity. *Proc. Natl. Acad. Sci.* 2010;107(24):10972–10977.
201. Linette GP, Stadtmauer EA, Maus MV, et al. Cardiovascular toxicity and titin cross-reactivity of affinity-enhanced T cells in myeloma and melanoma. *Blood*. 2013;122(6):863–871.
202. Raman MCC, Rizkallah PJ, Simmons R, et al. Direct molecular mimicry enables off-target cardiovascular toxicity by an enhanced affinity TCR designed for cancer immunotherapy. *Sci. Rep.* 2016;6:18851.

203. van der Veken LT, Coccoris M, Swart E, et al. Alpha beta T cell receptor transfer to gamma delta T cells generates functional effector cells without mixed TCR dimers in vivo. *J. Immunol. Baltim. Md 1950*. 2009;182(1):164–170.
204. Hiasa A, Nishikawa H, Hirayama M, et al. Rapid αβ TCR-mediated responses in γδ T cells transduced with cancer-specific TCR genes. *Gene Ther.* 2009;16(5):620–628.
205. van der Veken LT, Hagedoorn RS, van Loenen MM, et al. Alphabeta T-cell receptor engineered gammadelta T cells mediate effective antileukemic reactivity. *Cancer Res.* 2006;66(6):3331–3337.
206. Tan MP, Gerry AB, Brewer JE, et al. T cell receptor binding affinity governs the functional profile of cancer-specific CD8+ T cells. *Clin. Exp. Immunol.* 2015;180(2):255–270.
207. Zhao H, Xi X, Cui L, He W. CDR3δ -grafted γ9δ2T cells mediate effective antitumor reactivity. *Cell. Mol. Immunol.* 2012;9(2):147–154.
208. Marcu-Malina V, Heijhuurs S, van Buuren M, et al. Redirecting αβ T cells against cancer cells by transfer of a broadly tumor-reactive γδT-cell receptor. *Blood*. 2011;118(1):50–59.
209. Heemskerk MHM, Hagedoorn RS, van der Hoorn MAWG, et al. Efficiency of T-cell receptor expression in dual-specific T cells is controlled by the intrinsic qualities of the TCR chains within the TCR-CD3 complex. *Blood*. 2007;109(1):235–243.
210. Keast D. IMMUNOSURVEILLANCE AND CANCER. *The Lancet*. 1970;296(7675):710–712.
211. Hanahan D, Weinberg RA. Hallmarks of Cancer: The Next Generation. *Cell*. 2011;144(5):646–674.
212. Rosenberg SA. IL-2: The First Effective Immunotherapy for Human Cancer. *J. Immunol.* 2014;192(12):5451–5458.
213. Couzin-Frankel J. Cancer Immunotherapy. *Science*. 2013;342(6165):1432–1433.
214. Rosenberg SA, Yang JC, Restifo NP. Cancer immunotherapy: moving beyond current vaccines. *Nat. Med.* 2004;10(9):909–915.
215. Romero P, Banchereau J, Bhardwaj N, et al. The Human Vaccines Project: A roadmap for cancer vaccine development. *Sci. Transl. Med.* 2016;8(334):334ps9.
216. Theaker SM, Rius C, Greenshields-Watson A, et al. T-cell libraries allow simple parallel generation of multiple peptide-specific human T-cell clones. *J. Immunol. Methods*. 2016;430:43–50.
217. Chen J-L, Stewart-Jones G, Bossi G, et al. Structural and kinetic basis for heightened immunogenicity of T cell vaccines. *J. Exp. Med.* 2005;201(8):1243–1255.
218. Madura F, Rizkallah PJ, Holland CJ, et al. Structural basis for ineffective T-cell responses to MHC anchor residue-improved “heteroclitic” peptides. *Eur. J. Immunol.* 2015;45(2):584–591.
219. Bianchi V, Bulek A, Fuller A, et al. A Molecular Switch Abrogates Glycoprotein 100 (gp100) T-cell Receptor (TCR) Targeting of a Human Melanoma Antigen. *J. Biol. Chem.* 2016;291(17):8951–8959.
220. Schumacher T, Bunse L, Pusch S, et al. A vaccine targeting mutant IDH1 induces antitumour immunity. *Nature*. 2014;512(7514):324–327.
221. Apostolopoulos V, Pietersz GA, Tsibanis A, et al. Dendritic cell immunotherapy: clinical outcomes. *Clin. Transl. Immunol.* 2014;3(7):e21.
222. Brandes M, Willimann K, Moser B. Professional antigen-presentation function by human gammadelta T Cells. *Science*. 2005;309(5732):264–268.
223. Brandes M, Willimann K, Bioley G, et al. Cross-presenting human T cells induce robust CD8+ T cell responses. *Proc. Natl. Acad. Sci.* 2009;106(7):2307–2312.
224. Himoudi N, Morgenstern DA, Yan M, et al. Human T Lymphocytes Are Licensed for Professional Antigen Presentation by Interaction with Opsonized Target Cells. *J. Immunol.* 2012;188(4):1708–1716.
225. Mao C, Mou X, Zhou Y, et al. Tumor-Activated T Cells from Gastric Cancer Patients Induce the Antitumor Immune Response of T Cells via Their Antigen-Presenting Cell-Like Effects. *J. Immunol. Res.* 2014;2014:1–10.

226. Howard J, Loizon S, Tyler CJ, et al. The Antigen-Presenting Potential of Vγ9Vδ2 T Cells During Plasmodium falciparum Blood-Stage Infection. *J. Infect. Dis.* 2017;215(10):1569–1579.
227. Khan MWA, Curbishley SM, Chen H-C, et al. Expanded Human Blood-Derived Î³Î´T Cells Display Potent Antigen-Presentation Functions. *Front. Immunol.* 2014;5:.
228. Welton JL, Morgan MP, Martí S, et al. Monocytes and γδ T cells control the acute-phase response to intravenous zoledronate: Insights from a phase IV safety trial. *J. Bone Miner. Res.* 2013;28(3):464–471.
229. Bennouna J, Levy V, Sicard H, et al. Phase I study of bromohydrin pyrophosphate (BrHPP, IPH 1101), a Vγ9Vδ2 T lymphocyte agonist in patients with solid tumors. *Cancer Immunol. Immunother.* 2010;59(10):1521–1530.
230. Lang JM, Kaikobad MR, Wallace M, et al. Pilot trial of interleukin-2 and zoledronic acid to augment γδ T cells as treatment for patients with refractory renal cell carcinoma. *Cancer Immunol. Immunother.* 2011;60(10):1447–1460.
231. Kunzmann V, Smetak M, Kimmel B, et al. Tumor-promoting Versus Tumor-antagonizing Roles of γδ T Cells in Cancer Immunotherapy: Results From a Prospective Phase I/II Trial. *J. Immunother.* 2012;35(2):205–213.
232. Meraviglia S, Eberl M, Vermijlen D, et al. In vivo manipulation of Vγ9Vδ2 T cells with zoledronate and low-dose interleukin-2 for immunotherapy of advanced breast cancer patients: γδ T cells for immunotherapy of breast cancer. *Clin. Exp. Immunol.* 2010;no-no.
233. Dieli F, Vermijlen D, Fulfaro F, et al. Targeting human {gamma}delta} T cells with zoledronate and interleukin-2 for immunotherapy of hormone-refractory prostate cancer. *Cancer Res.* 2007;67(15):7450–7457.
234. James ND, Sydes MR, Clarke NW, et al. Addition of docetaxel, zoledronic acid, or both to first-line long-term hormone therapy in prostate cancer (STAMPEDE): survival results from an adaptive, multiarm, multistage, platform randomised controlled trial. *The Lancet*. 2016;387(10024):1163–1177.
235. Gnant M, Mlineritsch B, Stoeger H, et al. Zoledronic acid combined with adjuvant endocrine therapy of tamoxifen versus anastrozol plus ovarian function suppression in premenopausal early breast cancer: final analysis of the Austrian Breast and Colorectal Cancer Study Group Trial 12. *Ann. Oncol.* 2015;26(2):313–320.
236. Gnant M, Mlineritsch B, Stoeger H, et al. Adjuvant endocrine therapy plus zoledronic acid in premenopausal women with early-stage breast cancer: 62-month follow-up from the ABCSG-12 randomised trial. *Lancet Oncol.* 2011;12(7):631–641.
237. Hasegawa Y, Tanino H, Horiguchi J, et al. Randomized Controlled Trial of Zoledronic Acid plus Chemotherapy versus Chemotherapy Alone as Neoadjuvant Treatment of HER2-Negative Primary Breast Cancer (JONIE Study). *PLOS ONE*. 2015;10(12):e0143643.
238. Charehbili A, van de Ven S, Smit VTHBM, et al. Addition of zoledronic acid to neoadjuvant chemotherapy does not enhance tumor response in patients with HER2-negative stage II/III breast cancer: the NEOZOTAC trial (BOOG 2010-01). *Ann. Oncol.* 2014;25(5):998–1004.
239. Murakami H, Yamanaka T, Seto T, et al. Phase II study of zoledronic acid combined with docetaxel for non-small-cell lung cancer: West Japan Oncology Group. *Cancer Sci.* 2014;105(8):989–995.
240. Sharma P, Allison JP. The future of immune checkpoint therapy. *Science*. 2015;348(6230):56–61.
241. Schadendorf D, Hodi FS, Robert C, et al. Pooled Analysis of Long-Term Survival Data From Phase II and Phase III Trials of Ipilimumab in Unresectable or Metastatic Melanoma. *J. Clin. Oncol.* 2015;33(17):1889–1894.
242. Hamid O, Robert C, Daud A, et al. Safety and Tumor Responses with Lambrolizumab (Anti–PD-1) in Melanoma. *N. Engl. J. Med.* 2013;369(2):134–144.
243. Robert C, Long GV, Brady B, et al. Nivolumab in Previously Untreated Melanoma without *BRAF* Mutation. *N. Engl. J. Med.* 2015;372(4):320–330.

244. Wolchok JD, Kluger H, Callahan MK, et al. Nivolumab plus Ipilimumab in Advanced Melanoma. *N. Engl. J. Med.* 2013;369(2):122–133.
245. Postow MA, Manuel M, Wong P, et al. Peripheral T cell receptor diversity is associated with clinical outcomes following ipilimumab treatment in metastatic melanoma. *J. Immunother. Cancer*. 2015;3:23.
246. McGranahan N, Furness AJS, Rosenthal R, et al. Clonal neoantigens elicit T cell immunoreactivity and sensitivity to immune checkpoint blockade. *Science*. 2016;351(6280):1463–1469.
247. Iwasaki M, Tanaka Y, Kobayashi H, et al. Expression and function of PD-1 in human γδ T cells that recognize phosphoantigens. *Eur. J. Immunol.* 2011;41(2):345–355.
248. Rosenberg SA, Packard BS, Aebersold PM, et al. Use of Tumor-Infiltrating Lymphocytes and Interleukin-2 in the Immunotherapy of Patients with Metastatic Melanoma. *N. Engl. J. Med.* 1988;319(25):1676–1680.
249. Rosenberg SA, Restifo NP. Adoptive cell transfer as personalized immunotherapy for human cancer. *Science*. 2015;348(6230):62–68.
250. Dudley ME. Cancer Regression and Autoimmunity in Patients After Clonal Repopulation with Antitumor Lymphocytes. *Science*. 2002;298(5594):850–854.
251. Rosenberg SA, Yang JC, Sherry RM, et al. Durable Complete Responses in Heavily Pretreated Patients with Metastatic Melanoma Using T-Cell Transfer Immunotherapy. *Clin. Cancer Res.* 2011;17(13):4550–4557.
252. Paulos CM, Wrzesinski C, Kaiser A, et al. Microbial translocation augments the function of adoptively transferred self/tumor-specific CD8+ T cells via TLR4 signaling. *J. Clin. Invest.* 2007;117(8):2197–2204.
253. Donia M, Junker N, Ellebaek E, et al. Characterization and comparison of "standard" and "young" tumour-infiltrating lymphocytes for adoptive cell therapy at a Danish translational research institution. *Scand. J. Immunol.* 2012;75(2):157–167.
254. Donia M, Larsen SM, Met O, Svane IM. Simplified protocol for clinical-grade tumor-infiltrating lymphocyte manufacturing with use of the Wave bioreactor. *Cytotherapy*. 2014;16(8):1117–1120.
255. Ellebaek E, Iversen TZ, Junker N, et al. Adoptive cell therapy with autologous tumor infiltrating lymphocytes and low-dose Interleukin-2 in metastatic melanoma patients. *J. Transl. Med.* 2012;10:169.
256. Andersen R, Donia M, Ellebaek E, et al. Long-Lasting Complete Responses in Patients with Metastatic Melanoma after Adoptive Cell Therapy with Tumor-Infiltrating Lymphocytes and an Attenuated IL2 Regimen. *Clin. Cancer Res. Off. J. Am. Assoc. Cancer Res.* 2016;
257. Andersen R, Donia M, Westergaard MCW, et al. Tumor infiltrating lymphocyte therapy for ovarian cancer and renal cell carcinoma. *Hum. Vaccines Immunother.* 2015;11(12):2790–2795.
258. Kochenderfer JN, Wilson WH, Janik JE, et al. Eradication of B-lineage cells and regression of lymphoma in a patient treated with autologous T cells genetically engineered to recognize CD19. *Blood*. 2010;116(20):4099–4102.
259. Li Y, Moysey R, Molloy PE, et al. Directed evolution of human T-cell receptors with picomolar affinities by phage display. *Nat. Biotechnol.* 2005;23(3):349–354.
260. Straetemans T, Berrevoets C, Coccoris M, et al. Recurrence of Melanoma Following T Cell Treatment: Continued Antigen Expression in a Tumor That Evades T Cell Recruitment. *Mol. Ther.* 2015;23(2):396–406.
261. Maeurer MJ, Gollin SM, Martin D, et al. Tumor escape from immune recognition: lethal recurrent melanoma in a patient associated with downregulation of the peptide transporter protein TAP-1 and loss of expression of the immunodominant MART-1/Melan-A antigen. *J. Clin. Invest.* 1996;98(7):1633–1641.
262. Bialasiewicz AA, Ma JX, Richard G. Alpha/beta- and gamma/delta TCR(+) lymphocyte infiltration in necrotising choroidal melanomas. *Br. J. Ophthalmol.* 1999;83(9):1069–1073.
263. Yazdi AS, Morstedt K, Puchta U, et al. Heterogeneity of T-cell clones infiltrating primary malignant melanomas. *J. Invest. Dermatol.* 2006;126(2):393–398.

264. Cordova A, Toia F, La Mendola C, et al. Characterization of Human γδ T Lymphocytes Infiltrating Primary Malignant Melanomas. *PLoS ONE*. 2012;7(11):e49878.
265. Donia M, Ellebaek E, Andersen MH, Straten PT, Svane IM. Analysis of Vδ1 T cells in clinical grade melanoma-infiltrating lymphocytes. *Oncoimmunology*. 2012;1(8):1297–1304.
266. Lanca T, Costa MF, Goncalves-Sousa N, et al. Protective Role of the Inflammatory CCR2/CCL2 Chemokine Pathway through Recruitment of Type 1 Cytotoxic T Lymphocytes to Tumor Beds. *J. Immunol.* 2013;190(12):6673–6680.
267. Coffelt SB, Kersten K, Doornebal CW, et al. IL-17-producing γδ T cells and neutrophils conspire to promote breast cancer metastasis. *Nature*. 2015;522(7556):345–348.
268. Wu P, Wu D, Ni C, et al. γδT17 Cells Promote the Accumulation and Expansion of Myeloid-Derived Suppressor Cells in Human Colorectal Cancer. *Immunity*. 2014;40(5):785–800.
269. Daley D, Zambirinis CP, Seifert L, et al. γδ T Cells Support Pancreatic Oncogenesis by Restraining αβ T Cell Activation. *Cell*. 2016;166(6):1485–1499.e15.
270. Yi Y, He H-W, Wang J-X, et al. The functional impairment of HCC-infiltrating γδ T cells, partially mediated by regulatory T cells in a TGFβ- and IL-10-dependent manner. *J. Hepatol.* 2013;58(5):977–983.
271. Bennouna J, Bompas E, Neidhardt EM, et al. Phase-I study of Innacell γδ^{TM}, an autologous cell-therapy product highly enriched in γ9δ2 T lymphocytes, in combination with IL-2, in patients with metastatic renal cell carcinoma. *Cancer Immunol. Immunother.* 2008;57(11):1599–1609.
272. Nicol AJ, Tokuyama H, Mattarollo SR, et al. Clinical evaluation of autologous gamma delta T cell-based immunotherapy for metastatic solid tumours. *Br. J. Cancer*. 2011;105(6):778–786.
273. Kobayashi H, Tanaka Y, Yagi J, Minato N, Tanabe K. Phase I/II study of adoptive transfer of γδ T cells in combination with zoledronic acid and IL-2 to patients with advanced renal cell carcinoma. *Cancer Immunol. Immunother.* 2011;60(8):1075–1084.
274. Wilhelm M, Smetak M, Schaefer-Eckart K, et al. Successful adoptive transfer and in vivo expansion of haploidentical γδ T cells. *J. Transl. Med.* 2014;12(1):45.
275. Kang N, Zhou J, Zhang T, et al. Adoptive immunotherapy of lung cancer with immobilized anti-TCRgammadelta antibody-expanded human gammadelta T-cells in peripheral blood. *Cancer Biol. Ther.* 2009;8(16):1540–1549.
276. Zhou J, Kang N, Cui L, Ba D, He W. Anti-γδ TCR antibody-expanded γδ T cells: a better choice for the adoptive immunotherapy of lymphoid malignancies. *Cell. Mol. Immunol.* 2012;9(1):34–44.
277. Deniger DC, Maiti S, Mi T, et al. Activating and propagating polyclonal gamma delta T cells with broad specificity for malignancies. *Clin. Cancer Res.* 2014;
278. Almeida AR, Correia DV, Fernandes-Platzgummer A, et al. Delta One T cells for immunotherapy of chronic lymphocytic leukemia: clinical-grade expansion/ differentiation and preclinical proof-of-concept. *Clin. Cancer Res. Off. J. Am. Assoc. Cancer Res.* 2016;
279. Gentles AJ, Newman AM, Liu CL, et al. The prognostic landscape of genes and infiltrating immune cells across human cancers. *Nat. Med.* 2015;21(8):938–945.
280. Lee A-J, Kim S-G, Chae H-D, Lee GH, Shin I-H. γδ T cells are increased in the peripheral blood of patients with gastric cancer. *Clin. Chim. Acta*. 2012;413(19–20):1495–1499.
281. Kobayashi H, Tanaka Y, Nakazawa H, et al. A new indicator of favorable prognosis in locally advanced renal cell carcinomas: gamma delta T-cells in peripheral blood. *Anticancer Res.* 2011;31(3):1027–1031.
282. Wistuba-Hamprecht K, Martens A, Haehnel K, et al. Proportions of blood-borne Vδ1+ and Vδ2+ T-cells are associated with overall survival of melanoma patients treated with ipilimumab. *Eur. J. Cancer*. 2016;64:116–126.
283. Toia F, Buccheri S, Anfosso A, et al. Skewed Differentiation of Circulating Vγ9Vδ2 T Lymphocytes in Melanoma and Impact on Clinical Outcome. *PLOS ONE*. 2016;11(2):e0149570.
284. Capecchi MR. Altering the genome by homologous recombination. *Science*. 1989;244(4910):1288–1292.

285. Urnov FD, Miller JC, Lee Y-L, et al. Highly efficient endogenous human gene correction using designed zinc-finger nucleases. *Nature*. 2005;435(7042):646–651.
286. Miller JC, Tan S, Qiao G, et al. A TALE nuclease architecture for efficient genome editing. *Nat. Biotechnol.* 2011;29(2):143–148.
287. Sander JD, Dahlborg EJ, Goodwin MJ, et al. Selection-free zinc-finger-nuclease engineering by context-dependent assembly (CoDA). *Nat. Methods*. 2011;8(1):67–69.
288. Juillerat A, Dubois G, Valton J, et al. Comprehensive analysis of the specificity of transcription activator-like effector nucleases. *Nucleic Acids Res.* 2014;42(8):5390–5402.
289. Cong L, Ran FA, Cox D, et al. Multiplex Genome Engineering Using CRISPR/Cas Systems. *Science*. 2013;339(6121):819–823.
290. Deltcheva E, Chylinski K, Sharma CM, et al. CRISPR RNA maturation by trans-encoded small RNA and host factor RNase III. *Nature*. 2011;471(7340):602–607.
291. Jinek M, Chylinski K, Fonfara I, et al. A Programmable Dual-RNA-Guided DNA Endonuclease in Adaptive Bacterial Immunity. *Science*. 2012;337(6096):816–821.
292. Mali P, Yang L, Esvelt KM, et al. RNA-Guided Human Genome Engineering via Cas9. *Science*. 2013;339(6121):823–826.
293. Hsu PD, Scott DA, Weinstein JA, et al. DNA targeting specificity of RNA-guided Cas9 nucleases. *Nat. Biotechnol.* 2013;31(9):827–832.
294. Sternberg SH, Redding S, Jinek M, Greene EC, Doudna JA. DNA interrogation by the CRISPR RNA-guided endonuclease Cas9. *Nature*. 2014;507(7490):62–67.
295. Fu Y, Foden JA, Khayter C, et al. High-frequency off-target mutagenesis induced by CRISPR-Cas nucleases in human cells. *Nat. Biotechnol.* 2013;31(9):822–826.
296. Jensen KT, Fløe L, Petersen TS, et al. Chromatin accessibility and guide sequence secondary structure affect CRISPR-Cas9 gene editing efficiency. *FEBS Lett.* 2017;591(13):1892–1901.
297. Perez AR, Pritykin Y, Vidigal JA, et al. GuideScan software for improved single and paired CRISPR guide RNA design. *Nat. Biotechnol.* 2017;35(4):347–349.
298. Hough SH, Kancleris K, Brody L, et al. Guide Picker is a comprehensive design tool for visualizing and selecting guides for CRISPR experiments. *BMC Bioinformatics*. 2017;18(1):.
299. Ren J, Liu X, Fang C, et al. Multiplex Genome Editing to Generate Universal CAR T Cells Resistant to PD1 Inhibition. *Clin. Cancer Res.* 2017;23(9):2255–2266.
300. Ran FA, Hsu PD, Lin C-Y, et al. Double Nicking by RNA-Guided CRISPR Cas9 for Enhanced Genome Editing Specificity. *Cell*. 2013;154(6):1380–1389.
301. Gilbert LA, Horlbeck MA, Adamson B, et al. Genome-Scale CRISPR-Mediated Control of Gene Repression and Activation. *Cell*. 2014;159(3):647–661.
302. Konermann S, Brigham MD, Trevino AE, et al. Genome-scale transcriptional activation by an engineered CRISPR-Cas9 complex. *Nature*. 2014;517(7536):583–588.
303. Shalem O, Sanjana NE, Hartenian E, et al. Genome-Scale CRISPR-Cas9 Knockout Screening in Human Cells. *Science*. 2014;343(6166):84–87.
304. Sanjana NE, Wright J, Zheng K, et al. High-resolution interrogation of functional elements in the noncoding genome. *Science*. 2016;353(6307):1545–1549.
305. Wang T, Wei JJ, Sabatini DM, Lander ES. Genetic Screens in Human Cells Using the CRISPR-Cas9 System. *Science*. 2014;343(6166):80–84.
306. Doench JG, Fusi N, Sullender M, et al. Optimized sgRNA design to maximize activity and minimize off-target effects of CRISPR-Cas9. *Nat. Biotechnol.* 2016;34(2):184–191.
307. Fulco CP, Munschauer M, Anyoha R, et al. Systematic mapping of functional enhancer–promoter connections with CRISPR interference. *Science*. 2016;354(6313):769–773.
308. Marceau CD, Puschnik AS, Majzoub K, et al. Genetic dissection of Flaviviridae host factors through genome-scale CRISPR screens. *Nature*. 2016;535(7610):159–163.
309. Zhang R, Miner JJ, Gorman MJ, et al. A CRISPR screen defines a signal peptide processing pathway required by flaviviruses. *Nature*. 2016;535(7610):164–168.
310. Orchard RC, Wilen CB, Doench JG, et al. Discovery of a proteinaceous cellular receptor for a norovirus. *Science*. 2016;353(6302):933–936.
311. Chen S, Sanjana NE, Zheng K, et al. Genome-wide CRISPR Screen in a Mouse Model of Tumor Growth and Metastasis. *Cell*. 2015;160(6):1246–1260.

312. Canver MC, Smith EC, Sher F, et al. BCL11A enhancer dissection by Cas9-mediated in situ saturating mutagenesis. *Nature*. 2015;527(7577):192–197.
313. Korkmaz G, Lopes R, Ugalde AP, et al. Functional genetic screens for enhancer elements in the human genome using CRISPR-Cas9. *Nat. Biotechnol.* 2016;34(2):192–198.
314. Parnas O, Jovanovic M, Eisenhaure TM, et al. A Genome-wide CRISPR Screen in Primary Immune Cells to Dissect Regulatory Networks. *Cell*. 2015;162(3):675–686.
315. Nijmeijer BA, Szuhai K, Goselink HM, et al. Long–term culture of primary human lymphoblastic leukemia cells in the absence of serum or hematopoietic growth factors. *Exp. Hematol.* 2009;37(3):376–385.
316. Lang F, Wojcik B, Bothur S, et al. Plastic CD34 and CD38 expression in adult B–cell precursor acute lymphoblastic leukemia explains ambiguity of leukemia-initiating stem cell populations. *Leukemia*. 2017;31(3):731–734.
317. Evans M, Borysiewicz LK, Evans AS, et al. Antigen Processing Defects in Cervical Carcinomas Limit the Presentation of a CTL Epitope from Human Papillomavirus 16 E6. *J. Immunol.* 2001;167(9):5420–5428.
318. Trickett A, Kwan YL. T cell stimulation and expansion using anti-CD3/CD28 beads. *J. Immunol. Methods*. 2003;275(1–2):251–255.
319. Sanjana NE, Shalem O, Zhang F. Improved vectors and genome-wide libraries for CRISPR screening. *Nat. Methods*. 2014;11(8):783–784.
320. Richardson MW, Carroll RG, Stremlau M, et al. Mode of Transmission Affects the Sensitivity of Human Immunodeficiency Virus Type 1 to Restriction by Rhesus TRIM5. *J. Virol.* 2008;82(22):11117–11128.
321. Lissina A, Ladell K, Skowera A, et al. Protein kinase inhibitors substantially improve the physical detection of T-cells with peptide-MHC tetramers. *J. Immunol. Methods*. 2009;340(1):11–24.
322. Tungatt K, Bianchi V, Crowther MD, et al. Antibody Stabilization of Peptide–MHC Multimers Reveals Functional T Cells Bearing Extremely Low-Affinity TCRs. *J. Immunol.* 2015;194(1):463–474.
323. Dolton G, Tungatt K, Lloyd A, et al. More tricks with tetramers: a practical guide to staining T cells with peptide-MHC multimers. *Immunology*. 2015;146(1):11–22.
324. Ziegler SF, Ramsdell F, Alderson MR. The activation antigen CD69. *Stem Cells*. 1994;12(5):456–465.
325. Haney D, Quigley MF, Asher TE, et al. Isolation of viable antigen-specific CD8+ T cells based on membrane-bound tumor necrosis factor (TNF)-α expression. *J. Immunol. Methods*. 2011;369(1–2):33–41.
326. Petalidis L. Global amplification of mRNA by template-switching PCR: linearity and application to microarray analysis. *Nucleic Acids Res.* 2003;31(22):142e–142.
327. Kim JH, Lee S-R, Li L-H, et al. High Cleavage Efficiency of a 2A Peptide Derived from Porcine Teschovirus-1 in Human Cell Lines, Zebrafish and Mice. *PLoS ONE*. 2011;6(4):e18556.
328. Joung J, Konermann S, Gootenberg JS, et al. Genome-scale CRISPR-Cas9 knockout and transcriptional activation screening. *Nat. Protoc.* 2017;12(4):828–863.
329. Roederer M, Nozzi JL, Nason MC. SPICE: exploration and analysis of post-cytometric complex multivariate datasets. *Cytom. Part J. Int. Soc. Anal. Cytol.* 2011;79(2):167–174.
330. Katz SC, Bamboat ZM, Maker AV, et al. Regulatory T Cell Infiltration Predicts Outcome Following Resection of Colorectal Cancer Liver Metastases. *Ann. Surg. Oncol.* 2013;20(3):946–955.
331. Locke FL, Neelapu SS, Bartlett NL, et al. Phase 1 Results of ZUMA-1: A Multicenter Study of KTE-C19 Anti-CD19 CAR T Cell Therapy in Refractory Aggressive Lymphoma. *Mol. Ther.* 2017;25(1):285–295.
332. Kakarla S, Gottschalk S. CAR T Cells for Solid Tumors: Armed and Ready to Go? *Cancer J.* 2014;20(2):151–155.
333. Robbins PF, Morgan RA, Feldman SA, et al. Tumor Regression in Patients With Metastatic Synovial Cell Sarcoma and Melanoma Using Genetically Engineered Lymphocytes Reactive With NY-ESO-1. *J. Clin. Oncol.* 2011;29(7):917–924.

334. Robbins PF, Kassim SH, Tran TLN, et al. A Pilot Trial Using Lymphocytes Genetically Engineered with an NY-ESO-1-Reactive T-cell Receptor: Long-term Follow-up and Correlates with Response. *Clin. Cancer Res.* 2015;21(5):1019–1027.
335. Cole DK, Laugel B, Clement M, et al. The molecular determinants of CD8 co-receptor function. *Immunology*. 2012;137(2):139–148.
336. Ahmadi M, King JW, Xue S-A, et al. CD3 limits the efficacy of TCR gene therapy in vivo. *Blood*. 2011;118(13):3528–3537.
337. Kuball J, Dossett ML, Wolfl M, et al. Facilitating matched pairing and expression of TCR chains introduced into human T cells. *Blood*. 2007;109(6):2331–2338.
338. Voss R-H, Willemsen RA, Kuball J, et al. Molecular design of the Calphabeta interface favors specific pairing of introduced TCRalphabeta in human T cells. *J. Immunol. Baltim. Md 1950*. 2008;180(1):391–401.
339. Bialer G, Horovitz-Fried M, Ya'acobi S, Morgan RA, Cohen CJ. Selected Murine Residues Endow Human TCR with Enhanced Tumor Recognition. *J. Immunol.* 2010;184(11):6232–6241.
340. Sommermeyer D, Uckert W. Minimal Amino Acid Exchange in Human TCR Constant Regions Fosters Improved Function of TCR Gene-Modified T Cells. *J. Immunol.* 2010;184(11):6223–6231.
341. Tao C, Shao H, Zhang W, et al. ??TCR immunoglobulin constant region domain exchange in human ??TCRs improves TCR pairing without altering TCR gene-modified T cell function. *Mol. Med. Rep.* 2017;
342. Aggen DH, Chervin AS, Schmitt TM, et al. Single-chain VαVβ T-cell receptors function without mispairing with endogenous TCR chains. *Gene Ther.* 2012;19(4):365–374.
343. Rapoport AP, Stadtmauer EA, Binder-Scholl GK, et al. NY-ESO-1–specific TCR–engineered T cells mediate sustained antigen-specific antitumor effects in myeloma. *Nat. Med.* 2015;21(8):914–921.
344. Cameron BJ, Gerry AB, Dukes J, et al. Identification of a Titin-Derived HLA-A1-Presented Peptide as a Cross-Reactive Target for Engineered MAGE A3-Directed T Cells. *Sci. Transl. Med.* 2013;5(197):197ra103-197ra103.
345. Anderson EM, Haupt A, Schiel JA, et al. Systematic analysis of CRISPR–Cas9 mismatch tolerance reveals low levels of off-target activity. *J. Biotechnol.* 2015;211:56–65.
346. Katz ZB, Novotná L, Blount A, Lillemeier BF. A cycle of Zap70 kinase activation and release from the TCR amplifies and disperses antigenic stimuli. *Nat. Immunol.* 2016;18(1):86–95.
347. Bilal MY, Vacaflores A, Houtman JC. Optimization of methods for the genetic modification of human T cells. *Immunol. Cell Biol.* 2015;93(10):896–908.
348. Borthwick NJ, Lowdell M, Salmon M, Akbar AN. Loss of CD28 expression on CD8(+) T cells is induced by IL-2 receptor gamma chain signalling cytokines and type I IFN, and increases susceptibility to activation-induced apoptosis. *Int. Immunol.* 2000;12(7):1005–1013.
349. Cole DK, Edwards ESJ, Wynn KK, et al. Modification of MHC Anchor Residues Generates Heteroclitic Peptides That Alter TCR Binding and T Cell Recognition. *J. Immunol.* 2010;185(4):2600–2610.
350. Schodin BA, Tsomides TJ, Kranz DM. Correlation between the number of T cell receptors required for T cell activation and TCR-ligand affinity. *Immunity*. 1996;5(2):137–146.
351. Sallusto F, Lenig D, Förster R, Lipp M, Lanzavecchia A. Two subsets of memory T lymphocytes with distinct homing potentials and effector functions. *Nature*. 1999;401(6754):708–712.
352. Mahnke YD, Brodie TM, Sallusto F, Roederer M, Lugli E. The who's who of T-cell differentiation: Human memory T-cell subsets: HIGHLIGHTS. *Eur. J. Immunol.* 2013;43(11):2797–2809.
353. Fuertes Marraco SA, Neubert NJ, Verdeil G, Speiser DE. Inhibitory Receptors Beyond T Cell Exhaustion. *Front. Immunol.* 2015;6:.
354. Price DA, Sewell AK, Dong T, et al. Antigen-specific release of beta-chemokines by anti-HIV-1 cytotoxic T lymphocytes. *Curr. Biol. CB*. 1998;8(6):355–358.

355. Laugel B, Price DA, Milicic A, Sewell AK. CD8 exerts differential effects on the deployment of cytotoxic T lymphocyte effector functions. *Eur. J. Immunol.* 2007;37(4):905–913.
356. Wooldridge L, Ekeruche-Makinde J, van den Berg HA, et al. A Single Autoimmune T Cell Receptor Recognizes More Than a Million Different Peptides. *J. Biol. Chem.* 2012;287(2):1168–1177.
357. Ekeruche-Makinde J, Miles JJ, van den Berg HA, et al. Peptide length determines the outcome of TCR/peptide-MHCI engagement. *Blood*. 2013;121(7):1112–1123.
358. Tan MP, Gerry AB, Brewer JE, et al. T cell receptor binding affinity governs the functional profile of cancer-specific CD8 $^{+}$ T cells: TCR affinity governs T cell function. *Clin. Exp. Immunol.* 2015;180(2):255–270.
359. Tan MP, Dolton GM, Gerry AB, et al. Human leucocyte antigen class I-redirected anti-tumour CD4 $^{+}$ T cells require a higher T cell receptor binding affinity for optimal activity than CD8 $^{+}$ T cells: Anti-tumour HLA I-restricted CD4 $^{+}$ T cells. *Clin. Exp. Immunol.* 2017;187(1):124–137.
360. Cole DK, Bulek AM, Dolton G, et al. Hotspot autoimmune T cell receptor binding underlies pathogen and insulin peptide cross-reactivity. *J. Clin. Invest.* 2016;126(6):2191–2204.
361. Pageon SV, Tabarin T, Yamamoto Y, et al. Functional role of T-cell receptor nanoclusters in signal initiation and antigen discrimination. *Proc. Natl. Acad. Sci.* 2016;113(37):E5454–E5463.
362. Willcox CR, Pitard V, Netzer S, et al. Cytomegalovirus and tumor stress surveillance by binding of a human γδ T cell antigen receptor to endothelial protein C receptor. *Nat. Immunol.* 2012;13(9):872–879.
363. Roy S, Ly D, Castro CD, et al. Molecular Analysis of Lipid-Reactive V?1 ?? T Cells Identified by CD1c Tetramers. *J. Immunol.* 2016;196(4):1933–1942.
364. Rey J, Veuillen C, Vey N, Bouabdallah R, Olive D. Natural killer and γδ T cells in haematological malignancies: enhancing the immune effectors. *Trends Mol. Med.* 2009;15(6):275–284.
365. Newick K, O'Brien S, Moon E, Albelda SM. CAR T Cell Therapy for Solid Tumors. *Annu. Rev. Med.* 2017;68(1):139–152.
366. Abe Y, Muto M, Nieda M, et al. Clinical and immunological evaluation of zoledronate-activated Vγ9γδ T-cell-based immunotherapy for patients with multiple myeloma. *Exp. Hematol.* 2009;37(8):956–968.
367. Ramos CA, Savoldo B, Dotti G. CD19-CAR Trials: *Cancer J.* 2014;20(2):112–118.
368. Provasi E, Genovese P, Lombardo A, et al. Editing T cell specificity towards leukemia by zinc finger nucleases and lentiviral gene transfer. *Nat. Med.* 2012;18(5):807–815.
369. Torikai H, Reik A, Liu P-Q, et al. A foundation for universal T-cell based immunotherapy: T cells engineered to express a CD19-specific chimeric-antigen-receptor and eliminate expression of endogenous TCR. *Blood*. 2012;119(24):5697–5705.
370. Berdien B, Mock U, Atanackovic D, Fehse B. TALEN-mediated editing of endogenous T-cell receptors facilitates efficient reprogramming of T lymphocytes by lentiviral gene transfer. *Gene Ther.* 2014;21(6):539–548.
371. Poirot L, Philip B, Schiffer-Mannioui C, et al. Multiplex Genome-Edited T-cell Manufacturing Platform for "Off-the-Shelf" Adoptive T-cell Immunotherapies. *Cancer Res.* 2015;75(18):3853–3864.
372. Qasim W, Zhan H, Samarasinghe S, et al. Molecular remission of infant B-ALL after infusion of universal TALEN gene-edited CAR T cells. *Sci. Transl. Med.* 2017;9(374):eaaj2013.
373. Ren J, Zhang X, Liu X, et al. A versatile system for rapid multiplex genome-edited CAR T cell generation. *Oncotarget*. 2017;
374. Eyquem J, Mansilla-Soto J, Giavridis T, et al. Targeting a CAR to the TRAC locus with CRISPR/Cas9 enhances tumour rejection. *Nature*. 2017;543(7643):113–117.
375. Ding Z-C, Huang L, Blazar BR, et al. Polyfunctional CD4+ T cells are essential for eradicating advanced B-cell lymphoma after chemotherapy. *Blood*. 2012;120(11):2229–2239.
376. Bouchie A, DeFrancesco L, Sheridan C, Webb S. Nature Biotechnology's academic spinouts of 2016. *Nat. Biotechnol.* 2017;35(4):322–333.

377. Wilhelm M. T cells for immune therapy of patients with lymphoid malignancies. *Blood*. 2003;102(1):200–206.
378. Klebanoff CA, Gattinoni L, Restifo NP. Sorting Through Subsets: Which T-Cell Populations Mediate Highly Effective Adoptive Immunotherapy? *J. Immunother.* 2012;35(9):651–660.
379. Reissfelder C, Stamova S, Gossmann C, et al. Tumor-specific cytotoxic T lymphocyte activity determines colorectal cancer patient prognosis. *J. Clin. Invest.* 2015;125(2):739–751.
380. Donia M, Hansen M, Sendrup SL, et al. Methods to improve adoptive T-cell therapy for melanoma: IFN-γ enhances anticancer responses of cell products for infusion. *J. Invest. Dermatol.* 2013;133(2):545–552.
381. Parker BS, Rautela J, Hertzog PJ. Antitumour actions of interferons: implications for cancer therapy. *Nat. Rev. Cancer*. 2016;16(3):131–144.
382. Sen DR, Kaminski J, Barnitz RA, et al. The epigenetic landscape of T cell exhaustion. *Science*. 2016;354(6316):1165–1169.
383. Legut M, Cole DK, Sewell AK. The promise of γδ T cells and the γδ T cell receptor for cancer immunotherapy. *Cell. Mol. Immunol.* 2015;
384. Born WK, Reardon CL, O'Brien RL. The function of γδ T cells in innate immunity. *Curr. Opin. Immunol.* 2006;18(1):31–38.
385. Silva-Santos B, Strid J. γδ T cells get adaptive. *Nat. Immunol.* 2017;18(4):370–372.
386. Correia DV, Lopes AC, Silva-Santos B. Tumor cell recognition by γδ T lymphocytes: T-cell receptor vs. NK-cell receptors. *OncoImmunology*. 2013;2(1):e22892.
387. Shafi S, Vantourout P, Wallace G, et al. An NKG2D-Mediated Human Lymphoid Stress Surveillance Response with High Interindividual Variation. *Sci. Transl. Med.* 2011;3(113):113ra124-113ra124.
388. Gavlovsky P-J, Tonnerre P, Guitton C, Charreau B. Expression of MHC class I-related molecules MICA, HLA-E and EPCR shape endothelial cells with unique functions in innate and adaptive immunity. *Hum. Immunol.* 2016;77(11):1084–1091.
389. Xu B, Pizarro JC, Holmes MA, et al. Crystal structure of a T-cell receptor specific for the human MHC class I homolog MICA. *Proc. Natl. Acad. Sci.* 2011;108(6):2414–2419.
390. Aleksic M, Liddy N, Molloy PE, et al. Different affinity windows for virus and cancer-specific T-cell receptors: implications for therapeutic strategies. *Eur. J. Immunol.* 2012;42(12):3174–3179.
391. Hayday AC. γδ T Cells and the Lymphoid Stress-Surveillance Response. *Immunity*. 2009;31(2):184–196.
392. Robbins PF, Dudley ME, Wunderlich J, et al. Cutting edge: persistence of transferred lymphocyte clonotypes correlates with cancer regression in patients receiving cell transfer therapy. *J. Immunol. Baltim. Md 1950*. 2004;173(12):7125–7130.
393. Umeshappa CS, Xie Y, Xu S, et al. Th Cells Promote CTL Survival and Memory via Acquired pMHC-I and Endogenous IL-2 and CD40L Signaling and by Modulating Apoptosis-Controlling Pathways. *PLoS ONE*. 2013;8(6):e64787.
394. Wang H, Fang Z, Morita CT. V 2V 2 T Cell Receptor Recognition of Prenyl Pyrophosphates Is Dependent on All CDRs. *J. Immunol.* 2010;184(11):6209–6222.
395. Goodyear O. CD8+T cells specific for cancer germline gene antigens are found in many patients with multiple myeloma, and their frequency correlates with disease burden. *Blood*. 2005;106(13):4217–4224.
396. Kabelitz D, Pechhold K, Bender A, et al. Activation and Activation-Driven Death of Human gammadelta T Cells. *Immunol. Rev.* 1991;120(1):71–88.
397. Neller MA, Sewell AK, Burrows SR, Miles JJ. Tracking the repertoire of human adult and neonatal T cells during *ex vivo* amplification. *Br. J. Haematol.* 2012;159(3):370–373.
398. Schmittel A, Keilholz U, Scheibenbogen C. Evaluation of the interferon-gamma ELISPOT-assay for quantification of peptide specific T lymphocytes from peripheral blood. *J. Immunol. Methods*. 1997;210(2):167–174.
399. Giuntoli RL, Webb TJ, Zoso A, et al. Ovarian cancer-associated ascites demonstrates altered immune environment: implications for antitumor immunity. *Anticancer Res.* 2009;29(8):2875–2884.

400. Germeau C, Ma W, Schiavetti F, et al. High frequency of antitumor T cells in the blood of melanoma patients before and after vaccination with tumor antigens. *J. Exp. Med.* 2005;201(2):241–248.
401. Martina MN, Noel S, Saxena A, Rabb H, Hamad ARA. Double Negative (DN) αβ T Cells: misperception and overdue recognition. *Immunol. Cell Biol.* 2015;93(3):305–310.
402. Mori L, Lepore M, De Libero G. The Immunology of CD1- and MR1-Restricted T Cells. *Annu. Rev. Immunol.* 2016;34(1):479–510.
403. Voelkl S, Moore TV, Rehli M, et al. Characterization of MHC class-I restricted TCRαβ+ CD4− CD8− double negative T cells recognizing the gp100 antigen from a melanoma patient after gp100 vaccination. *Cancer Immunol. Immunother.* 2009;58(5):709–718.
404. Laugel B, Lloyd A, Meermeier EW, et al. Engineering of Isogenic Cells Deficient for MR1 with a CRISPR/Cas9 Lentiviral System: Tools To Study Microbial Antigen Processing and Presentation to Human MR1-Restricted T Cells. *J. Immunol.* 2016;197(3):971–982.
405. Posey AD, Schwab RD, Boesteanu AC, et al. Engineered CAR T Cells Targeting the Cancer-Associated Tn-Glycoform of the Membrane Mucin MUC1 Control Adenocarcinoma. *Immunity*. 2016;44(6):1444–1454.
406. Ledford H. Safety concerns blight promising cancer therapy. *Nature*. 2016;538(7624):150–151.
407. Oren R, Hod-Marco M, Haus-Cohen M, et al. Functional Comparison of Engineered T Cells Carrying a Native TCR versus TCR-like Antibody–Based Chimeric Antigen Receptors Indicates Affinity/Avidity Thresholds. *J. Immunol.* 2014;193(11):5733–5743.
408. Catellani S, Poggi A, Bruzzone A, et al. Expansion of V 1 T lymphocytes producing IL-4 in low-grade non-Hodgkin lymphomas expressing UL-16-binding proteins. *Blood*. 2007;109(5):2078–2085.
409. Siegers GM, Lamb LS. Cytotoxic and Regulatory Properties of Circulating Vδ1+ γδ T Cells: A New Player on the Cell Therapy Field? *Mol. Ther.* 2014;22(8):1416–1422.
410. Betts MR, Brenchley JM, Price DA, et al. Sensitive and viable identification of antigen-specific CD8+ T cells by a flow cytometric assay for degranulation. *J. Immunol. Methods*. 2003;281(1–2):65–78.
411. Dutta I, Postovit L-M, Siegers GM. Apoptosis Induced via Gamma Delta T Cell Antigen Receptor "Blocking" Antibodies: A Cautionary Tale. *Front. Immunol.* 2017;8:.
412. Harly C, Peyrat M-A, Netzer S, et al. Up-regulation of cytolytic functions of human V 2- T lymphocytes through engagement of ILT2 expressed by tumor target cells. *Blood*. 2011;117(10):2864–2873.
413. Trichet V, Benezech C, Dousset C, et al. Complex Interplay of Activating and Inhibitory Signals Received by V 9V 2 T Cells Revealed by Target Cell 2-Microglobulin Knockdown. *J. Immunol.* 2006;177(9):6129–6136.
414. Spencer CT, Abate G, Blazevic A, Hoft DF. Only a subset of phosphoantigen-responsive gamma9delta2 T cells mediate protective tuberculosis immunity. *J. Immunol. Baltim. Md 1950*. 2008;181(7):4471–4484.
415. Starick L, Riano F, Karunakaran MM, et al. Butyrophilin 3A (BTN3A, CD277)-specific antibody 20.1 differentially activates Vγ9Vδ2 TCR clonotypes and interferes with phosphoantigen activation. *Eur. J. Immunol.* 2017;47(6):982–992.
416. Bagchi S, Li S, Wang C-R. CD1b-autoreactive T cells recognize phospholipid antigens and contribute to antitumor immunity against a CD1b $^{+}$ T cell lymphoma. *OncoImmunology*. 2016;5(9):e1213932.
417. Lepore M, de Lalla C, Gundimeda SR, et al. A novel self-lipid antigen targets human T cells against CD1c+ leukemias. *J. Exp. Med.* 2014;211(7):1363–1377.
418. Gorini F, Azzimonti L, Delfanti G, et al. Invariant NKT cells contribute to chronic lymphocytic leukemia surveillance and prognosis. *Blood*. 2017;129(26):3440–3451.
419. Dougan SK, Kaser A, Blumberg RS. CD1 expression on antigen-presenting cells. *Curr. Top. Microbiol. Immunol.* 2007;314:113–141.
420. de Lalla C, Lepore M, Piccolo FM, et al. High-frequency and adaptive-like dynamics of human CD1 self-reactive T cells. *Eur. J. Immunol.* 2011;41(3):602–610.

421. de Jong A, Peña-Cruz V, Cheng T-Y, et al. CD1a-autoreactive T cells are a normal component of the human αβ T cell repertoire. *Nat. Immunol.* 2010;11(12):1102–1109.
422. Shamshiev A, Gober H-J, Donda A, et al. Presentation of the same glycolipid by different CD1 molecules. *J. Exp. Med.* 2002;195(8):1013–1021.
423. Moody DB. T Cell Activation by Lipopeptide Antigens. *Science*. 2004;303(5657):527–531.
424. Birkinshaw RW, Pellicci DG, Cheng T-Y, et al. αβ T cell antigen receptor recognition of CD1a presenting self lipid ligands. *Nat. Immunol.* 2015;16(3):258–266.
425. Szomolay B, Liu J, Brown PE, et al. Identification of human viral protein-derived ligands recognized by individual MHCI-restricted T-cell receptors. *Immunol. Cell Biol.* 2016;94(6):573–582.
426. Boutros M, Ahringer J. The art and design of genetic screens: RNA interference. *Nat. Rev. Genet.* 2008;9(7):554–566.
427. Jackson AL, Linsley PS. Recognizing and avoiding siRNA off-target effects for target identification and therapeutic application. *Nat. Rev. Drug Discov.* 2010;9(1):57–67.
428. Carette JE, Guimaraes CP, Wuethrich I, et al. Global gene disruption in human cells to assign genes to phenotypes by deep sequencing. *Nat. Biotechnol.* 2011;29(6):542–546.
429. Bürckstümmer T, Banning C, Hainzl P, et al. A reversible gene trap collection empowers haploid genetics in human cells. *Nat. Methods*. 2013;10(10):965–971.
430. Barsov EV. Telomerase and primary T cells: biology and immortalization for adoptive immunotherapy. *Immunotherapy*. 2011;3(3):407–421.
431. Jedema I, van der Werff NM, Barge RMY, Willemze R, Falkenburg JHF. New CFSE-based assay to determine susceptibility to lysis by cytotoxic T cells of leukemic precursor cells within a heterogeneous target cell population. *Blood*. 2004;103(7):2677–2682.
432. Petersen TN, Brunak S, von Heijne G, Nielsen H. SignalP 4.0: discriminating signal peptides from transmembrane regions. *Nat. Methods*. 2011;8(10):785–786.
433. Kasof GM, Lu JJ, Liu D, et al. Tumor necrosis factor-α induces the expression of DR6, a member of the TNF receptor family, through activation of NF-κB. *Oncogene*. 2001;20(55):7965–7975.
434. Zaretsky JM, Garcia-Diaz A, Shin DS, et al. Mutations Associated with Acquired Resistance to PD-1 Blockade in Melanoma. *N. Engl. J. Med.* 2016;375(9):819–829.
435. Strehl B, Seifert U, Kruger E, et al. Interferon-gamma, the functional plasticity of the ubiquitin-proteasome system, and MHC class I antigen processing. *Immunol. Rev.* 2005;207(1):19–30.
436. Challa-Malladi M, Lieu YK, Califano O, et al. Combined Genetic Inactivation of β2-Microglobulin and CD58 Reveals Frequent Escape from Immune Recognition in Diffuse Large B Cell Lymphoma. *Cancer Cell*. 2011;20(6):728–740.
437. Cao Y, Zhu T, Zhang P, et al. Mutations or copy number losses of *CD58* and *TP53* genes in diffuse large B cell lymphoma are independent unfavorable prognostic factors. *Oncotarget*. 2016;
438. Vitale G, van Eijck CHJ, van Koetsveld Ing PM, et al. Type I Interferons in the Treatment of Pancreatic Cancer: Mechanisms of Action and Role of Related Receptors. *Ann. Surg.* 2007;246(2):259–268.
439. Maeda S, Wada H, Naito Y, et al. Interferon-α Acts on the S/G_2 /M Phases to Induce Apoptosis in the G_1 Phase of an IFNAR2-expressing Hepatocellular Carcinoma Cell Line. *J. Biol. Chem.* 2014;289(34):23786–23795.
440. Gobin SJ, van Zutphen M, Westerheide SD, Boss JM, van den Elsen PJ. The MHC-specific enhanceosome and its role in MHC class I and beta(2)-microglobulin gene transactivation. *J. Immunol. Baltim. Md 1950*. 2001;167(9):5175–5184.
441. Gremion C, Grabscheid B, Wölk B, et al. Cytotoxic T lymphocytes derived from patients with chronic hepatitis C virus infection kill bystander cells via Fas-FasL interaction. *J. Virol.* 2004;78(4):2152–2157.
442. Sewell AK. Why must T cells be cross-reactive? *Nat. Rev. Immunol.* 2012;12(9):669–677.
443. Edwards PA, Ericsson J. Sterols and Isoprenoids: Signaling Molecules Derived from the Cholesterol Biosynthetic Pathway. *Annu. Rev. Biochem.* 1999;68(1):157–185.

444. Ohashi K, Osuga J, Tozawa R, et al. Early Embryonic Lethality Caused by Targeted Disruption of the 3-Hydroxy-3-methylglutaryl-CoA Reductase Gene. *J. Biol. Chem.* 2003;278(44):42936–42941.
445. Manguso RT, Pope HW, Zimmer MD, et al. In vivo CRISPR screening identifies Ptpn2 as a cancer immunotherapy target. *Nature*. 2017;547(7664):413–418.
446. Patel SJ, Sanjana NE, Kishton RJ, et al. Identification of essential genes for cancer immunotherapy. *Nature*. 2017;548(7669):537–542.
447. Travis J. Making the cut. *Science*. 2015;350(6267):1456–1457.
448. The Lancet. CAR T-cells: an exciting frontier in cancer therapy. *The Lancet*. 2017;390(10099):1006.
449. Maciocia PM, Wawrzyniecka PA, Philip B, Ricciardelli R, Akarca AU, Onuoha S, Legut M,, Cole DK, Sewell AK, Gritti G, Somja J, Piris MA, Peggs KS, Linch DC, Marafioti T, Pule MA. Targeting T-cell receptor β-constant for immunotherapy of T-cell malignancies. *Nat. Med.* 2017;(accepted for publication):
450. Irving M, Vuillefroy de Silly R, Scholten K, Dilek N, Coukos G. Engineering Chimeric Antigen Receptor T-Cells for Racing in Solid Tumors: Don't Forget the Fuel. *Front. Immunol.* 2017;8:.
451. Ruella M, Barrett DM, Kenderian SS, et al. Dual CD19 and CD123 targeting prevents antigen-loss relapses after CD19-directed immunotherapies. *J. Clin. Invest.* 2016;126(10):3814–3826.
452. Mackensen A, Meidenbauer N, Vogl S, et al. Phase I Study of Adoptive T-Cell Therapy Using Antigen-Specific CD8 $^{+}$ T Cells for the Treatment of Patients With Metastatic Melanoma. *J. Clin. Oncol.* 2006;24(31):5060–5069.
453. Debets R, Donnadieu E, Chouaib S, Coukos G. TCR-engineered T cells to treat tumors: Seeing but not touching? *Semin. Immunol.* 2016;28(1):10–21.
454. Obenaus M, Leitão C, Leisegang M, et al. Identification of human T-cell receptors with optimal affinity to cancer antigens using antigen-negative humanized mice. *Nat. Biotechnol.* 2015;33(4):402–407.
455. Morgan RA, Dudley ME, Wunderlich JR, et al. Cancer Regression in Patients After Transfer of Genetically Engineered Lymphocytes. *Science*. 2006;314(5796):126–129.
456. Johnson LA, Morgan RA, Dudley ME, et al. Gene therapy with human and mouse T-cell receptors mediates cancer regression and targets normal tissues expressing cognate antigen. *Blood*. 2009;114(3):535–546.
457. Hudecek M, Sommermeyer D, Kosasih PL, et al. The Nonsignaling Extracellular Spacer Domain of Chimeric Antigen Receptors Is Decisive for In Vivo Antitumor Activity. *Cancer Immunol. Res.* 2015;3(2):125–135.
458. Porter DL, Hwang W-T, Frey NV, et al. Chimeric antigen receptor T cells persist and induce sustained remissions in relapsed refractory chronic lymphocytic leukemia. *Sci. Transl. Med.* 2015;7(303):303ra139-303ra139.
459. Barrett DM, Singh N, Liu X, et al. Relation of clinical culture method to T-cell memory status and efficacy in xenograft models of adoptive immunotherapy. *Cytotherapy*. 2014;16(5):619–630.
460. Li Y, Zhi W, Wareski P, Weng N -p. IL-15 Activates Telomerase and Minimizes Telomere Loss and May Preserve the Replicative Life Span of Memory CD8+ T Cells In Vitro. *J. Immunol.* 2005;174(7):4019–4024.
461. Hurton LV, Singh H, Najjar AM, et al. Tethered IL-15 augments antitumor activity and promotes a stem-cell memory subset in tumor-specific T cells. *Proc. Natl. Acad. Sci.* 2016;113(48):E7788–E7797.
462. Terakura S, Yamamoto TN, Gardner RA, et al. Generation of CD19-chimeric antigen receptor modified CD8+ T cells derived from virus-specific central memory T cells. *Blood*. 2012;119(1):72–82.
463. Xu Y, Zhang M, Ramos CA, et al. Closely related T-memory stem cells correlate with in vivo expansion of CAR.CD19-T cells and are preserved by IL-7 and IL-15. *Blood*. 2014;123(24):3750–3759.

464. Borkner L, Kaiser A, van de Kasteele W, et al. RNA interference targeting programmed death receptor-1 improves immune functions of tumor-specific T cells. *Cancer Immunol. Immunother.* 2010;59(8):1173–1183.
465. Cherkassky L, Morello A, Villena-Vargas J, et al. Human CAR T cells with cell-intrinsic PD-1 checkpoint blockade resist tumor-mediated inhibition. *J. Clin. Invest.* 2016;126(8):3130–3144.
466. Brudno JN, Kochenderfer JN. Toxicities of chimeric antigen receptor T cells: recognition and management. *Blood*. 2016;127(26):3321–3330.
467. Lim WA, June CH. The Principles of Engineering Immune Cells to Treat Cancer. *Cell*. 2017;168(4):724–740.
468. Mikucki ME, Fisher DT, Matsuzaki J, et al. Non-redundant requirement for CXCR3 signalling during tumoricidal T-cell trafficking across tumour vascular checkpoints. *Nat. Commun.* 2015;6:7458.
469. Miller AM, Lundberg K, Ozenci V, et al. CD4+CD25high T Cells Are Enriched in the Tumor and Peripheral Blood of Prostate Cancer Patients. *J. Immunol.* 2006;177(10):7398–7405.
470. Gobert M, Treilleux I, Bendriss-Vermare N, et al. Regulatory T Cells Recruited through CCL22/CCR4 Are Selectively Activated in Lymphoid Infiltrates Surrounding Primary Breast Tumors and Lead to an Adverse Clinical Outcome. *Cancer Res.* 2009;69(5):2000–2009.
471. Facciabene A, Peng X, Hagemann IS, et al. Tumour hypoxia promotes tolerance and angiogenesis via CCL28 and Treg cells. *Nature*. 2011;475(7355):226–230.
472. Tan MCB, Goedegebuure PS, Belt BA, et al. Disruption of CCR5-Dependent Homing of Regulatory T Cells Inhibits Tumor Growth in a Murine Model of Pancreatic Cancer. *J. Immunol.* 2009;182(3):1746–1755.
473. Rosenberg SA, Yang JC, Sherry RM, et al. Durable Complete Responses in Heavily Pretreated Patients with Metastatic Melanoma Using T-Cell Transfer Immunotherapy. *Clin. Cancer Res.* 2011;17(13):4550–4557.
474. Kershaw MH, Wang G, Westwood JA, et al. Redirecting Migration of T Cells to Chemokine Secreted from Tumors by Genetic Modification with CXCR2. *Hum. Gene Ther.* 2002;13(16):1971–1980.
475. Peng W, Ye Y, Rabinovich BA, et al. Transduction of Tumor-Specific T Cells with CXCR2 Chemokine Receptor Improves Migration to Tumor and Antitumor Immune Responses. *Clin. Cancer Res.* 2010;16(22):5458–5468.
476. Moon EK, Carpenito C, Sun J, et al. Expression of a Functional CCR2 Receptor Enhances Tumor Localization and Tumor Eradication by Retargeted Human T cells Expressing a Mesothelin-Specific Chimeric Antibody Receptor. *Clin. Cancer Res.* 2011;17(14):4719–4730.
477. Di Stasi A, De Angelis B, Rooney CM, et al. T lymphocytes coexpressing CCR4 and a chimeric antigen receptor targeting CD30 have improved homing and antitumor activity in a Hodgkin tumor model. *Blood*. 2009;113(25):6392–6402.
478. Shah NN, Baird K, Delbrook CP, et al. Acute GVHD in patients receiving IL-15/4-1BBL activated NK cells following T-cell-depleted stem cell transplantation. *Blood*. 2015;125(5):784–792.
479. Ledford H. Broad Institute wins bitter battle over CRISPR patents. *Nature*. 2017;542(7642):401–401.

8. Appendix

Table 8.1 Sequences of primers used for PCR and Sanger sequencing.

Primer name	Sequence (5'-3')	Application
TRD R1	CAGTCTTTGCAAACAGCATTC	*trd PCR*
TRD R2	ATGGTTTGGTATGAGGCTGAC	*trd PCR*
TRG R1	CATGTCTGACGATACATCTGTG	*trg PCR*
TRG R2	ACATCTGCATCAAGTTGTTTAT	*trg PCR*
UPM F	CTAATACGACTCACTATAGGGC AAGCAGTGGTATCAACGCAGAGT	*trd/trg PCR*
Short UPM F	CTAATACGACTCACTATAGGGC	*trd/trg PCR*
M13 F	GTAAAACGACGGCCAG	*TOPO PCR and sequencing*
M13 R	CAGGAAACAGCTATGAC	*TOPO PCR and sequencing*
pELNS F1	GAGTTTGGATCTTGGTTCATTC	*pELNS PCR*
pELNS F2	CTTCCATTTCAGGTGTCGTG	*pELNS sequencing*
pELNS R1	GCATTAAAGCAGCGTATCCAC	*pELNS PCR*
pELNS R2	CCAGAGGTTGATTGTCGAC	*pELNS sequencing*
pELNS R3	AGAAACTTGCACCGCATATG	*pELNS sequencing*
GeCKO F1	AATGGACTATCATATGCTTACCGTAACTTGAA AGTATTTCG	*pLentiCRISPR PCR and sequencing*
GeCKO R1	TGTGGGCGATGTGCGCTCTG	*pLentiCRISPR PCR*
GeCKO F2	TCTTGTGGAAAGGACGAAACACCG	*pLentiCRISPR PCR*
GeCKO R2	ACCGGAGCCAATTCCCACTCCTTTC	*pLentiCRISPR PCR*
GeCKO seq	AAAAGCACCGACTCGGTGCCAC	*pLentiCRISPR PCR and sequencing*
C1orf74 F	ATTCCCTGCTCCTGCTTTGTTTC	*c1orf74 PCR*
C1orf74 R	CTACAGCATTGTGCCTTAGTG	*c1orf74 PCR*
C1orf74 seq	CAACCTAGAGATGATCATTTAC	*c1orf74 sequencing*
Adaptor F	AATGGACTATCATATGCTTACCGTAACTTGAA AGTATTTCG	*GeCKO library PCR*
Adaptor R	TCTACTATTCTTTCCCCTGCACTGTTGTGGGC GATGTGCGCTCTG	*GeCKO library PCR*

Table 8.2 Amino acid sequence of γδ TCRs synthesised and cloned into the lentiviral vector pELNS. CDR3 sequences are underlined while the constant domains are shown in colour (blue – TRGC1, red – TRDC), and the 2A sequence with linker is shown in grey.

γδ20 TCR:

MLSLLHTSTLAVLGALCVYGAGHLEQPQISSTKTLSKTARLECVVSGITISATSVYWYRERPGEVIQFLVSISYDGTVRK
ESGIPSGKFEVDRIPETSTSTLTIHNVEKQDIATYYCALWEVHQELGKKIKVFGPGTKLIITDKQLDADVSPKPTIFLPSI
AETKLQKAGTYLCLLEKFFPDVIKIHWQEKKSNTILGSQEGNTMKTNDTYMKFSWLTVPEKSLDKEHRCIVRHENNK
NGVDQEIIFPPIKTDVITMDPKDNCSKDANDTLLLQLTNTSAYYMYLLLLLKSVVYFAIITCCLLRRTAFCCNGEKSGS
GSGEGRGSLLTCGDVEENPGPMQRISSLIHLSLFWAGVMSAIELVPEHQTVPVSIGVPATLRCSMKGEAIGNYYIN
WYRKTQGNTMTFIYREKDIYGPGFKDNFQGDIDIAKNLAVLKILAPSERDEGSYYCACDTVTGGFRPNTDKLIFGKG
TRVTVEPRSQPHTKPSVFVMKNGTNVACLVKEFYPKDIRINLVSSKKITEFDPAIVISPSGKYNAVKLGKYEDSNSVTC
SVQHDNKTVHSTDFEVKTDSTDHVKPKETENTKQPSKSCHKPKAIVHTEKVNMMSLTVLGLRMLFAKTVAVNFLL
TAKLFFL

ML5.15 TCR:

MLSLLHTSTLAVLGALCVYGAGHLEQPQISSTKTLSKTARLECVVSGITISATSVYWYRERPGEVIQFLVSISYDGTVRK
ESGIPSGKFEVDRIPETSTSTLTIHNVEKQDIATYYCALWGSLYYKKLFGSGTTLVVTDKQLDADVSPKPTIFLPSIAETK
LQKAGTYLCLLEKFFPDVIKIHWQEKKSNTILGSQEGNTMKTNDTYMKFSWLTVPEKSLDKEHRCIVRHENNKNGV
DQEIIFPPIKTDVITMDPKDNCSKDANDTLLLQLTNTSAYYMYLLLLLKSVVYFAIITCCLLRRTAFCCNGEKSGSGEGR
GSLLTCGDVEENPGPMLFSSLLCVFVAFSYSGSSVAQKVTQAQSSVSMPVRKAVTLNCLYETSWWSYYIFWYKQLP
SKEMIFLIRQGSDEQNAKSGRYSVNFKKAAKSVALTISALQLEDSAKYFCALGEEWGHTDLGQRFYTDKLIFGKGTR
VTVEPRSQPHTKPSVFVMKNGTNVACLVKEFYPKDIRINLVSSKKITEFDPAIVISPSGKYNAVKLGKYEDSNSVTCSV
QHDNKTVHSTDFEVKTDSTDHVKPKETENTKQPSKSCHKPKAIVHTEKVNMMSLTVLGLRMLFAKTVAVNFLLTA
KLFFL

ML15.15 TCR:

MLSLLHTSTLAVLGALCVYGAGHLEQPQISSTKTLSKTARLECVVSGITISATSVYWYRERPGEVIQFLVSISYDGTVRK
ESGIPSGKFEVDRIPETSTSTLTIHNVEKQDIATYYCALWEVQELGKKIKVFGPGTKLIITDKQLDADVSPKPTIFLPSIA
ETKLQKAGTYLCLLEKFFPDVIKIHWQEKKSNTILGSQEGNTMKTNDTYMKFSWLTVPEKSLDKEHRCIVRHENNK
NGVDQEIIFPPIKTDVITMDPKDNCSKDANDTLLLQLTNTSAYYMYLLLLLKSVVYFAIITCCLLRRTAFCCNGEKSGS
GSGEGRGSLLTCGDVEENPGPMQRISSLIHLSLFWAGVMSAIELVPEHQTVPVSIGVPATLRCSMKGEAIGNYYIN
WYRKTQGNTMTFIYREKDIYGPGFKDNFQGDIDIAKNLAVLKILAPSERDEGSYYCACDLLYWGTPTTDKLIFGKGT
RVTVEPRSQPHTKPSVFVMKNGTNVACLVKEFYPKDIRINLVSSKKITEFDPAIVISPSGKYNAVKLGKYEDSNSVTCS
VQHDNKTVHSTDFEVKTDSTDHVKPKETENTKQPSKSCHKPKAIVHTEKVNMMSLTVLGLRMLFAKTVAVNFLLT
AKLFFL

BC1.18 TCR:

MLSLLHASTLAVLGALCVYGAGHLEQPQISSTKTLSKTARLECVVSGITISATSVYWYRERPGEVIQFLVSISYDGTVR
KESGIPSGKFEVDRIPETSTSTLTIHNVEKQDIATYYCALWELLDYYKKLFGSGTTLVVTDKQLDADVSPKPTIFLPSIAE
TKLQKAGTYLCLLEKFFPDVIKIHWQEKKSNTILGSQEGNTMKTNDTYMKFSWLTVPEKSLDKEHRCIVRHENNKN
GVDQEIIFPPIKTDVITMDPKDNCSKDANDTLLLQLTNTSAYYMYLLLLLKSVVYFAIITCCLLRRTAFCCNGEKSGSGS
GEGRGSLLTCGDVEENPGPMLFSSLLCVFVAFSYSGSSVAQKVTQAQSSVSMPVRKAVTLNCLYETSWWSYYIFW
YKQLPSKEMIFLIRQGSDEQNAKSGRYSVNFKKAAKSVALTISALQLEDSAKYFCALAPRVALVPERLIFGKGTRVTVE
PRSQPHTKPSVFVMKNGTNVACLVKEFYPKDIRINLVSSKKITEFDPAIVISPSGKYNAVKLGKYEDSNSVTCSVQHD
NKTVHSTDFEVKTDSTDHVKPKETENTKQPSKSCHKPKAIVHTEKVNMMSLTVLGLRMLFAKTVAVNFLLTAKLF

CMV1530 TCR:

MLLALALLLAFLPPASQKSSNLEGRTKSVTRPTGSSAVITCDLPVENAVYTHWYLHQEGKAPQRLLYYDSYNSRVVLE
SGISREKYHTYASTGKSLKFILENLIERDSGVYYCATWDYYKKLFGSGTTLVVTDKQLDADVSPKPTIFLPSIAETKLQK
AGTYLCLLEKFFPDVIKIHWQEKKSNTILGSQEGNTMKTNDTYMKFSWLTVPEKSLDKEHRCIVRHENNKNGVDQE
IIFPPIKTDVITMDPKDNCSKDANDTLLLQLTNTSAYYMYLLLLLKSVVYFAIITCCLLRRTAFCCNGEKSGSGSGEGRG
SLLTCGDVEENPGPMLFSSLLCVFVAFSYSGSSVAQKVTQAQSSVSMPVRKAVTLNCLYETSWWSYYIFWYKQLPS
KEMIFLIRQGSDEQNAKSGRYSVNFKKAAKSVALTISALQLEDSAKYFCALGESPISYYWGIRGTDKLIFGKGTRVTVE
PRSQPHTKPSVFVMKNGTNVACLVKEFYPKDIRINLVSSKKITEFDPAIVISPSGKYNAVKLGKYEDSNSVTCSVQHD
NKTVHSTDFEVKTDSTDHVKPKETENTKQPSKSCHKPKAIVHTEKVNMMSLTVLGLRMLFAKTVAVNFLLTAKLFF

Table 8.3 Amino acid sequence of γδ TCRs synthesised and cloned into the lentiviral vector pELNS. CDR3 sequences are underlined while the constant domains are shown in colour (blue – TRAC, red – TRBC2), and the 2A sequence with linker is shown in grey.

Mel13 TCR:

MMKSLRVLLVILWLQLSWVWSQQKEVEQNSGPLSVPEGAIASLNCTYSDRGSQSFFWYRQYSGKSPELIMFIYSN
GDKEDGRFTAQLNKASQYVSLLIRDSQPSDSATYLCAVNVAGKSTFGDGTTLTVKPNIQNPDPAVYQLRDSKSSDK
SVCLFTDFDSQTNVSQSKDSDVYITDKTVLDMRSMDFKSNSAVAWSNKSDFACANAFNNSIIPEDTFFPSPESSCD
VKLVEKSFETDTNLNFQNLSVIGFRILLLKVAGFNLLMTLRLWSSSGSGEGRGSLLTCGDVEENPGPMLCSLLALLLG
TFFGVRSQTIHQWPATLVQPVGSPLSLECTVEGTSNPNLYWYRQAAGRGLQLLFYSVGIGQISSEVPQNLSASRPQ
DRQFILSSKKLLLSDSGFYLCAWSETGLGTGELFFGEGSRLTVLEDLKNVFPPEVAVFEPSEAEISHTQKATLVCLATGF
YPDHVELSWWVNGKEVHSGVCTDPQPLKEQPALNDSRYCLSSRLRVSATFWQNPRNHFRCQVQFYGLSENDEW
TQDRAKPVTQIVSAEAWGRADCGFTSESYQQGVLSATILYEILLGKATLYAVLVSALVLMAMVKRKD

C1orf74:

MLLLDLMSSPSPQLLVAAAQQTLGMGKRRSPPQAICLHLAGEVAVARGLKPAVLYDCNCAGASELQSYLEELKGLG
FLTFGLHILEIGENLIVSPEHVCQHLEQVLLGTIAFVDVSSCQRHPSVCSLDQLQDLKALVAEIITHLQGLQRDLSLAVS
YSRLHSSDWNLCTVFGILLGYPVPYTFHLNQGDDNCLALTPLRVFTARISWLLGQPPILLYSFSVPESLFPGLRILNTW
EKDLRTRFRTQNDFADLSISSEIVTLPAVAL

Table 8.4 Guide RNA sequences for CRISPR/Cas9 knock-outs. PAM sequences are not shown.

gRNA	Sequence (5'-3')
TCR-β g1	CAAACACAGCGACCTCGGGT
TCR-β g2	TGGCTCAAACACAGCGACCT
TCR-β g3	AGCTCAGCTCCACGTGGTCG
TCR-β g4	GCGGCTGCTCAGGCAGTATC
BTN3 g1	AGGCAGAGTGCACCGTATCG
BTN3 g3	CTGCACTCATGGTCGGGAAC
EPCR g2	TCCGCGACCCCTATCACGTG
EPCR g4	TACCAGGGCAACGCGTCGCT
MICA/B g1	CAGTCTTCGTTATAACCTCA
MICA/B g3	AGGTTATAACGAAGACTGTG
β2m g1	ACTCACGCTGGATAGCCTCC
CD1a g1	ATGACCGAATGGTGCGTATA
CD1a g2	TATTCCGTATACGCACCATT
CD1b g1	AAAGGAGGTCGGCCCCTGGA
CD1b g2	TAAGGAGGTTGCTGAGTTAG
CD1c g1	TGCCCTTGGACCAGTTATGC
CD1c g2	GTCAACCAATCCTGGGCACG
CD1d g1	GGCGAATTCCTTCACGTCCC
CD1d g2	ACCGACGGCTTGGCGTGGCT
C1orf74 g1	GAGCAAGGCGGTCACTGGTA
C1orf74 g2	GCTGCTGTCCAACCCGACGT
C1orf74 g3	TCCGATCCAGCGGCGACACC
C1orf74 g4	TCAGGACTTGAAGGCCCTCG
C1orf74 g5	GTCCCAGAGAGTTTGTTCCC
C1orf74 g6	AGCAGACAGAAGGGTGACGC
JAK1 g1	TCTCGTCATACAGGGCAAAG
C10orf62 g1	ACATAGAGACCTTCACCACG

Table 8.5 Primer sequences for HiSeq (Illumina) sequencing of GeCKO libraries.

Primer name	Illumina P5 and seq F	stagger	barcode F	priming site
Illumina F01	AATGATACGGCGACCACCGAGATCTACACTCTTTCCCTACACGACGCTCTTCCGATCT	T	AAGTAGAG	TCTTGTGGAAAGGACGAAACACC
Illumina F02		AT	CATGCTTA	
Illumina F03		GAT	GCACATCT	
Illumina F04		CGAT	TGCTCGAC	

Primer name	Illumina P7	barcode R	Illumina seq R	priming site
Illumina R01	CAAGCAGAAGACGGCATACGAGAT	TCGCCTTG	GTGACTGGAGTTCAGACGTG	CCGACTCGGTGCCACTTTTTCAA
Illumina R02		ATAGCGTC	TGCTCTTCCGATCT	

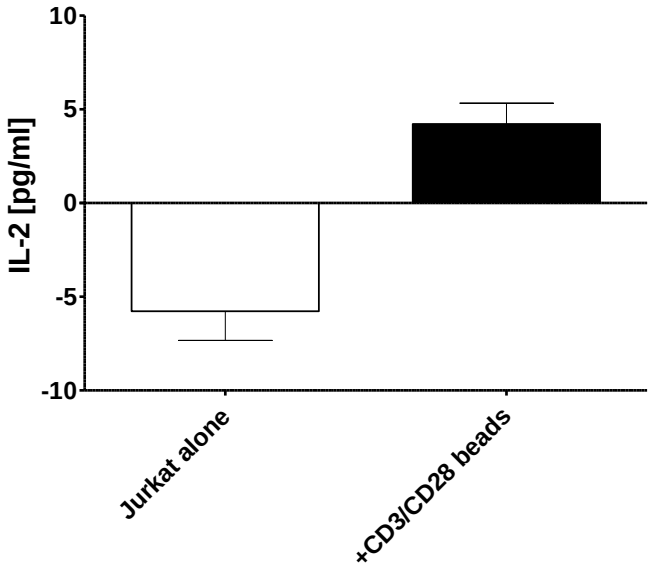

Figure 8.1 IL-2 production by Jurkat cell line. TCR-proficient Jurkat cells were incubated for 16 h, alone or with CD3/CD28 Activator beads. Following incubation, IL-2 concentration in the supernatant was quantified. Standard error of the mean is shown.

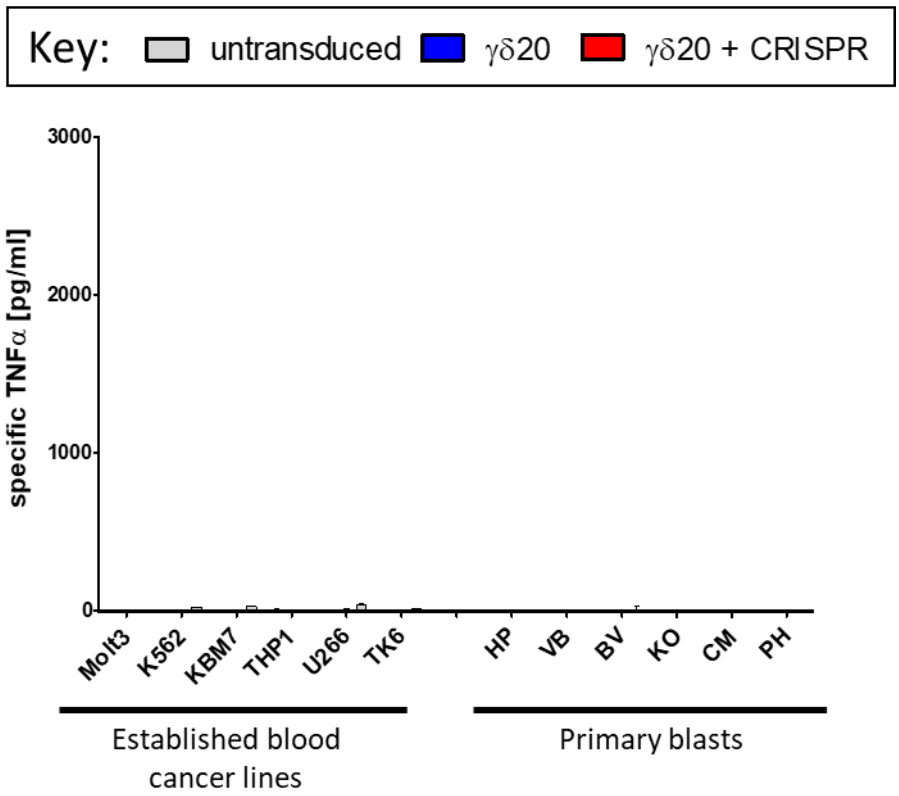

Figure 8.2 γδ20 TCR transduced cells do not recognise haematological malignancies in absence of aminobisphosphonate treatment. TNFα secretion by γδ20 TCR transduced $CD8^+$ T-cells in response to a panel of established blood cancer cell lines of diverse myeloid or lymphoid lineages, as well as primary B lymphoblastic leukaemia blasts. Specific TNFα secretion was calculated by subtracting TNFα secreted from cancer lines alone, and T-cells alone. Representative data from two experiments carried out in duplicate are shown.

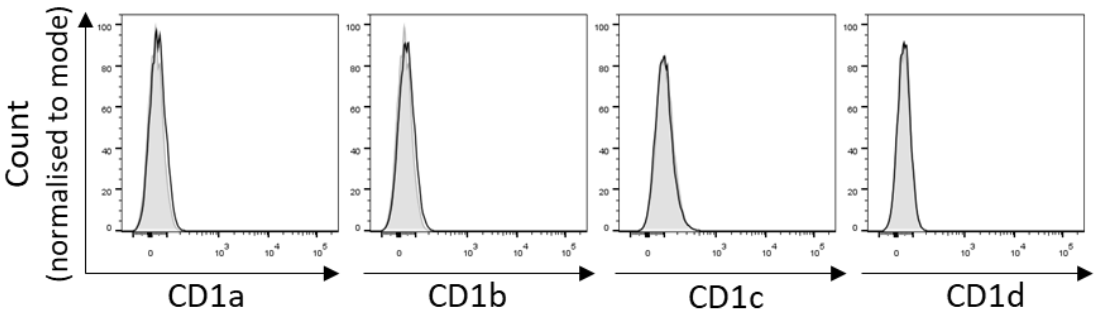

Figure 8.3 Melanoma cell line t15 does not express detectable quantities of CD1 family members. T15 was stained for CD1a-CD1d surface expression by flow cytometry. Only live events were included in the analysis. Unstained cells are shown as a grey histogram while cells stained with CD1 antibodies are shown as a black histogram.

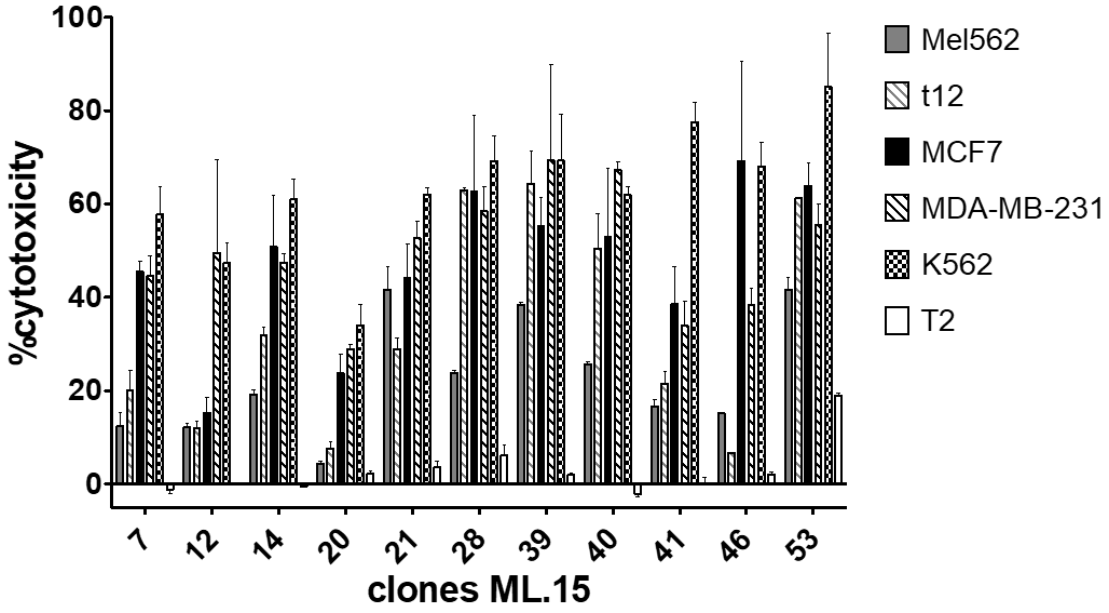

Figure 8.4 MM TIL 15 derived γδ T-cell clones lyse allogeneic cancer cell lines. Cytotoxicity of autologous tumour-reactive γδ T-cell clones from MM TIL 15 was determined by ^{51}Cr release after 4 h co-incubation with cancer cell lines at effector to target ratio of 10:1. Mel562 and t12 are melanoma cell lines, MCF7 and MDA-MB-231 are breast cancer cell lines, K562 is a leukaemia cell line, and T2 is a lymphoblast cell line.

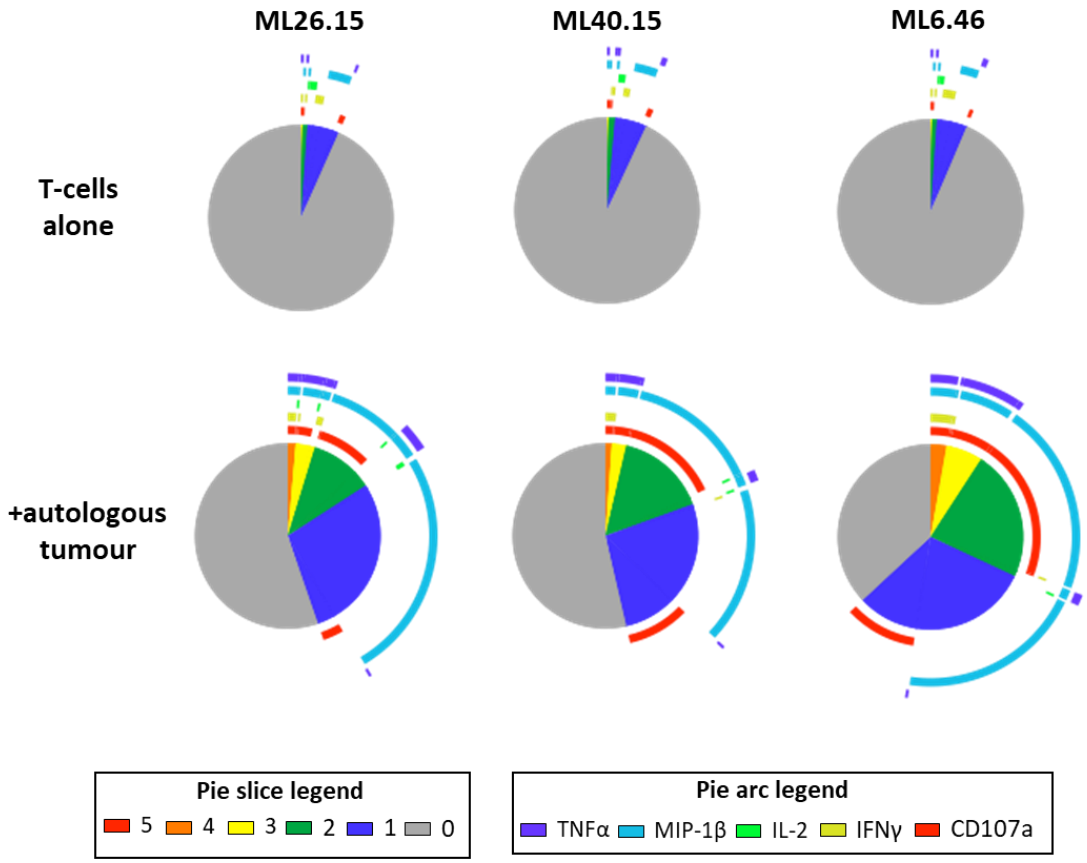

Figure 8.5 TIL-derived γδ T-cell clones show polyfunctional response to the autologous tumour. Polyfunctional profile of response of representative γδ T-cell clones to autologous tumours was determined by intracellular cytokine staining after 5 h of co-incubation. Only viable $CD3^+$ cells were included in the analysis, and the gates were set based on appropriate biological and fluorescence minus one controls. Pie slices represent fractions of cells positive for a given number of effector functions simultaneously, while arcs specify the effector function.

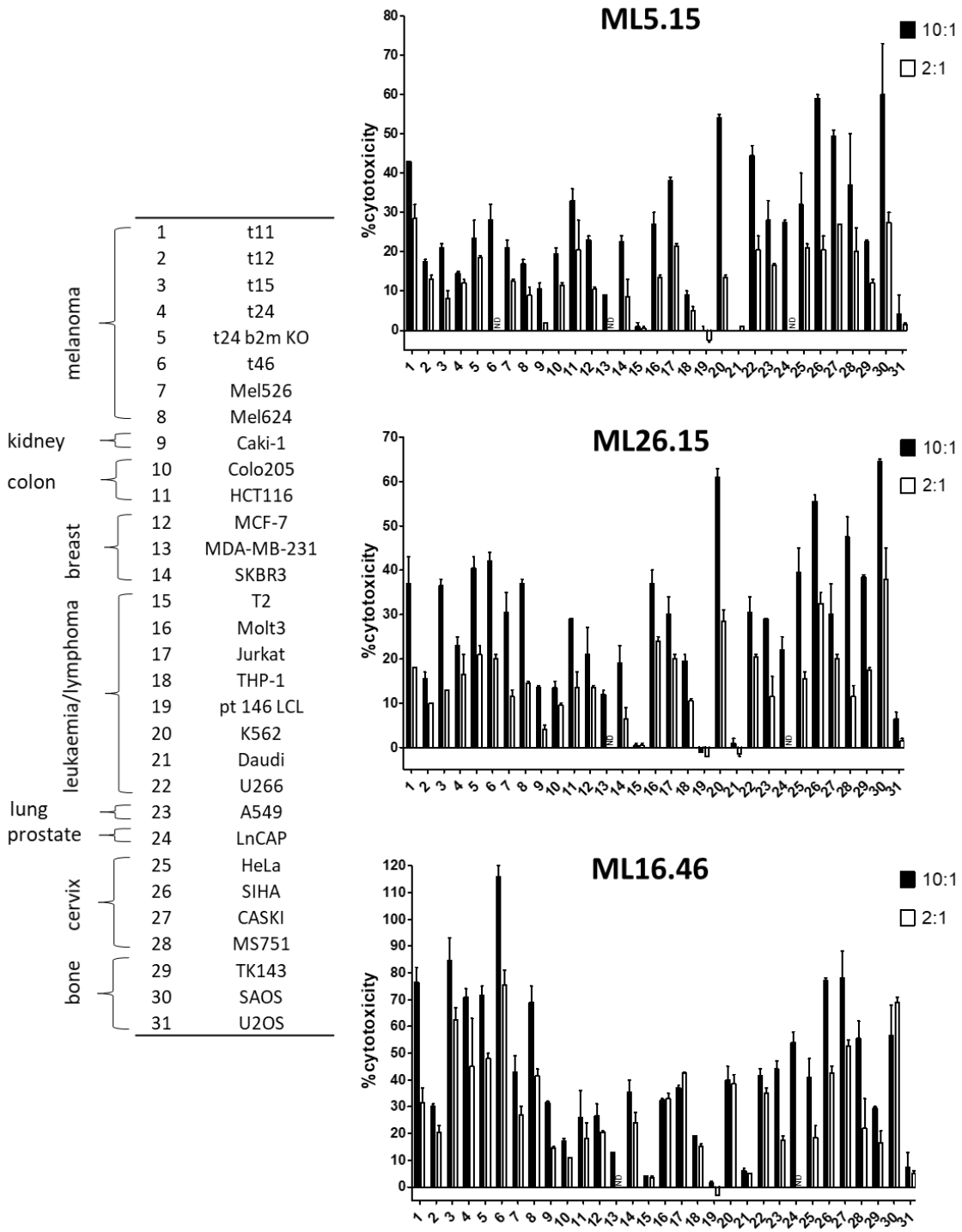

Figure 8.6 TIL-derived γδ T-cell clones recognise cancer cell lines of diverse origin. Cytotoxicity against a panel of cancer cell lines (listed on the left hand side) was determined by ^{51}Cr release after 6 h of co-incubation with T-cells at 10:1 and 2:1 effector to target ratio. ND – not determined.

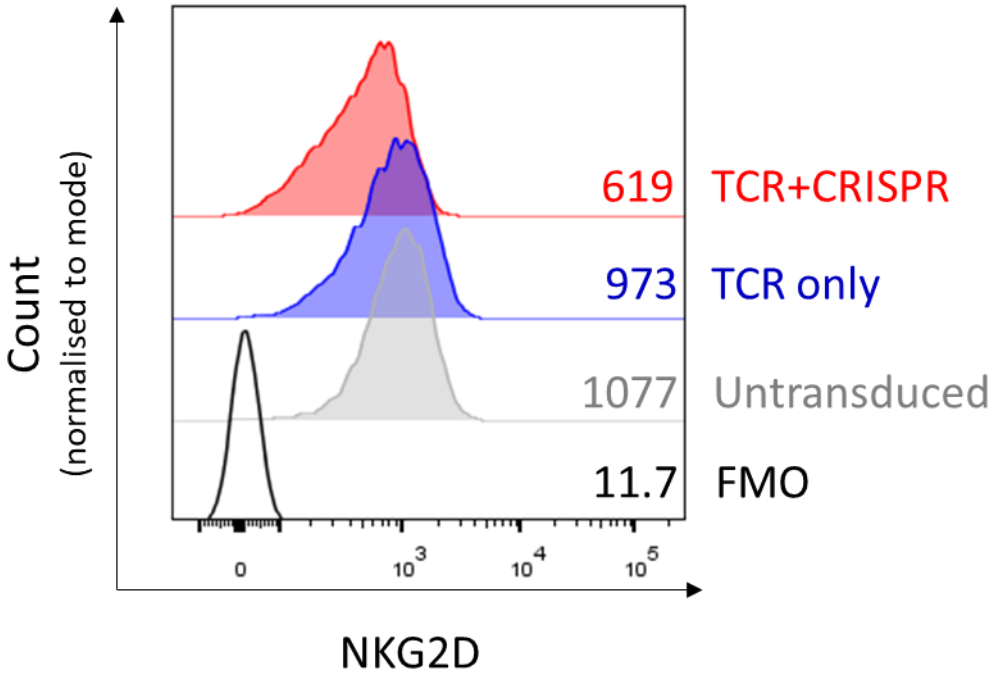

Figure 8.7 NKG2D is expressed by TCR-transduced and untransduced CD8$^+$ T-cells. Primary CD8$^+$ αβ T-cells, transduced with TCR only or TCR+TCR-β CRISPR, or the untransduced control, were stained for NKG2D surface expression. Only viable CD3+ T-cells were included in the analysis. The numbers on histograms correspond to the MFI of staining. FMO – fluorescence minus one (unstained control).

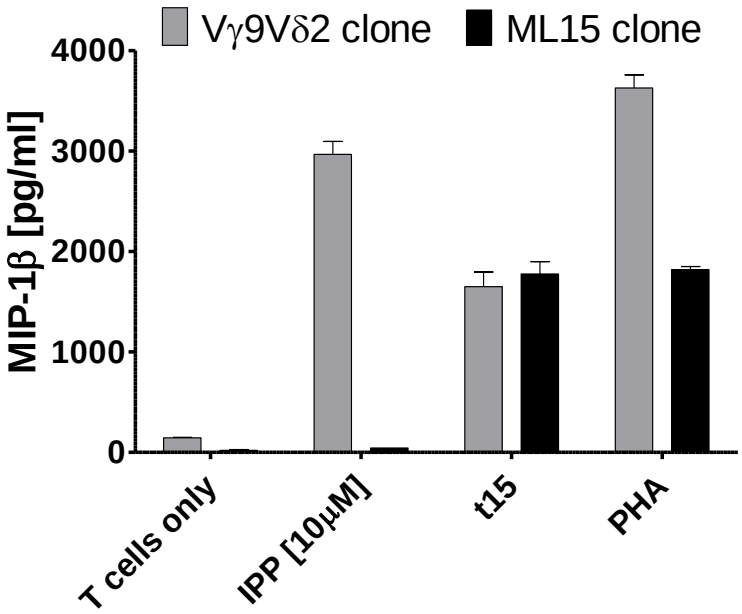

Figure 8.8 TIL-derived Vγ9Vδ2 clone ML15 fails to self-present the mammalian phosphoantigen IPP. Clone ML15 and a conventional, peripheral blood derived Vγ9Vδ2 clone were stimulated 10 μM IPP for 16 h, followed by quantification of secreted MIP-1β. Autologous tumour t15 and non-specific T-cell activator PHA were included as positive controls.

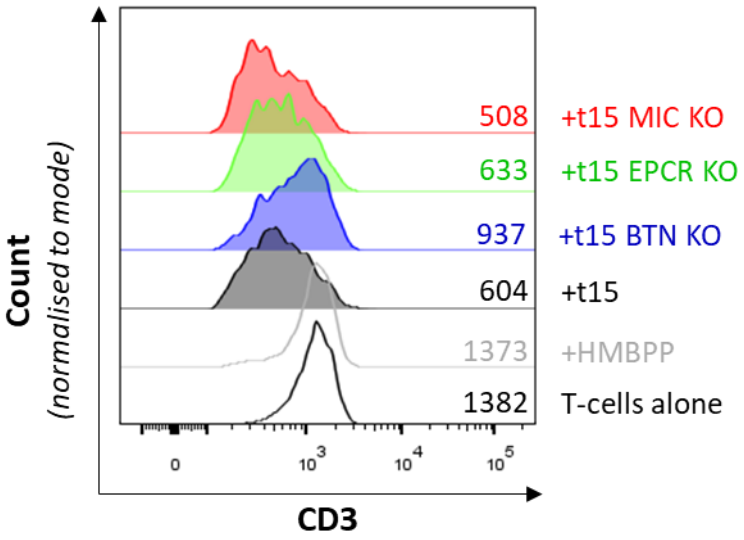

Figure 8.9 Clone ML15 shows a smaller degree of TCR down-regulation in response to BTN3 knock-out compared with the parental tumour t15. Clone ML15 was co-incubated with 1 μM HMBPP, or autologous tumour (wild type or deficient in BTN3, EPCR or MICA/B) for 5 h. Only live $CD3^+$ cells were taken for the analysis. The numbers on histograms indicate the MFI of CD3 staining.

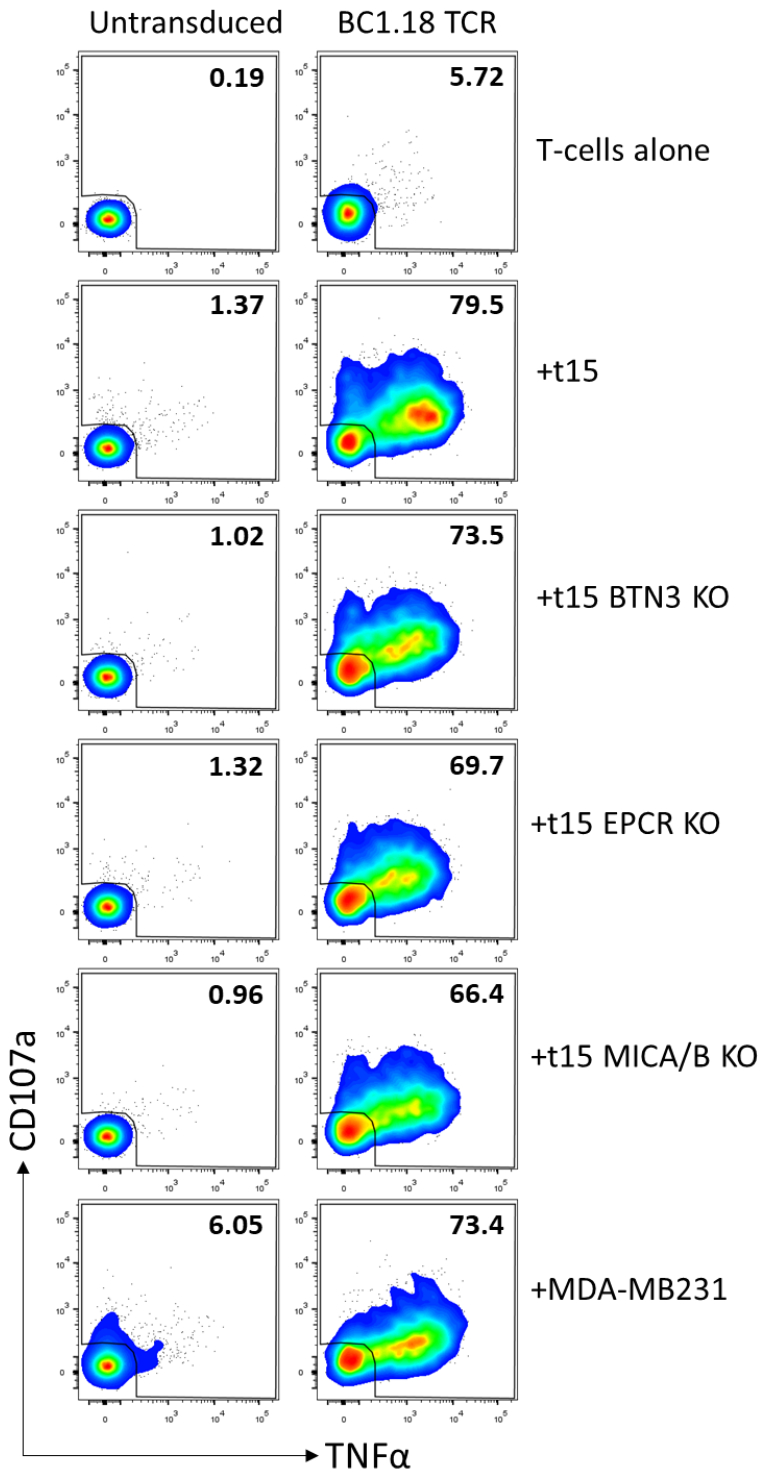

Figure 8.10 BC.18 TCR-transduced cells recognise do not require BTN3, EPCR or MICA/B for cancer cell recognition. Primary CD8+ T-cells, either untransduced or transduced with BC1.18 TCR, were co-incubated with melanoma cell line t15 (wild type or deficient in BTN3, EPCR or MICA/B) for 5 h. MDA-MB231 breast cancer cell line was included as a positive control. Only live $CD3^{+}$ cells were taken for the analysis. The numbers on dot plots correspond to the percentage of gated populations.

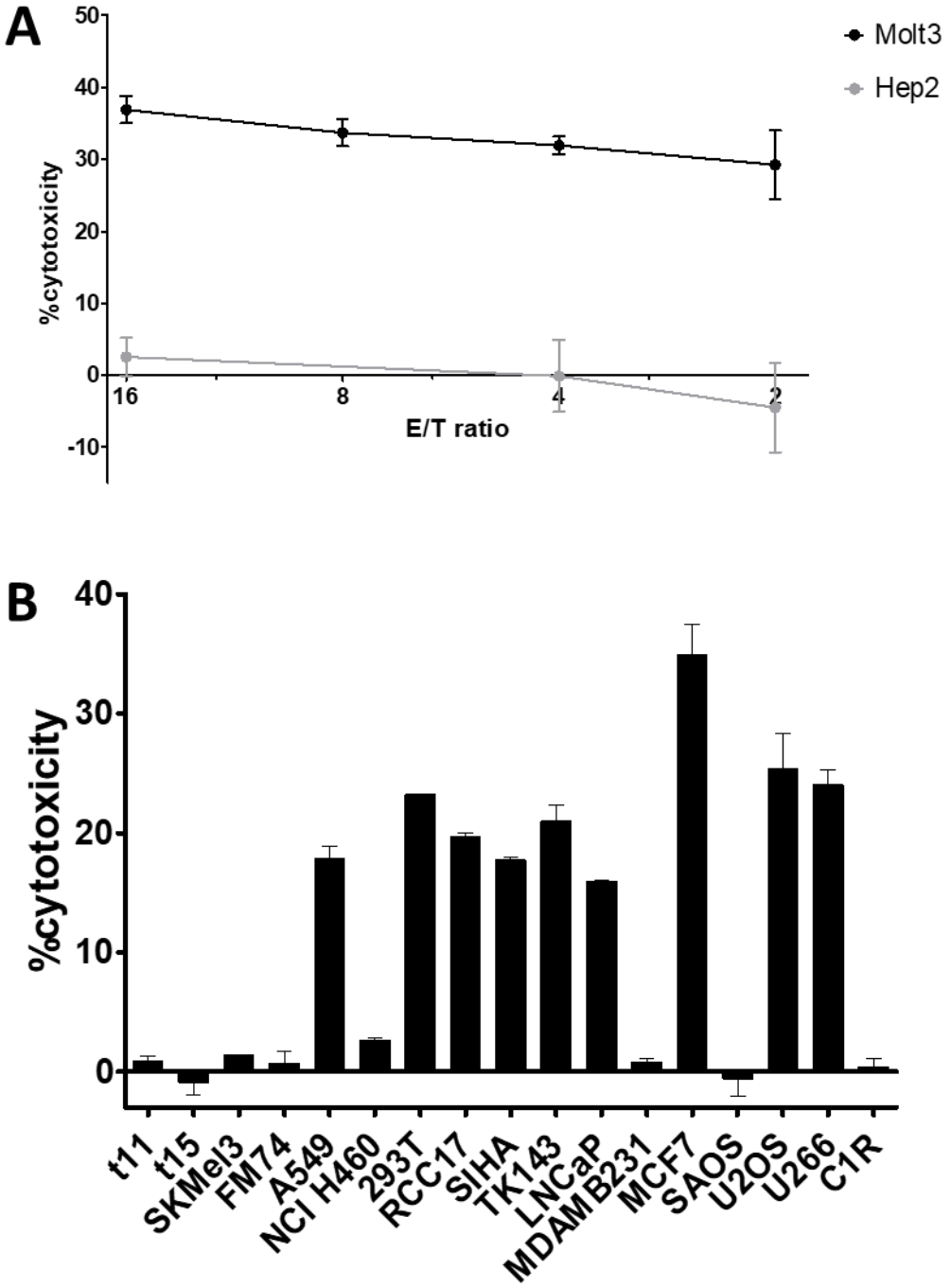

Figure 8.11 Cancer reactive clone 40E.22 DN lyses diverse cancer cell lines, but not normal cells. (**A**) Clone 40E.22 DN was co-incubated with Molt-3 cell line or normal hepatocyte cell line Hep2 for 4 h at different effector to target ratios. The cytotoxicity was determined by 51Cr release assay. (**B**) Clone 40E.22 DN was co-incubated with diverse cancer cell lines for 4 h at 2:1 effector to target ratio. The cytotoxicity was determined by ^{51}Cr release assay.

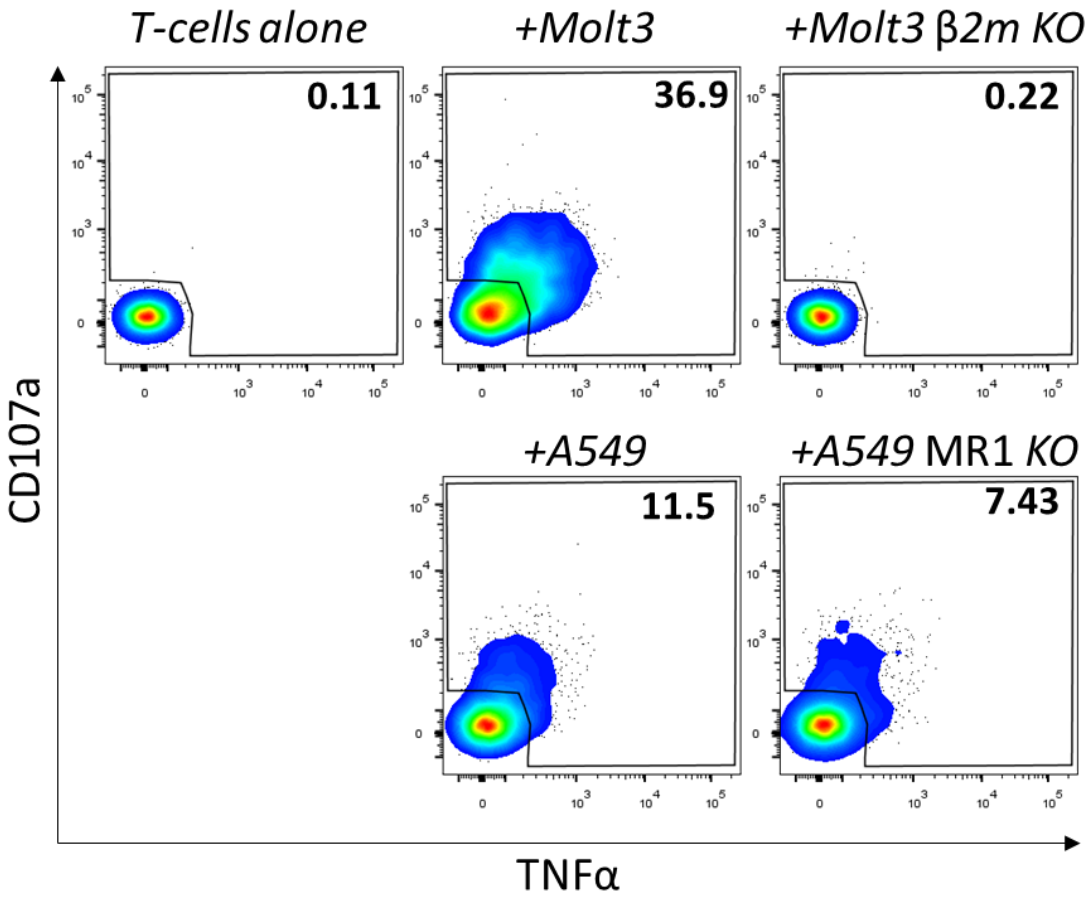

Figure 8.12 Cancer reactive clone 40E.22 DN does not require MR1 expression on target cells for target recognition. Clone 40E.22 was co-incubated with a lung cancer line A549, either wild type or deficient in MR1, for 5 h. Molt-3 cell lines, wild type or deficient in β2m, were used as a positive and a negative control, respectively. Only live $CD3^+$ cells were taken for the analysis. The numbers on dot plots correspond to the percentage of gated populations.

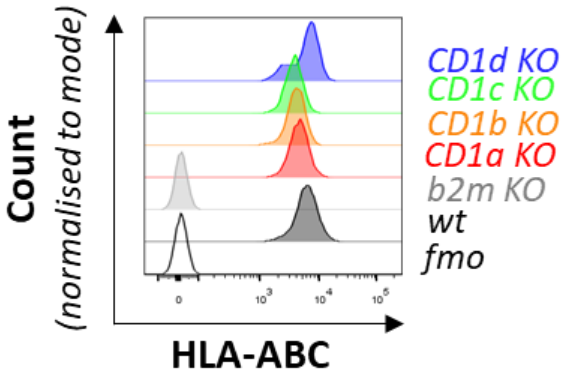

Figure 8.13 CD1 knock-outs do not abrogate the surface expression of MHC-Ia molecules HLA-A, B and C. gRNAs targeting CD1a, CD1b, CD1c and CD1d were transduced into Molt-3 cell line together with Cas9 protein by electroporation. After 14 days, the cells were subjected to single cell cloning. The clones were then stained for HLA-ABC. Unstained Molt-3 cell line (fmo) and β2m knockout (b2m KO) were used as negative controls while wild type Molt-3 cell line was shown as a positive control.

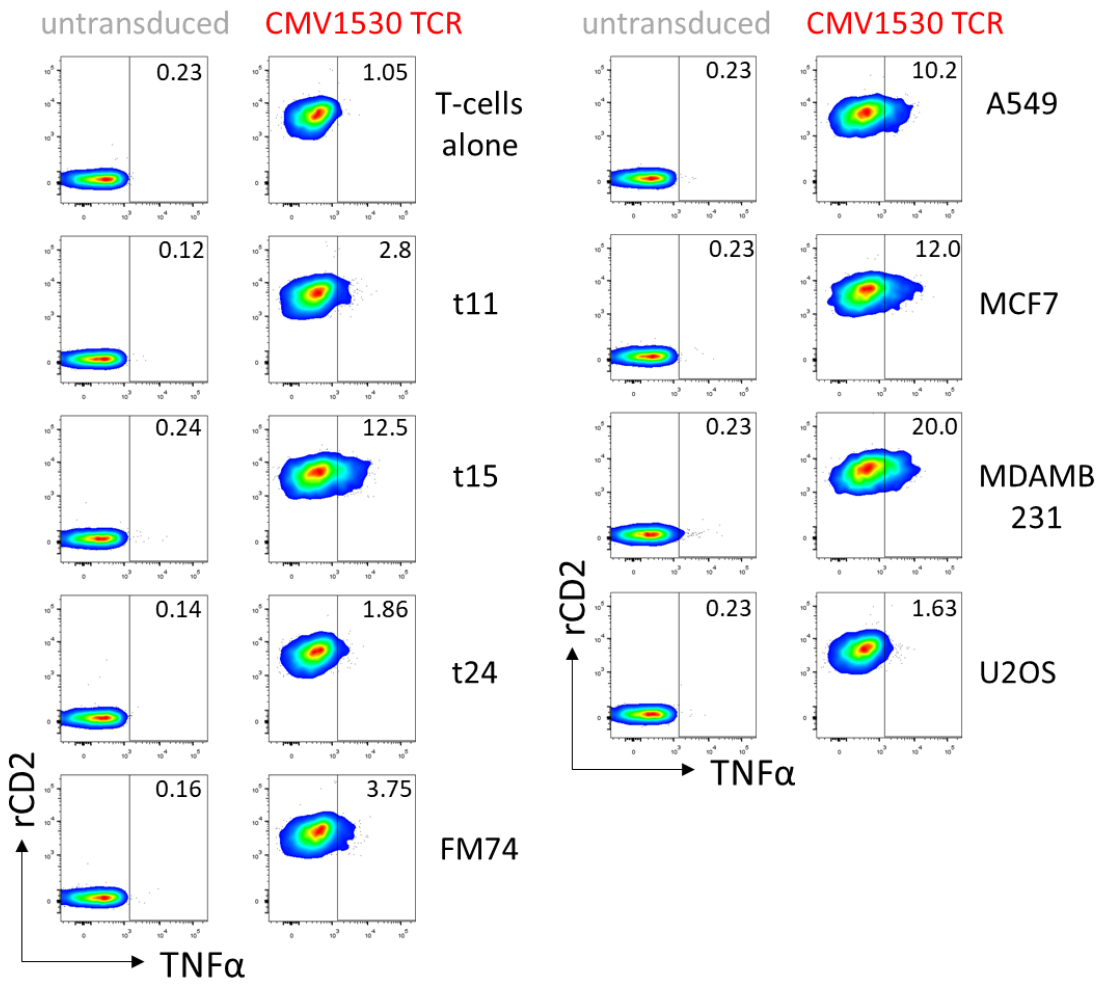

Figure 8.14 T-cells transduced with CMV1530 TCR recognise several cancer cell lines. $CD8^+$ T-cells transduced with CMV1530 TCR together with TCR-β CRISPR were co-incubated with a panel of cancer cell lines for 5 h. Following incubation, the T-cell response was measured as percentage of $TNF\alpha^+$ cells. Only viable $CD3^+CD8^+$ cells were taken for analysis. CMV1530 TCR was the dominant clonotype discovered by Ravens *et al.* in patient 1530 on day 120 and has the following CDR3 sequences: CDR3γ CATWDYYKKLF, CDR3δ CALGESPISYYWGIRGTDKLIF.

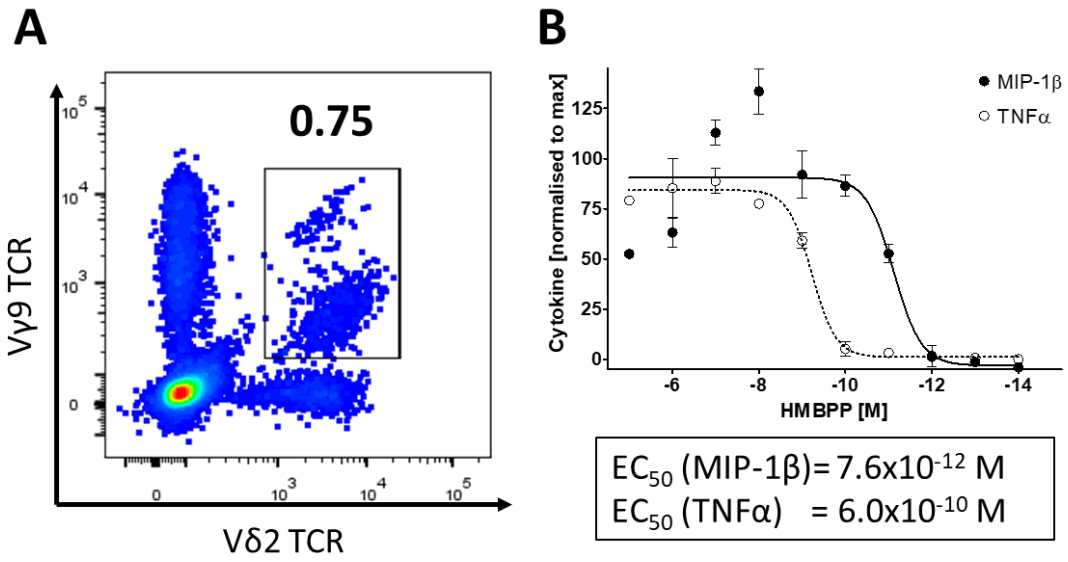

Figure 8.15 Procurement of phosphoantigen-reactive clones from TIL 15. (**A**) TIL 15 was stained with anti-Vγ9 and Vδ2 TCR antibodies and $V\gamma9^{+}V\delta2^{+}$ population was sorted. The cells were treated with protein kinase inhibitor dasatinib prior to staining with antibodies to prevent from TCR signalling and resulting activation-induced cell death. The number on dot plots indicates the percentage of gated population. (**B**) The sensitivity of the representative Vγ9Vδ2 T-cell clone was determined by MIP-1β and TNFα release after 16 h of stimulation with titrated concentrations of HMBPP. The cytokine concentrations were normalised by subtracting the cytokine concentration from unstimulated T-cells, and taking the concentration of cytokines in wells stimulated with PHA as 100%.

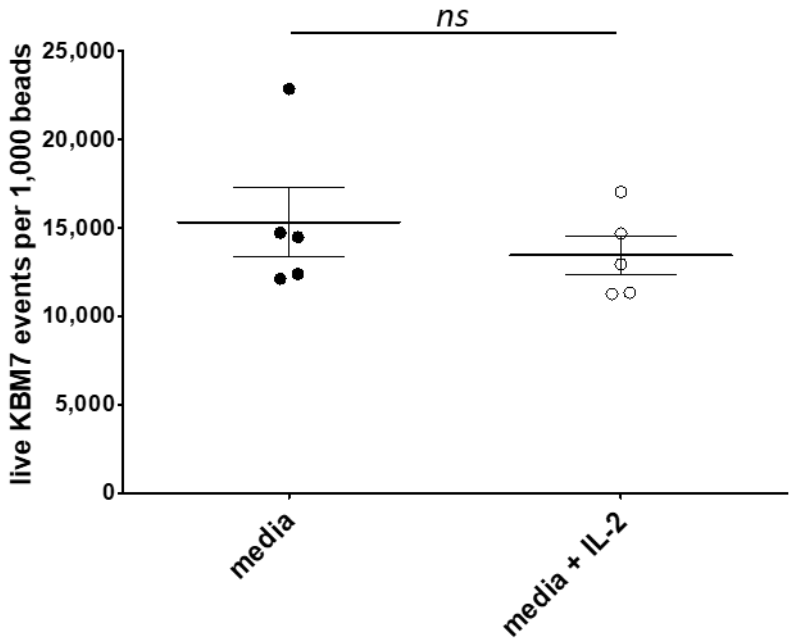

Figure 8.16 Low dose IL-2 supplementation does not affect KBM7 cell growth. KBM7 cells were cultured in R10 media or T-cell priming media containing 20 IU/ml of IL-2. The number of live cancer cells in each well was established after 14 days as described in Materials and Methods. Student's t-test, ns – not significant. Standard error of the mean is shown.

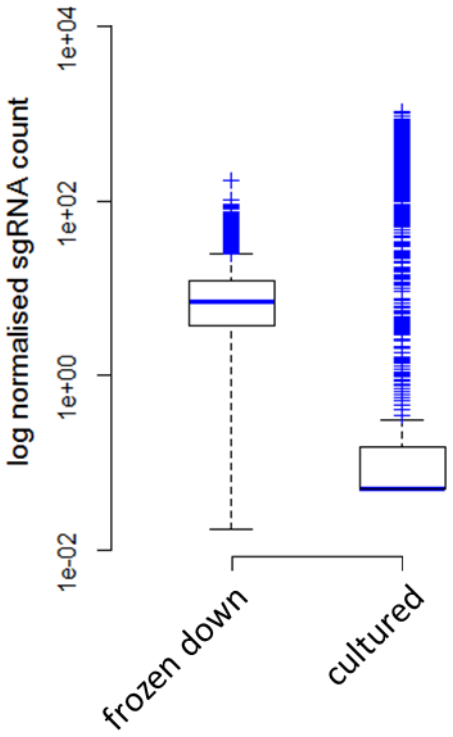

Figure 8.17 Long term culture introduces bias in the whole genome library. KBM7 cells transduced with GeCKO library were either cryopreserved on the day of library selection setup, or cultured in 96U well plates at the density of 100,000 cells per well for 14 days. Due to excessive cell growth, the cultured library was passaged twice weekly. After the culture period, the DNA from at least 30×10^6 cells from the frozen down and the cultured libraries was extracted, and the gRNA sequences were amplified by PCR and sequenced in high throughput manner, as described in **Materials and Methods Section 2.12.4**. The normalised gRNA representation was visualised using the R software.

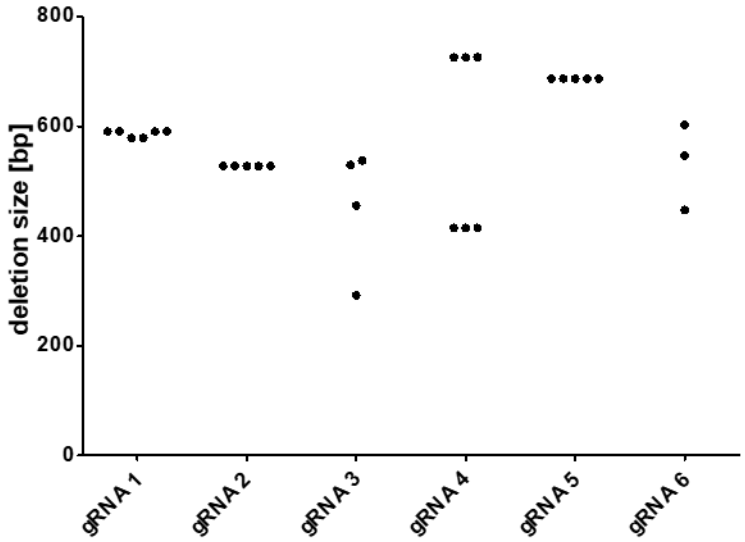

Figure 8.18 KBM7 clones transduced with *c1orf74* specific gRNAs harbour large deletions. KBM7 line was transduced with six different gRNAs targeting the protein coding region of *c1orf74* exon 2. Following selection of cells that had taken up lentivirus, single cell clones were procured. The protein coding region of *c1orf74* exon 2 was then amplified from the genomic DNA of the clones as described in Materials and Methods, and the size of the deletion was determined by alignment of sequenced PCR products to wild type *c1orf74* sequence. Each data point corresponds to an independent cell clone.

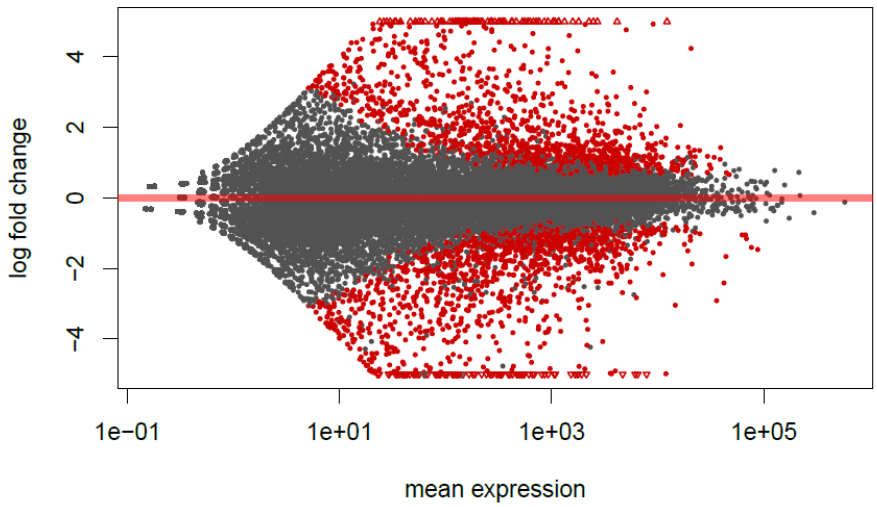

Figure 8.19 The comparison of transcriptomes between wild type KBM7 cell line and C1orf74-deficient, whole genome library-derived clone 2 unravels differential expression of nearly 5,000 genes. Total RNA was extracted from wild type KBM7 cell line, as well as C1orf74-deficient clone 2 derived from the selected whole genome library. RNA was extracted from three independent aliquots of cells per sample. mRNA was then enriched by poly(A) selection, transcribed into cDNA, and sequenced on Illumina HiSeq. Genes overexpressed (log fold change >0) or downregulated (log fold change <0) in clone 2 compared to wild type KBM7 in a statistically significant manner ($p<0.001$) are shown in red. RNAseq was performed and analysed courtesy of John Phillips, University of Utah.

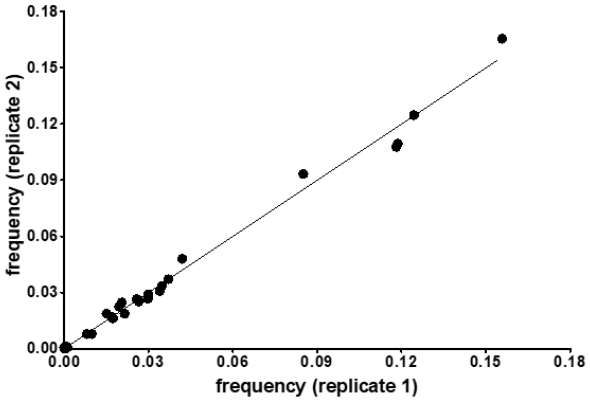

	Replicate 1	Replicate 2
Reads	7,363	9,188
Unique gRNAs	35	40
R^2	0.9928	

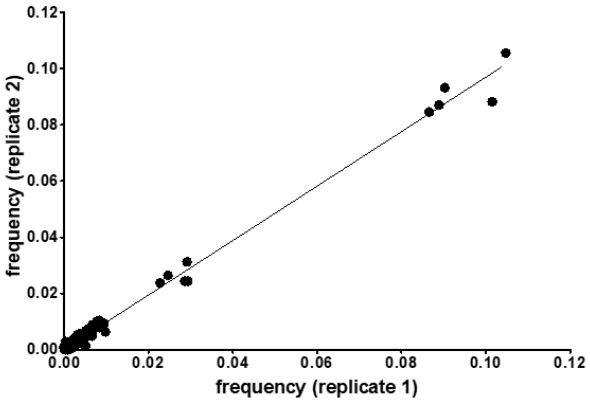

	Replicate 1	Replicate 2
Reads	5,939	5,986
Unique gRNAs	279	265
R^2	0.9921	

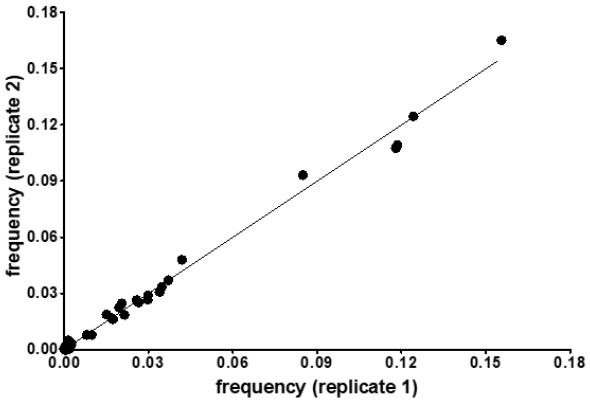

	Replicate 1	Replicate 2
Reads	3,787	4,628
Unique gRNAs	30	29
R^2	0.9936	

Figure 8.20 T-cell selected whole genome CRISPR/Cas9 libraries can be reproducibly sequenced on Illumina MiSeq. Whole genome libraries in melanoma cell line t24 were subjected to three independent T-cell selections. gDNA was extracted from the two independent samples per library (5 mln cells per sample), and 2.5 μg of the DNA (5-10% of the sample) was amplified by PCR as described in Materials and Methods. The PCR products were then multiplexed and sequenced on MiSeq (Illumina). The correlation between frequencies of respective gRNAs in library duplicates is shown as Pearson's correlation coefficient R^2. The lentivirally packaged whole genome libraries were provided by John Phillips, University of Utah.

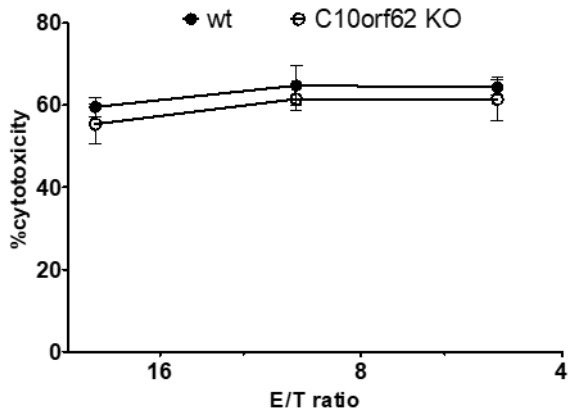

Figure 8.21 Knock-out of C10orf62 from a melanoma cell line does not affect cytotoxicity of a Melan-A specific T-cell clone. C10orf62-specific gRNA enriched in sub-library B was independently transduced into t24 melanoma cell line. The transduced cells, as well as the untransduced parental line, were co-incubated with a Melan-A specific T-cell clone KT B17 for 4 h. Cytotoxicity was determined by ^{51}Cr release assay. Standard error of the mean is shown.

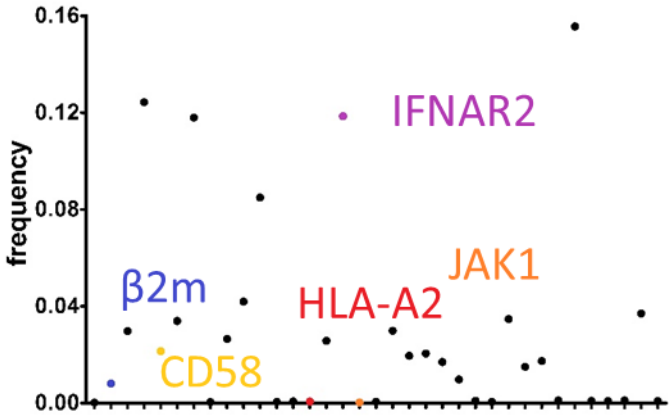

Figure 8.22 Whole genome screening with a melanoma specific αβ T-cell clone KT B17 identifies targets involved in the MHC-I processing and presentation pathway. Whole genome library GeCKO v2 (sub-library B) was transduced into a HLA-A2^{+} melanoma cell line t24. The transduced cells were co-incubated with an αβ T-cell clone KT B17 specific for a Melan-A epitope presented by HLA-A2 at E:T of 1:1 for 14 days. Genomic DNA from sub-library B after the selection was extracted and sequenced as described in Materials and Methods, and the frequencies of individual gRNAs are shown. gRNAs targeting genes of known function in antigen processing and presentation are shown in colour. The lentivirally packaged whole genome library was provided by John Phillips, University of Utah.

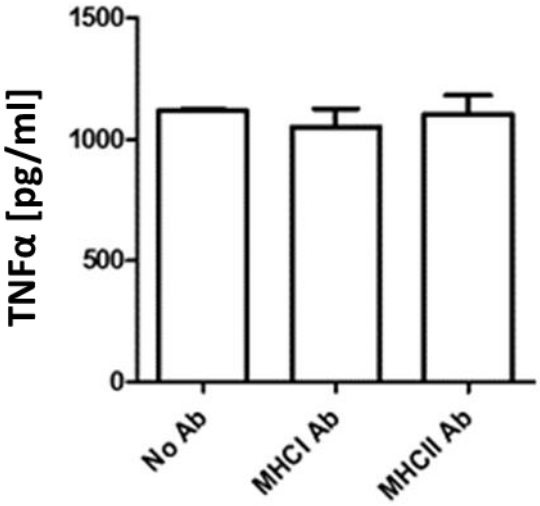

Figure 8.23 Blocking antibodies against conventional MHC-I and MHC-II molecules do not abrogate the cancer cell recognition by clone MC.7G5. Clone MC.7G5 was co-incubated with melanoma cell line t24 for 16 h, followed by quantification of secreted TNFα. TNFα secreted by T-cells incubated alone was subtracted from the experimental values. Where indicated, melanoma cell line t24 was pre-incubated with MHC class I or class II antibodies (30 min at 37ºC, using 10 μg/ml antibody). Data provided as a courtesy of Michael Crowther, Cardiff University.